TP 15533E

Towards a Standard for Vessel URN Measurement in Shallow Water

Final Report on Transport Canada Innovation Centre Project MMP2

JASCO Applied Sciences (Canada) Ltd

30 May 2022

Submitted to:

Véronique Nolet
Transport Canada Innovation Centre
Contract T8009-190191/002/XLV

Authors:

Alexander O. MacGillivray
S. Bruce Martin
Michael A. Ainslie
Joshua N. Dolman
Zizheng Li
Graham A. Warner
Carmen B. Lawrence
Federica Pace
Max Schuster
Dietrich Wittekind

P001556-002
Document 02427
Version 2.0

JASCO APPLIED SCIENCES

TP 15533E

Suggested citation:

MacGillivray, A.O., Martin, S.B., M.A. Ainslie, J.N. Dolman, Z. Li, G.A. Warner, C.B. Lawrence, F. Pace, M. Schuster, and D. Wittekind. 2022. Towards a Standard for Vessel URN Measurement in Shallow Water: Final Report on Transport Canada Innovation Centre Project MMP2. Document 02427, Version 2.0. Technical report by JASCO Applied Sciences for Transport Canada Innovation Centre.

Author Affiliations:

JASCO Applied Sciences
Alexander O. MacGillivray
S. Bruce Martin
Michael A. Ainslie
Joshua N. Dolman
Zizheng Li
Graham A. Warner
Carmen B. Lawrence
Federica Pace

DW-ShipConsult
Max Schuster
Dietrich Wittekind

This report reflects the views of the JASCO Applied Sciences and not necessarily those of the Innovation Centre of Transport Canada.

The Innovation Centre does not endorse products or manufacturers. Trade or manufacturers' names appear in this report only because they are essential to its objectives.

Un sommaire français se trouve avant la table des matières

Transport Canada / Transports Canada

PUBLICATION DATA FORM

1. Transport Canada Publication No.	2. Project No.	3. Recipient's Catalogue No.
TP 15533E	P001556-002	T89-17/2022E-PDF

4. Title and Subtitle	5. Publication Date
Towards a Standard for Vessel URN Measurement in Shallow Water	May 30th, 2022
	6. Performing Organization Document No.: 02427

7. Author(s)	8. Transport Canada File No.
A. O. MacGillivray, S. B. Martin, M. A. Ainslie, J. D. Dolman, Z. Li, G. A. Warner, C. B. Lawrence, F. Pace, M. Schuster, and D. Wittekind	-

9. Performing Organization Name and Address	10. PWGSC File No.
JASCO Applied Sciences (Canada) Ltd. Suite 2305, 4464 Markham St. Victoria, BC V8Z 7X8 Canada	- 11. PWGSC or Transport Canada Contract No.: T8009-190191/002/XLV

12. Sponsoring Agency Name and Address	13. Type of Publication and Period Covered
Transport Canada, Innovation Centre Place de Ville, Tower C 330 Sparks Street, Ottawa ON K1A 0N5	Technical report, 2020-2022 14. Project Officer: Véronique Nolet

15. Supplementary Notes (Funding programs, titles of related publications, etc.)

16. Abstract

Performing repeatable vessel source level (SL) measurements is difficult in shallow water because of the way that the environment affects received sound pressure. In deep water, with a hydrophone far from the seabed, it is relatively straightforward to estimate propagation loss (PL) and convert sound pressure level (SPL) measurements into SL using methods codified in existing standards (ISO 17208 and ANSI S12.64). Estimating PL is more difficult in shallow water because of the way that sound reflects from the seabed and multiple propagation paths contribute to the received sound pressure. Obtaining repeatable SL measurements in shallow water therefore requires straightforward and robust methods to estimate PL. A field experiment, developed in consultation with an ISO working group on shallow water URN measurement, was carried out to evaluate several different methods of measuring vessel SL in shallow water. Three anonymized partner vessels were measured many times, in three different water depths and with six different hydrophone arrays. Results of the experiment confirmed that it is possible to obtain repeatable vessel SL estimates in shallow water, comparable to those obtained in deep water. Furthermore, the methods required are only moderately more complex than those codified in the existing standards.

17. Key Words	18. Distribution Statement
vessel underwater radiated noise; shallow water; international standards; acoustic measurement	Digital copy

19. Security Classification (of this publication)	20. Security Classification (of this page)	21. Declassification (date)	22. No. of Pages	23. Price
Unclassified	Unclassified	—	180	

CI/IC 79-005
Rev. 96

Canada

Transport Canada Transports Canada

FORMULE DE DONNÉES POUR PUBLICATION

1. No de la publication de Transports Canada.	2. No de l'étude	3. No de catalogue du destinataire
TP 15533E	P001556-002	T89-17/2022E-PDF

4. Titre et sous-titre	5. Date de la publication
Vers une norme pour la mesure du bruit rayonné en eau peu profonde	30 mai 2022
	6. No de document de l'organisme exécutant: 02427

7. Auteur(s)	8. No de dossier-Transports Canada
A. O. MacGillivray, S. B. Martin, M. A. Ainslie, J. D. Dolman, Z. Li, G. A. Warner, C. B. Lawrence, F. Pace, M. Schuster, and D. Wittekind	-

9. Nom et adresse de l'organisme exécutant	10. No de dossier-TPSGC
JASCO Applied Sciences (Canada) Ltd. Suite 2305, 4464 Markham St. Victoria, BC V8Z 7X8 Canada	- 11. No de contrat-TPSGC ou Transports Canada: T8009-190191/002/XLV

12. Nom et adresse de l'organisme parrain	13. Genre de publication et période visée
Transports Canada, Centre d'Innovation Place de Ville, Tour C 330 rue Sparks, Ottawa ON K1A 0N5	Rapport technique, 2020-2022 14. Agent de projet: Véronique Nolet

15. Remarques additionnelles (programmes de financement, titres de publications connexes, etc.)

16. Résumé

Il est difficile d'effectuer des mesures reproductibles au niveau source des navires en eau peu profonde en raison de la façon dont l'environnement affecte la pression sonore reçue. En eau profonde, avec un hydrophone éloigné du fond marin, il est relativement simple d'estimer la perte de propagation et de convertir les mesures de niveau de pression sonore en niveau source en utilisant des méthodes codifiées dans les normes existantes (ISO 17208 et ANSI S12.64). L'estimation de la perte de propagation est plus difficile en eau peu profonde en raison de la façon dont le son se reflète sur le fond marin et les multiples voies de propagation contribuent à la pression sonore reçue. L'obtention de mesures reproductibles au niveau source en eau peu profonde nécessite donc des méthodes simples et très fiables pour estimer la perte de propagation. Une expérience sur le terrain, élaborée en consultation avec un groupe de travail de l'ISO sur la mesure du bruit rayonné en eau peu profonde, a été réalisée pour évaluer plusieurs méthodes différentes de mesure au niveau source des navires en eau peu profonde. Trois navires partenaires anonymes ont été mesurés à plusieurs reprises, à trois profondeurs d'eau différentes et avec six réseaux d'hydrophones différents. Les résultats de l'expérience ont confirmé qu'il est possible d'obtenir des estimations reproductibles au niveau source des navires en eau peu profonde, comparables à celles obtenues en eau profonde. De plus, les méthodes requises ne sont que modérément plus complexes que celles codifiées dans les normes existantes.

17. Mots clés	18. Diffusion
	Copie numérique

19. Classification de sécurité (de cette publication)	20. Classification de sécurité (de cette page)	21. Déclassification (date)	22. Nombre de pages	23. Prix
Non classifiée	Non classifiée	—	180	

CI/IC 79-005
Rev. 96

Canada

EXECUTIVE SUMMARY

This report is a deliverable for JASCO Applied Sciences' project MMP2: *Support ISO TC43/SC3 to Develop Measurement Standard for Shallow Water Vessel Source Level Measurements*. The project is supported by Transport Canada's Innovation Centre under the Marine Mammal Protection (MMP) umbrella of projects, with the objective of providing input to the International Organization for Standardization (ISO) Technical Committee (TC) 43, Sub-Committee (SC) 3, Working Group (WG) 1 (ISO TC 43/SC 3/WG 1), who are developing ISO standard 17208-3 for the measurement of vessel underwater radiated noise (URN) in shallow water. The knowledge gap addressed in this project is summarized as follows:

> *What combinations of sensors and analysis methods yield measurements of vessel underwater sound levels in shallow water consistent with those that are known to be accurately obtained in deep water using ISO Standard 17208-1/−2?*

This project was carried out in two phases:

1. Development of a White Paper that describes the issues associated with shallow-water vessel URN measurements, followed by development of a measurement plan for a field experiment to address the identified knowledge gaps.
2. Execution of the field experiment, followed by analysis and reporting of the collected URN measurements to address the identified knowledge gaps.

This is the project's final report and the fifth major document delivered to Transport Canada.

The motivation for this project is that predicting the effects of vessels on the marine ecosystem requires measuring their URN emissions in terms of a source level (SL). Note that URN is used as a generic term for source level (SL) and radiated noise level (RNL), as well as for their adjusted quantities (aSL and aRNL). Conceptually, the source level of a vessel is found by measuring its sound pressure levels (SPL) as it passes a recorder and then adding the propagation loss (PL) that accounts for the attenuation of the sound as it travelled from source to receiver. For measurements made in deep water, with a hydrophone far from the seabed, it is relatively straightforward estimate PL and convert the received sound pressure level into a source level, using methods in the existing standards for vessel source level measurement (ISO standards 17208-1, −2 and ANSI S12.64). However, many groups interested in the measurement of vessel URN are based in coastal areas where the water depths are shallower than those recommended in existing standards (ISO 17208-2 or ANSI S12.64). In shallow water, it is much more difficult to estimate PL because sounds interact with the seabed and multiple propagation paths contribute to the received sound level at a recording location. An accurate PL estimate in shallow water must account for the bathymetry, sound speed profile, and acoustic properties of the seabed at the measurement site. To support development of a shallow-water URN measurement standard, a straightforward and robust method is needed to estimate shallow-water PL.

An experimental measurement plan was designed to verify the acoustic propagation modelling performed for the White Paper, provide the data needed to develop a data collection Best Practice Guide in the future, and help determine the best method of computing URN in shallow

water so that it is comparable to deep-water URN. To meet the project objectives, URN was measured from the same vessels many times, in different water depths and with different hydrophone geometries. The planned water depths were 30, 70, and 180 m, referred to here as the shallow, intermediate and deep-water sites. The measurements at the deep site followed ISO Standard 17208-2 and served as the reference results to which all other results were compared. A local vessel operator in British Columbia's Southern Gulf Islands was identified as a project collaborator and assisted in planning of hydrophone deployment locations. The operator instructed their crew to transit past the hydrophone arrays and provided JASCO with voyage logs for three of their vessels.

In total, URN data were obtained from a total of 16 hydrophone nodes, distributed across three moored vertical line arrays (VLAs), two moored horizontal line arrays (HLAs), and a single drifting vertical line array. Hydrophone recording systems were AMAR G4 (JASCO Applied Sciences) acoustic recorders. All hydrophones were GeoSpectrum type M36 with a nominal sensitivity of −164 dB re 1 V/µPa. All hydrophones were calibrated prior to deployment and on retrieval using G.R.A.S 42AC pistonphone calibrators.

The measurement plan was successfully carried out from May 5th through Jul 22nd 2021. At the beginning the experiment, PL measurements were conducted at all three sites using a controlled acoustic source to measure the geoacoustic properties of the seabed. Measurements were made with the drifting vertical array in early May, early June, and late July just prior to retrieval of the moored recorders. Water column sound speed profiles were measured during the drifting array measurements.

During the experiment, the identity, position, and speed over ground of three anonymized partner vessels (referred to as A, B, and C) were obtained from the Automated Identification System (AIS). To obtain URN measurements for each vessel pass, the hydrophone recordings were automatically analyzed with ShipSound, a component of JASCO’s custom vessel noise measurement system, PortListen®. Each automated URN measurement from ShipSound was subjected to a manual quality review by a human analyst. A total of 2732 vessel passes were recorded at the three test sites during the field measurement period, which resulted in 12,079 single-hydrophone URN measurements. All measurements underwent a manual quality review, which yielded a total of 1880 vessels passes with 7675 single hydrophone measurements retained for subsequent analysis.

Analysis of the measurements confirmed that it is possible to obtain repeatable vessel source level estimates in shallow water that are comparable to those obtained in deep water. The data collection and analysis methods required are only moderately more complex than those in the existing ISO 17208-1/−2 standards. Nonetheless, the precision of source levels measured in shallow water may be limited to some extent by knowledge of the acoustic properties of the seabed.

Reference source levels for vessels A–C were obtained by analyzing URN measurements from the deep VLA according to the procedure from ISO standard 17208-2. Using these source levels as a reference, five different source level metrics were evaluated at the intermediate and shallow sites, reflecting five different approaches to analyzing vessel URN measurements:

1. ISO (Method for Deep Water Source Levels from ISO 17208-2): This is the method for analyzing deep-water RNL measurements performed according to ISO standard 17208-1 and converting them to source levels using formulae codified in ISO standard 17208-2. It does not account for the influence of the seabed but averages URN over a range of pre-defined grazing angles (15°, 30°, and 45°, which requires the vessel to pass the recorder array at a specific distance).
2. HWB (Hybrid Wavenumber Integration & Beam Tracing Method): This is a method for estimating PL of a URN measurement in any water depth using a hybrid model based on low-frequency wavenumber integration and high-frequency beam tracing. This method requires a detailed description of the acoustic properties of the environment (assumed to be range-independent) and sophisticated numerical models. The PL estimate from the numerical models is used to calculate a monopole source level directly from the URN data.
3. ECA (ECHO Certification Alignment Method): This is a method for calculating propagation loss for a URN measurement performed at any grazing angle, but which neglects the influence of the seabed. This method is similar in principle to the ISO method, but it does not assume a fixed set of grazing angles and is based on an exact Lloyds mirror PL calculation, integrated over decidecade frequency bands.
4. SCA (Seabed Critical Angle Method): This is a method for calculating source levels from single-node RNL measurements in any water depth by applying physics-based correction factors to account for the critical angle of the seabed (which must be known or estimated) and the water depth. This method can be averaged over multiple hydrophone nodes (i.e., at different grazing angles) to yield a higher-precision source level estimate.
5. M-A (Meyer-Audoly Method): This is a method for calculating source levels from array-averaged RNL measurements in shallow water by applying an empirical correction formula to account for the frequency-dependent influence of the seabed and water depth. This method includes an empirical parameter (ε), which is selected according to the seabed type (which must be known). This method was developed for a vertical array of three hydrophones, spanning the water column.

Of these five metrics, M-A and SCA provided the most robust source level estimates over a wide range of frequencies and water depths while accounting for the influence of the seabed on URN measurements. Uncertainty regarding the seabed properties was naturally found to affect the accuracy of both these methods. Of the remaining metrics, the ISO method performed well for estimating array-averaged source levels, especially considering it did not account for the influence of the seabed on shallow-water propagation loss. The ECA method performed well at short closest point of approach (CPA) distances but not at longer CPA distances. The HWB method performed well at high frequencies (1000 Hz and above), but it was not robust at lower frequencies where it had difficulty estimating source levels at longer CPA distances.

Experimental data indicated that both horizontal line array and vertical line array geometries performed well in intermediate and shallow-water depths, provided they sampled a range of grazing angles. While ISO standard 17208-1 specifies that a URN measurement be averaged over an array of three hydrophones, the experimental results at the shallow and intermediate sites suggested that single-node measurements may also be used to obtain consistent source level estimates. The uncertainty of single-hydrophone measurements is more sensitive to placement of the sensor which was minimized by deploying the hydrophones at the seabed and close to the source (50–150 m horizontal range from the vessel). The experimental results also suggested that it was possible to obtain consistent source level measurements at CPA distances closer than one vessel length from the source (though it remains important to avoid the near field, e.g., not closer than 50 m). Results from this experiment indicated that measurements from drifting hydrophones were more difficult to obtain and analyze than measurements from moored hydrophone arrays.

Results from this study are expected to provide valuable information for development of a shallow-water measurement standard, and the authors of this study have prepared a list of conclusions and recommendations for the ISO working group. The findings of this study are believed to be particularly robust, as they are based on a very large data set, consisting of 7675 individual URN measurements of three vessels from 13 hydrophones on 7 different moorings and a drifting vertical array distributed across three measurement locations at different depths. This is a comprehensive and unique data set that should be used to investigate other topics in future. Possible avenues for future research include methods for measuring directivity of vessel noise, examining the effect of source depth on source level estimates, further examination of adjusted source level metrics, and studying whether vessel URN test data may be used to directly estimate seabed geoacoustic properties.

SOMMAIRE

Ce rapport est un livrable pour le projet MMP2 de JASCO Applied Sciences : *Support ISO TC43/SC3 to Develop Measurement Standard for Shallow Water Vessel Source Level Measurements*. Le projet est soutenu par le Centre d'innovation de Transports Canada sous l'égide des projets de protection des mammifères marins, afin de fournir des commentaires au Comité technique 43 de l'Organisation internationale de normalisation (ISO), sous-comité 3, Groupe de travail 1 (ISO TC 43/SC 3/WG 1), qui élabore la norme ISO 17208-3 pour la mesure du bruit rayonné des navires en eau peu profonde. Les lacunes dans les connaissances abordées dans ce projet se résument comme suit :

Quelles combinaisons de capteurs et de méthodes d'analyse donnent des mesures des niveaux sonores sous-marins des navires en eau peu profonde, cohérentes avec ceux qui sont connus pour être obtenus avec précision en eau profonde à l'aide de la norme ISO 17208-1/−2?

Le présent projet s'est déroulé en deux étapes :

1. Élaboration d'un livre blanc pour décrire les problèmes associés aux mesures du bruit rayonné des navires en eau peu profonde, suivi de l'élaboration d'un plan de mesure pour une expérience sur le terrain afin de combler les lacunes identifiées dans les connaissances.
2. Exécution de l'expérience sur le terrain, suivie d'une analyse et d'un rapport des mesures recueillies du bruit rayonné sous l'eau pour combler les lacunes en matière de connaissances.

Il s'agit du rapport final du projet et du cinquième document majeur remis à Transports Canada.

La motivation pour ce projet réside dans le fait que, pour prévoir les effets des navires sur l'écosystème marin, il faut mesurer leurs émissions du BRSE en ce qui concerne le niveau source. Notez que le bruit rayonné sous l'eau (BRSE) est utilisé comme terme générique pour le niveau source et le niveau de bruit rayonné, ainsi que pour leurs quantités ajustées. Conceptuellement, le niveau source d'un navire est trouvé en mesurant ses niveaux de pression sonore lorsqu'il passe devant un enregistreur, puis en ajoutant la perte de propagation qui tient compte de l'atténuation du son lors de son trajet de la source au récepteur. Pour les mesures effectuées en eau profonde, avec un hydrophone éloigné du fond marin, il est relativement simple d'estimer la perte de propagation et de convertir le niveau de pression sonore reçu au niveau source, en utilisant les méthodes des normes actuelles pour la mesure du niveau source des navires (normes ISO 17208-1, −2 et ANSI S12.64). Cependant, de nombreux groupes intéressés par la mesure du BRSE des navires sont basés dans des zones côtières où les profondeurs d'eau sont inférieures à celles recommandées dans les normes actuelles (ISO 17208-2 ou ANSI S12.64). En eau peu profonde, il est beaucoup plus difficile d'estimer la perte de propagation parce que les sons interagissent avec le fond marin et que de multiples voies de propagation contribuent au niveau sonore reçu à un emplacement d'enregistrement. Une estimation précise de la perte de propagation en eau peu profonde doit tenir compte de la bathymétrie, du profil de vitesse du son et des propriétés sonores du fond marin sur le site de mesure. Pour soutenir le développement d'une norme de mesure du bruit rayonné en eau peu

profonde, une méthode simple et très fiable est nécessaire pour estimer la perte de propagation en eau peu profonde.

Un plan de mesure expérimental a été conçu pour vérifier la modélisation de la propagation sonore effectuée pour le livre blanc, pour fournir les données nécessaires pour développer un guide des meilleures pratiques de collecte de données à l'avenir et pour aider à déterminer la meilleure méthode de calcul du bruit rayonné en eau peu profonde afin qu'il soit comparable au bruit rayonné en eau profonde. Pour atteindre les objectifs du projet, le BRSE a été mesuré plusieurs fois à partir des mêmes navires, à différentes profondeurs d'eau et avec différentes géométries d'hydrophones. Les profondeurs d'eau prévues étaient de 30, de 70 et de 180 m, désignées ici par les sites en eaux peu profondes, intermédiaires et profondes. Les mesures sur le site profond ont suivi la norme ISO 17208-2 et ont servi de résultats de référence auxquels tous les autres résultats ont été comparés. Un opérateur de navire local dans le sud des îles Gulf de la Colombie-Britannique a été identifié comme collaborateur du projet et a aidé à planifier les emplacements de déploiement des hydrophones. L'opérateur a demandé à son équipage de passer devant les réseaux d'hydrophones et a fourni les carnets de route de trois de ses navires à JASCO.

Au total, les données du BRSE ont été obtenues à partir d'un total de 16 nœuds d'hydrophones, répartis sur trois réseaux d'antennes linéaires verticales, deux réseaux d'antennes linéaires horizontales et un seul réseau d'antennes dérivantes verticales. Les systèmes d'enregistrement hydrophone étaient des enregistreurs sonores AMAR G4 (JASCO Applied Sciences). Tous les hydrophones étaient de type GeoSpectrum M36 avec une sensibilité nominale de −164 dB re 1 V/µPa. Tous les hydrophones ont été étalonnés avant le déploiement et lors de la récupération à l'aide d'étalonneurs de pistonphone GRAS 42AC.

Le plan de mesure a été réalisé avec succès à partir du 5 mai jusqu'au 22 juillet 2021. Au début de l'expérience, des mesures de perte de propagation ont été effectuées sur les trois sites à l'aide d'une source sonore contrôlée pour mesurer les propriétés géosonores du fond marin. Des mesures ont été faites avec le réseau d'antennes dérivantes verticales en début mai, en début juin et à la fin juillet, juste avant la récupération des enregistreurs amarrés. Les profils de vitesse du son dans la colonne d'eau ont été mesurés pendant les mesures du réseau d'antennes dérivantes.

Au cours de l'expérience, l'identité, la position et la vitesse au sol de trois navires partenaires anonymes (appelés A, B et C) ont été obtenues à partir du système d'identification automatique (SIA). Pour obtenir des mesures du BRSE pour chaque passage de navire, les enregistrements d'hydrophone ont été automatiquement analysés avec ShipSound, un composant du système personnalisé de mesure du bruit des navires de JASCO, PortListen[MD]. Chaque mesure automatisée du BRSE de ShipSound a été soumise à un examen manuel de la qualité par un analyste humain. Au total, 2 732 passages de navires ont été enregistrés sur les trois sites d'essai au cours de la période de mesure sur le terrain, ce qui a donné lieu à 12 079 mesures de BRSE à hydrophone unique. Toutes les mesures ont fait l'objet d'un examen manuel de la qualité, qui a donné un total de 1 880 passages de navires avec 7 675 mesures d'hydrophones uniques conservées pour une analyse ultérieure.

L’analyse des mesures a confirmé qu’il est possible d’obtenir des estimations reproductibles du niveau source des navires en eau peu profonde, comparables à celles obtenues en eau profonde. Les méthodes de collecte et d’analyse de données requises ne sont que modérément plus complexes que celles des normes ISO 17208-1/−2 existantes. Néanmoins, la précision des niveaux source mesurés en eau peu profonde peut être limitée dans une certaine mesure par la connaissance des propriétés sonores du fond marin.

Les niveaux source de référence pour les navires A à C ont été obtenus en analysant les mesures du BRSE de la VLA profonde selon la procédure de la norme ISO 17208-2. En utilisant ces niveaux source comme référence, cinq métriques de niveau source différentes ont été évaluées aux sites intermédiaires et peu profonds, en reflétant cinq approches différentes pour analyser les mesures de l’URN des navires :

1. ISO (Méthode pour les niveaux source en eau profonde de l’ISO 17208-2) : Il s’agit de la méthode d’analyse des mesures de niveaux de bruit rayonné en eau profonde effectuées selon la norme ISO 17208-1 et de leur conversion en niveaux source à l’aide de formules codifiées dans la norme ISO 17208-2. Elle ne tient pas compte de l’influence du fond marin, mais fait la moyenne de l’URN sur une plage d’angles rasants prédéfinis (15 °, 30 ° et 45 °, ce qui oblige le navire à passer le réseau d’enregistreurs à une distance précise).
2. HWB (méthode d’intégration du nombre d’ondes et du traçage des faisceaux) : Il s’agit d’une méthode d’estimation de la perte de propagation d’une mesure URN à n’importe quelle profondeur d’eau à l’aide d’un modèle hybride basé sur l’intégration du nombre d’ondes à basse fréquence et le traçage de faisceaux à haute fréquence. Cette méthode nécessite une description détaillée des propriétés sonores du milieu (supposées indépendantes de la portée) et des modèles numériques sophistiqués. L’estimation de la perte de propagation des modèles numériques est utilisée pour calculer un niveau source de monopole directement à partir des données d’URN.
3. ECA (méthode d’harmonisation de la certification ECHO) : Il s’agit d’une méthode de calcul de la perte de propagation pour une mesure d’URN effectuée à n’importe quel angle rasant, mais qui néglige l’influence du fond marin. Cette méthode est semblable en ce qui concerne son principe à la méthode ISO, mais elle ne présuppose pas un ensemble fixe d’angles rasants et se base sur un calcul de la perte de propagation qui représente un miroir Lloyds exact, intégré sur des bandes de fréquences de plusieurs décennies.
4. SCA (méthode de l’angle critique du fond marin) : Il s’agit d’une méthode de calcul des niveaux source à partir de mesures des niveaux de bruit rayonné à nœud unique à n’importe quelle profondeur d’eau en appliquant des facteurs de correction basés sur la physique pour tenir compte de l’angle critique du fond marin (qui doit être connu ou estimé) et de la profondeur d’eau. Cette méthode peut être étalée sur plusieurs nœuds d’hydrophones (c.-à-d. à différents angles rasants) pour produire une estimation plus précise du niveau source.

5. MA (méthode Meyer-Audoly) : Il s'agit d'une méthode de calcul des niveaux source à partir de mesures des niveaux moyens de bruit rayonné en eau peu profonde, en appliquant une formule de correction empirique pour tenir compte de l'influence dépendante de la fréquence du fond marin et de la profondeur de l'eau. Cette méthode comprend un paramètre empirique (ε), qui est choisi en fonction du type de fond marin (qui doit être connu). Cette méthode a été développée pour un réseau d'antennes verticales de trois hydrophones, qui couvrent la colonne d'eau.

Parmi ces cinq mesures, la MA et la SCA ont fourni les estimations de niveau source les plus fiables sur une large gamme de fréquences et de profondeurs d'eau, tout en tenant compte de l'influence du fond marin sur les mesures de l'URN. L'incertitude concernant les propriétés du fond marin a naturellement affecté la précision de ces deux méthodes. Parmi les mesures restantes, la méthode ISO a fourni un bon rendement pour estimer les niveaux source en moyenne par réseau, d'autant plus qu'elle ne tenait pas compte de l'influence du fond marin sur la perte de propagation en eau peu profonde. La méthode ECA a donné de bons résultats aux courtes distances du point d'approche minimale (CPA), mais pas aux distances plus longues du CPA. La méthode HWB a bien fourni un bon rendement à de hautes fréquences (1 000 Hz et plus), mais elle n'était pas robuste à de basses fréquences où elle avait des difficultés à estimer les niveaux source à des distances CPA plus longues.

Les données expérimentales ont indiqué que les géométries de réseaux d'antennes linéaires horizontales et de réseaux d'antennes linéaires verticales fonctionnaient bien à des profondeurs d'eau intermédiaires et peu profondes, à condition qu'elles aient échantillonné une gamme d'angles rasants. Alors que la norme ISO 17208-1 spécifie qu'une mesure URN doit être moyennée sur un réseau de trois hydrophones, les résultats expérimentaux sur les sites peu profonds et intermédiaires suggèrent que des mesures à un seul nœud peuvent également être utilisées pour obtenir des estimations cohérentes du niveau source. L'incertitude des mesures d'un seul hydrophone est plus sensible au placement du capteur, qui a été minimisé en déployant les hydrophones au fond de la mer et à proximité de la source (portée horizontale de 50 à 150 m du navire). Les résultats expérimentaux ont également suggéré qu'il était possible d'obtenir des mesures cohérentes du niveau source à des distances CPA à moins d'une longueur de navire de la source (bien qu'il reste important d'éviter le champ proche, p. ex., pas à moins de 50 m). Les résultats de cette expérience ont indiqué que les mesures des hydrophones dérivants étaient plus difficiles à obtenir et à analyser que les mesures des réseaux d'hydrophones ancrés.

Les résultats de cette étude devraient fournir des renseignements précieux pour l'élaboration d'une norme de mesure en eau peu profonde; les auteurs de cette étude ont préparé une liste de conclusions et de recommandations pour le groupe de travail ISO. On pense que les résultats de cette étude sont particulièrement fiables, car ils sont basés sur un très grand ensemble de données, composé de 7 675 mesures individuelles du BRSE de trois navires, à partir de 13 hydrophones sur 7 mouillages différents et d'un réseau vertical dérivant réparti sur trois emplacements de mesure à différentes profondeurs. Il s'agit d'un ensemble de données complet et unique qui devrait être utilisé pour étudier d'autres sujets à l'avenir. Les pistes de recherche possibles incluent des méthodes de mesure de la directivité du bruit des navires, l'examen de l'effet de la profondeur de la source sur les estimations du niveau source, un

examen plus approfondi des mesures ajustées du niveau source et l'étude de la possibilité d'utiliser les données d'essai du BRSE du navire pour estimer directement les propriétés géosonores du fond marin.

TABLE OF CONTENTS

APPENDICES

FIGURES

TABLES

LIST OF ABBREVIATIONS AND ACRONYMS

AIS	Automatic Identification System
AMAR	Autonomous Multichannel Acoustic Recorder
ANSI	American National Standards Institute
aRNL	adjusted RNL
ASA	Acoustical Society of America
aSL	adjusted SL
BC	British Columbia
BPG	Best Practice Guide
BV	Bureau Veritas
CD	Committee Draft
CHS	Canadian Hydrographic Service
CPA	closest point of approach
CPP	controllable pitch propeller
CTD	conductivity-temperature-depth
DFO	Department of Fisheries and Oceans
DIS	Draft International Standard
DNV	Det Norske Veritas Germanischer Lloyd
ECA	ECHO Certification Alignment Method
FDIS	Final Draft International Standard
FFT	Fast Fourier Transform
GPS	Global Positioning System
HLA	horizontal line array
HWB	Hybrid Wavenumber Integration & Beam Tracing Method
IEC	International Electrotechnical Commission
ISO	International Organization for Standardization
M-A	Meyer-Audoly (Method)
MAP	maximum *a posteriori*
MONM	Marine Operations Noise Model
NL	noise level
NWIP	ISO New Work Item Proposal
OSM	Ocean Sound Meter
PAM	passive acoustic monitoring
PE	parabolic equation
PL	propagation loss
PPD	posterior probability density
PSD	power spectral density
PSO	protected species observer
RINA	Registro Italiano Navale
rjMCMC	reversible-jump Markov Chain Monte Carlo
RNL	radiated noise level
RPM	revolutions per minute
SC	Sub-Committee
SC3	ISO TC 43/SC 3
SCA	Seabed Critical Angle Method
SL	source level
SNR	signal-to-noise ratio
SPL	sound pressure level
STW	speed through water
TC	Technical Committee
TC-IC	Transport Canada’s Innovation Centre
trans-D	trans-Dimensional
TVR	Transmission Voltage Response
ULS	underwater listening station
URN	underwater radiated noise
VLA	vertical line array
WG	Working Group
WG1	ISO TC 43/SC 3/WG 1

1. INTRODUCTION AND BACKGROUND

JASCO Applied Sciences, in collaboration with DW-ShipConsult, executed a project, supported by Transport Canada's Innovation Centre (TC-IC), intended to provide experimental results to assist the International Standards Organization (ISO) in developing Standard 17208-3 for the measurement of vessel underwater radiated noise (URN)[1] in shallow water. Measurements in shallow water are difficult to perform because of the ways in which sound interacts with the seafloor and sea surface.

In assisting the ISO to develop standard 17208-3, this project aimed to answer the question:

> *What combinations of sensors and analysis methods yield measurements of vessel underwater sound levels in shallow water consistent with those that are known to be accurately obtained in deep water using ISO Standard 17208-1/−2?*

The project had two phases: 1) development of a White Paper that describes the issues associated with shallow-water vessel URN measurements followed by development of a measurement plan for a field experiment to address the identified knowledge gaps and 2) execution of the field experiments, followed by analysis and reporting of the collected URN measurements to address the knowledge gaps. Experimental measurements were performed in shallow, intermediate, and deep water with numerous repeat vessels transits by a local vessel operator who collaborated with the TC-IC study.

This is the project's final report and the fifth major document delivered to Transport Canada. The previous documents were as follows:

1. The 'White Paper' (Ainslie et al. 2020b), which was an acoustic propagation modelling study investigating how sound from ships is affected by shallow-water conditions. The White Paper included recommendations for how measurements should be performed during the field experiment.
2. The Final Measurement Plan (Martin et al. 2021), which detailed where the acoustic measurements would be performed using bottom mounted hydrophone recorders, vertical arrays of hydrophone recorders, and vertical arrays of recorders suspended over the side of a vessel. It also detailed the plans for determining sediment properties at the mooring sites by emitting sound in the 600–1200 Hz band and inverting the measured propagation losses. To obtain authorization from the Fisheries and Oceans Canada (DFO) to generate the sounds in Southern Resident killer whale habitat, the plan implemented mitigation measures to prevent marine mammals from being exposed to potentially disruptive levels of underwater sound.
3. Long-term Recorder Deployment Report, which documents the deployment of the long-term recorders and the methods employed for the May 2021 drift measurements and Propagation Loss measurements (Lawrence et al. 2021).

[1] Throughout this report, underwater radiated noise (URN) is used as a generic term for source level (SL) and radiated noise level (RNL), as well as for their adjusted quantities (aSL and aRNL).

4. Shallow Water Vessel Source Level Data Set & QC Report, which contains the full description of the May to July 2021 measurement methods and provides an overview of the data quality (Lawrence et al. 2021).

JASCO performed engineering trials in September 2020 and February 2021. A summary of the September 2020 and February 2021 trials are included in this report.

The contents of the remainder of this report are as follows:

1. Section 1 describes the motivations for the project, including issues that make shallow-water vessel source level measurements more difficult than those in deep water, need for a best practice guidance for making the measurements, and how to compute the propagation loss between vessel and sensors.
2. Section 2 provides definitions of key acoustical terminology that are used throughout the document and an overview of the ISO process that will lead to the ratification of Standard 17208-3.
3. Section 3 provides a high-level summary of previous reports, including a synopsis of the key modelling results from the White Paper, the recommendations for acoustic recorder placements that resulted from the modelling, and the recommended methods of analyzing the data to obtain source levels. Section 3 also describes the lessons learned from JASCO's September 2020 and February 2021 engineering trials of different acoustic recorder systems and analysis of the container ship source levels that were recorded.
4. Section 4 presents a review of the May to July 2021 measurement plan and provides a detailed report on the methods and results of the field experiment. This section also includes a discussion of the results of the field experiment and a summary of its conclusions.
5. Section 5 provides recommendations to the ISO working group for the international standard on measurement of vessel source levels in shallow water, based on the findings of this study.

1.1. What is Different About Shallow Water?

Predicting the effects of man-made sounds on the marine ecosystem requires knowledge of amplitude and frequency content of those sounds. The source level of a marine vessel depends on its size, speed, draught, and trim as well as design considerations such as engine mounting, propeller design, and the flow of water over the propeller and rudders. Because of the wide range of factors that influence vessel source levels, many measurements are required to characterize the world-wide fleet. Conceptually, the source level (SL, symbol L_S) of a vessel is easily found by measuring the sound pressure levels (SPL, symbol L_p) of the vessel as it passes a recorder and then adding the propagation loss (PL, symbol N_{PL}) that accounts for the attenuation of the sound as it travelled from source to receiver:

$$L_S = L_p + N_{\mathrm{PL}}\,. \tag{1}$$

For measurements made in deep water, with a hydrophone far from the seabed, the direct and surface reflected propagation paths arrive at hydrophones in the upper half of the water column with more energy than any paths interacting with the seabed. As a result, it is relatively straightforward to account for the two propagation paths and convert the received sound pressure level into a monopole source level without employing numerical acoustic propagation modelling. In the existing standards for vessel source level measurement (ISO standards 17208-1, −2 and ANSI 12.64), the purpose of measuring at 15, 30, and 45° elevations (Figure 1) and averaging over repeated measurements is to smooth out the frequency dependence of the interference between the direct and reflected paths so that the URN measurement is stable.

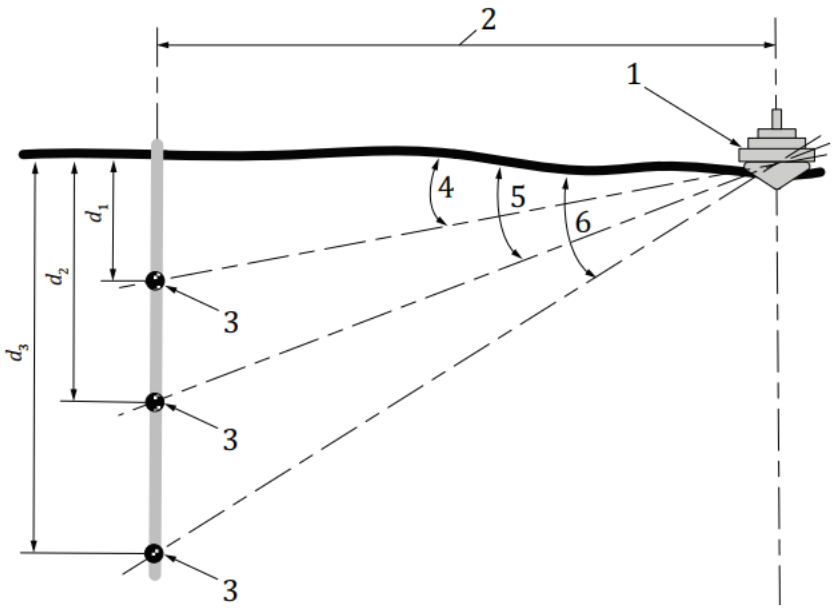

Figure 1. Recommended geometry from ISO Standard 17208-1 (2016) for making underwater radiated noise measurements in deep water conditions: (1) The vessel; (2) the closest point of approach (CPA) distance, which should the longer of 100 m or the vessel length; (3) hydrophones; and (4, 5, 6) angles to the hydrophones with target angles of 15, 30, and 45 degrees. The water depth must be greater than the CPA distance for this geometry.

Many groups interested in the measurement of vessel URN are located in coastal areas where the water depths are shallower than recommended in ISO 17208-1/2 or ANSI S12.64. In shallow water, sounds interact with the seabed and surface and multiple paths contribute to the received sound level at a recording location. The number of paths will depend on the distance between the recorder and vessel; more paths contribute significantly to the received level at longer ranges (e.g., Figure 2). The amplitude of the seabed and surface reflected paths depends on the incidence angles, seabed composition, and bathymetric profiles. If the seabed composition, speed of sound in the water column and bathymetry are known, acoustic propagation modelling may be employed to estimate PL, and hence arrive at the source level.

The bounds on how to account for the shallow-water propagation need to be defined before an approach can be considered for an international standard. For practitioners who employ acoustic propagation models, a standard could define requirements on how the geoacoustic properties were determined and how to demonstrate that the acoustic propagation model is reliable.

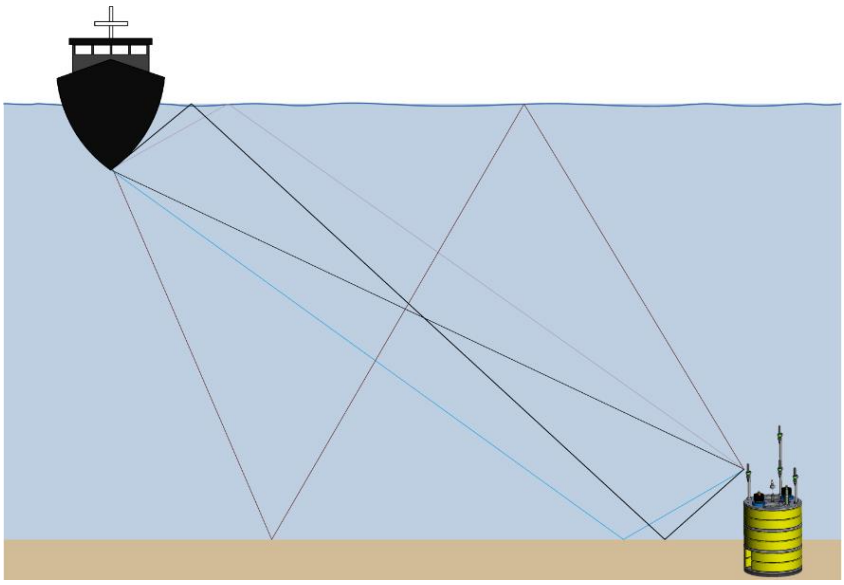

Figure 2. Diagram of multiple paths that sound travels from a ship to a recorder in shallow water.

Measurements in shallow water are not only affected by interactions of the sound with the seabed but also by propagation and sound generation effects that are unique this environment. First, shallow water inhibits the propagation of low frequencies in a manner that depends on the water depth and seabed composition. For most applications, 10 Hz is the minimum frequency of interest; for a typical sand seabed, a 10 Hz cut-off frequency requires a water depth of ~65 m. To avoid a situation when one single normal mode[2] dominates, there needs to be at least two normal modes present, which in turn requires the water depth to exceed this value by a factor of three, leading to a minimum water depth of 120 m if one wanted to cover the entire frequency range of interest without entering the single mode regime. At closer ranges, this single mode

[2] The term "normal mode" refers to the depth resonances of propagating sound waves in the water column. The number of normal modes strongly influences propagation loss in shallow water.

criterion is less important; however, this view of propagation supports the use of 150 m depth as the division between deep and shallow water contained in ISO 17208-2.

The second effect to be considered is that resistance of water to a ship's passage increases in shallow water, which could increase propeller loading and hence noise. The International Towing Tank Committee recommends that no correction is needed if the water depth H satisfies the following criterion:

$$H < \max\left(3\sqrt{BT}, 0.3\text{m}\left(\frac{V}{\text{m/s}}\right)^2\right), \quad (2)$$

where B is the beam of the vessel, T is the draught, and V is the vessel speed. For a vessel with a 27 m beam and a 6 m draught travelling at 10 m/s (~20 knots), the minimum water depth is max (38.2, 30), which is 38.2 m.

These two constraints indicate that a minimum water depth of at least 65 m is needed to accurately measure the sound from large vessels. However, there are many places in the world where accessing water deeper than 50 m is logistically challenging. For example, much of the North Sea and Baltic Sea, both of which have heavy vessel traffic, is less than 40 m deep. Therefore, it is relevant to assess how to make measurements in these shallow areas that are comparable to the accepted deep-water methods.

1.2. A Need for Best Practices in Measurement

Figure 1, copied from ISO 17208-1, requires the use of a hydrophone array whose length is on the order of the vessel length. It implies that the hydrophones are suspended from the surface in some manner. The Specification goes on to suggest that bottom mounted or surface deployed hydrophones could be used, but there is limited guidance on issues that arise with the different options and what must be controlled to obtain a valid measurement. Both types of measurements present technical challenges. The following are the key constraints essential for URN measurements:

1. The location of the hydrophones relative to the vessel must be known to within 10 % of the distance (10 % range error is equivalent to ~0.5 dB in source level).
2. The measurement platform must not introduce noise levels that are within 10 dB of the measured sound level from the target vessel in any of the decidecades[3] of interest. Possible sources of measurement noise are movement of the hydrophones and sound from the platform (e.g., engines, hull slap).

Currents are a substantial source of error for both hydrophone location and noise. For bottom mounted hydrophone arrays, currents cause 'knock-down' of the hydrophones. For surface mounted systems, they can 'knock-up' the hydrophones. The associated movement of the hydrophones and flow over them generates flow noise at low frequencies that overlap with the frequencies of greatest interest for source level measurements (30–100 Hz).

[3] A decidecade (0.1 dec) is approximately equal to one third of an octave, and for this reason is sometimes referred to as a 'one-third octave'.

Deploying hydrophones from the surface presents the following other substantial challenges:

1. Navigational safety: The desired CPA distance between the hydrophone array and measured vessel (dimension 2 in Figure 1) is on the order of the vessel length. To meet the noise requirements, the engines on the deployment vessel must be shut down. This means that the deployment vessel will be without engine power in close proximity to a large vessel that has virtually no ability to turn or stop. There are many vessel masters who will not accept this risk. Similarly, there are many traffic areas where small craft are not allowed to stop inside the traffic lanes without special permission.
2. Movement noise: The hydrophones must be suspended from the surface in some way. Even small vertical movements (on the order of centimeters) from waves generates noise in the recorded data at frequencies below 100 Hz that can exceed the measured sound levels. Methods to isolate the hydrophones from the surface noise complicate knowing where the hydrophones are and are complex to design and ensure are working well.
3. Hull-slap: Small waves and chop striking the slides of a metal boat generate a surprising level of underwater noise.

Taken together, these constraints and considerations mean that there is a need for a Best Practices Guide (BPG) for improving the likelihood of obtaining high quality acoustic data. Providing measurements that could inform the development of a BPG in the future was a motivation for this project.

1.3. How to Compute Propagation Loss?

The term ‘propagation loss’ appears to be a simple concept in Equation 1. However, there are two approaches to determining PL: compute the geometric spreading loss (i.e., $20\log_{10}$(CPA distance)), which results in a URN estimate called the Radiated Noise Level (RNL); or compute the attenuation with numerical models that include all propagation effects to obtain the source level (SL). RNL is viewed as useful for comparing one vessel to another. SL is required if one wants to perform ‘forward modelling’ that predicts the sound level at any distance from the vessel. Because RNL is easy to compute for the deep-water case, it was the only approach included in the first vessel URN standards (ANSI 12.64 and ISO 17208-1). For the deep-water case, ISO 17208-2 proposed a method of computing the source level from RNL assuming the sea surface is a perfect reflector and that the analyst knows the depth of the source (often the tip of the vessel’s propeller). However, the nominal propeller depths are often not well known, and even when they are, in reality propellers are extended sources, not point sources, and thus the SL is an estimate when following the ISO 17208-2 approach (with levels of certainty provided in the Specification). The ISO 17208-2 methods do not account for the sound speed profile as a function of water depth, nor do they account for differential absorption of sound by seawater. Both of these effects can be significant, even with relatively short measurement ranges of hundreds of meters.

As discussed in Section 1.1, in shallow water the sound interacts with the seabed and sea surface which complicates both the RNL and SL computations. A goal of this project is to provide sufficient data to allow for the development of adjusted expressions for RNL and SL that are comparable, within a specified uncertainty, to the values obtained in deep water.

2. BACKGROUND

2.1. Acoustical Terminology

The process towards a shallow-water URN measurement standard will require effective communication between stakeholders, which is facilitated by a harmonized and precise terminology with wide acceptance. Given that international consensus exists for ISO 18405 (2017), this document follows that standard throughout. In the following, distinctions are made between abbreviations, such as SPL to stand for sound pressure level in text and symbols such as L_p to stand for sound pressure level in equations.

2.1.1. General

Geometrical parameters and fractional decade frequency bands are defined in Tables 1 and 2. The speed of sound in water is c_w and the compressional wave speed in the seabed is c_p.

Table 1. Terms and definitions: Geometry. All quantities are evaluated at the closest point of approach between the source and receiver.

Term	Definition	Equation/Symbol
horizontal range	horizontal distance between source and receiver	x
receiver depth	vertical distance between sea surface and receiver (i.e., a hydrophone)	z
slant range	Pythagorean distance between source and receiver	$r = \sqrt{x^2 + z^2}$
grazing angle (θ)	Angle below sea surface to receiver at closest point of approach	$\theta = \text{atan}(z/x)$
seabed critical angle (ψ)	Grazing angle at which sound is totally reflected from the seabed	$\psi = \text{acos}(c_w/c_p)$*

* The critical angle formula provided in this table is only valid for an idealized, homogeneous seabed (i.e., without vertical structure). For the more general case of a stratified seabed composed of elastic layers, the critical angle must be calculated using a numerical model (see Section 4.2.1).

Table 2. Terms and definitions: Decade and fractional decade frequency bands.

Term	Definition	Notes
decade (dec)	ISO 80000-8:2020	
decidecade (ddec)	0.1 dec	One decidecade is approximately equal to one third of an octave.
Centidecade (cdec)	0.01 dec	One centidecade is equal to one tenth of a decidecade.

2.1.2. Levels, Power Quantities, and Reference Values

The general formula for level of a power quantity Q is:

$$L_Q = 10 \log_{10} \frac{Q}{Q_0} \text{ dB}, \tag{3}$$

relative to a reference value Q_0 of the same quantity. For example, sound pressure level (SPL, symbol L_p) is the level of the power quantity:

$$\text{Q} = \overline{p^2}, \tag{4}$$

relative to 1 µPa²:

$$L_p = 10 \log_{10} \frac{\overline{p^2}}{1\ \mu\text{Pa}^2} \text{ dB}. \tag{5}$$

Similarly, source level (SL, symbol L_S) is the level of the source factor S:

$$Q = S \tag{6}$$

$$S = 10^{L_S/(10\ \text{dB})}\ \mu\text{Pa}^2 \cdot \text{m}^2 \tag{7}$$

relative to 1 µPa²·m²:

$$L_S = 10 \log_{10} \frac{S}{1\ \mu\text{Pa}^2 \cdot \text{m}^2} \text{ dB}. \tag{8}$$

Finally, radiated noise level (RNL, symbol L_{RN}) is the level of the power quantity:

$$Q = \overline{p^2} r^2, \tag{9}$$

where *r* is slant distance from the source to the receiver. The level is computed relative to the same reference quantity of 1 µPa²·m²:

$$L_{\text{RN}} = 10 \log_{10} \frac{\overline{p^2} r^2}{1\ \mu\text{Pa}^2 \cdot \text{m}^2} \text{dB}. \tag{10}$$

2.2. Sound Propagation: Concepts and Specialized Terminology

Following ISO 18405, SL is the sum of the received SPL and the propagation loss (PL, symbol N_{PL}) between source and receiver:

$$L_S = L_p + N_{\mathrm{PL}}\,. \tag{11}$$

N_{PL} may be estimated using numerical acoustic propagation models or through the use of a number of proposed simplified approaches.

An estimate of PL is fundamental to calculating SL. Rearranging Equation 11, PL can be written:

$$N_{\mathrm{PL}} = L_S - L_p\,, \tag{12}$$

and the propagation factor is

$$F = 10^{-N_{\mathrm{PL}}/(10\ \mathrm{dB})}\ \mathrm{m}^{-2}\,. \tag{13}$$

The term ‘spherical spreading’ is used to indicate a propagation factor inversely proportional to slant range (r) squared:

$$F \propto r^{-2}\,. \tag{14}$$

The term ‘cylindrical spreading’ is used to indicate a propagation factor inversely proportional to *horizontal* range (x):

$$F \propto x^{-1}\,. \tag{15}$$

For spherical spreading, PL is given by $10\log_{10}(r^2)$ dB.

2.3. URN Metrics

Several URN metrics have been evaluated for the current study, which are discussed in this section. The first URN metric of interest for many applications is the radiated noise level (RNL), which is defined in ISO standard 17208-1 (2016):

$$L_{\mathrm{RN}} = L_p + 10\log_{10} r^2 \ \mathrm{dB}\,, \tag{16}$$

which is equivalent to Equation 10. The RNL described in Equation 16 will be included in the analysis for this project as a reference point for comparisons between methods, however, source level (SL) is of greater interest here because the objective of the project is to assist ISO TC 43/SC 3/WG 1 in developing a standard for measurement of vessel SL in shallow water.

Note that *underwater radiated noise (URN)* is used as a generic term for SL and RNL, as well as for their adjusted quantities (aSL and aRNL). These quantities all have the same reference value, which may be written either as 1 µPa·m or 1 µPa^2·m^2. There is no material difference in meaning between these two reference values. A reference value of 1 µPa^2·m^2 is used throughout this report.[4]

2.3.1. SL.ISO – Method for Deep Water Source Levels from ISO 17208-2

ISO standard 17208-2 provides a method for correcting the RNL to obtain the SL that is known to be valid in deep water:

$$L_{S(ISO)} = L_{RN} + \Delta L_{ISO} \tag{17}$$

$$\Delta L_{ISO} = -10\log_{10}\frac{14(kd)^2 + 2(kd)^4}{14 + 2(kd)^2 + (kd)^4}\ \mathrm{dB} \tag{18}$$

where the wavenumber $k = \frac{2\pi f}{c}$, f is the frequency of interest, c the speed of sound in water, and d is the source depth. This approach is based on the interference between the surface reflected sound and the direct path sound, and it is computed from the power average of the PL measured on a VLA at grazing angles of 15°, 30°, and 45°. Despite being developed for hydrophone array averaged measurements, this correction factor is commutative and can be applied to single-node measurements. In this study, SL.ISO is used as a reference source level to test how measurements with shallower depths and other URN metrics compare to the accepted standard in deep water.

In the present report, the SL.ISO metric was calculated according to Equation 18, regardless of actual measurement grazing angle at the vessel CPA. Note that Annex B of ISO 17208-2 provides a set of alternative correction formulae for measurements that deviate from the nominal grazing angles specified by ISO 17208-1. While the alternative formulae were not used in the present analysis, the SL.ECA metric (see Section 2.3.3) provides a single-channel correction factor that is nonetheless similar to the Annex B formulae and is based upon the same set of

[4] Source level is sometimes stated with reference to '1 µPa @ 1 m'. While there is no difference in the intended meaning between '1 µPa·m' and '1 µPa @ 1 m', here we prefer the international standard reference value, 1 µPa·m because source level is a far-field characteristic of the source (i.e., not at 1 m).

assumptions regarding deep-water PL. Thus, readers interested in the performance of the 17208-2 Annex B formulae are instead referred to results for the SL.ECA metric for comparison.

2.3.2. SL.HWB – Hybrid Wavenumber Integration & Beam Tracing Method

Full-wave numerical propagation methods are widely viewed as the reference standard for computing propagation loss in realistic ocean environments (Jensen et al. 2011). For this project, JASCO initially employed a hybrid parabolic Equation and geometric spreading solution during the early trials (see Section 3.2.2). As a result of lessons learned from the early trial, for the final analysis a hybrid propagation model was employed that used a fully-elastic wave-number integration solution up to 4 kHz, and a finite-element beam tracing method above 4 kHz (see Section 4.1.10). This is referred to as the Hybrid Wavenumber Integration & Beam Tracing method (HWB):

$$L_{S(HWB)} = L_p + N_{\mathrm{PL}(HWB)}\,.$$

For this study, $N_{\mathrm{PL}(HWB)}$ has been calculated at a single source depth, under the simplifying assumption that the vessel itself is a point-like source of sound. It should be noted, however, that the point-source assumption is not the only available choice when using this method. Indeed, several past studies have calculated vessel URN with full-wave methods under the assumption that the source of radiation is not point-like but is instead distributed with depth. One common assumption is to apply an incoherent depth-averaging technique whereby $N_{\mathrm{PL}(HWB)}$ is calculated assuming a normal distribution of source depths (e.g., Wales and Heitmeyer 2002, MacGillivray et al. 2019, Jiang et al. 2020). While the assumption of a vertically distributed source may result in a more robust source level estimate, as originally demonstrated by Wales and Heitmeyer (2002), depth averaging has not been used for calculating $N_{\mathrm{PL}(HWB)}$ in the current study because there exists no widely agreed-upon approach for applying this technique. Attenuation of acoustic energy by molecular absorption in seawater was accounted for with frequency-dependent absorption coefficients calculated using the formulae of François and Garrison (1982b, 1982a).

2.3.3. SL.ECA – ECHO Certification Alignment Method

In shallow water, it is unlikely that measurements will be made at an incidence angle of 30^0. In Ainslie et al. (2022) the formula that lead to Equation 18 are provided, which are reproduced here. This approach is valid for any angle and was employed here as an alternative approach, however, it does not include energy reflecting from the seabed.

$$L_{S(ECA)} = L_{RN} - \Delta L_{ECA} + \Delta L_{\alpha} \tag{19}$$

$$\Delta L_{ECA} = 10\log_{10}\gamma \text{ dB}. \tag{20}$$

where γ is the dipole to monopole conversion factor, shown in Equation 21 as a function of grazing angle θ:

$$\gamma(\theta) = 2 - \frac{\sin(2\pi T f_2) - \sin(2\pi T f_1)}{\pi T (f_2 - f_1)}; T = \frac{2d\sin\theta}{c}. \tag{21}$$

Here f_1 and f_2 are the lower and upper frequencies of the decidecade being analyzed, d is the depth of the source and c is the speed of sound in water. This approach includes an absorption factor ΔL_α which accounts for sound energy lost to seawater across the slant range (Ainslie and McColm 1998).

2.3.4. SL.SCA – Seabed Critical Angle Method

In shallow water, the bottom reflected sound also contributes to the received sound pressure, which must be accounted for in the propagation loss. This leads to a more general version of the approximation employed in ISO 17208-2 that includes a term for the bottom reflection via the bottom's critical angle, as well as an explicit term for the direct path arrival:

$$L_{S(SCA)} = L_{RN} - \Delta L_{SCA} + \Delta L_\alpha \tag{22}$$

$$\Delta L_{SCA} = 10 \log_{10} \sigma_1 + \frac{\psi}{rH} \sigma_\psi \text{ dB} \tag{23}$$

where r is the slant range from the source to receiver and H is the water depth The correction terms for the direct path – surface interference (σ_1) and the direct path – seabed reflection interference (σ_ψ) are given in Equations 24 and 25. The grazing angle θ and critical angle ψ are defined in Table 1.

$$\sigma_1 \approx \left(\frac{1}{2} + \frac{1}{4\eta \sin^2 \theta} \right)^{-1} ; \eta = k^2 d^2 \tag{24}$$

$$\sigma_\psi \approx \left(\frac{1}{2} + \frac{3}{4\eta \sin^2 \psi} \right)^{-1} \tag{25}$$

The wavenumber k and source depth d are identical to the term used in Section 2.3.1. This approach includes the same absorption factor (ΔL_α) used in Section 2.3.3. Derivation of the various terms included in the SCA method are discussed in detail in Appendix B.

2.3.5. SL.M-A – Meyer-Audoly Method

Meyer and Audoly (2020) proposed an empirical formula to correct RNL, measured on a vertical array of hydrophones, for the influence of multiple reflections on the sea surface and seafloor in shallow water to obtain source level. Their empirical formula was developed using numerical simulations performed for a variety of measurement conditions, sound speed profiles, and seafloor compositions. The correction factor is shown in Equation 27), where $Q = 0.75$, $i^2 = -1$, d is the depth of the source and c_w is the speed of sound in water. The correction factor is formulated as a second-order high-pass filter, where the correction factor is constant above the cut-off frequency f_0 and follows a constant increase of 20 dB per decade band below f_0:

$$L_{S(M-A)} = L_{RN} - \Delta L_{M-A} + \Delta L_{\alpha} \tag{26}$$

$$\Delta L_{M-A} = 10 \log_{10} \left| \frac{\varepsilon K}{\frac{f_0^2}{f^2} + \frac{i}{Q}\frac{f_0}{f} - 1} \right| \text{ dB};\ f_0 = \frac{c_w}{2\pi d} \tag{27}$$

where K represents the influence of sound energy in high frequency due to sea surface reflections and ε represents the influence of additional reflections on the seafloor. In the case of a hard seafloor such as basalt, this factor represents a doubling of sound energy.

$$\varepsilon = \begin{cases} 1, \text{ if the seafloor is considered soft} \\ 2, \text{ if the seafloor is considered hard} \end{cases} \tag{28}$$

$$K = 2 \max\left(\sqrt{\frac{x}{H}}, 1\right) \tag{29}$$

This approach includes the same absorption factor (ΔL_{α}) used in Section 2.3.3. This method was specifically developed for three channel hydrophone arrays, so SL.M-A has only been applied to array-averaged RNL measurements to be consistent with the intended methodology.

2.3.6. Adjusted Source Levels

The previously discussed URN metrics model the vessel sound field as a monopole point source at a source depth d. Adjusted source level (aSL) instead models the vessel sound field as a dipole consisting of the point source and its image reflected over the sea surface. While unsuitable for modelling sound propagation due to an insensitivity to source depth, this method is useful for direct comparisons of URN between vessels. This is closely related to RNL and in some cases, functionally equivalent to RNL in deep water. Equations 30 and 31 show the adjustment to be applied to each source level metric (Ainslie et al, 2020a):

$$L_S^{'} = L_S + \Delta L_S \tag{30}$$

$$\Delta L_S = 10 \log_{10} \frac{14(kd)^2 + 2(kd)^4}{14 + 2(kd)^2 + (kd)^4} \text{ dB} \tag{31}$$

where the wavenumber k and source depth d are identical to the term used in Section 2.3.1, and the adjustment is evaluated at a grazing angle of 30°. Interestingly, this adjustment is the inverse of the SL.ISO correction, meaning that aSL.ISO is exactly equal to RNL.

2.4. The ISO 17208-3 Process

This section provides an overview of the process being followed to develop the ISO 17208 standard.

2.4.1. ISO 17208 and ISO TC 43/SC 3/WG 1

ISO standards in underwater acoustics are developed by Sub-Committee 3 (SC 3) of ISO Technical Committee 43 (TC 43). In the following, this sub-committee is referred to as ISO TC 43/SC 3, abbreviated as 'SC3'. Within SC3, the working group responsible for the development of ISO 17208 is ISO TC 43/SC 3/WG 1, abbreviated 'WG1'. For the duration of this project, the convenor of WG1 was Christian Audoly.

ISO 17208 is planned as a three-part standard:

- Underwater acoustics — Quantities and procedures for description and measurement of underwater sound from ships — Part 1: Requirements for precision measurements in deep water used for comparison purposes (ISO 17208-1:2016)
- Underwater acoustics — Quantities and procedures for description and measurement of underwater sound from ships — Part 2: Determination of source levels from deep water measurements (ISO 17208-2:2019)
- Underwater acoustics — Quantities and procedures for description and measurement of underwater sound from ships — Part 3: Determination of source levels from shallow-water measurements (ISO 17208-3, under development)

2.4.2. ISO 17208-1:2016

The development of Part 1 (ISO 17208-1) started in SC1/WG55, based on ANSI S12.64 (2009). It became the first standard produced by SC3. Work started ca. 2010 in SC 1/WG55 to develop ISO 17208. First step was the PAS (ISO 17208-1 2016).

Parts 1 and 2 are already published. Part 1 describes a procedure for measuring radiated noise level (RNL) in deep water, Equation 16. This quantity is used by most Classification Societies to rank vessels according to whether they meet specified requirements for their silent classes.

2.4.3. ISO 17208-2:2019

Part 2 (ISO 17208-2) describes a procedure for determining source level (SL) in deep water (see Equation 11). This quantity permits computation of sound pressure level at a distant location using the sonar equation from propagation loss (PL): SPL = SL – PL. The difference between RNL and SL is illustrated by Figure 3. Above ~800 Hz, the two quantities differ by 3 dB, which is related to the surface reflection that is accounted for in the source level but not in the radiated noise level.

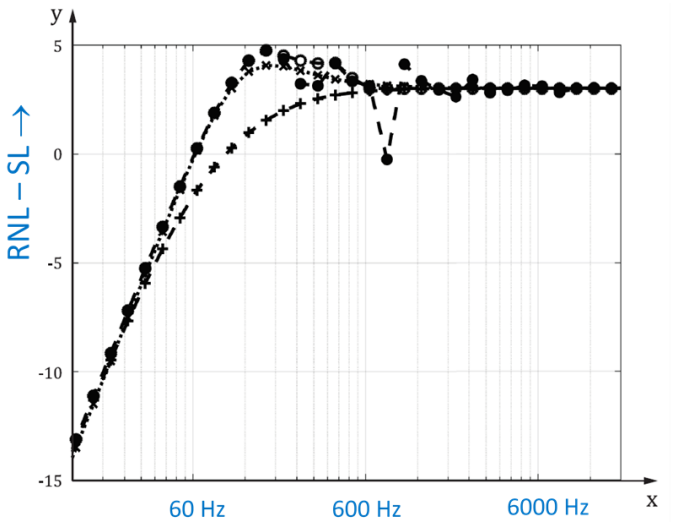

Figure 3. Graph of radiated noise level minus source level (RNL – SL) versus frequency. In the range of frequencies considered (12 Hz to 18 kHz), the difference varies between −14 dB and +5 dB for a source at a depth of 4 m.

2.4.4. ISO 17208 Part 3

At the time of writing, work on the development of Part 3 is ongoing, under the project leadership of Christ de Jong (TNO). The material described in the White Paper was presented to an online meeting of SC3/WG 1 held on 11 Aug 2020. The first step towards the development of Part 3 was the submission of a New Work Item Proposal (NWIP). The NWIP was approved by the ISO working group in September 2021 and included a draft measurement procedure for shallow-water SL. Subsequent steps in the standardization process are as follows:

- Committee Draft (CD, optional),
- Draft International Standard (DIS, required), and
- Final Draft International Standard (FDIS, optional).

At each WG1 meeting (typically held annually) proposals are made and discussed for different aspects of the standard. Such proposals are made by individual WG1 members. Consensus is obtained at each step usually by incrementally improving on the initial draft, included in the NWIP. The complete process typically takes 2–4 years.

3. PREVIOUS RESULTS AND DELIVERABLES

3.1. Results and Recommendations from the White Paper

The objective of the acoustic propagation modelling during preparation of the White Paper (Ainslie et al. 2020b) was to investigate the following:

- Which of the metrics considered (SL, RNL, aSL, and aRNL) best characterizes vessel URN in shallow water?
- What shallow-water geometry is best suited to characterizing vessel URN? (i.e., which geometry most closely reproduces deep-water value measured using ISO 17208-1 or −2)?

The overall approach to the modelling had two steps. First, predict the sound field generated by a source ship using centidecade (cdec) bands, sum the cdec bands to synthesize decidecade (ddec) band quantities; the ddec band levels become the 'truth' received levels. Second, the original source properties were estimated from the synthesized ddec band quantities by considering propagation only at the ddec centre frequencies. The difference between the two values is an anomaly that was minimized by optimizing the configuration of data collection hydrophones and choice of URN metric, and by selecting seabeds with desirable propagation properties.

The specific steps followed were as follows:

1. Verify propagation models used for estimating properties of individual cdec bands and of ddec band centre frequencies
2. Estimate source properties as a function of frequency from 10 Hz to 100 kHz. The main metrics considered are SL and RNL. Also considered are aSL and aRNL (Ainslie et al. 2020a).
3. Assess the suitability of these source properties at selected frequencies (30 Hz, 300 Hz, 3 kHz, and 30 kHz). Most of the sound radiated by surface vessels is at frequencies below 1 kHz, so it is tempting to focus on 30 and 300 Hz only. This temptation was avoided because of the need to consider animals' hearing sensitivity. For example, if an animal's hearing range is limited to frequencies above 10 kHz, the most relevant frequency for that animal would be 30 kHz.
4. Compare the inferred URN values (SL, RNL, aSL, and aRNL) with expected values of these metrics by plotting in the form of the difference between the inferred value and the expected value.

The following are the key results from the study:

1. The sound levels measured in shallow water depend strongly on the sediment type.
2. To stabilize estimates of URN, the use of adjusted source level (aSL) and radiated noise level (aRNL) should be considered. Adjusted levels consider sound radiating from the source and its surface reflection together as a dipole source.
3. Source level (and aSL) is difficult to accurately obtain in shallow water due to the interference patterns between the direct and reflected paths. Computing propagation loss for multiple frequencies within each decidecade helps mitigate this effect. Using the incoherent version of ray trace models also mitigates the effects for higher frequencies (>3 kHz).
4. In shallow water, placing recorders between 100 and 200 m from the planned vessel measurement location is effective for obtaining the RNL, except for the interference frequency range (around 300 Hz, depth dependent). The null can be mitigated by averaging over frequencies or averaging over hydrophones.
5. To obtain source levels in shallow water, coherent methods must be employed, which requires accurate knowledge of the source (propeller) depths, water depths and seabed composition. Detailed knowledge of the sound speed profile is not typically required, as it has only a weak influence on short range (<500 m) sound propagation in shallow water.
6. In very shallow water (30 m water depth), three or more hydrophones should be placed at the seabed, with closest point of approach (CPA) approximately equal to one ship length. This hydrophone has a prominent null at the frequency determined by $kd \sin\theta = \pi$ where d is the source depth. Therefore, it is preferable to also place a second hydrophone at the peak ($kd \sin\theta = \pi/2$), and a third hydrophone between these ($kd \sin\theta = 3\pi/4$). For a 30 m water depth and a vessel length of 170 m, these distances work out to 170, 343, and 228 m.
7. In intermediate water depth (say 70 m), three or more equally spaced hydrophones should be placed in a vertical array, spanning at least half of the water column, at a CPA of about five water depths. The purpose is to place the receivers in the cylindrical spreading region, and thus reduce sensitivity to detailed interference patterns by averaging over depth.
8. Propagation loss measurements using a controlled sound source should be conducted during the field experiment to measure the seabed properties.

The adjusted radiated noise level (aRNL) was considered during the White Paper analysis. However, since the goal of this project was to support ISO TC43/SC 3/WG 1 in developing a standard for shallow water vessel *source level* measurement, aRNL was not evaluated using the collected data (see Section 2.3 for the metrics evaluated).

3.2. Lessons Learned from Test Deployments of Vertical Arrays and Bottom-Mounted Hydrophones for Shallow-Water Vessel Source Level Measurements

3.2.1. Engineering Trials Overview

The analysis of the acoustic modelling work undertaken for the White Paper indicated that vertical line arrays were a preferred method of measuring vessel source levels in shallow water, as depth-averaged sound levels are more robust than a point measurement. An assessment of the conditions at planned trial sites in British Columbia (see Section 4.1.2) indicated that relatively strong currents were expected. Past experience suggested that one could expect noise due to flow around the hydrophones and movement (knockdown) of vertical arrays. It was also desired to demonstrate that measurements near the seabed were repeatable and reliable. Therefore, trials were conducted to evaluate the performance of different sensor geometries. In September 2020, a three-channel vertical array was evaluated, along with a 'C-lander' that positioned four-hydrophones near the seabed. The results indicated that improvements to the vertical arrays were required, which were tested in February 2021. The trials and their results are described in this section.

3.2.1.1. September 2020 Trial

Trial Overview

Two measurement stations (identified as C-lander and vertical array) were deployed outside of Halifax harbour, Nova Scotia, in the proximity of the shipping lanes entering the port of Halifax in September 2020; the C-lander consisted of a single acoustic recorder fitted with four hydrophone sensors (Figure 4), while the vertical high flow array consisted of three separate acoustic omni-directional recorders. On the vertical array, the bottom and middle instruments were fitted with a single hydrophone while the top instrument with two hydrophones (Figure 5). All hydrophones used were GeoSpectrum M36-V35-100 with a nominal sensitivity of −165±1 dB re 1µPa/V.

Underwater sound was recorded with Autonomous Multichannel Acoustic Recorders (AMARs; JASCO). Before deployment, each AMAR was calibrated at the JASCO facility with a pistonphone type 42AC precision sound source (G.R.A.S. Sound & Vibration A/S). The AMARs were also calibrated on deployment or retrieval. The pistonphone calibrator produces a constant tone at 250 Hz at a fixed distance from the hydrophone sensor in an airtight space with known volume. The recorded level of the reference tone on the AMAR yields the system gain for the AMAR and hydrophone. To determine absolute sound pressure levels, this gain is applied during data analysis. Typical calibration variance using this method is less than 0.7 dB absolute pressure.

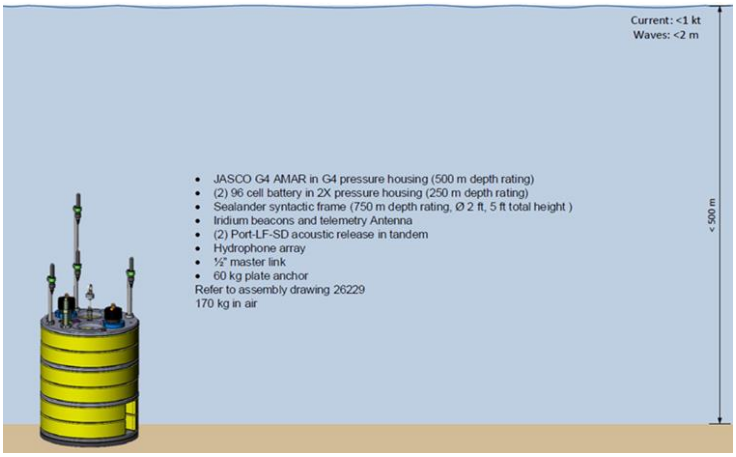

Figure 4.The C-lander mooring design (design 230).

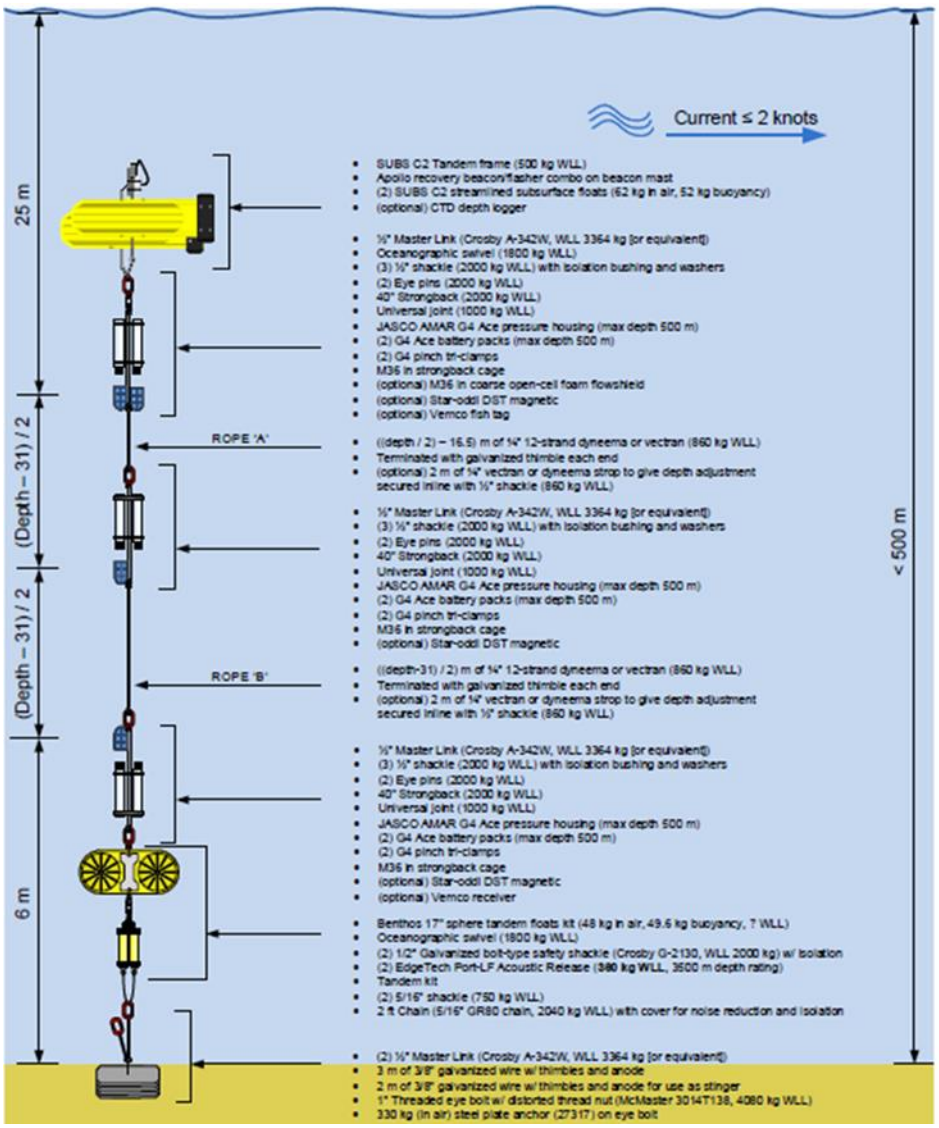

Figure 5.The vertical array mooring design (design 240).

Table 3. List of acoustic recorders, including setup and deployment coordinates and dates.

Measurement station	AMAR serial number	Sampling frequency (kHz)	Number of hydrophones	Lat. (dd.dddd)	Long (dd.dddd)	Bathymetry (m)	Instrument depth (m)	Deployment	
								Start	End
Array	611	512	2	44.48037	-63.512	71.6	21.6	2020 Sep 9 16:12	2020 Sep 29 12:46
	613		1				44.6		
	625		1				66.6		
C-lander	615	128	4	44.4803	-63.5131	70	69	2020 Sep 8 15:02	2020 Sep 29 13:03

The recording schedule (Table 3) was the same for all AMARs; however; AMAR 615 recorded at lower sampling frequency, i.e., 128000 samples per second as opposed to 512000 samples per second (Table 3).

The recorders were deployed at the locations shown in Figure 6 (and Table 3). Figure 6 also has black dots for all AIS vessel positions received during the September field trial.

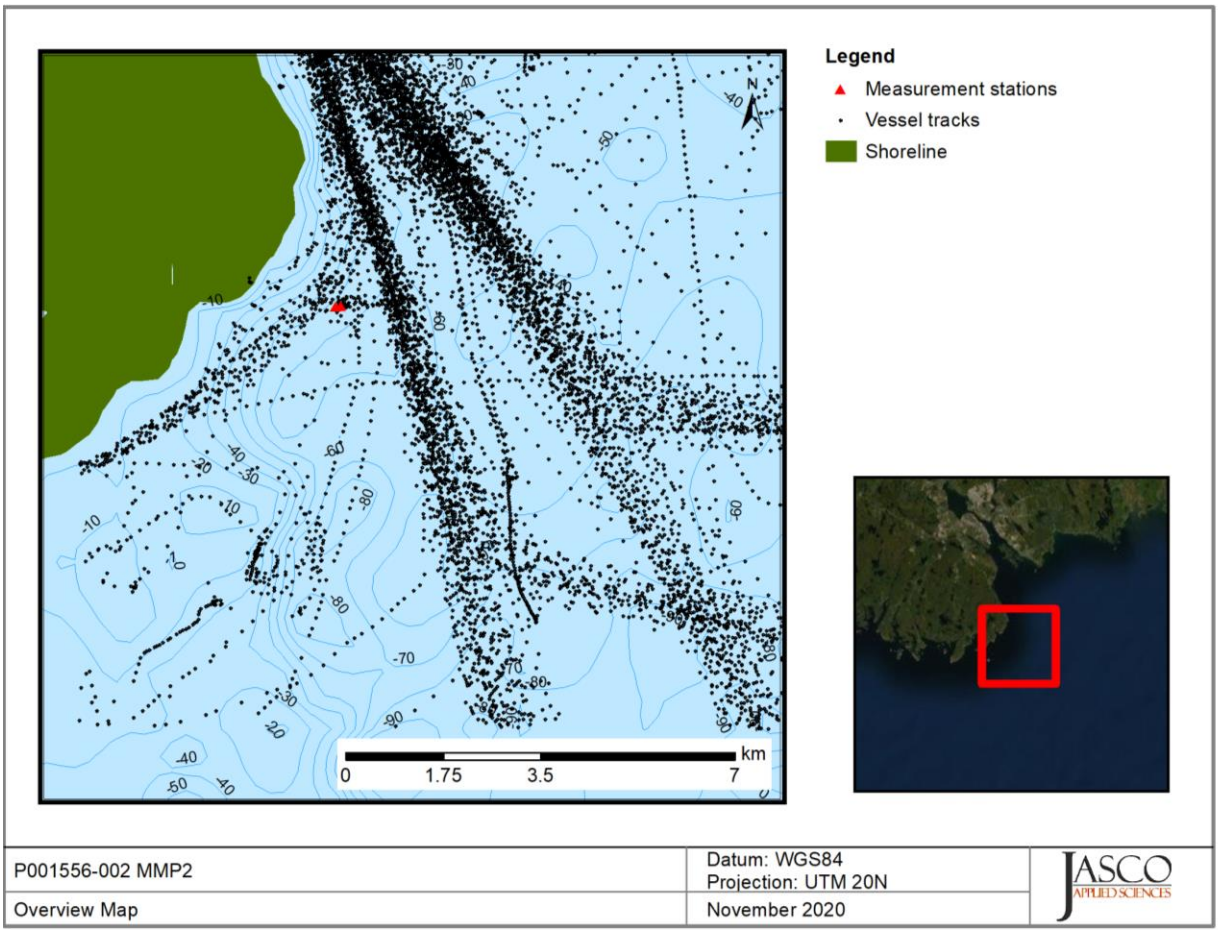

Figure 6. Location of the moorings for the Sept 2020 measurements (red triangles) and vessel tracks recorded from Automatic Identification System (AIS; black dots).

Data from vessel tracks (Figure 6) that passed within 1 km of the vertical array were used in the analyses of the September 2020 data. In the period of the deployment, tracks for 166 different vessels were present in the automatic identification system (AIS) data. The majority of vessels recorded along the shipping routes were either container or fishing vessels (Figure 7). The source level analysis focused on large cargo and commercial vessels, due to their higher URN emissions. Fishing vessels, recreational vessels, and other small vessels were excluded from the SL analysis as their lower URN emissions yielded poorer-quality measurements (i.e., due to their lower signal-to-noise ratio [SNR]). Source levels were analyzed for a total of 70 vessels. Most vessels were only measured while leaving Halifax because the inbound shipping lane was farther than 1 km from the measurement site. Most measurements were at distances longer than 600 m.

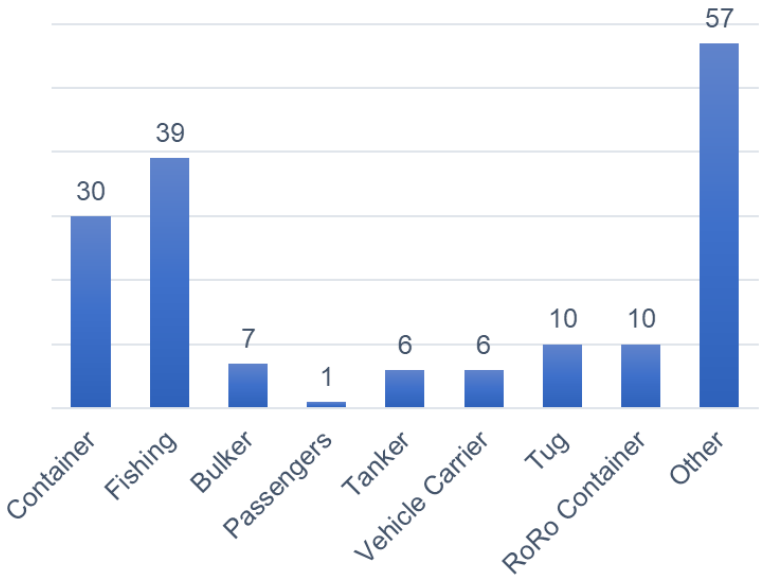

Figure 7. Bar plot showing the distribution of vessels that passed within 1 km of the measurement stations during the monitoring period. Key vessel classes are specified while smaller recreational vessels, sailing boats, and less common vessels are classed as ‘other’.

Summary of Results

The results from the initial analysis of the September 2020 trial data are summarized in Figure 8. This figure shows the source levels computed by adding a modelled propagation loss (N_{PL}) to the received sound pressure levels averaged over the time taken for each vessel to transit ±30 degrees relative to the closest point of approach, in accordance with ISO 17208-1.

The following were the important features of the results:

1. For all decidecades, the results on the four C-lander hydrophones were the same, within ~1 dB. It was concluded that the measurements near the seabed are repeatable and only a single hydrophone at each seabed site would be needed for the British Columbia measurements.
2. For all sensors locations, the lowest decidecades (10.0 and 12.6 Hz) were affected by flow noise and would not have been reported as valid data. On the vertical array, this problem was worse for the higher hydrophones (611, 613 – see Table 3), and extends up to at least 40 Hz. Since it is desirable to measure the source level down to at least 20 Hz, these results indicated that a second trial to control noise levels on the vertical arrays was needed.
3. There was a 5 dB increase in SL at 5 kHz, indicating that the two-step propagation loss method was not accurately representing the conditions at the Halifax harbour location. This is discussed further in Section 3.2.2.
4. The SL estimates on the vertical array hydrophones showed substantial variability in most of the decidecades from 40 to 4000 Hz, which further suggests that the propagation loss estimates were not representing the conditions at the test site.

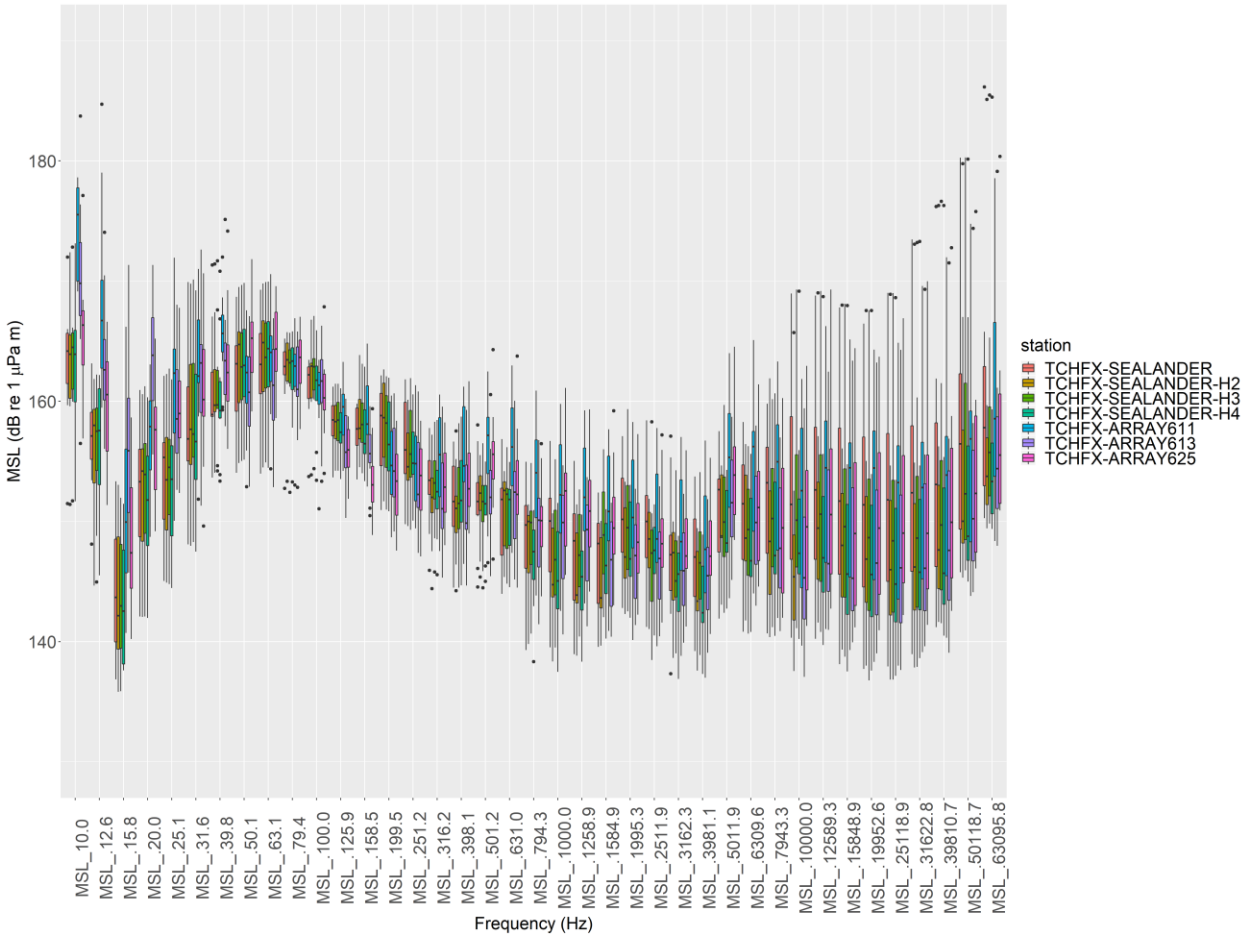

Figure 8. Summary of the source levels (SLs) computed from the closest points of approach (CPAs) that were within 1 km of the vertical array. The results are plotted by decidecade, with a box and whisker plot per-sensor for each decidecade. Each box shows the 25th and 75th percentile of the measurements as a the bottom and top of the box, with the median value as the line within the box. The total range of values is shown as the lines above and below the boxes, with outliers added as dots. For each decidecade, the four hydrophones on the C-lander are drawn first, then the three hydrophones of the vertical array. The vertical array hydrophones (611, 613, 625) are plotted in order of depth from shallowest to deepest.

A detailed analysis of the vertical array hydrophone data indicated that there was evidence of strum noise whose frequency was modulated by the tidal velocity on all of the array hydrophones (Figure 9). A re-analysis of the mooring design identified that these frequencies could be expected based on the tension, length, and diameter of the mooring cables.

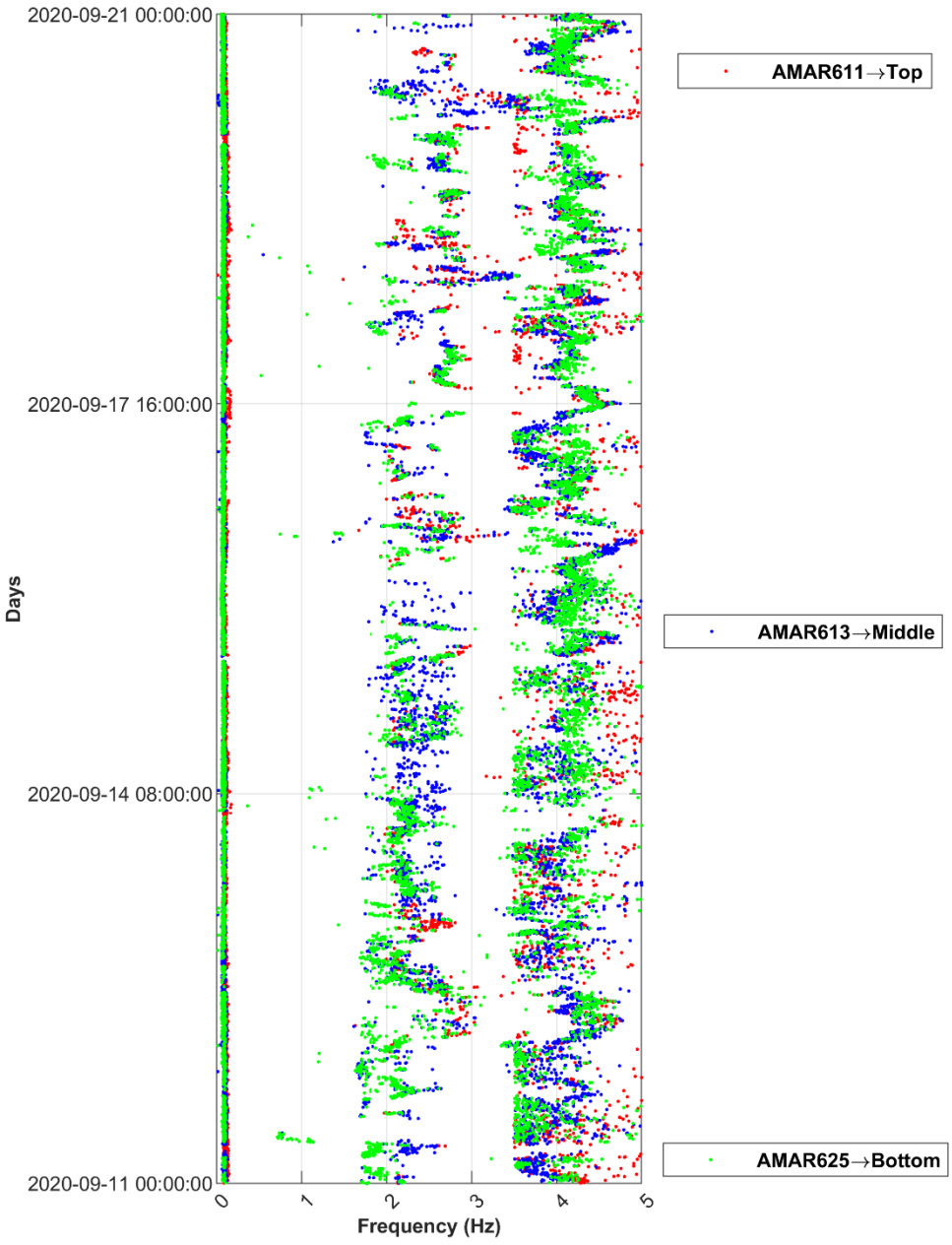

Figure 9. Time (vertical) versus peak frequency induced by strum for the bottom (green), mid (blue) and top (red) hydrophones. The frequencies increase during periods of higher currents.

3.2.1.2. February 2021 Trial

Trial Overview

The presence of flow and strum noise identified in the September 2020 trial data was unsatisfactory and lead to a redesign of the mooring to include vortex shedding elements (Figure 10) as well as experimenting with additional flow shielding over the hydrophones. Vortex shedding elements reduce the vortices that occur when the current flows over the cables and instruments, which reduces strum as well as knockdown. The size of the flaps to add to a cylinder to reduce vortices depends on the diameter of the cylinder. The effects of stagnation and flow around a hydrophone can also be mitigated by using flow shields. During the February 2021 trial, the field team experimented with open cell foam covers.

Two moorings were deployed 26 Feb to 14 Mar 2021 very close to the site of the September 2020 trial (Figure 11, Table 4). One of these moorings was identical to Figure 5, while the other had the vortex shedding and flow shield treatments (Figure 10). To compare the effects of the flow shields, one hydrophone on the top AMAR had the flow shield while the other did not.

Figure 10. The top-most AMAR from mooring 240A showing vortex shedding elements added for the February 2021 trial. Four pieces of 5 cm duct tape were required for the AMAR tubes, and a 5 cm hairy fairing wrap for the vectran cables. The black open-cell foam flow shield can be seen on the right hand hydrophone. The untreated left hand hydrophone is visible inside the steel protective cage.

Table 4. Locations of the February 2021 vertical array trial moorings.

Mooring/Equipment	Location	Latitude/deg.min (N)	Longitude/deg.min (W)	Depth (m)
TC240A Array (treated)	Outbound SL	44.4804 N	63.512 W	71
TC240 Array (original)		44.477 N	63.511 W	71

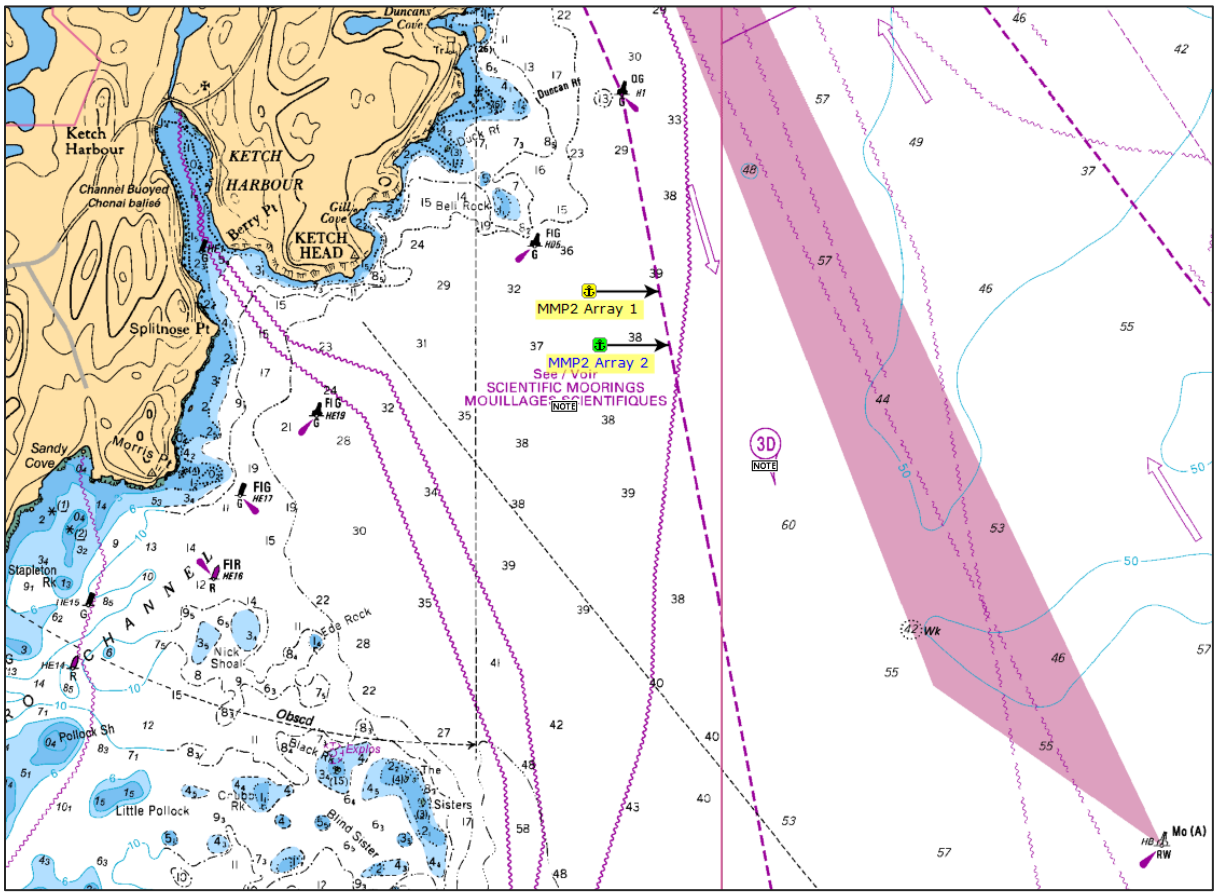

Figure 11. Location of the moorings for the February 2021 flow noise reduction measurements, 500 m from limits of outbound shipping lane. (Nautical charts © Canadian Hydrographic Service).

February 2021 Trial Results

The results of the February 2021 vertical array trials are summarized in Figure 12. The top row shows that the treatments reduced flow and strum noise by ~30 dB at 10 Hz, with benefits continuing up to ~200 Hz. The bottom row suggests that the foam on the treated array also helped reduce the flow and strum noise levels, however, the results are not as definitive. A minute-by-minute difference between the two hydrophones shows there was a NL reduction in most frequencies below 125 Hz; however, there was an increase in flow and strum noise around 30 Hz on the top hydrophone. This was not replicated at the middle hydrophone.

The results confirmed that the treatments would be used for the measurements in British Columbia.

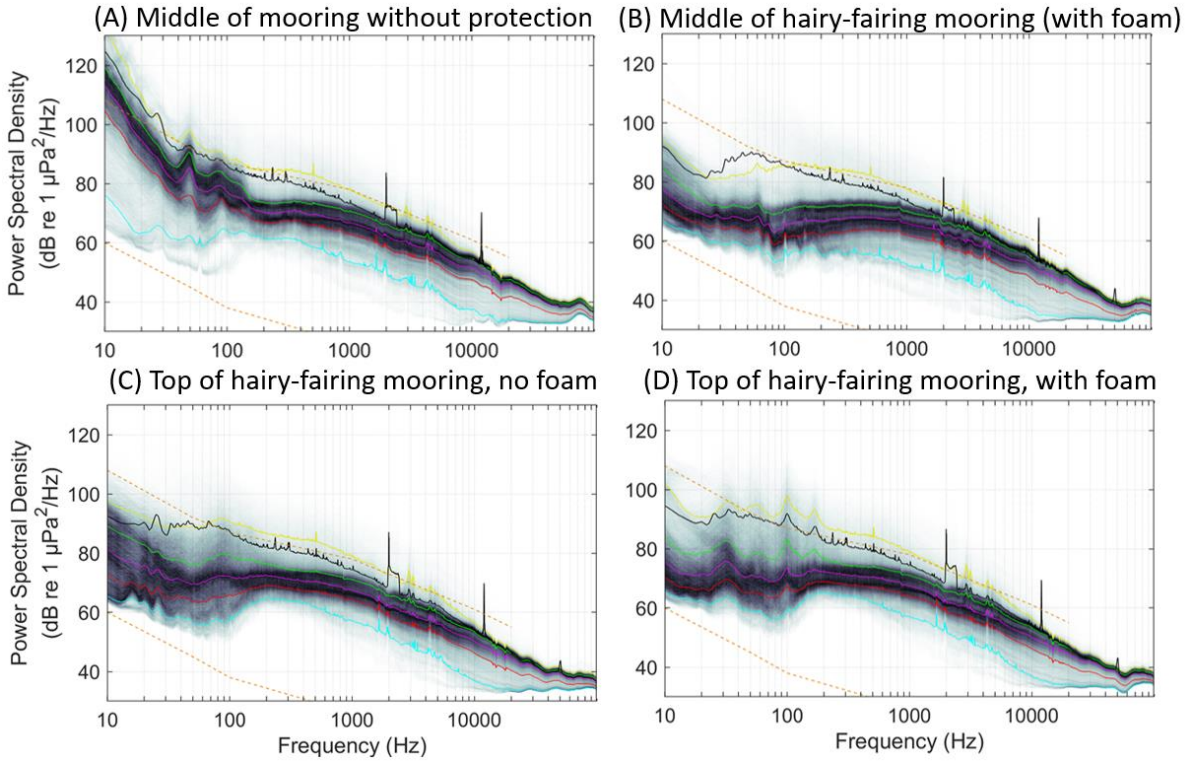

Figure 12. Comparison of the power spectral density measurements during the February 2021 trial. Each figure is a plot of the power spectral density recorded over the whole duration of the trial, with the 5th, 25th, 50th, 75th, and 95th percentile values at each frequency shown as the cyan, red, magenta, green and yellow lines, respectively. The mean value is shown by the black line. The limits of prevailing noise from (Wenz 1962) are shown as the orange dotted lines for reference. (A) shows the reference spectrum taken from the untreated mooring's middle hydrophone, which can be directly compared to (B), the middle hydrophone on the treated array. The effects of including the foam on the upper hydrophones of the treated array are compared in (C) and (D). The vortex shedding elements improved performance below 200 Hz. The foam improved noise performance at 100 Hz and below.

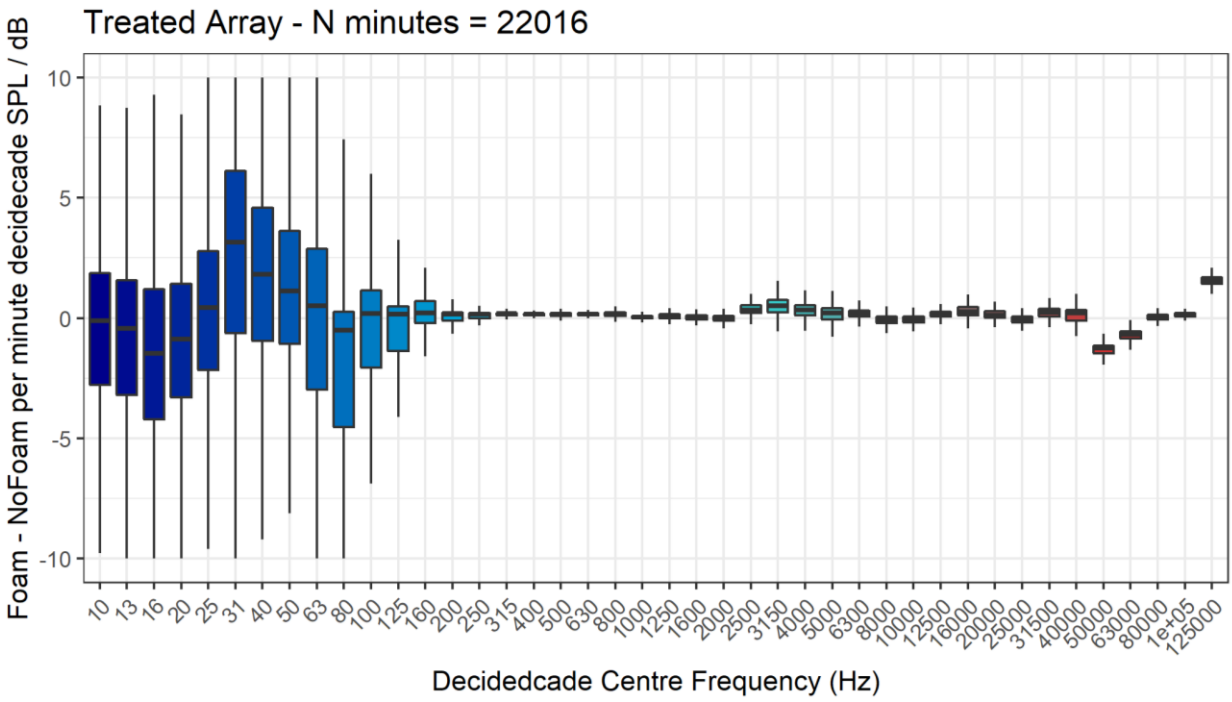

Figure 13. Minute-by-minute subtraction of the sound level without foam from the decidecade sound level with foam. Negative values indicate the foam improved performance.

3.2.2. Approaches to Propagation Loss Modelling and Source Level Analysis

The results of the initial SL analysis, carried out using ShipSound®, showed that a fluid seabed approximation was unsuitable for calculating PL in Halifax Harbour. At this location, there is a thin coarse sand sediment overlying a hard bedrock that supports elastic shear wave propagation. Numerical experiments were conducted to verify which approaches to modelling the sound propagation would provide convergent solutions at both low and high frequency. It was determined that a parabolic equation (PE) model was not appropriate for this location because of the thin sediment and high shear speeds in the bedrock layer. Thus, ShipSound was configured to use a fully elastic wave-number integration solution (Jensen et al. 2011) for calculating monopole source levels below 4 kHz and a beam tracing solution (BELLHOP, Porter and Liu 1994), with an elastic seabed reflection coefficient, above 4 kHz. The beam tracing solution was required at high frequency because the wave-number integration solution becomes computationally prohibitive above 4 kHz for the large number of receiver locations and source locations that ShipSound uses to calculate PL. ShipSound was also configured to use the hybrid wavenumber integration and beam tracing approach for analysis of the BC data set since the conditions in the trial area were similar to those in Halifax.

4. FIELD MEASUREMENTS MAY–JULY 2021

The field measurements were designed to verify the acoustic propagation modelling performed for the White Paper, provide the data needed to develop a data collection Best Practice Guide (BPG) in the future, and help determine the best method of computing the URN in shallow water so that it is comparable to the deep-water URN. To meet the project objectives, the experimental plan called for measuring the same vessel's URN many times, in different water depths (30, 70, and 180 m) and with different hydrophone–ship geometries. A local vessel operator in British Columbia's Southern Gulf Islands was identified as a project collaborator and assisted in planning of hydrophone deployment locations. This operator's vessels were chosen because of their large size, regular routes, and frequent trips, which made it possible to gather a large data set for statistical analysis.

During the review of the White Paper with ISO TC 43/SC 3/WG 1 in August 2020, it was determined that the preferred configurations for acoustic recorders were as follows:

1. At the deep-water site (180 m), the preferred configuration was a vertical line array of three hydrophones so that the measurements are fully compliant with ISO 17208-1 (2019) and 17208-2 (2019) (for the measurement of the radiated noise level and source level of a vessel in deep water, respectively). SL.ISO (see Section 2.3) from this location was considered the 'correct' reference value to be compared to the other locations and hydrophone geometries.
2. At the mid-water depth site (70 m), the preferred configuration was two vertical line arrays of three hydrophones at 150 and 350 m from the vessel's nominal track line as well as a bottom-mounted hydrophone at 121 m from the nominal track line. The latter hydrophone effectively formed a horizontal line array when combined with the bottom hydrophones of the two vertical line arrays. The modelling predictions from the White Paper suggested that water depths of at least 70 m were required to obtain reliable estimates of the source level for frequencies as low as 10 Hz. Measurements close to the vessels, and at five times the water depth both had predicted advantages for obtaining reliable source levels, which guided the choice of mooring geometries and locations at this site.
3. At the shallow-water site (30 m), the preferred configuration was a horizontal line array of three bottom-mounted hydrophones deployed 170, 228, and 344 m from the vessel's nominal track line. This water depth was considered too shallow for a vertical array but is typical of areas such as the North and Baltic seas where future shallow-water measurements are likely to be performed.

The plan also called for measurements of vessel source levels using a drifting hydrophone array at three times during the experiment: during the initial deployment, halfway through the deployment period, and before retrieval. Drifting hydrophone measurements are presented as an option for data collection in ISO 17208-1. The purpose of collecting measurements using moored vertical arrays, bottom-mounted horizontal arrays, and drifting arrays simultaneously was to compare the variability in source level estimates from the three methods. It is also to compare the complexity of making the measurements and analyzing the data with each method.

A propagation loss (PL) data collection experiment was planned during the initial array deployments to better characterize sound propagation conditions at the three measurement sites. Acoustic inversion methods were applied to the collected PL data to determine the geoacoustic properties of the seabed at each site. These properties were then used to select the seabed parameters required in the calculation of three of the SL metrics (SL.HWB, SL.SCA, SL.ECA; see Section 2.3).

The trial plan was implemented successfully, and fieldwork occurred in three phases:

- 5–9 May 2021: Deployment, Drift Measurements and PL Measurements,
- 8–10 Jun 2021: Mid-Trial Drift Measurements, and
- 19–23 Jul 2021: Drift Measurements and Equipment Retrieval.

Further details on the vessels measured, recorder geometries, measurement equipment and fieldwork schedules are provided below. Detailed reports on the fieldwork are provided in Lawrence et al. (2021).

4.1. Methods

4.1.1. Source Vessels

It was determined during the development of this project concept that to understand the relative variability of shallow-water measurements compared to deep-water ones, the same vessel's URN would be measured many times, in different water depths and with different measurement geometries. A local operator collaborated with the project by supporting measurements of their vessels along a frequently transited route between Tsawwassen and Swartz Bay. The operator instructed their crew to transit past the hydrophone arrays and provided JASCO with voyage logs for three of their vessels (Table 5). The logs contained the following information for each voyage:

- Number of passengers aboard,
- Departure and arrival time, and
- Fore and aft draft.

The identity, position, and speed over ground of vessels A–C were obtained from the Automated Identification System (AIS). A total of 2732 vessel passes were recorded at the three test sites during the field measurement period (Table 6). Following a manual quality review to identify unsuitable measurements (see Section 4.1.4) a total of 1880 vessels passes were retained for subsequent analysis. The measurement acceptance rate of approximately 70% exceeded expectations, due to the relatively high traffic volume in the study area and the opportunistic nature of the measurement schedule. Note that each individual vessel pass resulted in multiple URN measurements because multiple hydrophone nodes were deployed at each site.

Table 5. Vessel design specifications. The identities of the vessels have been anonymized.

Vessel	Length (m)	Breadth (m)	Propeller type	Propeller diameter (m)	Blades per propeller	Nominal prop. RPM	Installed power (kW)	Drive type
A	167	27	Twin screw CPP	3.4	4	210	15,600	Diesel/LNG
B								
C	160	28	Single screw CPP	5.0	4	140	16,000	Diesel-Electric

CPP = controllable pitch propeller.
RPM = revolutions per minute

Table 6. Number of vessel trips measured at each site during May, June, and July 2021. The number accepted indicates how many trips had one or more underwater radiated noise (URN) measurements that passed a manual data quality review.[5]

Vessel	Median speed (kn)	Median draft (m)	Trips measured (Accepted)		
			Deep	Intermediate	Shallow
A	20.1	4.6	434 (239)	384 (206)	372 (261)
B	19.3	4.4	541 (398)	269 (253)	359 (266)
C	20.1	5.5	114 (73)	128 (77)	131 (107)

[5] one knot (1 kn) is equal to one nautical mile per hour (approximately 0.5144 m/s)

4.1.2. Measurement Sites

URN measurements were performed at three locations, with nominal water depths of 30, 70, and 180 m (Figure 14). The Deep site (180 m) served as the reference deep-water location for comparison to the shallow-water sites. The Intermediate site (70 m) met the 65 m minimum criteria for acceptable acoustic propagation at 10 Hz (see section 1.4 in Ainslie et al. 2020b). The shallow-water site (30 m) did not meet the criteria but had a typical water depth for measurements made in the Baltic and North Seas and hence was relevant for informing international standards. The bathymetry at the shallow site was sloping along the vessel track but relatively flat across-track. The bathymetry at the intermediate site was flat all around the site. The deep site was in a bowl that rose to 160 m depth ~1 km from the measurement site in all directions.

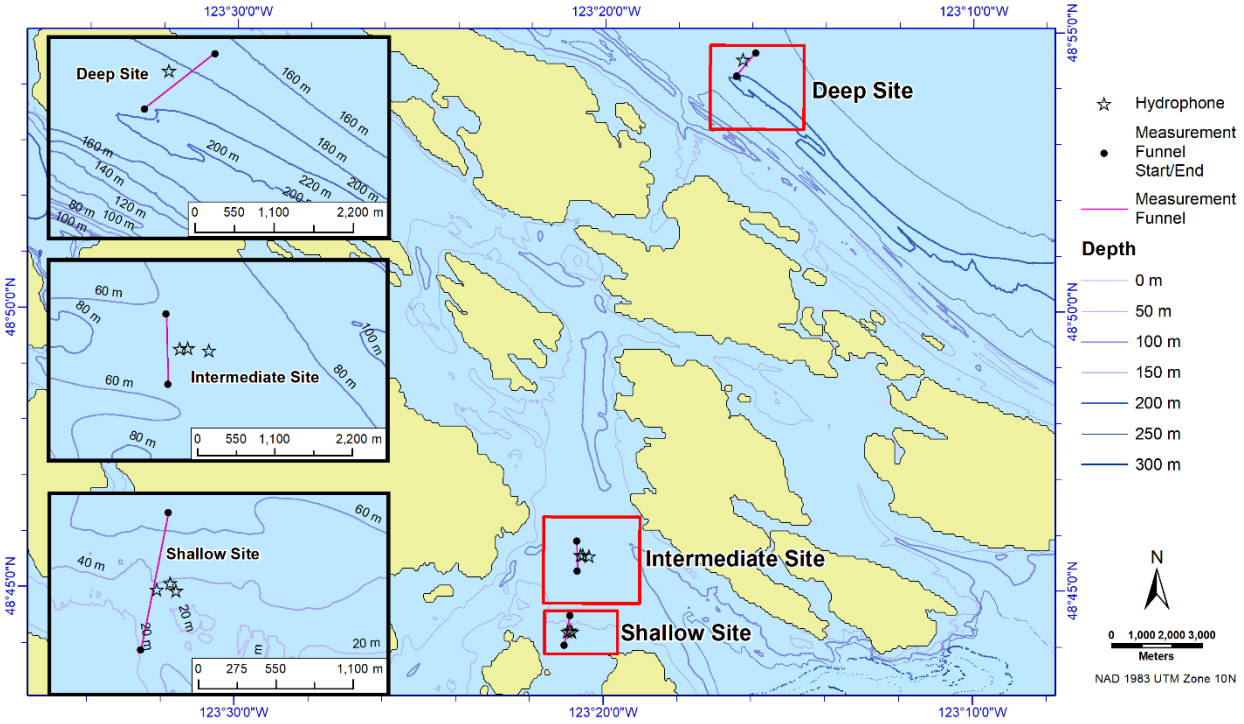

Figure 14. Hydrophone deployment locations in the BC Salish Sea for vessel underwater radiated noise (URN) recording and analysis. The shallow and intermediate sites were located in Swanson Channel, between Salt Spring and North Pender Islands. The deep site was located in Georgia Strait, near the entrance of Active Pass.

4.1.3. Measurement Equipment and Geometries

4.1.3.1. Moored Hydrophones

Moored hydrophones were deployed for this study from 5 May through 22 Jul 2021. Figure 15 shows the planned deployment geometries of the hydrophones relative to the nominal vessel tracks. The actual locations and depths of the hydrophone elements, which differed slightly from the planned arrangement, were recorded by the field team following deployment of the moored hydrophones (Table 7). The sensors near the seabed were bottom plate hydrophones (Figure 16). The vertical arrays of hydrophones used the high-flow array mooring (Figure 17). The three vertical arrays incorporated depth loggers at the top-most hydrophone, which were used for measuring array knockdown due to tidal currents.

All moored hydrophones were sampled continuously using AMAR G4 (JASCO Applied Sciences) acoustic recorders at 128 kHz sampling rate. All hydrophones were GeoSpectrum M36-V35 with a nominal sensitivity of −164 dB re 1 V/µPa. The hydrophones were calibrated prior to deployment and on retrieval using a G.R.A.S 42AC pistonphone calibrator at 250 Hz. The real-time clocks on the AMAR G4s were synchronized with Global Positioning System (GPS) time prior to deployment. The maximum clock drift for the deployment period was estimated at 52 s.

The bottom plate hydrophones were lowered to the seabed using a ‘parachute-rig’ that has an acoustic release and float attached to the lifting ring (Figure 16). The ranging feature of the acoustic release was used to localize each mooring so that the as-deployed location on the seabed was known. The acoustic releases at the bottom of the vertical arrays were used to locate those moorings. The GPS coordinates of the moorings at the seabed were localized to within ±1.5 m (RMS) accuracy.

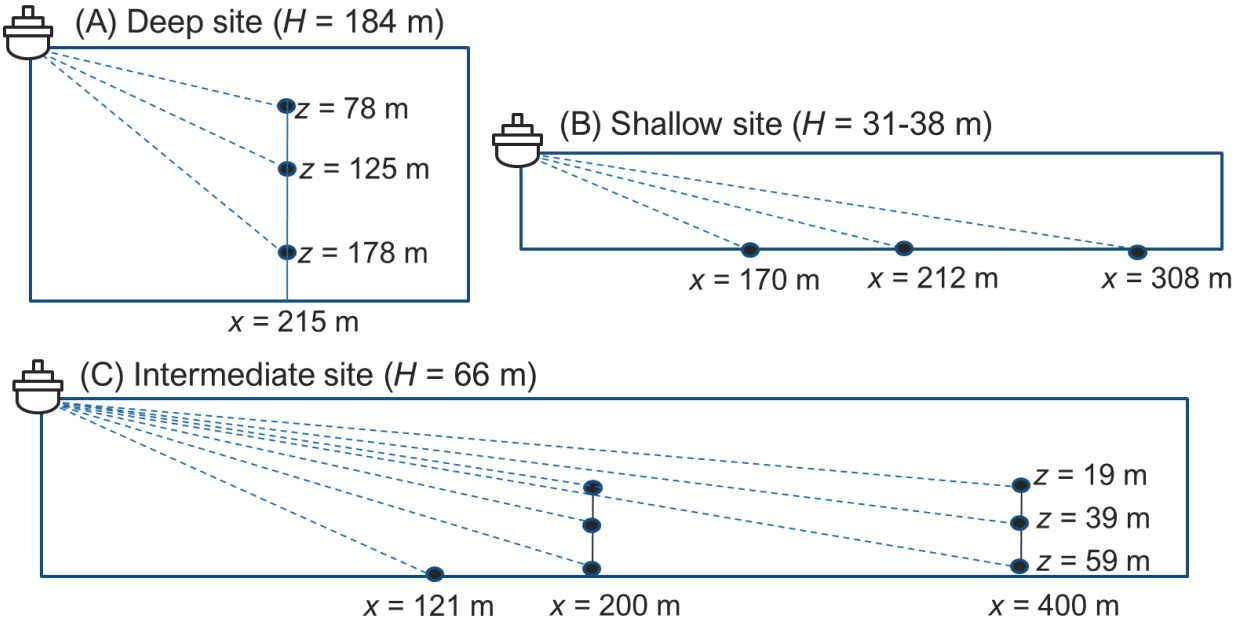

Figure 15. As-deployed measurement geometries for MMP2 data collection in 2021. Dots represent the hydrophone nodes. Horizontal distance (*x*) indicates nominal closest point of approach (CPA) distance of the mooring from the planned vessel track—note that actual CPA distances varied between vessel transits (see Section 4.2.2). Receiver depth (*z*) indicates hydrophone node depths below the sea-surface on the vertical arrays. Water depth (*H*) indicates mean low-tide water depth at chart datum. See Table 7.

Table 7. As-deployed hydrophone geometry and mooring coordinates for underwater radiated noise (URN) data collection. Water depth at each site is the Canadian Hydrographic Service (CHS) NONNA-10 (CHS 2021) surveyed water depth at the deployment location (mean low tide reference). Depth below sea-surface for each hydrophone element is the nominal value calculated from the water depth assuming the array is oriented vertically in the water column.

Site	Mooring type	Mooring ID	Longitude	Latitude	Depth below sea-surface (m)			Water depth (m)
					Element 1	Element 2	Element 3	
Deep	VLA	D.VLA.150	123° 16' 14.9697" W	48° 54' 30.8389" N	77.5	124.6	177.6	184.2
Intermediate	VLA	I.VLA.150	123° 20' 33.2397" W	48° 45' 37.5228" N	19.0	39.1	59.1	65.7
		I.VLA.350	123° 20' 23.5431" W	48° 45' 36.5146" N	19.4	39.4	59.5	66.1
	Base plate	I.BP.121	123° 20' 37.0585" W	48° 45' 37.5060" N	65.4	—	—	65.9
Shallow	Base plate	S.BP.170	123° 20' 51.0784" W	48° 44' 15.0527" N	30.8	—	—	31.3
		S.BP.228	123° 20' 53.1136" W	48° 44' 16.8535" N	37.2	—	—	37.7
		S.BP.344	123° 20' 57.8190" W	48° 44' 15.3470" N	36.8	—	—	37.3

VLA = vertical line array.

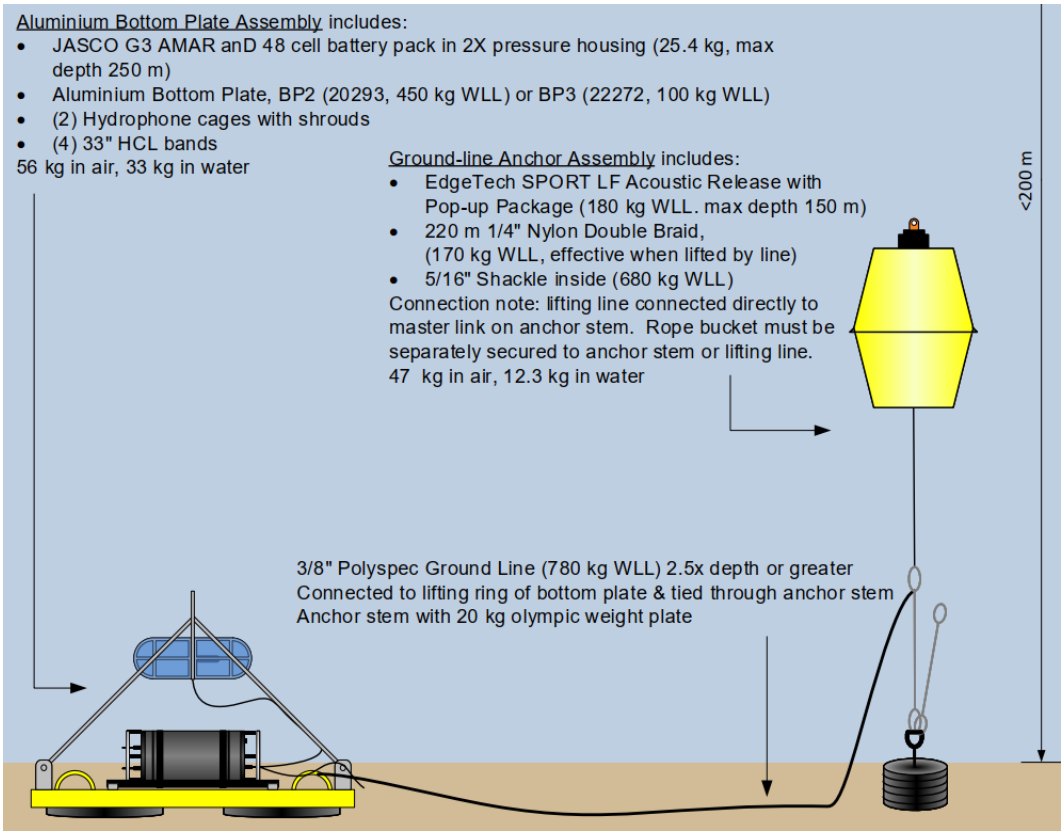

Figure 16. Mooring diagram for bottom plate mooring with a stand-alone pop-up acoustic release. This mooring does not leave any anchors behind. This mooring was employed for the bottom mounted hydrophones at the 70 and 30 m water depths.

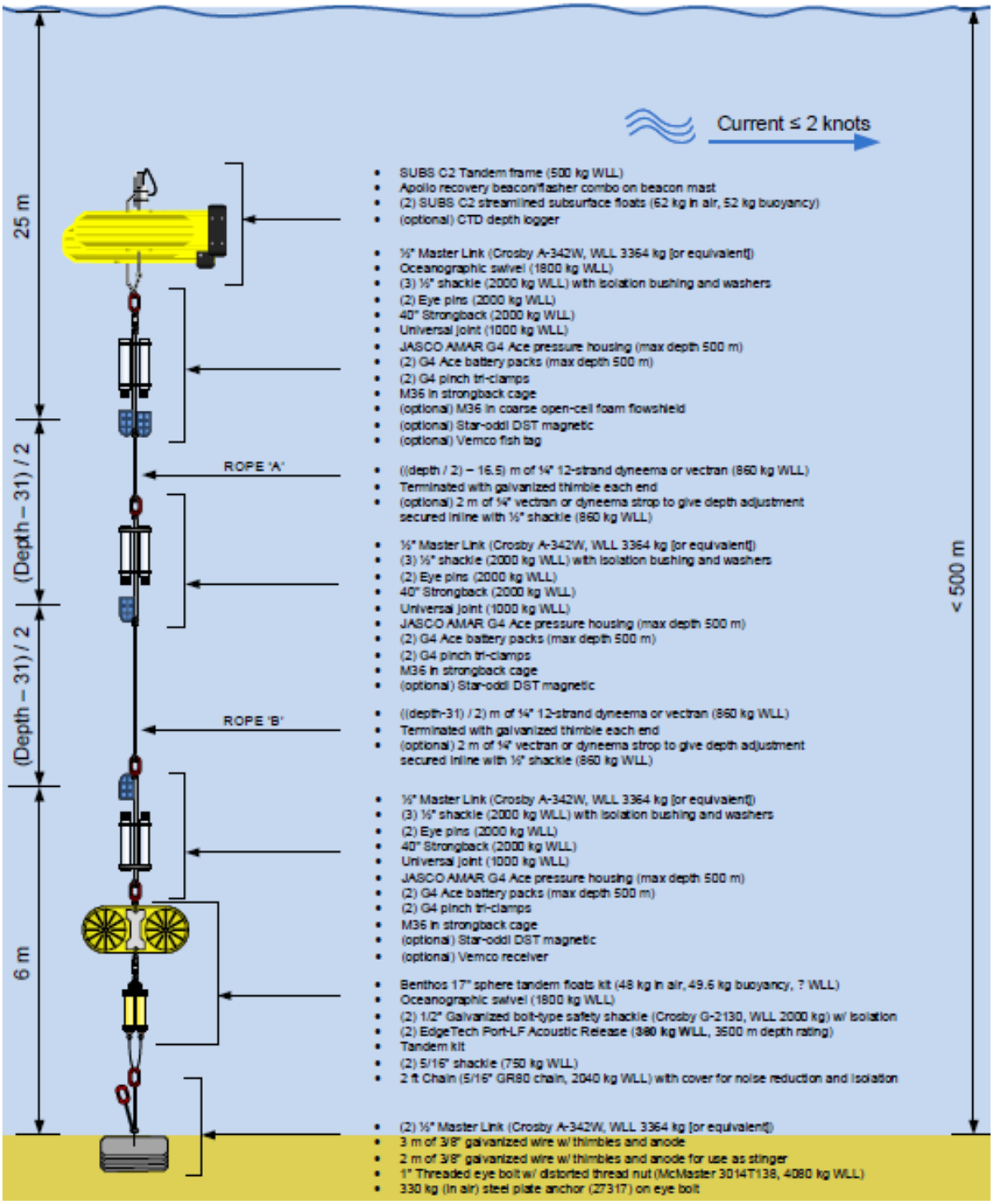

Figure 17. Mooring diagram for the bottom mounted vertical arrays that were employed for the source level measurements. Sensor spacings are shown for the 70 m site. Sensor depths for the 180 m site are 40, 87, and 150 m as shown in Figure 15.

4.1.3.2. Horizontal Line Arrays

In addition to the three vertical arrays referred to as D.VLA.150, I.VLA.150, and I.VLA.350, the hydrophone geometry includes two horizontal line arrays. At the intermediate site, the bottom hydrophone of the two VLAs and the base plate at 121 m from the nominal track line were combined to form I.HLA.121. At the shallow site, all three base plate hydrophones were combined to create S.HLA.170.

4.1.3.3. Drifting Vertical Arrays

Vertical arrays of hydrophones suspended from a drifting auxiliary vessel are the suggested sensor configurations for ISO 17208-1/−2 compliant vessel source level measurements in deep water (e.g., Figure 1). Thus, this sensor configuration was included in the project for comparison to the seabed mounted sensors. On three occasions throughout the deployment period, at least four measurements at each location were conducted using a vertical array suspended over the side of a drifting vessel. The drifting measurements were made at a nominal distance of 200 m from the vessel at its closest point of approach. All sound sources on the drifting vessel were turned off during the measurements. The deployment vessel was positioned down-current from the vessel to avoid any risk of collision.

The drifting array hydrophones were sampled continuously by an AMAR G4 at 128 kHz. All hydrophones were M36-C35 (GeoSpectrum Technologies Inc.) with a nominal sensitivity of −164 dBV/µPa. The hydrophones were calibrated on deck each day using a G.R.A.S 42AC pistonphone calibrator at 250 Hz. The real-time clocks on the AMAR G4s were synchronized with GPS time prior to deployment. A conductivity-temperature-depth (CTD) cast was performed before or after each drifting measurement.

The vertical array configuration is shown in Figure 18. During the May measurement program, it was quickly determined that the double damper plate did an excellent job of isolating the hydrophones from the non-acoustic noise associated with vertical movement surface due to waves. However, the array was unsuitable for retrieval without mechanical assistance, and even with assistance it was felt that the strain on the system was unacceptable. Therefore, the May and June deployments employed the configuration shown in Figure 19, which did not isolate the hydrophones from surface movement and added low-frequency noise to the data. In July, a single damper plate configuration with retrieval line (Figure 20) was successfully employed and is recommended for future programs that opt for a drifting vertical array configuration.

A depth logger was affixed to the bottom of the array to measure knock-over of the hydrophones while drifting and a GPS logger was run with a 10 s update rate to measure the position of the measurement vessel. A sea anchor was also used to reduce movement of the measurement vessel due to wind (Figure 21).

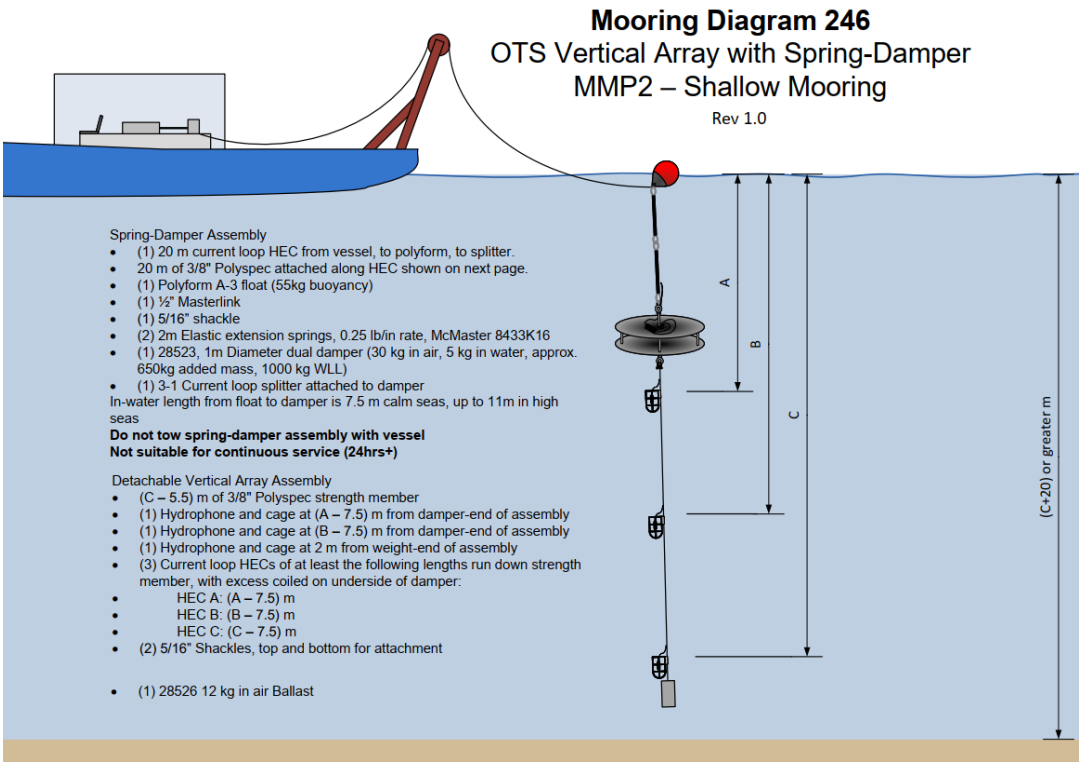

Figure 18. Mooring diagram for the three-element drifting vertical array configured for a water depth of 200 m or more.

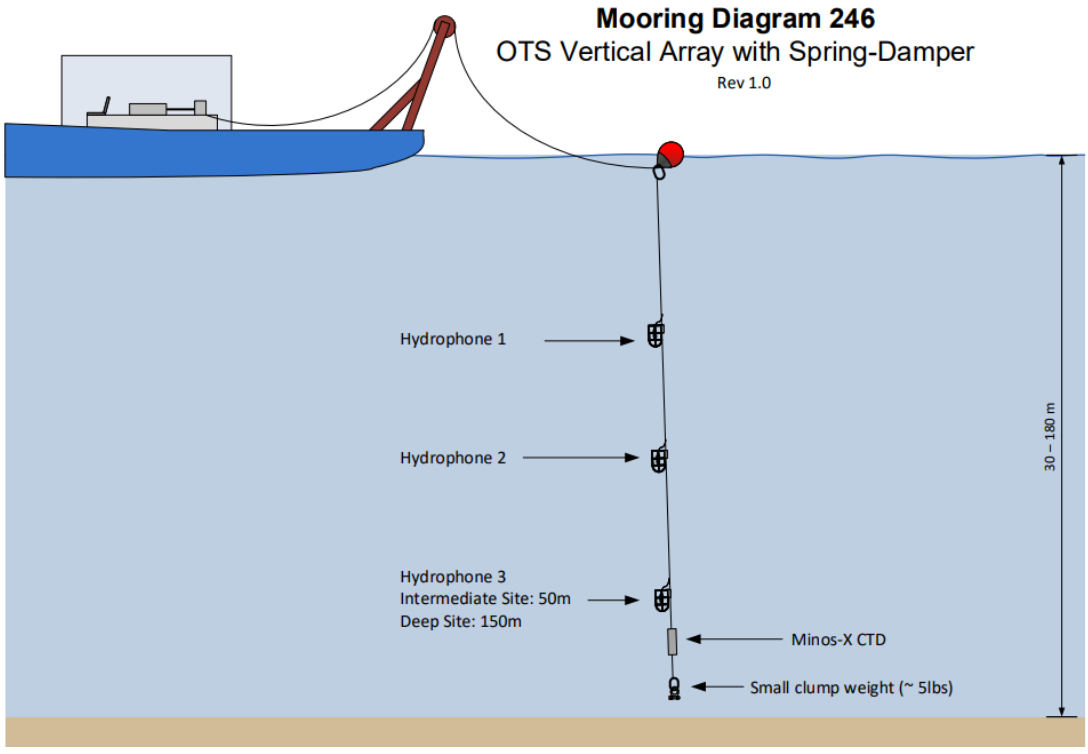

Figure 19. Over-the-side vertical array mooring as deployed in May 2021.

Table 8. Approximate hydrophone depths with modified drift system.

Site	Depth (m)		
	Element 1	Element 2	Element 3
Shallow	15		
Intermediate	10	30	50
Deep	30	80	140

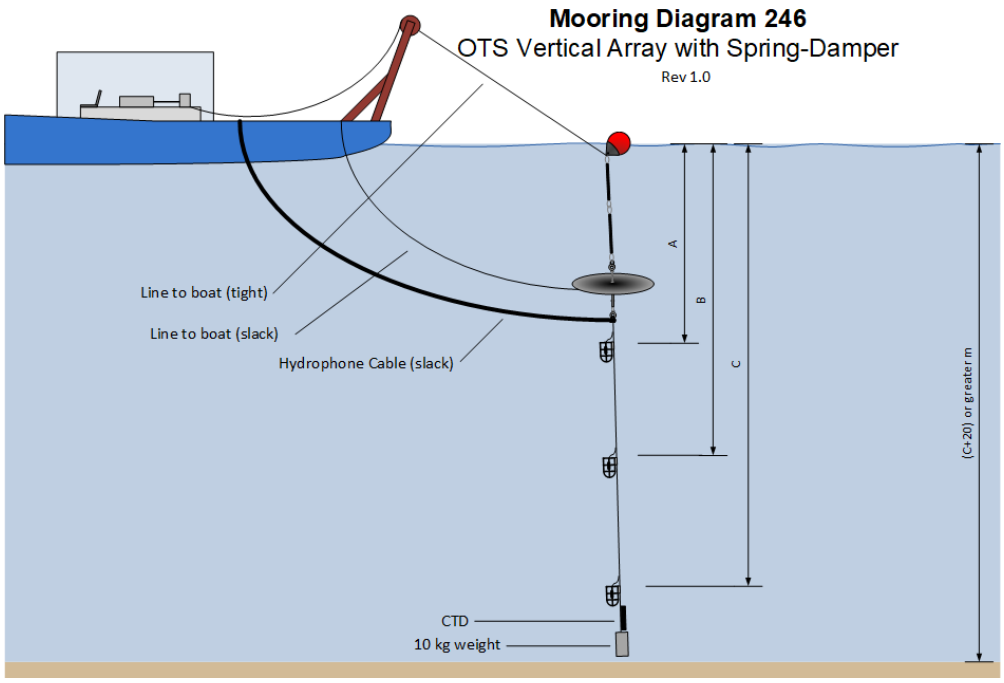

Figure 20. Over-the-side vertical array mooring as deployed in June and July 2021.

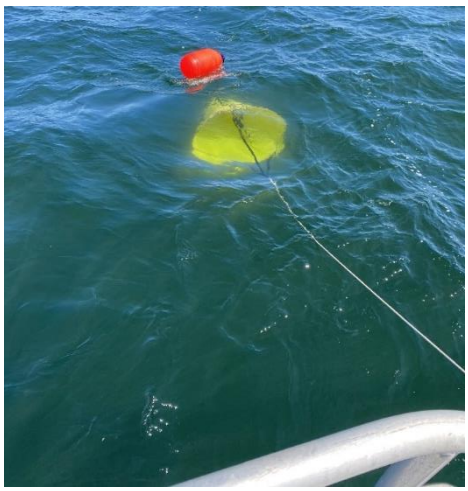

Figure 21. The 72-inch sea anchor deployed from the *Celtic V* in July 2021. Photo by Graham Warner, JASCO Applied Sciences.

4.1.4. Propagation Loss Experiment

To carry out numerical modelling of propagation loss, an accurate estimate of the seabed geoacoustic properties was required. To infer seabed properties, measurements of propagation loss were carried out at each recording site using a controlled acoustic source and calibrated hydrophone receiver. The experiments measured the PL between a M21-175-900 (GeoSpectrum Technologies Inc.) sound source deployed from a drifting vessel (Figure 22) and a bottom plate hydrophone on the seabed (see Figure 16). The source had a 900 Hz centre resonant frequency and a 500–1200 Hz usable bandwidth. It generated linear frequency-modulated sweeps in this frequency range (Figures 23 and 24). The projector was suspended from a deployment vessel at 8 m depth and allowed to transmit for ~60 min while the vessel drifted past the seabed recorder.

In accordance with the Fisheries and Oceans Canada permit to perform the PL measurements in Southern Resident killer whale habitat, JASCO performed the following mitigations to avoid harm to marine mammals:

1. Visual monitoring for 30 min prior to energizing the source.
2. Visual and passive acoustic monitoring throughout the experiment.
3. Ramping up of acoustic power over 15 min.
4. Ensuring that the per-pulse SPL did not exceed 170 dB re 1 µPa².

Visual observations were conducted by a trained protected species observer (PSO) during the PL experiment. Passive acoustic monitoring (PAM) for marine mammal calls was performed using a separate hydrophone suspended at a depth of approximately 15 m below the observation vessel. The PAM hydrophone was also used to verify that the SPL from the projector did not exceed the permitted threshold. No marine mammals were visually observed by the PSO or acoustically detected during the PL measurements. Detailed activity and observation logs from the PL experiment are provided in the Long-term Recorder Deployment Report (Lawrence et al. 2021).

A near-field monitoring hydrophone provided a real-time view of the projector source level and logged data for later analysis. The near-field hydrophone was a M36-C0 (GeoSpectrum Technologies Inc.) with a sensitivity of −199 dB re 1 V/µPa. The hydrophone was calibrated on deck prior to deployment using a G.R.A.S 42AC pistonphone calibrator at 250 Hz. The hydrophone data were sampled and logged using a JASCO Ocean Sound Meter (OSM) system at 128 kHz. The OSM clock was synchronized with GPS time. A handheld GPS logger kept track of the projector location throughout the drift measurements.

The bottom plate hydrophone system was identical to the ones used for the main data collection. The same ‘parachute rig’ was employed to localize the mooring prior to making the drifting measurements. The bottom plate hydrophone was deployed prior to the drift measurements and retrieved at the end of each drift. CTD casts were performed at the beginning and end of each PL drift (see Section 4.1.3.1).

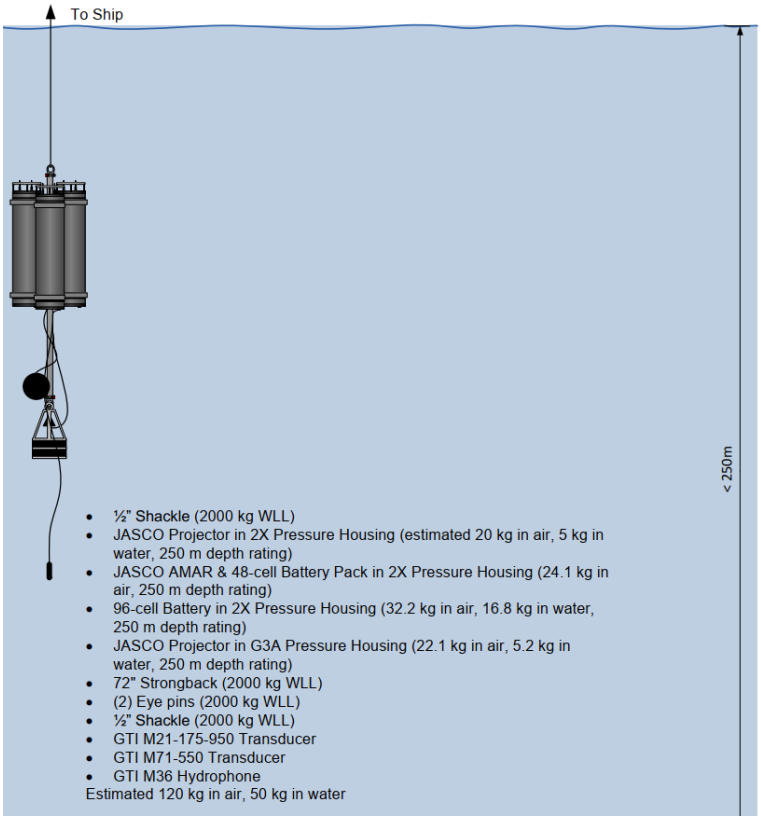

Figure 22. Mooring diagram for the over-the-side projector and hydrophone employed for the propagation loss study. The projectors are omnidirectional.

The projector was an M21-175-900 'bender' (GeoSpectrum Technologies Inc.). The Transmission Voltage Response (TVR) curve for the projector is shown in Figure 23. The TVR is not constant with frequency, i.e., 1 V at the input to the projector results in a source level of 136 dB re 1 µPa²m² if the frequency is 900 Hz but only 116 dB re 1 µPa²m² at 600 Hz. The projector was driven with a 600–1200 Hz linear-frequency modulated pulse lasting 2 s (Figure 24). The amplitude of the pulse increased for the first second (as the frequency increases toward resonance at 900 Hz) and decreased for the second (as the sensitivity decreases for frequencies above resonance), so that the projector source level, averaged over the 2 s pulse was less than 170 dB re 1 µPa²m². The pulse was repeated every 10 s.

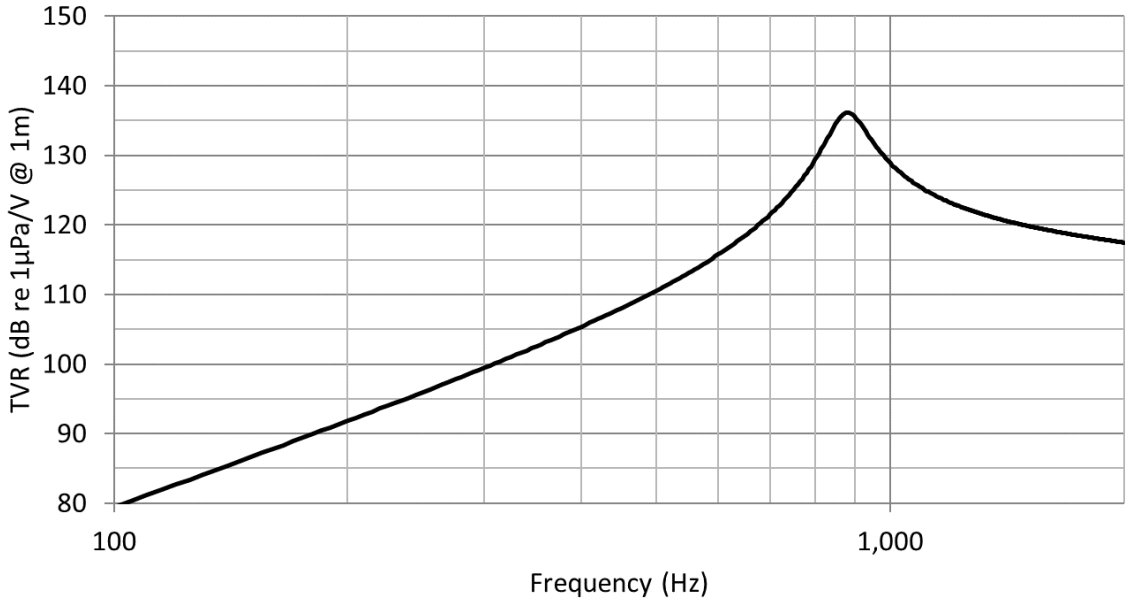

Figure 23. Transmission Voltage Response (TVR) for the M21-175-900 projector.

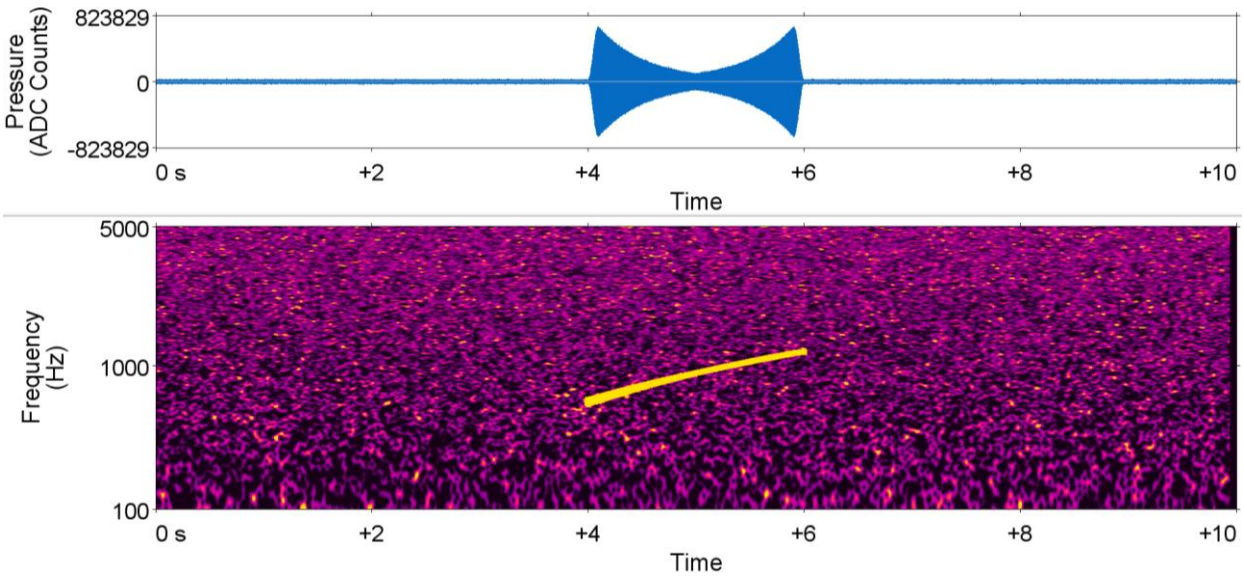

Figure 24. (Top) time series and (bottom) spectrogram of the propagation loss test pulse employed for the inversion study.

A summary of the PL drift data at the deep site recorded at the hydrophone 1 m from the source is shown in Figure 25; note the increase in source level over the first 15 min, which was implemented to comply with the DFO Permit Conditions. The sound level measured at the seabed is shown in Figure 26. The inversion of these data is discussed in the next section.

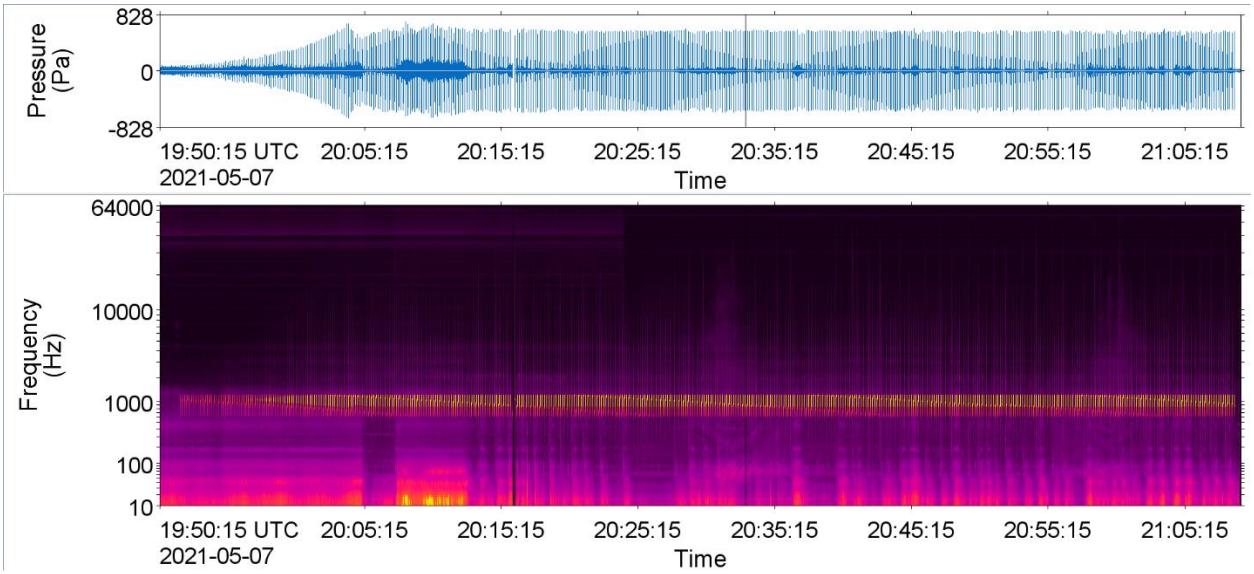

Figure 25. Acoustic data for measuring propagation loss (PL) at the deep site, as recorded on the 1 m source monitoring hydrophone.

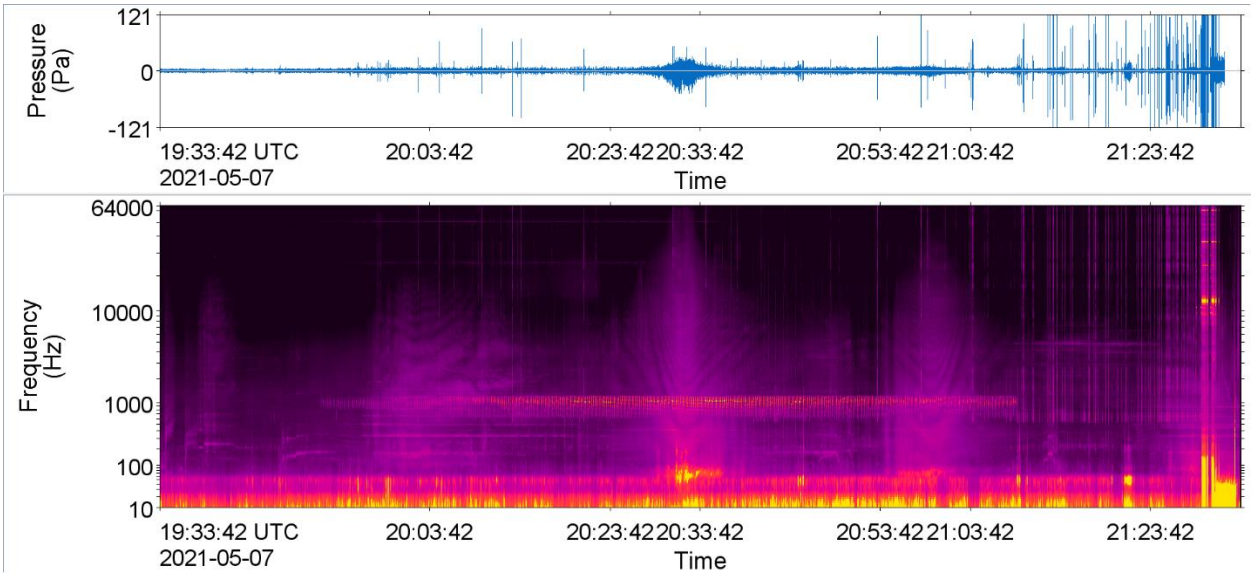

Figure 26. Acoustic data for measuring propagation loss (PL) at the deep site, as recorded on the bottom-mounted hydrophone.

4.1.5. Geoacoustic Inversion

Underwater acoustic propagation loss (PL) depends on the source depth, receiver depth, water sound speed profile, bathymetry, and seabed geoacoustic properties. If these parameters are known, acoustic propagation models can accurately predict propagation loss as a function of distance and frequency. Of these parameters, geoacoustic properties are typically the most difficult to measure and are often unknown for many areas of the world's oceans. Geoacoustic properties can be measured directly from laboratory analysis of sediment cores but collecting and analyzing core data is costly and time consuming. Thus, the acoustic inversion technique was preferred for the MMP2 experiment.

For this study, a remote sensing method was used to infer representative geoacoustic properties that can be used for accurately modelling sound propagation from vessels. This involved playing underwater acoustic signals while measuring the SL (L_S), source depth, received SPL (L_p), receiver depth, and the water sound speed profile. Depth sounder measurements were also collected to verify available bathymetric data. Propagation loss (N_{PL}) was calculated from the difference between SL and received SPL:

$$N_{\mathrm{PL}} = L_S - L_p. \tag{32}$$

A non-linear Bayesian inversion method that employed JASCO's Marine Operations Noise Model (MONM) was used to estimate the sediment layering and geoacoustic properties from the PL measurements. In essence, MONM was used to predict PL that would replicate the measurements for the known source and receiver depths, water sound speed profile, and bathymetry, by varying the geoacoustic parameters (see Appendix C for details). The most likely (i.e., maximum *a posteriori*, or MAP) set of geoacoustic properties for each site were those that resulted in the best match to the PL measurements.

4.1.6. Conductivity-Temperature-Depth Measurements

Profiles of water temperature and salinity were collected throughout the trials using a Minos-X (AML Oceanographic) conductivity-temperature-depth (CTD) probe. The profiles from the CTD probe were used to calculate sound speed profiles for each month and site during the experiment (Figure 27). The CTD data suggested that sound speed profiles were weakly stratified with depth during the experiment and would thus have negligible influence on URN measurements. Numerical tests, undertaken to investigate this assumption, indicated that there was no significant difference between PL calculations performed using actual measured profiles and iso-velocity profiles, out to 1 km range (Figure 28). Thus, it was concluded that the iso-velocity approximation was valid for calculating vessel source levels from the experimental data.

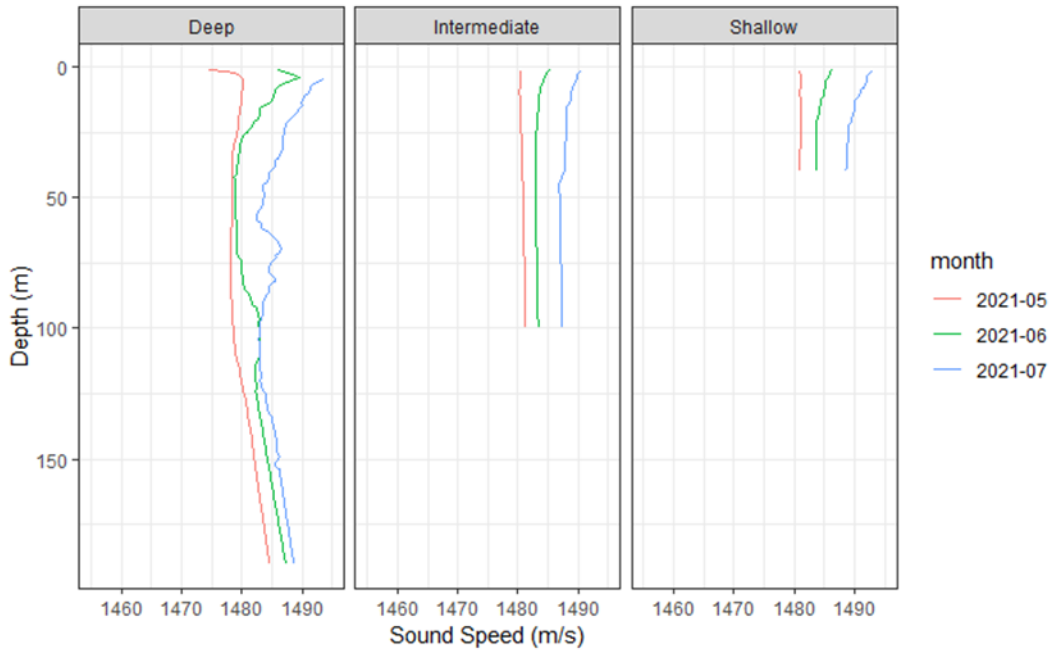

Figure 27. Mean profiles of sound speed in water versus depth measured during the experiment at each site. Profiles represent the average of upcast and downcast data.

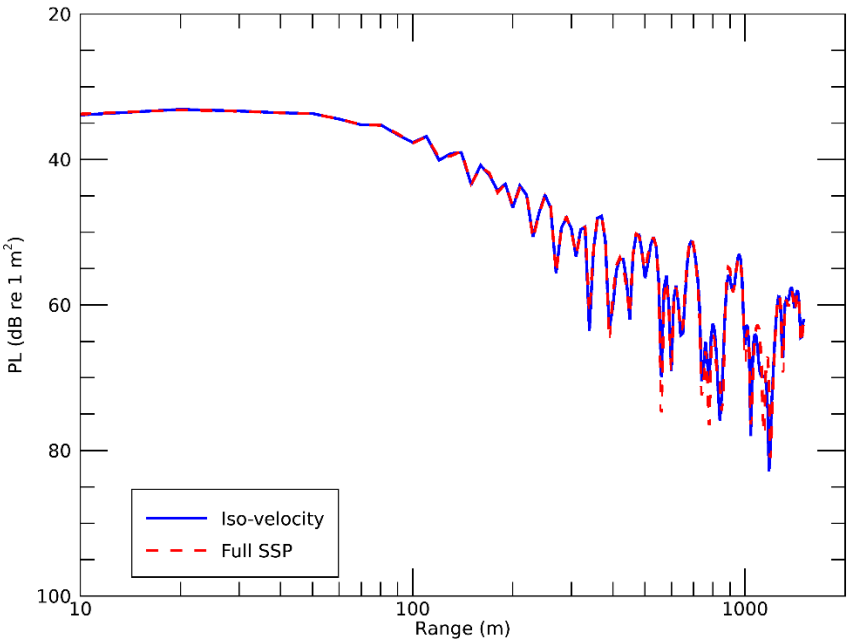

Figure 28. Propagation loss (PL) versus range at 100 Hz for an iso-velocity profile (red dashed line) compared with PL versus range for measured sound speed profile data (solid blue line) collected at the deep site during May 2021. PL was calculated using MONM (eight Padé terms) using 5 m source depth and 69 m receiver depth.

4.1.7. Weather and Current Data

Wind and ocean currents are the two environmental factors expected to have the most influence on vessel URN measurements. Wind affects the sea state (i.e., by increasing wave height), which in turn can induce rolling or pitching of the vessel and destabilize wake inflow to the propeller. The ISO 17208-1 standard recommends a maximum wind speed of 20 knots, for ships greater than 100 m, to ensure stability of the vessel during a URN measurement. Ocean currents, on the other hand, affect the measured speed of the vessel, since speed over ground as measured on AIS is not equal to speed of the vessel through water. It is assumed that the latter speed is the most relevant for measuring URN from surface vessels, as it relates directly to propeller inflow.

Windspeed data (10 min average) for all URN measurements were obtained from the Environment Canada weather station nearest to the measurement site. The nearest weather stations to the three measurement sites were as follows:

- TSAWASSEN FERRY AUTO (TC ID: VTF) at the deep site; and
- VICTORIA INTL A (TC ID: YYJ) at the shallow and intermediate sites.

Logged wind speeds did not exceed the 20 knot maximum for any accepted URN measurements collected during the experiment (Figure 29).

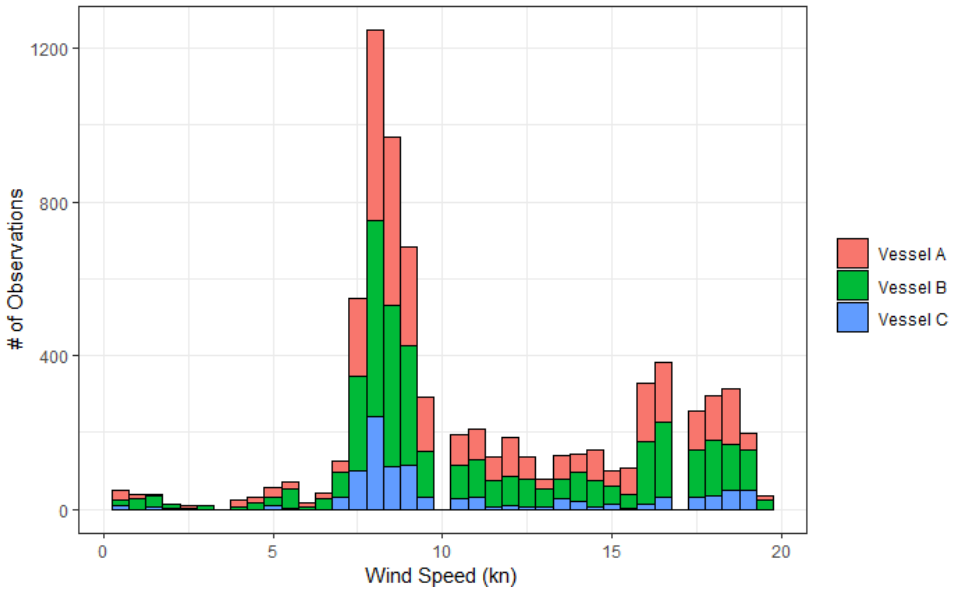

Figure 29. Histogram of wind speeds recorded during accepted underwater radiated noise (URN) measurements.

Direct current measurements were unavailable for the three measurement sites, so surface current data were estimated using the WebTide Tidal Prediction Model (v 0.7.1), provided by Fisheries and Oceans Canada (Bedford Institute of Oceanography 2015). The speed through water vector was computed from the difference of the AIS speed over ground vector ($\vec{v}_{sog}$) and the ocean current vector from WebTide ($\vec{u}_c$):

$$\vec{v}_{sow} = \vec{v}_{sog} - \vec{u}_c \, .$$

The magnitude of the resulting speed over water vector, $|\vec{v}_{sow}|$, was used for binning the URN measurements when comparing source levels measured between different sites and hydrophone arrays.

4.1.8. ShipSound Analysis

To obtain URN measurements for each vessel pass, the hydrophone recordings were analyzed with ShipSound, a component of JASCO's custom vessel noise measurement system, PortListen®. ShipSound automatically tracks the identity, position, and speed over ground of vessels transiting past the hydrophone arrays using the Automated Identification System (AIS). Any AIS vessels transiting through a 1 × 4 km measurement funnel around each measure site (Figure 14) were automatically analyzed by ShipSound to obtain a URN measurement. Environmental conditions (wind speed, current speed) and the coordinates of nearby AIS vessels were also recorded for each automated measurement. Source level reports were automatically produced for each valid pass from the hydrophone and vessel tracking data.

ShipSound computes RNL and SL.HWB (see Section 4.1.10) within a data window defined by a ±30° azimuth angle centred from the CPA to the hydrophone. For acoustic data within the measurement window, ShipSound analyzes acoustic data in decidecade frequency bands from 10 Hz to 63,100 Hz. Each sound recording is processed using 1-s sliding Fast Fourier Transforms (FFTs) using a power-normalized Hann window and 50 % overlap, to obtain power spectral density (PSD) levels versus time. Vessel track information is obtained from AIS data. Since the AIS transmitter/receiver is not necessarily coincident with the vessel's acoustic source, the acoustic closest point of approach (CPA) is determined by tracking the range and speed of the source using an automated tracking algorithm based on the cepstrogram method (Hannay et al. 2016). The automated CPA time may be verified (and adjusted if necessary) during manual quality review by a human analyst (see Section 4.1.9). The RNL and SL.HWB values (broadband and decidecade-band) are computed in decibels as a linear average from the RNL and SL.HWB from all 1-s sample locations along the vessel track within the ±30° data window. Background noise sound pressure levels (NL) are computed by averaging measured sound levels over two one-minute intervals: 1 min just before the vessel enters the entrance funnel and 1 min after it leaves the exit zone. Measured SPL is compared with the NL in decidecade frequency bands and is adjusted if $3\ dB \leq \mathrm{SPL} - \mathrm{NL} < 10\ dB$, according to the method prescribed in the ISO 17208-1 standard. Decidecade band levels are discarded when $\mathrm{SPL} - \mathrm{NL} < 3\ dB$.

In all instances, array-average RNL and SL.HWB values (i.e., for the HLA and VLA measurements) were computed from the power-mean value of the three individual hydrophone nodes, according to the method prescribed by ISO standard 17208-1:

$$L_X = 10 \log_{10} \left[\frac{10^{L_X(h_1)/10} + 10^{L_X(h_2)/10} + 10^{L_X(h_3)/10}}{3} \right] \text{dB}$$

where L_X is the array-average value of RNL or SL.HWB and $L_X(h_n)$ is the single-node measurement from hydrophone n. In some instances, a single-hydrophone measurement was excluded from the array-average value if it was rejected following a manual data-quality review (see Section 4.1.9).

4.1.9. Data Quality Review

Each automated URN measurement from ShipSound was subjected to a manual quality review by a human analyst. For each measurement, the analyst inspected the vessel track, spectrogram, background noise levels, received levels, and source levels recorded by ShipSound. Measurements were rejected under the following circumstances:

1. Other AIS vessels were present within four times the measured CPA of the vessel of interest;
2. Spectrograms visibly contained contaminating noise from sources other than the vessel of interest (including non-AIS vessels);
3. Measurements had three or more decidecade bands with signal-to-noise-ratio less than 3 dB in the range 50–1000 Hz;
4. Pressure waveforms contained clipped samples inside more than six 1 s intervals inside the data window;
5. Vessel AIS tracks had an unsteady speed or heading in the measurement window.

In addition, measurements on the vertical arrays were automatically rejected when data from the depth loggers indicated that knock-down due to tidal currents was sufficient to introduce >10 % error in the CPA estimate, as suggested by ISO standard 17208-1.

4.1.10. Source Level Calculation

A modelled SL value (SL.HWB) was calculated in ShipSound using the Hybrid Wavenumber Integration Beam Trace method described in Section 2.3.2. This method is based on the numerical solution of the acoustic wave equation, which accounts for the effect of the ocean environment on sound transmission. Since no single acoustic model is applicable at all sampled ranges and frequencies, a hybrid PL model was applied as follows: in decidecade bands at 4 kHz and below PL was calculated using the VSTACK wavenumber integration model and in decidecades above 4 kHz PL was calculated using the Bellhop beam tracing model.

VSTACK computes PL versus depth and range for arbitrarily layered, range-independent, acoustic environments using the wavenumber integration approach to solving the exact (range-independent) acoustic wave equation (Jensen et al. 2011). This model is valid over the full

angular range of the wave equation and can fully account for the elasto-acoustic properties of the sub-bottom. Wavenumber integration methods are extensively used in the fields of underwater acoustics and seismology where they are often referred to as reflectivity methods or discrete wavenumber methods. VSTACK computes sound propagation in arbitrarily stratified water and seabed layers by decomposing the outgoing field into a continuum of outward-propagating plane cylindrical waves. Seabed reflectivity in the model is dependent on the seabed layer properties: compressional and shear wave speeds, attenuation coefficients, and layer densities.

BELLHOP computes PL versus range and depth using the finite-element beam tracing method (Porter and Liu 1994), which is a variant of the ray-trace method. While BELLHOP is a fully range-dependent propagation model, only range-independent predictions were used for the current application. Bottom loss was included in the BELLHOP model by using tabulated, frequency-dependent reflection coefficients for a layered elastic seabed, generated using the reflectivity method (i.e., as in VSTACK). Attenuation of acoustic energy by molecular absorption in seawater was accounted for with frequency-dependent absorption coefficients calculated using the formulae of François and Garrison (1982b, 1982a).

Both numerical models assumed iso-velocity sound speed profiles in the water column and fully-elastic, vertically-stratified geoacoustic profiles in the seabed. Seabed geoacoustic properties at each site were estimated using the inversion procedures described in Sections 4.1.3.1, 4.2.1 and Appendix C. Seawater absorption coefficients for BELLHOP were calculated using mean water temperature and salinity values from CTD profiles measured during the experiment. For the moored hydrophones, the environment was assumed to be range-independent for all PL calculations, with constant water depth at each site as follows:

- 184 m at the deep site,
- 66 m at the intermediate site, and
- 31 m at the shallow site.

The range-independent approximation was expected to be good at the deep and intermediate sites, where the seabed was approximately flat across the measurement funnel. The range-independent approximation was expected to be poorer at the shallow site, where the slope of the seabed was approximately 4 degrees across the measurement funnel. The range-independent assumption is discussed further in Section 4.3.

Average PL in each decidecade band was based on the mean propagation factor calculated at 50 frequencies, which were spaced logarithmically between the minimum and maximum decidecade band limits. Other SL metrics were calculated by adjusting RNL from ShipSound according to the procedures described in Section 2.3. All PL calculations were performed assuming a single source depth, which was taken to be 70 % of the logged vessel draft as specified in ISO standard 17208-1.

4.2. Results

This section presents results of the field experiments and uses statistical analysis of the URN measurements to compare the performance of different source level metrics at the three measurement sites. Many of the results in this section use box-and-whisker plots to represent the distributions of measured values. In these figures, the box represents the central 50% of the measurements, with the line in the middle of the box representing the median values. The lines below the boxes show the ranges of values for the first quartile of the data, while the lines above the boxes show the upper quartile. In some of the figures, dots above or below the lines are included to indicate when outliers are present.

Many of the results in this section also apply averaging to URN data to reduce the variance of source levels estimates (i.e., thereby increasing measurement accuracy). When averaging source levels, care must be taken to specify how the averaging was performed, since different averaging methods will yield different results. The following approach used in this study was deliberately chosen to follow as closely as possible the averaging procedures described in ISO standard 17208-1:

- When averaging source levels measured on *different* hydrophones from the *same* vessel pass, the average source level was computed as the decibel level of the mean source factor (i.e., see ISO 17208-1:2016 Equation 8). This method is referred to henceforth as the ‘power average’.
- When averaging source levels measured on the *same* hydrophone node, or array, from *different* vessel passes, the average source level was computed as the mean of the decibel source level values (i.e., see ISO 17208-1:2016 Equation 9). This method is referred to henceforth as the ‘arithmetic average’[6].

Finally, measurements from different vessel passes were generally grouped (or ‘binned’) according to their speed through water before averaging, since speed through water strongly influences vessel URN. Note that this quantity is referred to by the ISO standard as ‘speed over water’. However, the authors of this report prefer ‘speed through water’ and have used this terminology in the remainder of this section.

[6] The arithmetic average has sometimes been referred to as the 'geometric mean' in other work. We have used the term 'arithmetic average' here for consistency with ISO standard 17208-1.

4.2.1. Determination of Sediment Properties by Inversion

Characterization of the sound propagation properties at the three measurement sites was a key input to the vessel source level analysis. Thus, calibrated measurements of propagation loss versus source-receiver range were collected at the deep, intermediate, and shallow URN measurements sites on 7 May 2021 (see Figures 30–32), as described in Section 4.1.3. A non-linear Bayesian inversion algorithm was applied to these data to estimate the geoacoustic properties of the seabed at each site (see Appendix C). The result of the algorithm was a set of geoacoustic profiles (referred to as the maximum *a posteriori*, or MAP, estimates), describing the elastic properties of the seabed materials versus depth below the seafloor (Table 9). The MAP geoacoustic profiles were used as input to the VSTACK and Bellhop full-wave propagation models (Section 2.3.2) for calculating vessel source levels in ShipSound using the HWB method. The MAP profiles were also used to determine the seabed critical angle (ψ) versus frequency (Figure 33) for calculating vessel source levels using the seabed critical angle (SCA) method.

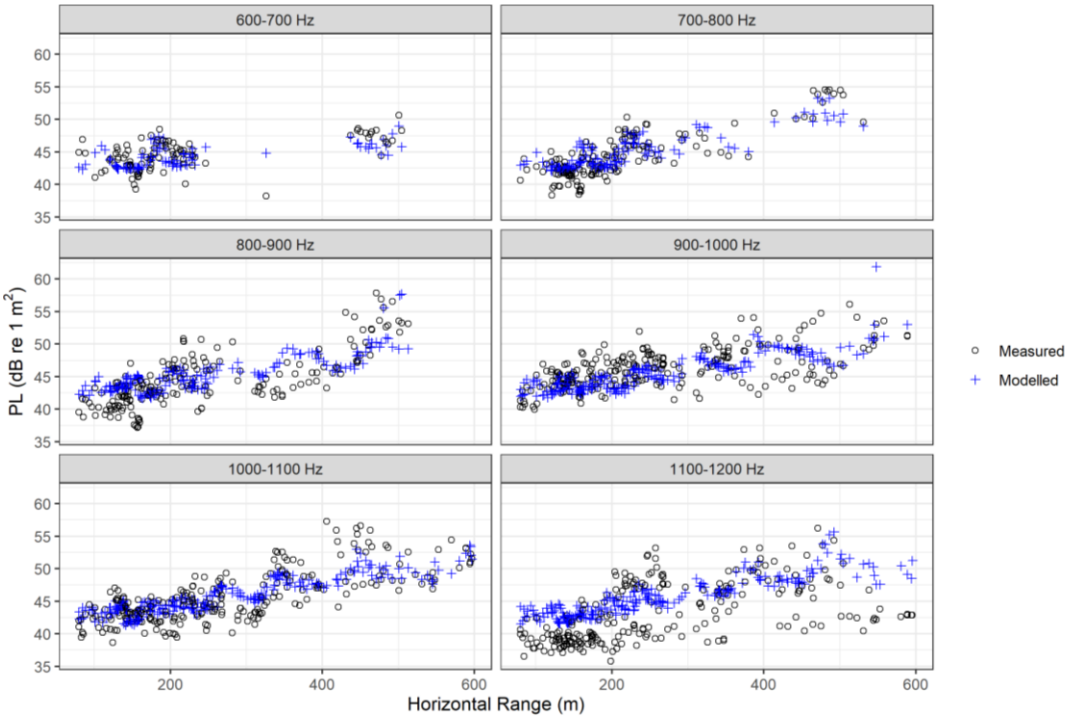

Figure 30. Deep site: Measured and modelled propagation loss (PL) versus horizontal distance from the source. Modelled PL are from the maximum *a posteriori* (MAP) geoacoustic model (Table 9).

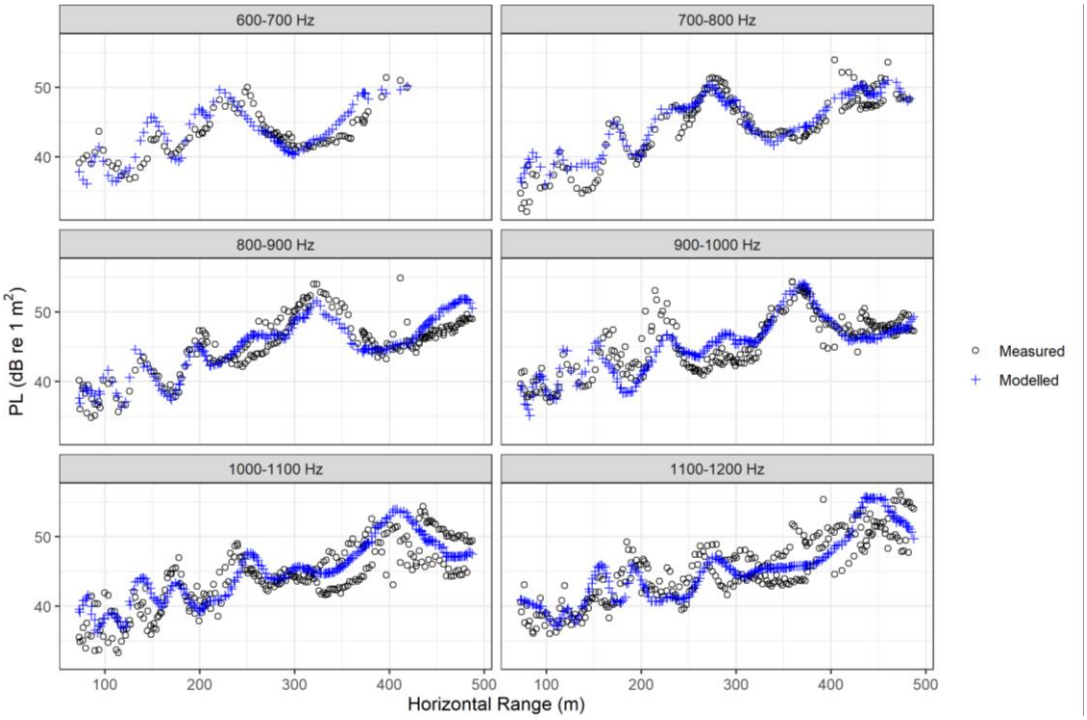

Figure 31. Intermediate site: Measured and modelled propagation loss (PL) versus horizontal distance from the source. Modelled PL are from the maximum *a posteriori* (MAP) geoacoustic model (Table 9).

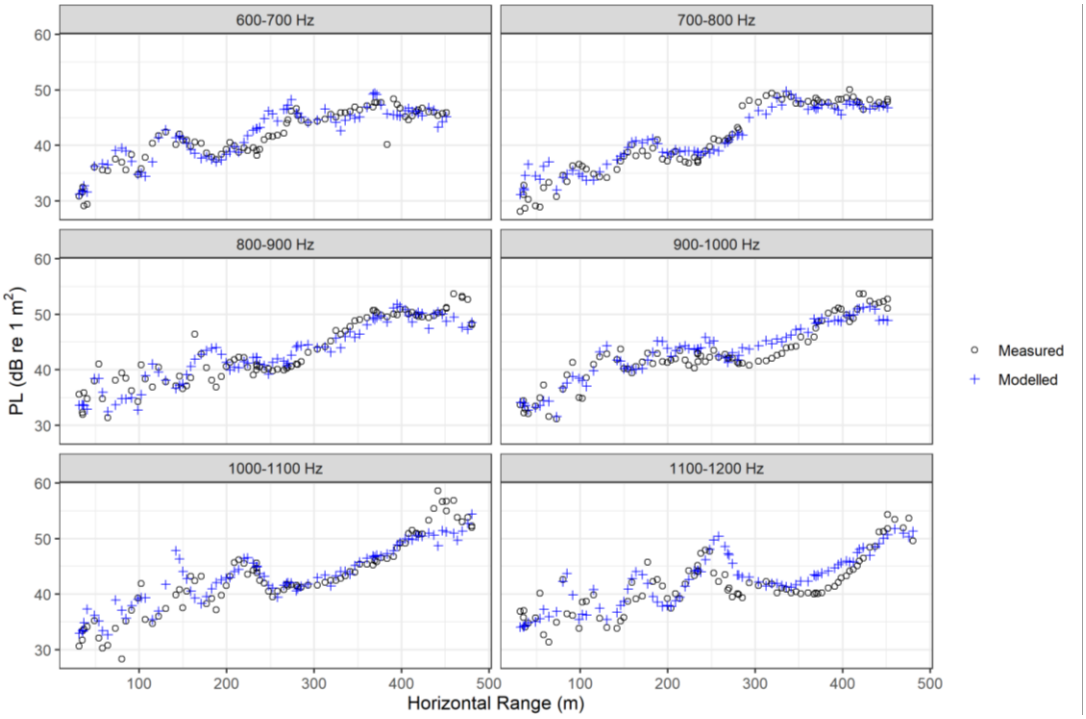

Figure 32. Shallow site: Measured and modelled propagation loss (PL) versus horizontal distance from the source. Modelled PL are from the maximum *a posteriori* (MAP) geoacoustic model (Table 9).

Table 9. Estimated geoacoustic parameters versus depth below seafloor for the deep, intermediate, and shallow sites, based on the maximum *a posteriori* (MAP) inverted models. Shear-wave speed and attenuation were only estimated for the top sediment layer.

Depth below seafloor (m)	C_p (m/s)	ρ (g/cm^3)	α_p (dB/λ)	C_s (m/s)	α_s (dB/λ)
Deep site					
0–2.8	1460–1466	1.32–1.33	0.80–0.12	260	0.61
>2.8	2496	2.47	0.47		
Intermediate site					
0–2.9	1545–1549	1.82	1.00–0.97	40	2.59
2.9–4.9	1565–1637	1.86–1.91	0.10–0.03		
4.9–10.3	1942–1970	2.00–2.20	0.02–0.03		
>10.3	2238	2.45	0.81		
Shallow site					
0–1.4	1480–1488	1.61–1.63	0.86–0.13	94	2.10
1.4–13.2	1838–2261	2.29–2.44	0.02–0.07		
>13.2	2401	2.46	0.97		

C_p = compressional-wave speed, ρ = density, α_p = compressional-wave attenuation, C_s = shear-wave speed, α_s = shear-wave attenuation.

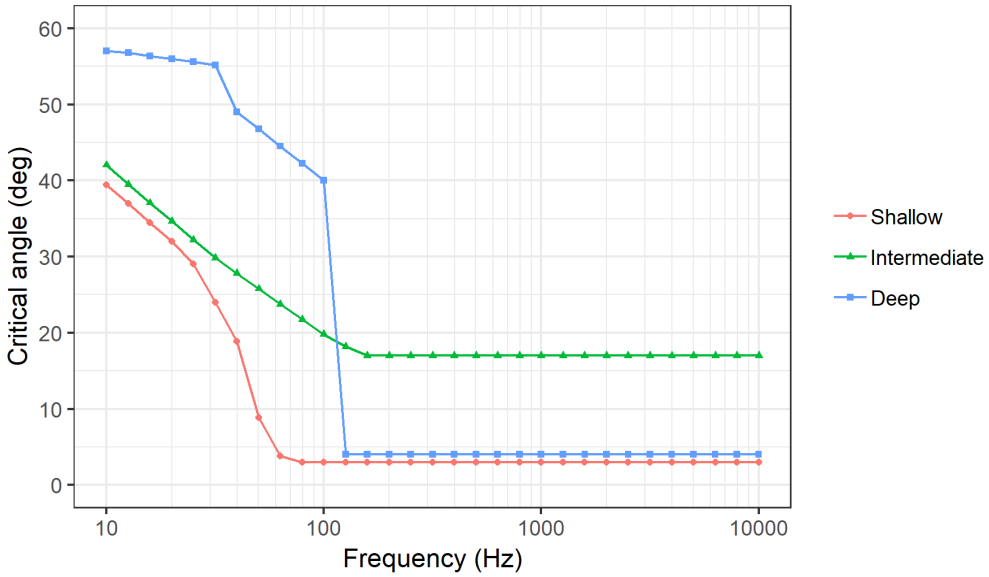

Figure 33. Estimated seabed critical angle versus frequency, by measurement site.

4.2.2. URN Measurement Summary

From the experimental data, ShipSound automatically analyzed a total of 12,079 unique URN measurements on 13 individual hydrophone nodes for vessels A–C. Of this total, 7675 measurements passed a manual data quality review. Speeds of the vessels varied during the experiment, but most URN measurements were collected at speeds between 17–22 knots with a mixture of both port and starboard aspects for each vessel (Figure 34). The routes of the vessels also varied during the experiment and thus URN measurements were sampled at a range of horizontal CPA distances, out to a maximum distance of 1 km (Figure 35).

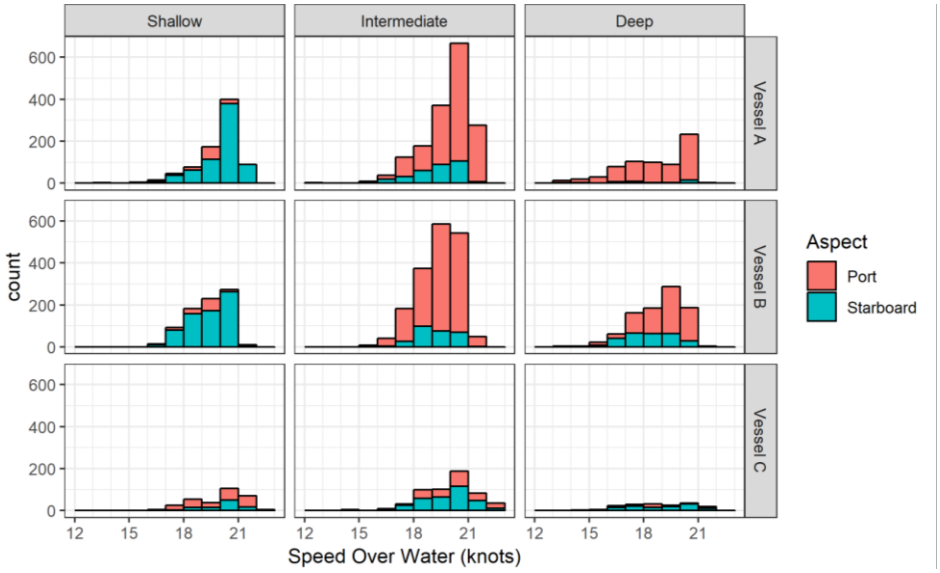

Figure 34. Histograms of speed over water at each site showing number of single-hydrophone underwater radiated noise (URN) measurements for port and starboard aspect for each vessel.

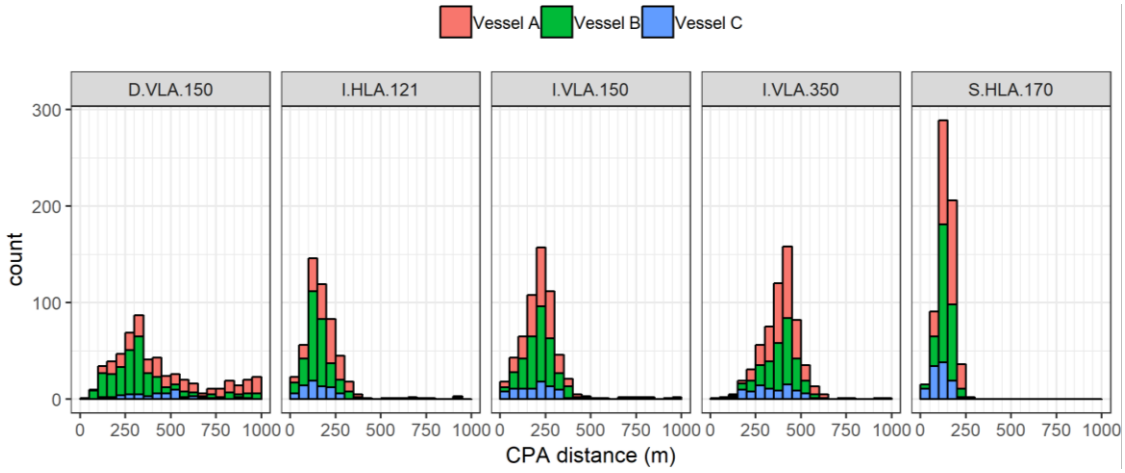

Figure 35. Histogram of vessel closest point of approach (CPA) distances to each hydrophone array for accepted underwater radiated noise (URN) passes. CPA distances for the horizontal arrays are referenced to the closest hydrophone to the vessel track.

Initial analysis of source level data from ShipSound indicated that the URN of vessels A–C were strongly dependent on speed through water at the time of measurement (Figure 36). All three vessels exhibited a U-shaped trend of source level versus speed through water, with minimum sound emissions in the 17–19 knot range. This type of SL-versus-speed curve is characteristic of controllable-pitch propellers, which were used on all three vessels (Baudin and Mumm 2015, Traverso et al. 2015). Mean draft of the vessels did not vary substantially over the course of the experiment, and variations in vessel trim did not appear to have a significant influence on measured source levels (Figures 37 and 38). Comparison of port and starboard URN measurements suggested that vessels B and C did not exhibit significant differences between these two aspects, whereas vessel A had higher slightly noise emissions for the port aspect (see Figure 39). Differences between port and starboard RNL for vessel A should be kept in mind when interpreting results, since URN sampling was heavily weighted toward starboard aspect measurements at the shallow site for this vessel (see Figure 34).

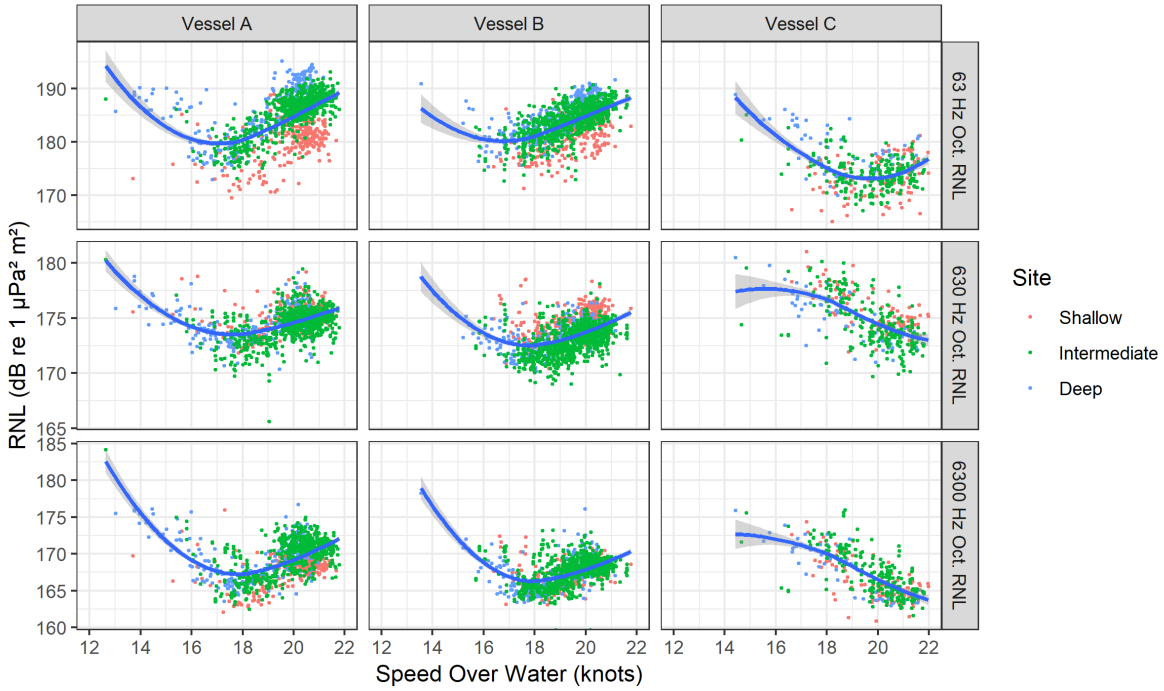

Figure 36. Scatter plot of array-average radiated noise level (RNL) in octave-bands (63, 630, and 6300 Hz) versus speed through water for each vessel, as measured at the three measurements sites. Line shows smoothed trend of data using the locally-weighted-smoothing (lowess) method (R Core Team 2020).

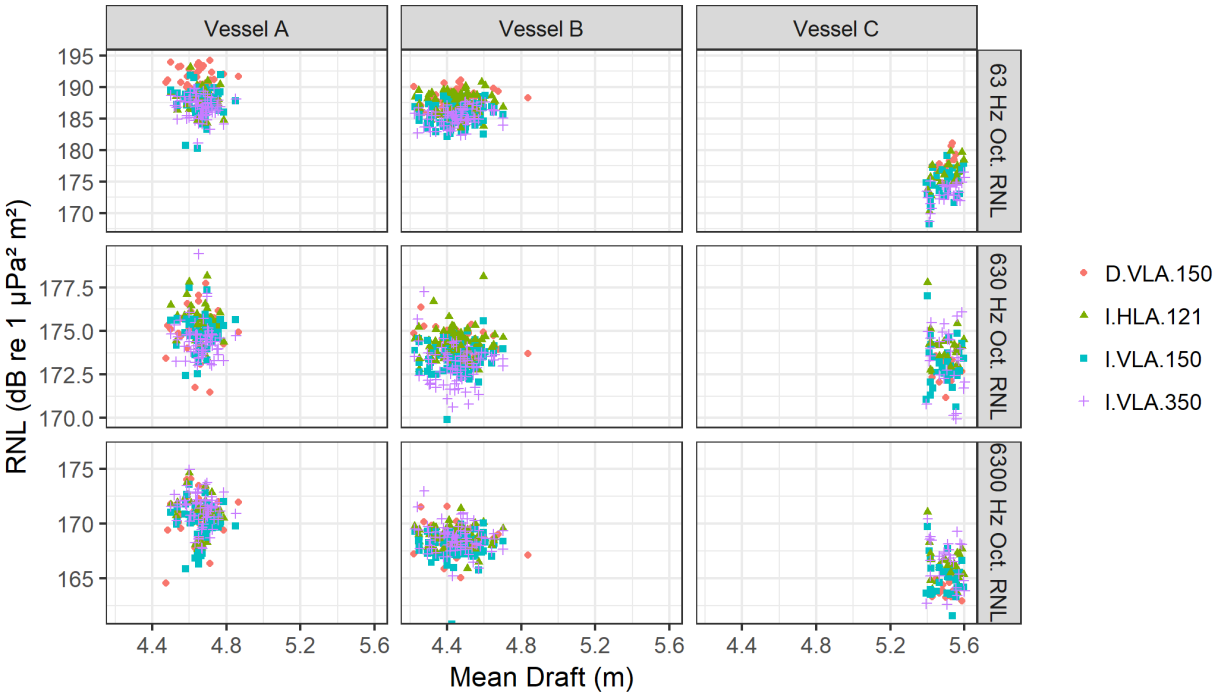

Figure 37. Scatter plot of array-average radiated noise level (RNL) in octave-bands (63, 630, and 6300 Hz) versus mean vessel draft. To control for the effect of water depth and speed on measured RNL, speeds through water below 20 knots and measurements from the shallow HLA have been excluded.

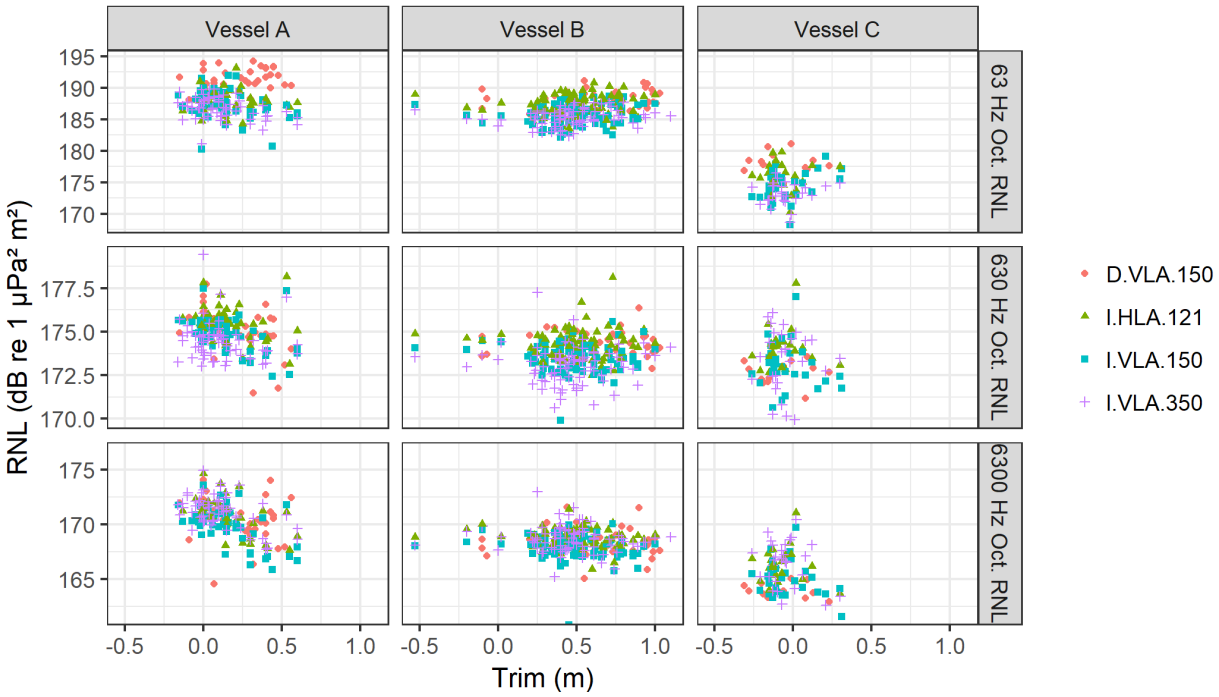

Figure 38. Scatter plot of array-average radiated noise level (RNL) in octave-bands (63, 630, and 6300 Hz) versus trim (i.e., fore draft — aft draft). To control for the effect of water depth and speed on measured RNL, speeds through water below 20 knots and measurements from the shallow HLA have been excluded.

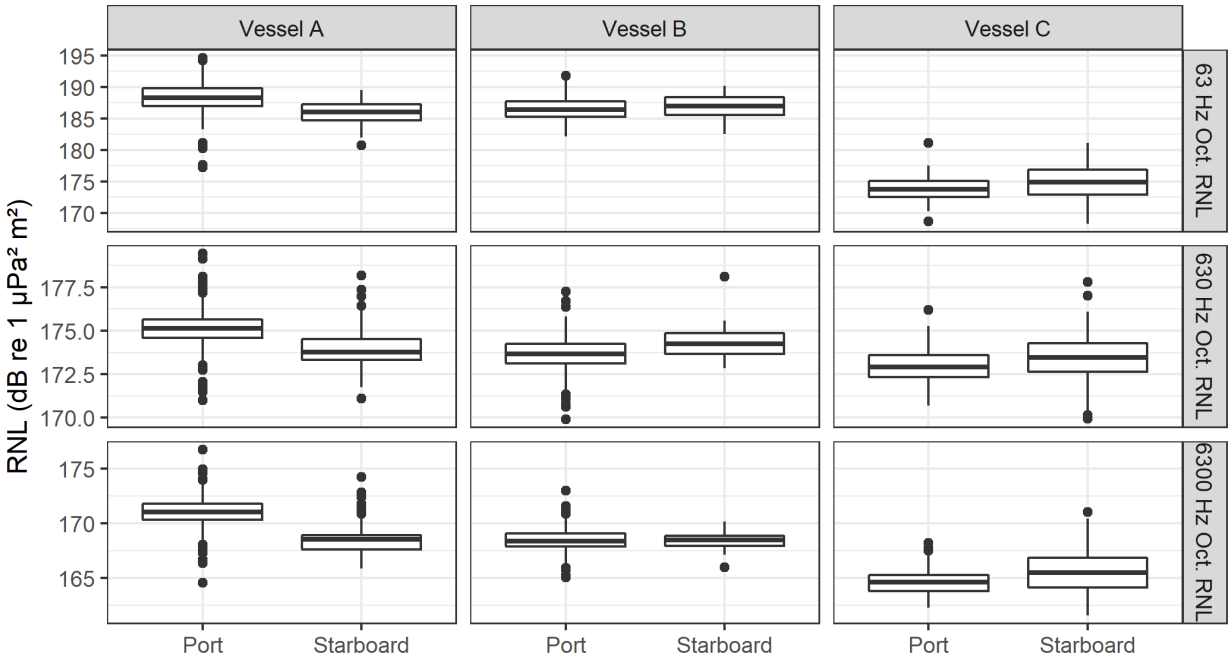

Figure 39. Box-and-whisker plot of array-average radiated noise level (RNL) in octave-bands (63, 630, and 6300 Hz) versus vessel aspect. To control for the effect of water depth and speed on measured RNL, speeds below 20 knots and measurements from the shallow HLA have been excluded.

4.2.3. Reference Source Level Measurements

Reference source levels for vessels A–C were obtained from URN measurements on the deep VLA and were analyzed according to the procedure from ISO standard 17208-2 (see Section 2.3.1). For each vessel pass, array-average source levels were computed from the power-mean values of the VLA nodes, as discussed in 4.1.8. Source level measurements were then binned by speed through water (in 1 knot bins), filtered by CPA distance, and arithmetically averaged to compute reference decidecade band source levels (Figure 40). Inspection of the reference measurements suggested that source levels of vessels A–C were most repeatable in the 20–21 knot speed range, and in frequency bands above 100 Hz.

The reference measurements were filtered by CPA distance before averaging, so that the mean range conformed as closely as possible to the measurement angles specified by ISO standard 17208-1 (see Figure 1). At the deep VLA, a CPA distance of 215 m yielded nominal measurement angles of 20°, 30°, and 40°. While this was a slightly narrower range of angles than those specified by the ISO standard (15°, 30°, and 45°), this difference was not expected to significantly affect the quality of the reference measurements. After filtering, reasonable conformance with the ISO geometry was possible for vessels A and B, but not for vessel C because it consistently passed too far from the VLA (Tables 10 and 11). This suggests that reference source levels for vessel C were of a lower grade than the other two vessels. Therefore, reference source levels for vessels A and B were expected to provide a better

representation of standards-conformant measurements, for the purpose of evaluating different metrics at the shallow and intermediate depth sites.

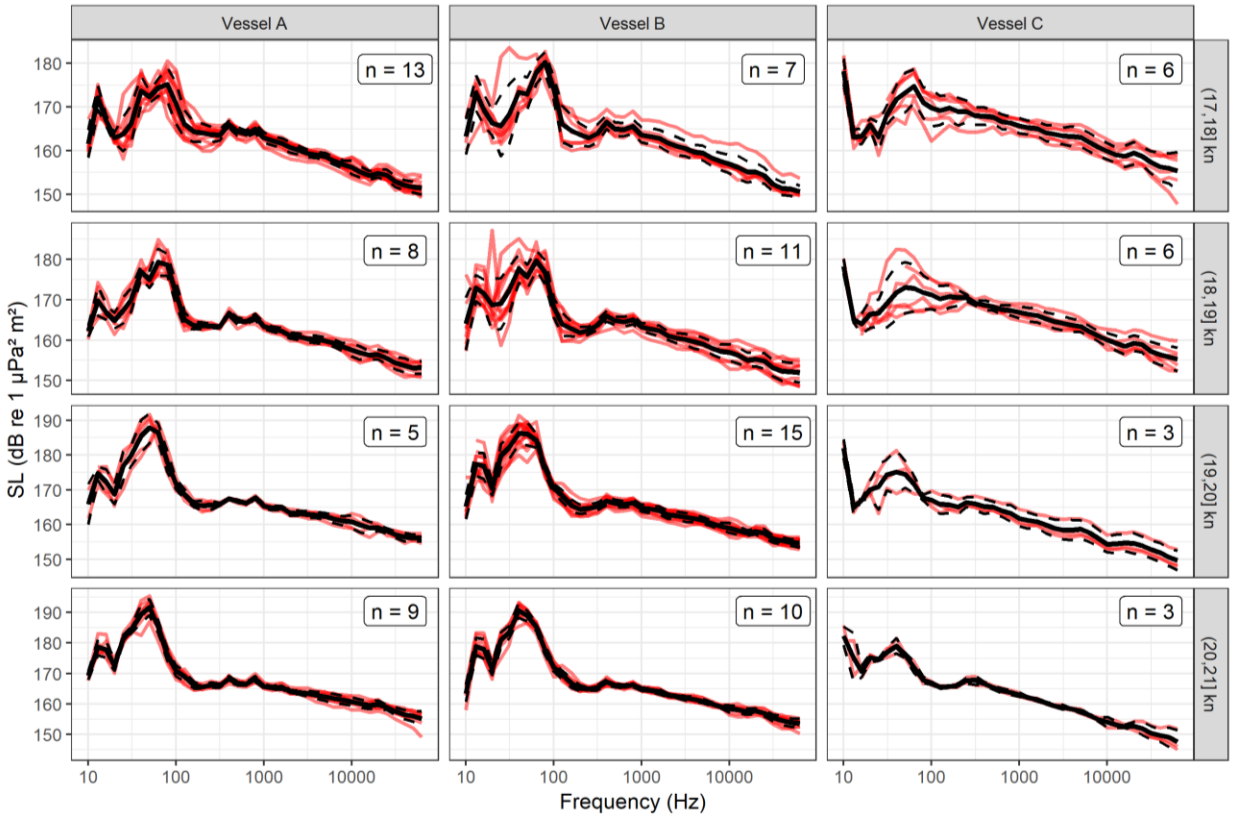

Figure 40. Reference source levels for vessel A–C (columns) computed in 1 knot speed through water bins (rows) from vertical line array (VLA) measurements at the deep site. Measurements for vessels A were filtered between 100–300 m horizontal closest point to approach (CPA) distance to the VLA. Measurements for vessels B were filtered between 150–250 m horizontal CPA distance to the VLA. Measurements for vessel C were filtered between 50–450 m horizontal CPA distance to the VLA. Red lines = individual array-average measurements, solid black line = arithmetic mean value, dashed black line = standard deviation. The n values indicate the number of individual array-average measurements contributing to the mean. Mean and standard deviation CPA distances for these measurements are provided in Table 10.

Table 10. Mean (± standard deviation) closest point of approach (CPA) distances to the deep VLA for reference source level measurements of vessels A–C. Note that the round and square brackets are mathematical notation indicating open and closed intervals, respectively (e.g., (17, 18] means >17 and ≤18).

Speed bin (kn)	CPA (m)		
	Vessel A	Vessel B	Vessel C
(17,18]	226 ± 61	213 ± 24	265 ± 89
(18,19]	221 ± 33	203 ± 30	286 ± 43
(19,20]	219 ± 70	193 ± 30	373 ± 44
(20,21]	215 ± 65	210 ± 23	343 ± 121

Table 11. Mean (± standard deviation) grazing angle to the deep VLA for reference source level measurements of vessels A–C. Channel 1–3 refer to the bottom, middle, and top hydrophones respectively. Note that the round and square brackets are mathematical notation indicating open and closed intervals, respectively (e.g., (17, 18] means >17 and ≤18).

Speed bin (kn)	Hydrophone channel	Grazing angle (°)		
		Vessel A	Vessel B	Vessel C
(17,18]	Channel 1	39.4 ± 8.4	40.1 ± 3.4	35.4 ± 8.8
	Channel 2	30.3 ± 7.8	30.6 ± 3.0	26.8 ± 7.5
	Channel 3	20.3 ± 6.1	20.2 ± 2.3	17.6 ± 5.4
(18,19]	Channel 1	39.1 ± 4.3	41.4 ± 4.3	32.2 ± 4.1
	Channel 2	29.7 ± 3.8	31.9 ± 3.9	23.9 ± 3.4
	Channel 3	19.6 ± 2.8	21.2 ± 3.0	15.5 ± 2.4
(19,20]	Channel 1	40.6 ± 10.0	43.0 ± 4.4	25.6 ± 2.6
	Channel 2	31.4 ± 9.3	33.3 ± 4.1	18.6 ± 2.0
	Channel 3	21.1 ± 7.2	22.3 ± 3.1	11.8 ± 1.4
(20,21]	Channel 1	41.6 ± 9.2	40.3 ± 3.1	29.2 ± 10.3
	Channel 2	32.3 ± 8.5	30.8 ± 2.8	21.7 ± 8.5
	Channel 3	21.8 ± 6.5	20.4 ± 2.1	14.0 ± 5.9

4.2.4. Single-node URN Measurements

To evaluate the performance of source level metrics for single-node hydrophone measurements, single-node source levels for vessels A–C were binned according to CPA distance and speed, and then arithmetically averaged so that they could be compared against reference source levels from the deep VLA (Figures 41 to 43 and Appendix D.1). Note that the Meyer-Audoly (SL.M-A) metric was excluded from the single-node comparisons, as it was only intended for use with array-averaged data. Trends of the single-node comparisons were generally consistent between vessels A–C.

At the deep site, all source level metrics exhibited good consistency with reference levels with only mild sensitivity to CPA distance. At the shallow and intermediate sites, consistency with reference levels was much more variable between metrics, with greatest differences apparent at low frequencies (below approximately 500 Hz). In this frequency range, SCA and ECA metrics had best consistency with reference source levels, particularly at CPA distances less than 250 m where the HWB and ISO metrics tended to underestimate reference source levels. Mismatch with reference source levels was typically highest at the shallow site for all metrics, as expected for reasons discussed in Section 1.1.

Where the consistency was poor, the tendency of many of the metrics was to underestimate, rather than overestimate reference source levels (with the notable exception of the ECA method below 300 Hz at the intermediate-depth site). This suggested that many of the metrics underestimated propagation loss, particularly at lower frequencies. Surprisingly, the HWB method performed relatively poorly below 1000 Hz using the single-hydrophone data, compared to the simpler methods. This may have been related to the relatively narrow frequency band used for the geoacoustic inversion analysis (see Section 4.3).

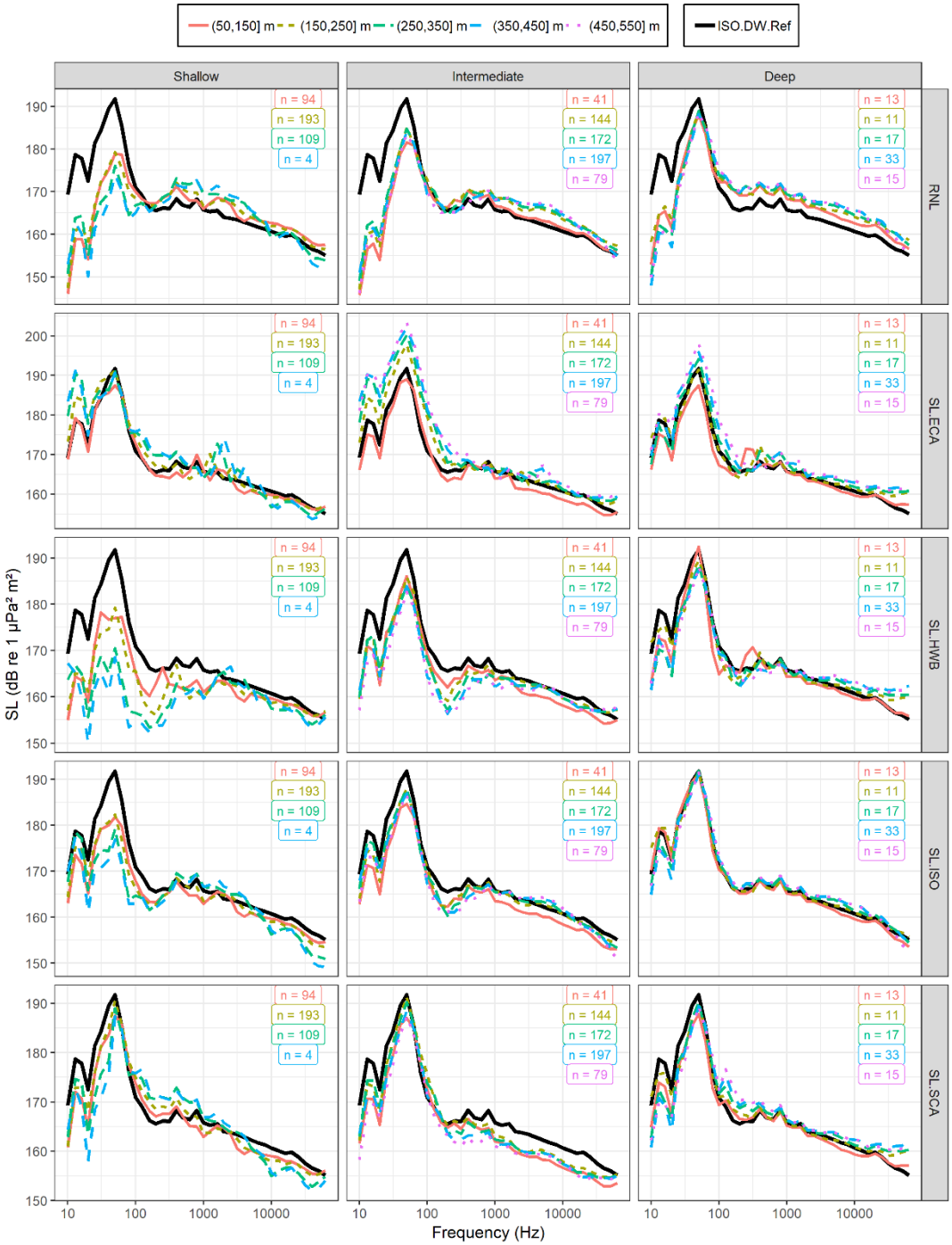

Figure 41. Vessel A: Mean source level versus frequency for single-node hydrophone measurements with speeds through water between 20 and 21 knots. Columns show different sites and rows show different source level (SL) metrics. Coloured lines show different closest point of approach (CPA) distance bins. Black lines show reference measurements (SL.ISO) from the deep VLA. The ‘n’ values indicate the number of individual measurements contributing to the average.

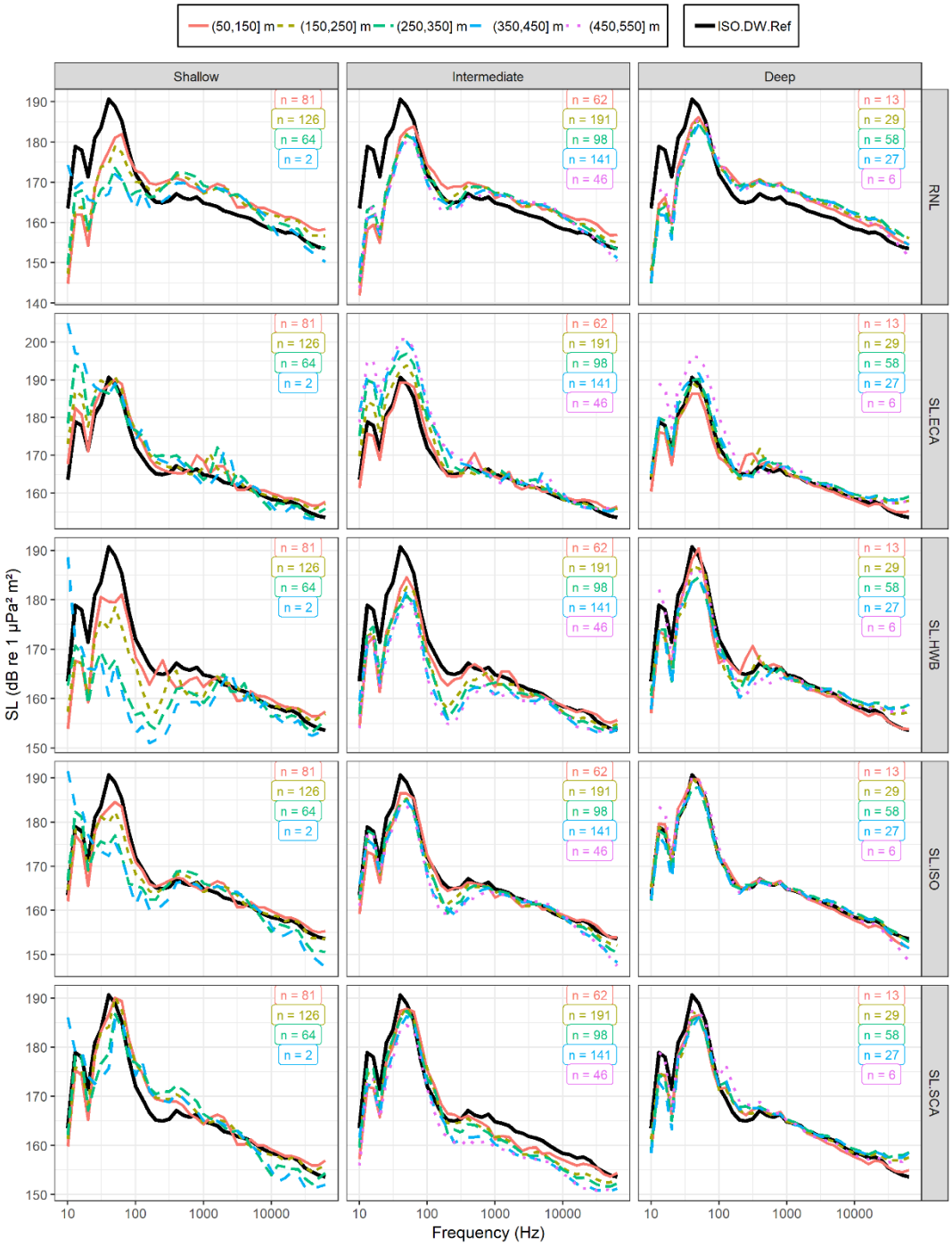

Figure 42. Vessel B: Mean source level versus frequency for single-node hydrophone measurements with speed through water between 20 and 21 knots. Columns show different sites and rows show different source level (SL) metrics. Coloured lines show different closest point of approach (CPA) distance bins. Black lines show reference measurements (SL.ISO) from the deep VLA. The ‘n’ values indicate the number of individual measurements contributing to the average.

Figure 43. Vessel C: Mean source level versus frequency for single-node hydrophone measurements with speeds through water between 20 and 21 knots. Columns show different sites and rows show different source level (SL) metrics. Coloured lines show different closest point of approach (CPA) distance bins. Black lines show reference measurements (SL.ISO) from the deep VLA. The ‘n’ values indicate the number of individual measurements contributing to the average.

4.2.5. Array-average URN Measurements

To evaluate the performance of source level metrics for different array geometries, the array-average source levels for vessels A–C were binned according to CPA range and speed through water, and then arithmetically averaged so that they could be compared against reference source levels from the deep VLA (Figures 44 to 46 and Appendix D.2). Note that data from the two different VLAs at the intermediate site were grouped together for this analysis, since their source-receiver geometry was effectively identical after applying range binning. The results for the array-average measurements exhibited similar trends with CPA distance and water depth as the single-node measurements (see Section 4.2.4). Inspection of the data suggested that the SCA, M-A, and ECA methods were most consistent with reference source levels on the various hydrophone arrays, and their performance was best at shorter CPA distances (<250 m). Both the HLA and VLA geometries appeared to yield consistent source level metrics, when used with these metrics.

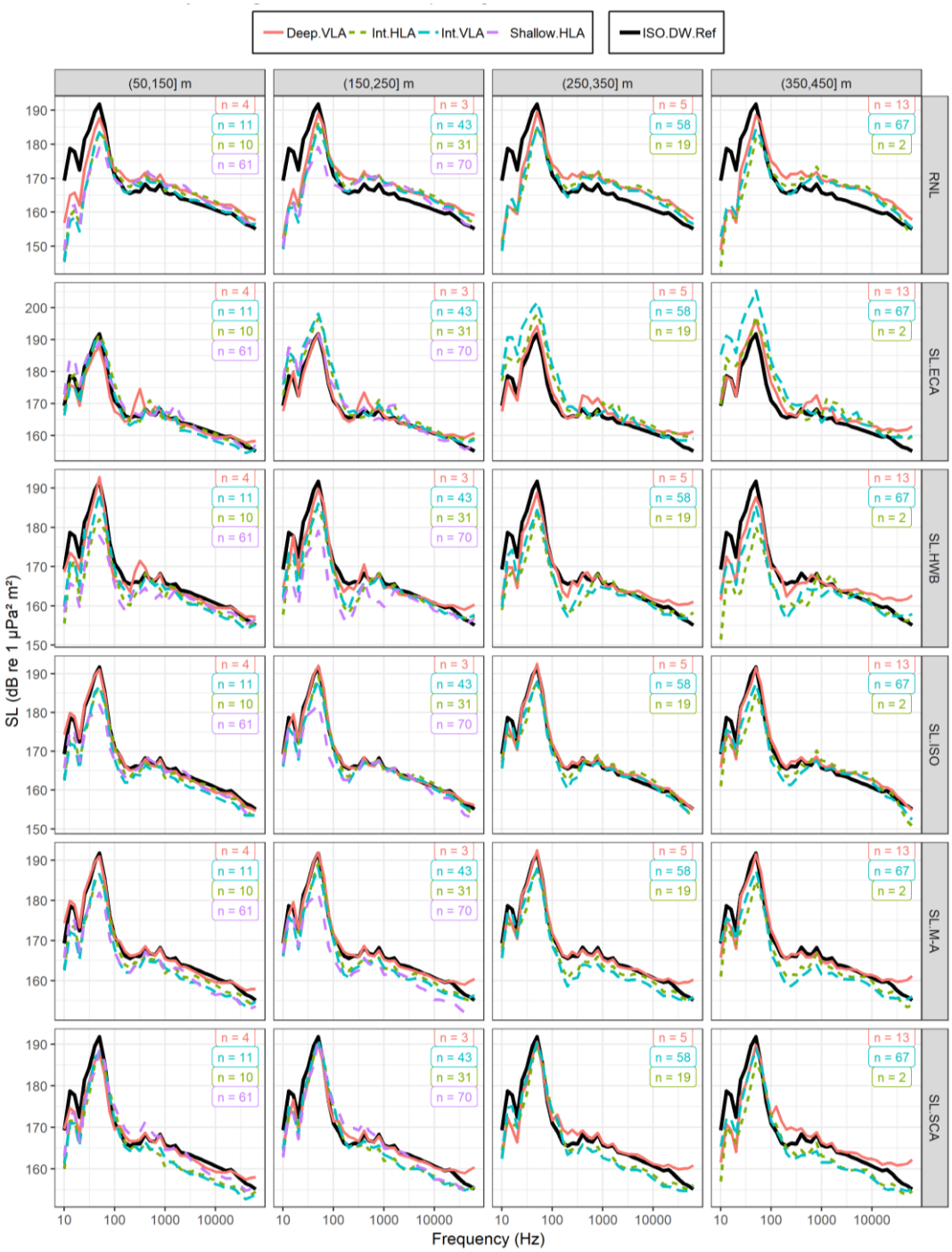

Figure 44. Vessel A: Mean source level versus frequency for array-average hydrophone measurements with speeds through water between 20 and 21 knots. Columns show different source level (SL) metrics and rows show different closest point of approach (CPA) bins from the arrays. Coloured lines show different HLA and VLA combinations. Black lines show reference measurements (SL.ISO) from the deep VLA. The ‘n’ values indicate the number of individual measurements contributing to the average.

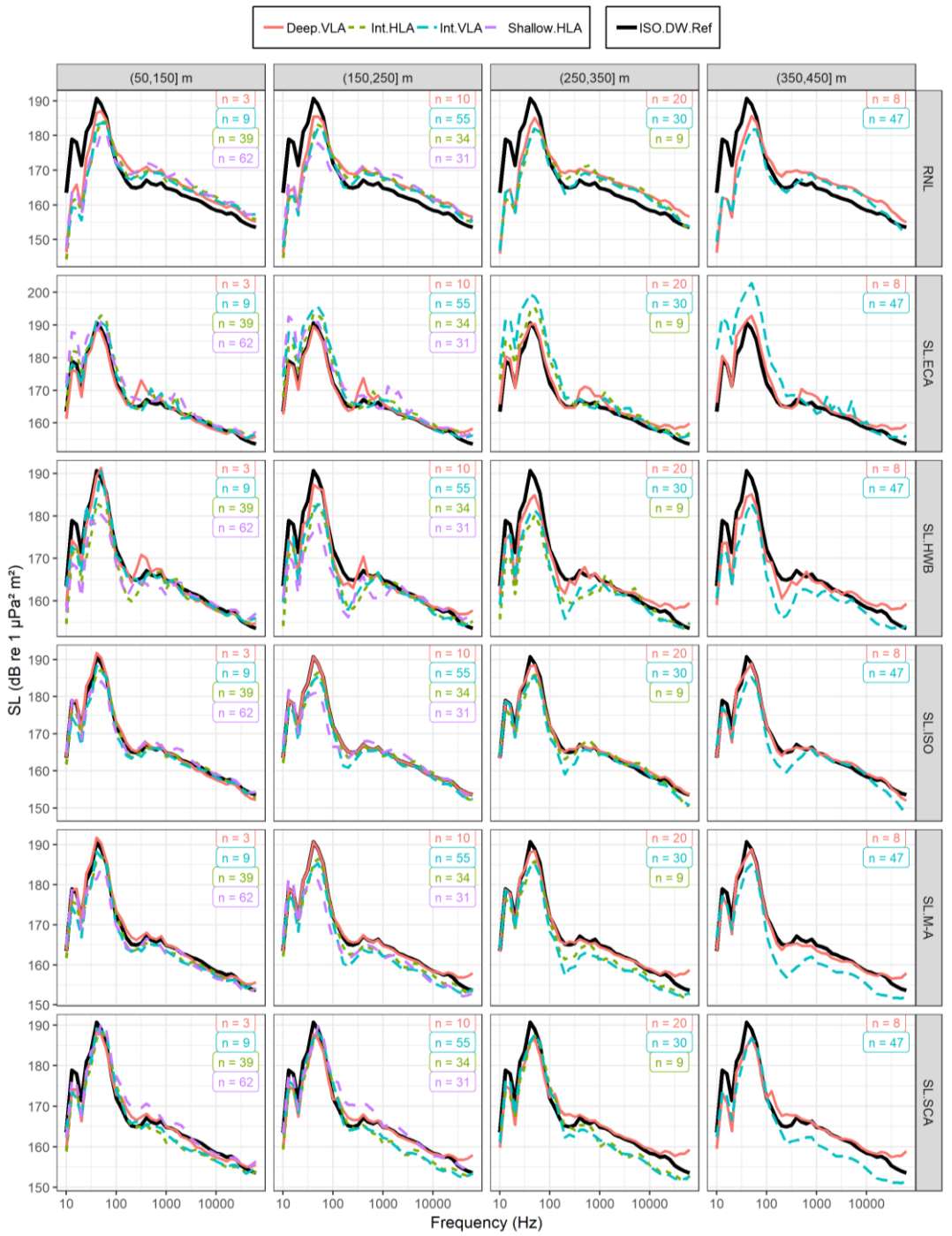

Figure 45. Vessel B: Mean source level versus frequency for array-average hydrophone measurements with speeds through water between 20 and 21 knots. Columns show different source level (SL) metrics and rows show different closest point of approach (CPA) bins from the arrays. Coloured lines show different HLA and VLA combinations. Black lines show reference measurements (SL.ISO) from the deep VLA. The 'n' values indicate the number of individual measurements contributing to the average.

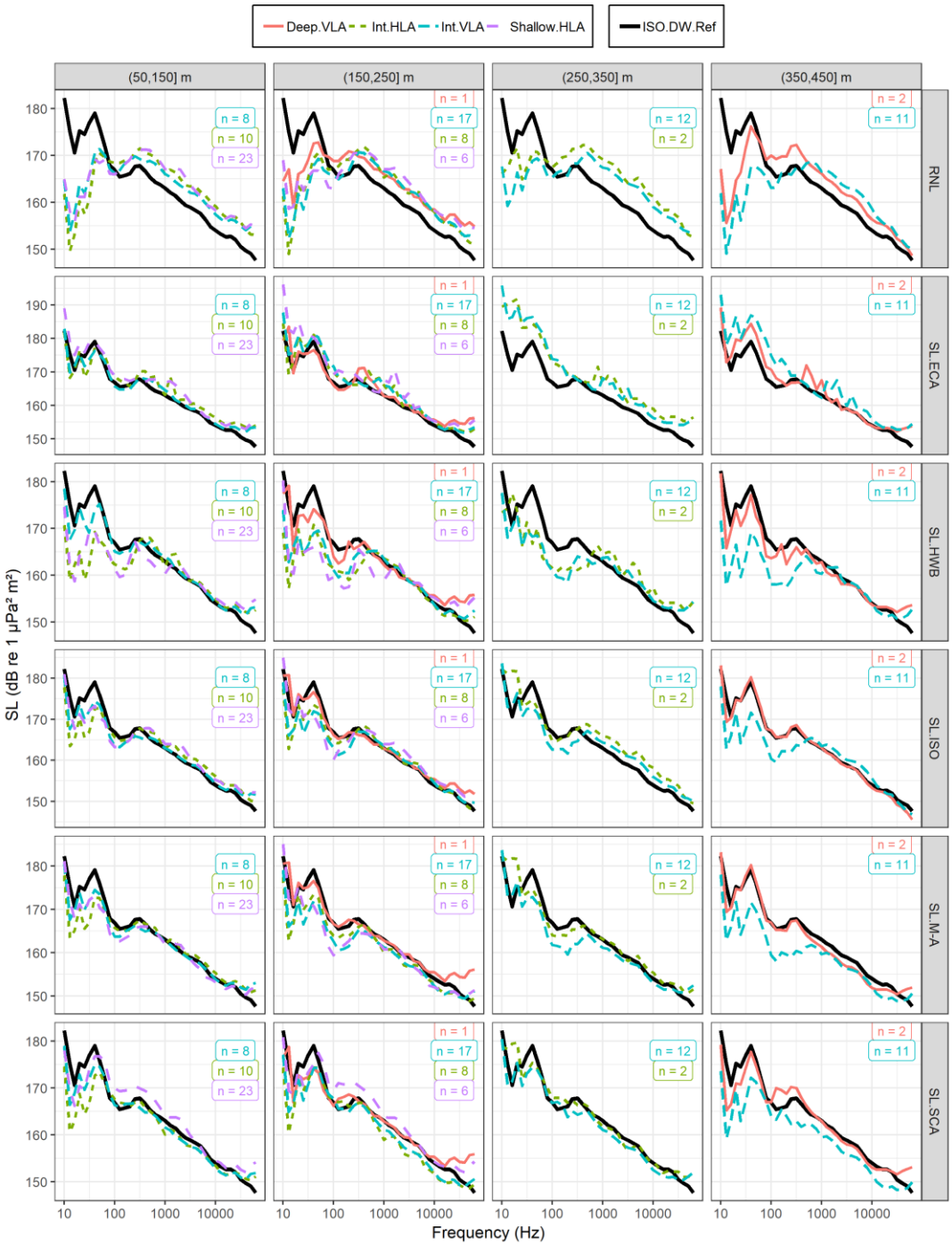

Figure 46. Vessel C: Mean source level versus frequency for array-average hydrophone measurements with speeds through water between 20 and 21 knots. Columns show different source level (SL) metrics and rows show different closest point of approach (CPA) bins from the arrays. Coloured lines show different HLA and VLA combinations. Black lines show reference measurements (SL.ISO) from the deep VLA. The ‘n’ values indicate the number of individual measurements contributing to the average.

4.2.6. Array Geometry Comparisons

To compare the performance of the different hydrophone array geometries deployed during the experiment, ten measurements of each vessel were identified at each array, with speeds between 20–21 knots and CPA distances closest to the planned measurement funnel at each site. The single-node and array-averaged metrics for these ten measurements were then arithmetically averaged and compared to reference source levels (Figures 47 to 51). Note that single-node comparisons are not shown for the Meyer-Audoly metric as it was only intended for use with array-averaged data. The means and standard deviations of the vessel CPA distances and measurement grazing angles to the array nodes were calculated for each set of ten measurements (Tables 12 and 13). Differences between hydrophone array channels are analyzed in more detail in Appendix E.

As expected, single-node values exhibited more variability than the array-average values. Furthermore, the VLA nodes closer to the seabed and HLA nodes closer to the vessel track matched the reference values more closely than those near the sea-surface and farther from the vessel track, respectively. On all arrays, the observed mismatch was greater for vessel C than for vessels A and B, which was most likely due to the lower quality of the reference source levels for this vessel (see Section 4.2.3).

Notwithstanding the difficulties with the vessel C comparisons, all array-averaged source level metrics (i.e., excluding RNL) generally did a good job of matching reference levels on the deep VLA (D.VLA.150) across the entire frequency range. At the intermediate site, the various metrics generally matched reference levels better on the two nearest arrays (I.HLA.121 and I.VLA.150) than on the one farthest array (I.VLA.350). The main issue with the array-averaged metrics at the intermediate site was underestimation of the low-frequency reference levels, particularly at longer ranges. On the HLA at the shallow site, mismatch for all metrics was generally greater than at the other two sites. This was particularly the case for low frequencies, although the SCA and ECA metrics still appeared to perform reasonably well in this frequency range.

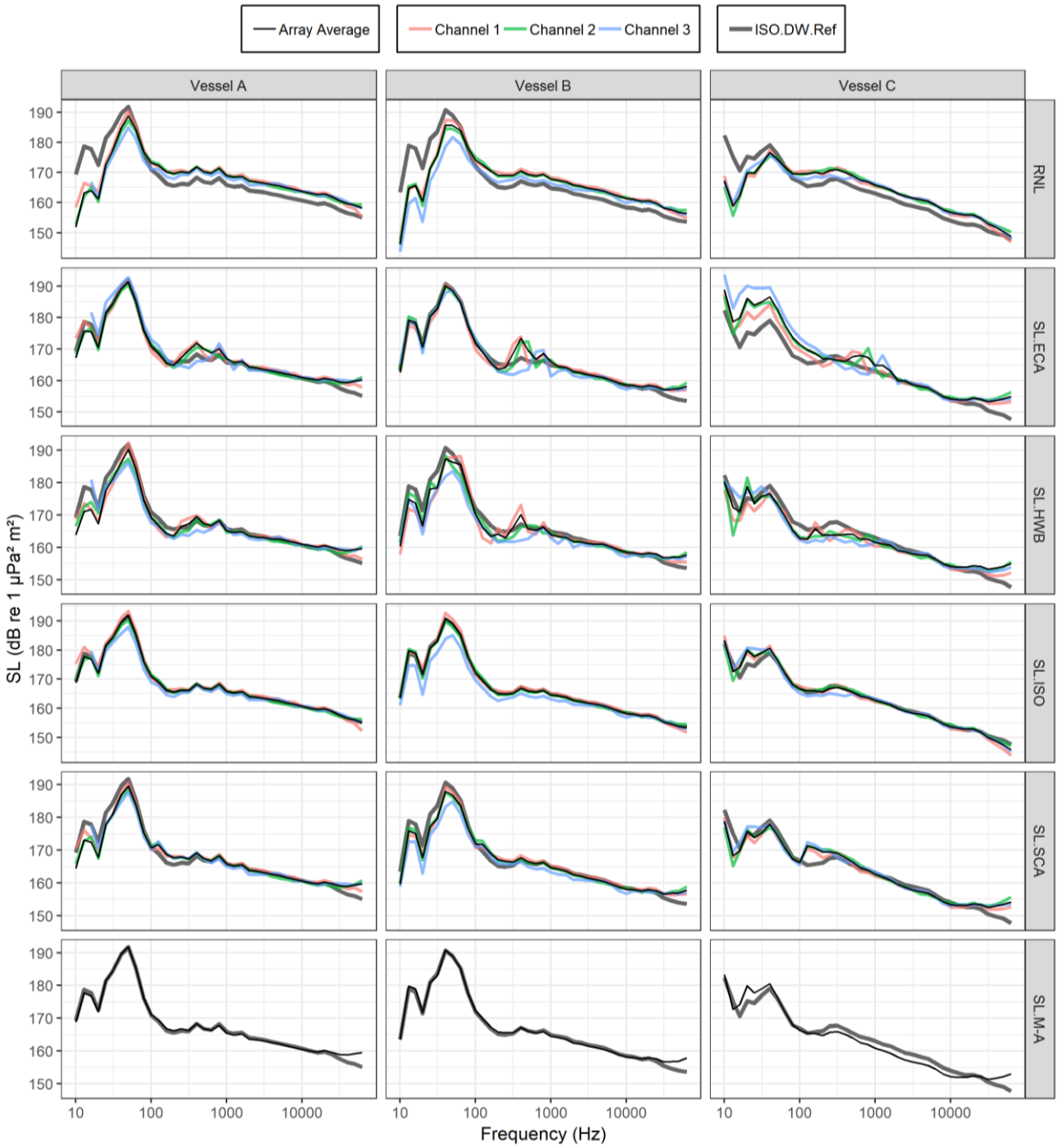

Figure 47. Comparisons of mean source levels for vessels A–C on different channels of deep VLA (D.VLA.150). Average values are shown for the ten measurements of each vessel with closest point of approach (CPA) closest to 215 m from the VLA and speeds through water between 20–21 knots. Channels 1, 2, and 3 refer to the bottom, middle, and top hydrophones, respectively. Coloured solid lines indicate single-node values and dashed black lines indicate array-average values. See Figure E-1 for differences between individual hydrophone channels.

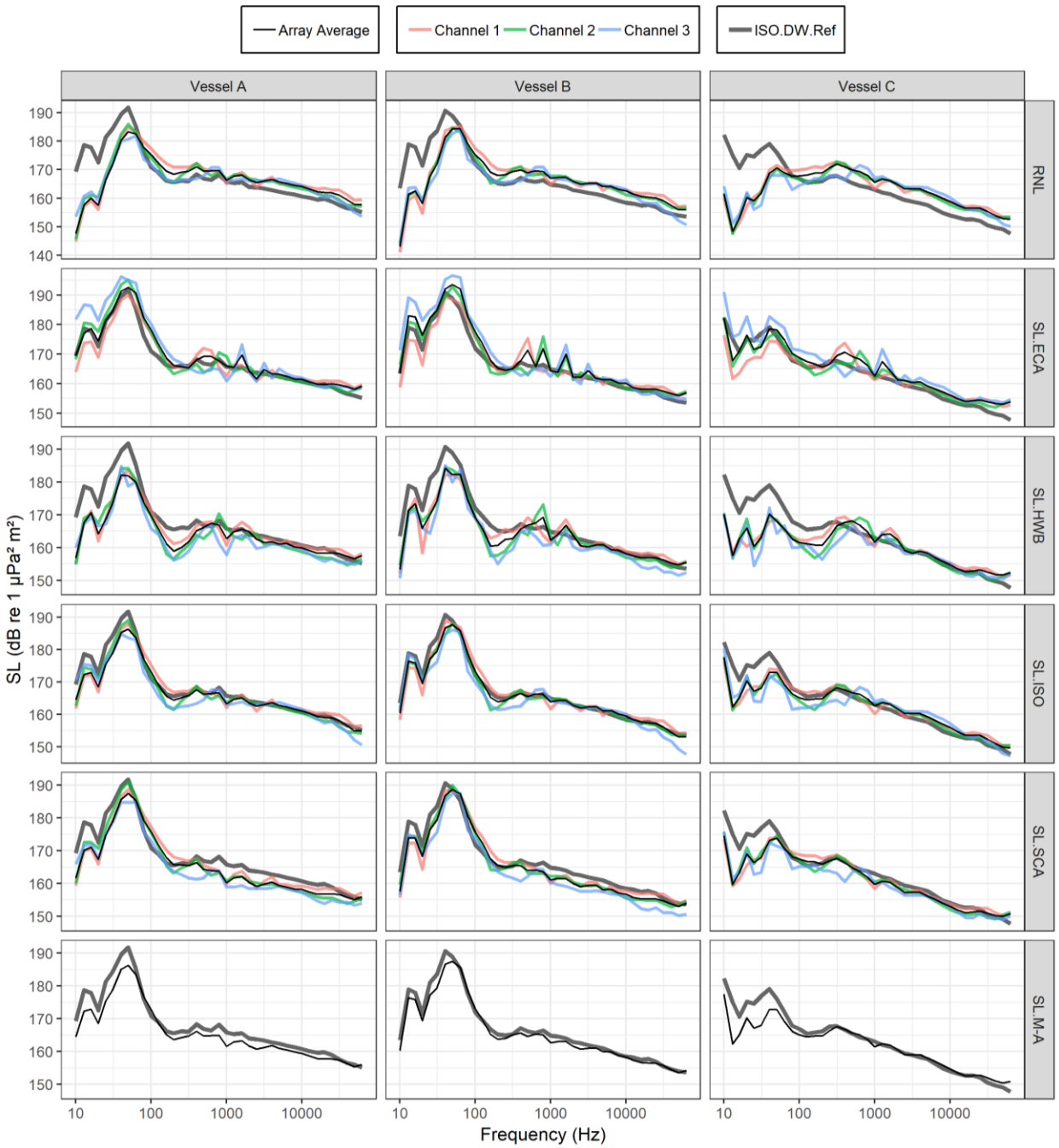

Figure 48. Comparisons of mean source levels for vessels A–C on different channels of the 121 m intermediate HLA (I.HLA.121). Average values are shown for the ten measurements of each vessel with closest point of approach (CPA) closest to 121 m from the HLA and speeds through water between 20–21 knots. Channels 1, 2, and 3 refer to the nearest, middle, and farthest hydrophones from the vessel track, respectively. Coloured solid lines indicate single-node values and dashed black lines indicate array-average values. See Figure E-2 for differences between individual hydrophone channels.

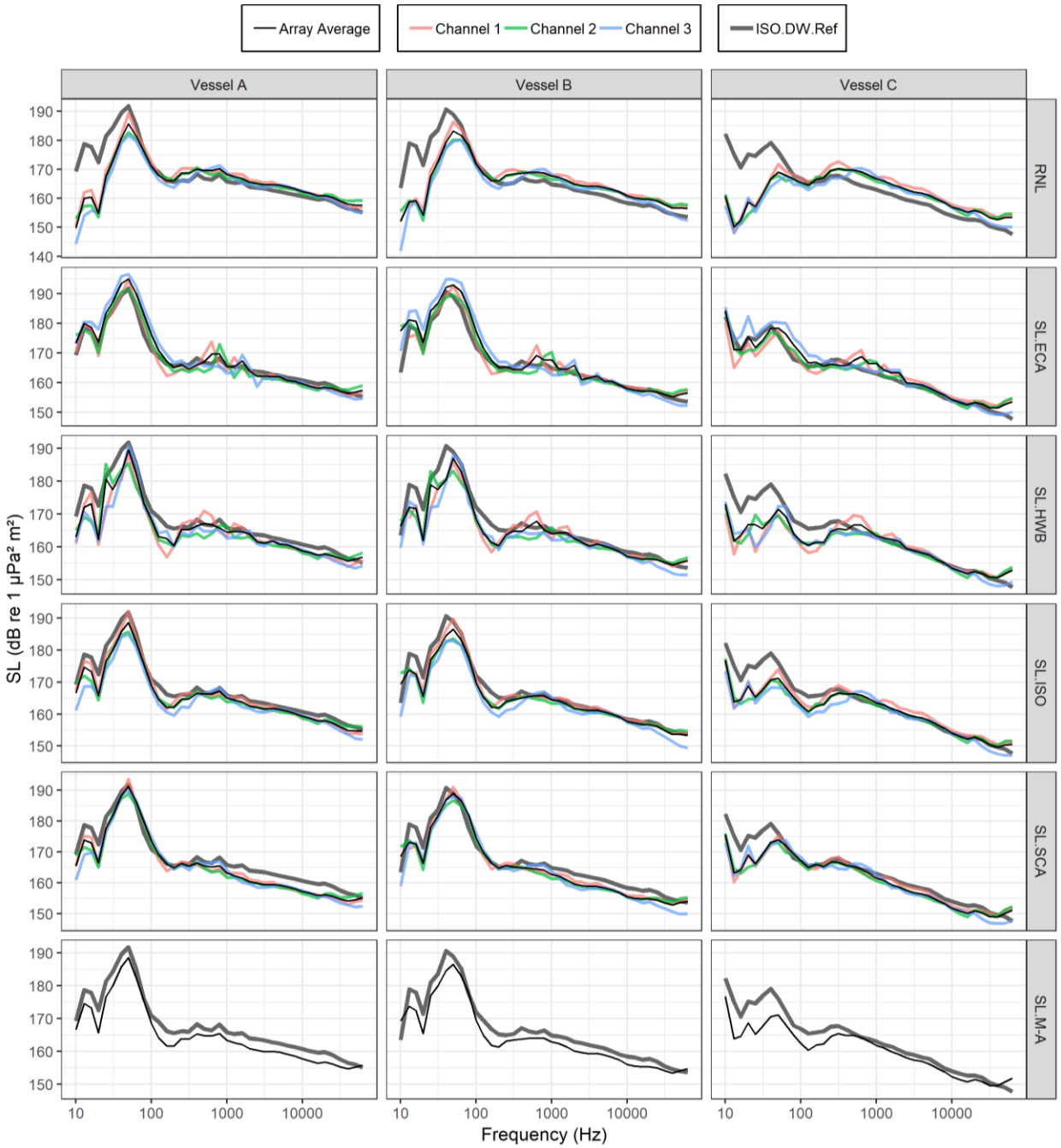

Figure 49. Comparisons of mean source levels for vessels A–C on different channels of the 150 m intermediate VLA (I.VLA.150). Average values are shown for the ten measurements of each vessel with closest point of approach (CPA) closest to 150 m from the VLA and speeds through water between 20–21 knots Channels 1, 2, and 3 refer to the bottom, middle, and top hydrophones, respectively. Coloured solid lines indicate single-node values and dashed black lines indicate array-average values. See Figure E-3 for differences between individual hydrophone channels.

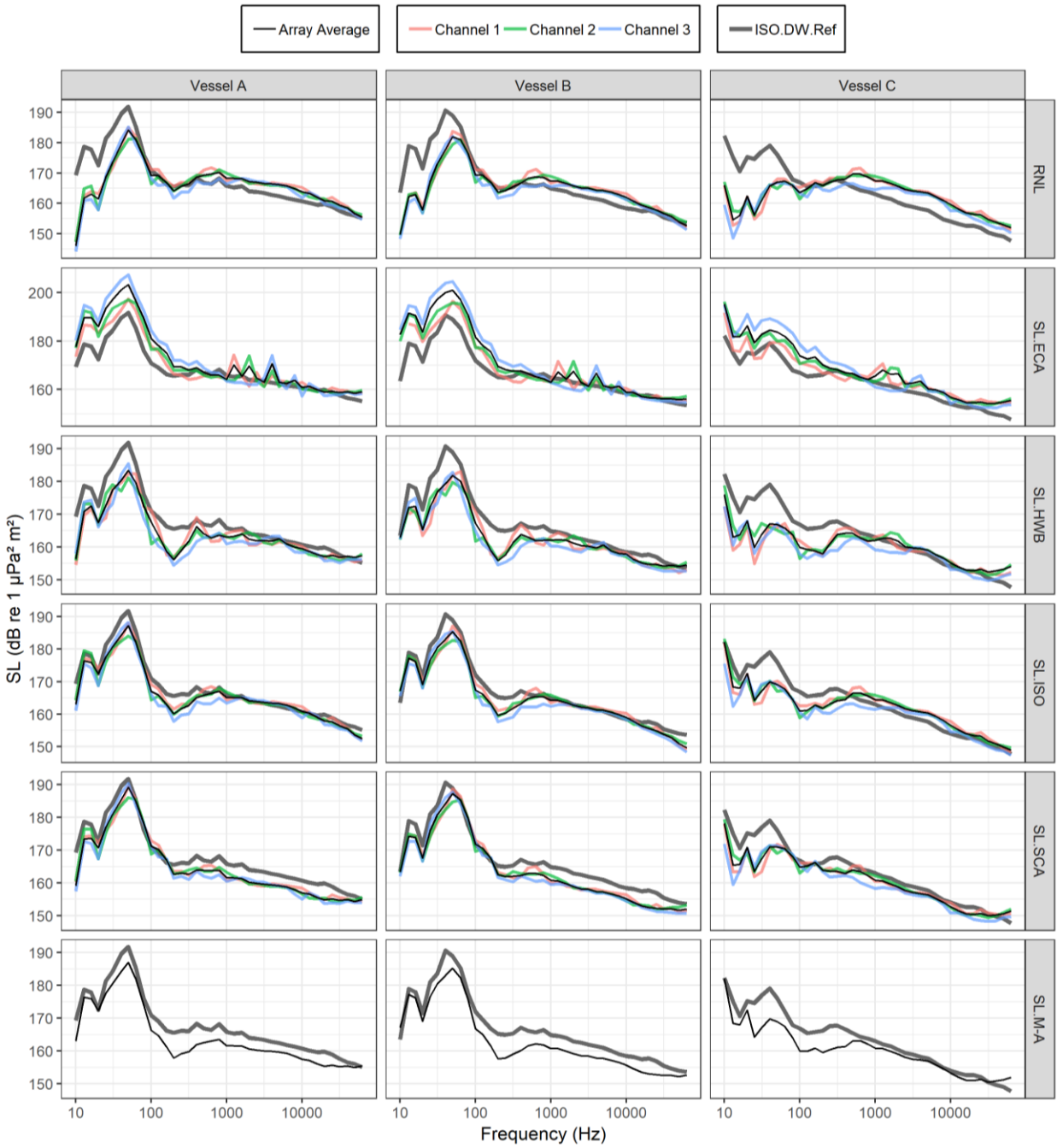

Figure 50. Comparisons of mean source levels for vessels A–C on different channels of the 350 m intermediate VLA (I.VLA.350). Average values are shown for the ten measurements of each vessel with closest point of approach (CPA) closest to 350 m from the VLA and speeds through water between 20–21 knots. Channels 1, 2, and 3 refer to the bottom, middle, and top hydrophones, respectively. Coloured solid lines indicate single-node values and dashed black lines indicate array-average values. See Figure E-4 for differences between individual hydrophone channels.

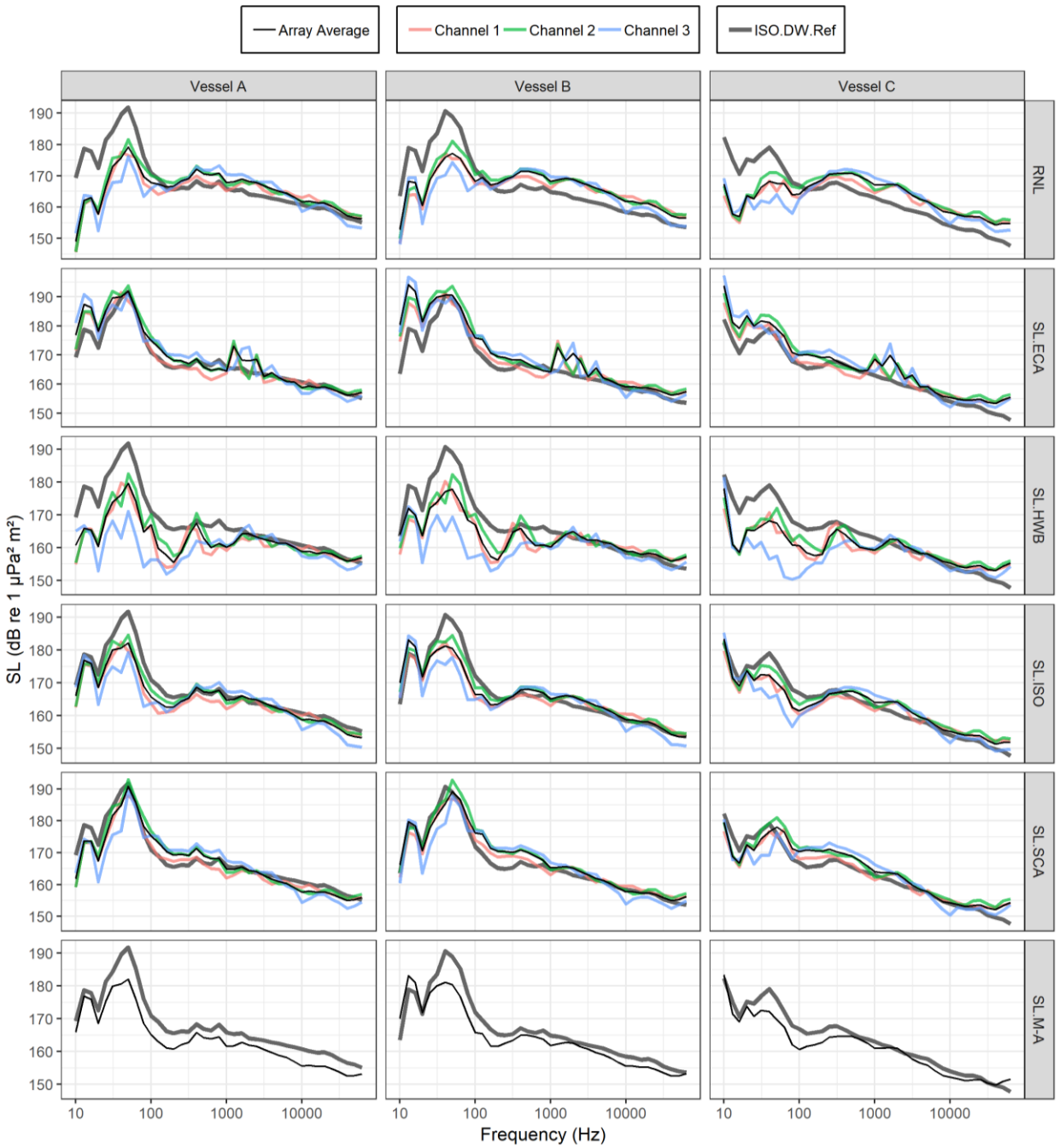

Figure 51. Comparisons of mean source levels for vessels A–C on different channels of the 170 m shallow HLA (S.HLA.170). Average values are shown for the ten measurements of each vessel with closest point of approach (CPA) closest to 170 m from the HLA and speeds through water between 20–21 knots. Channels 1, 2, and 3 refer to the nearest, middle, and farthest hydrophones from the vessel track, respectively. Coloured solid lines indicate single-node values and dashed black lines indicate array-average values. See Figure E-5 for differences between individual hydrophone channels.

Table 12. Mean (± standard deviation) grazing angles at each array node for source level measurements of vessels A–C. Values are shown for the ten measurements of each vessel with closest point of approach (CPA) closest to the ideal geometry for each line array and speeds through water between 20–21 knots.

Array	Hydrophone channel	Grazing Angle (°)		
		Vessel A	Vessel B	Vessel C
D.VLA.150	Channel 1	40.2 ± 9.6	39.3 ± 3.0	22.1 ± 7.1
	Channel 2	31.1 ± 8.8	29.9 ± 2.6	16 ± 5.7
	Channel 3	17.1 ± 4	18.6 ± 1.2	10.3 ± 4.4
I.HLA.121	Channel 1	23.5 ± 4.1	28.6 ± 1.0	29.2 ± 5.4
	Channel 2	14.3 ± 1.9	16.6 ± 0.4	16.9 ± 2.1
	Channel 3	7.7 ± 0.4	8.5 ± 0.1	8.4 ± 0.5
I.VLA.150	Channel 1	21.5 ± 1.3	21.1 ± 2.3	19.7 ± 3.5
	Channel 2	14.7 ± 1.0	14.3 ± 1.6	14.2 ± 3.3
	Channel 3	7.3 ± 0.5	7.1 ± 0.8	7.2 ± 1.8
I.VLA.350	Channel 1	9.6 ± 0.1	9.7 ± 0.5	9.6 ± 1.2
	Channel 2	6.4 ± 0.1	6.4 ± 0.3	6.4 ± 0.8
	Channel 3	3.1 ± 0.1	3.1 ± 0.2	3.1 ± 0.4
S.HLA.170	Channel 1	10.2 ± 0.1	10.2 ± 0.3	11.2 ± 1.1
	Channel 2	9.9 ± 0.1	9.9 ± 0.2	10.8 ± 0.9
	Channel 3	6.9 ± 0.1	6.9 ± 0.1	7.2 ± 0.4

Table 13. Mean (± standard deviation) closest point of approach (CPA) distances at each array for source level measurements of vessels A–C. Values are shown for the ten measurements of each vessel with closest point of approach (CPA) closest to the ideal geometry for each line array and speeds through water between 20–21 knots.

Array	CPA (m)		
	Vessel A	Vessel B	Vessel C
D.VLA.150	223 ± 69	218 ± 22	467 ± 108
I.HLA.121	154 ± 26	120 ± 5	121 ± 24
I.VLA.150	149 ± 10	155 ± 16	161 ± 32
I.VLA.350	350 ± 4	349 ± 16	353 ± 41
S.HLA.170	170 ± 2	169 ± 4	155 ± 15

4.2.7. Residual Differences from Reference Source Levels

The performance of the different metrics and array geometries was quantified by calculating statistics of the residual differences between measured decidecade band source levels and their reference values. Residuals of the decidecade band source levels were calculated for all URN measurements as the following difference:

$$e_i(f) = L'_{S,i}(f) - L_{S(\mathrm{ref})}(f)$$

where $L_{S,i}{}'(f)$ is the decidecade band source level for measurement i at frequency f, computed using any of the metrics described in Section 2.3, and $L_{S(\mathrm{ref})}(f)$ is the reference source level from the deep VLA for the same vessel and speed bin. Statistics of the residuals were collected inside the following three frequency ranges, for Vessels A and B and speed through water bins between 17–21 knots:

1. The 10 decidecade bands from 10–80 Hz,
2. The 10 decidecade bands from 100–800 Hz, and
3. The 19 decidecade bands above 1000 Hz.

Vessel C was excluded from the residual statistics, as reference measurements for this vessel were of a lower grade than the other two study vessels (see Section 4.2.3). Statistics of the residuals were summarized in box-and-whisker plots for both the single-node and array-averaged measurements (Figures 52 to 57). These statistics were further summarized by calculating the arithmetic mean of the absolute residuals (i.e., $\overline{|e_i(f)|}$) versus CPA bin for the single-node and array-averaged measurements (Figures 58 to 61).

As expected, the results showed that the ISO source level metric had the best match with reference source levels at the deep site. Under ideal circumstances, where URN was identical for each vessel pass, the residual difference of the ISO metric would be zero at the deep site. Thus, residual differences at the deep site are primarily attributable to the fact that vessel URN and measurement geometry were not perfectly repeatable between vessel passes (see Figure 40).

At the intermediate site, the array-average residuals appeared to show that both the VLA and HLA geometries were suitable for reproducing deep-water reference measurements. The HLA geometry appeared to be slightly more robust to variations in CPA distance, but this difference was small. At the shallow site, the array measurements appeared to be less robust to CPA distance, with lowest residuals generally measured at CPA distances less than 150 m to the nearest hydrophone.

Performance of the various metrics may be summarized as follows:

- The RNL metric was generally a poor match to the reference source levels, as expected. Surprisingly, however, RNL performed better than some of the other metrics in the 100–800 Hz frequency range at the intermediate and shallow sites, particularly at longer CPA distances.
- The ECA metric performed well at short CPA distances (<150 m), over all frequency ranges at all sites. However, mismatch of this metric increased at longer CPA distances, indicating that it was less robust to variations in CPA distance than some of the other metrics.
- The HWB metric performed well above 1000 Hz, but at lower frequencies, this metric was generally less robust and tended to have large mismatch compared to the other metrics at the intermediate and shallow sites. Possible reasons for the low-frequency mismatch are discussed in Section 4.3.
- The ISO metric performed well at all sites and frequencies over a wide range of CPA distances. This metric was remarkably robust, given the simplicity of the method. It also worked surprisingly well on the horizontal arrays, given that it was developed for vertical array geometry.
- The M-A metric performed well in the 10–800 Hz frequency range at all sites and CPA distances (with the exception of the 100–800 Hz on the shallow HLA). At 1000 Hz and above, this metric tended to underestimate reference source levels, although the mismatch was smaller at short CPA distances (<150 m).
- The SCA metric also performed well in the 10–800 Hz frequency range at all sites and CPA distances, with lowest single-node residuals generally at shorter CPA distances. At 1000 Hz and above, performance of this metric was best at the shallow and deep sites. As with the M-A method, it tended to underestimate reference source levels at 1000 Hz and above.

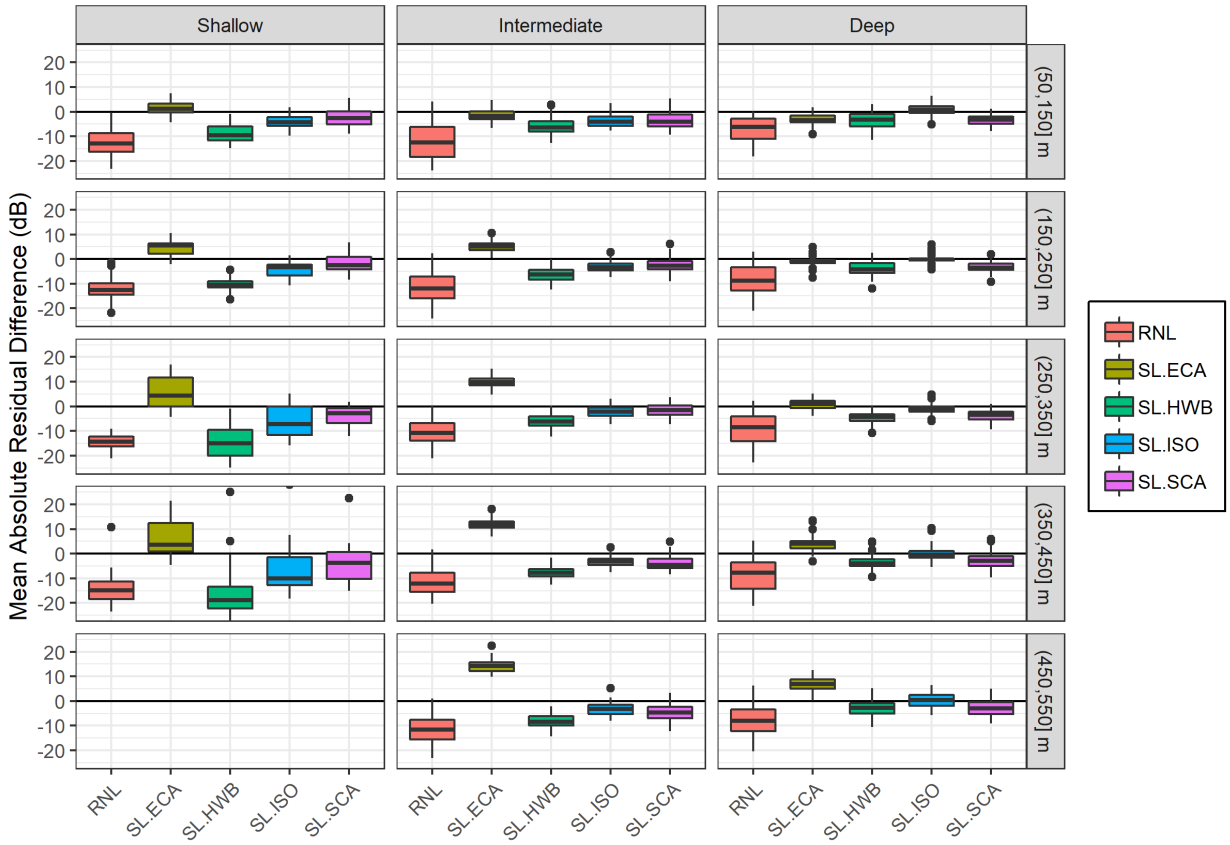

Figure 52. Box-and-whisker plots summarizing residual differences of single-node source level metrics in decidecade bands from 10–80 Hz, relative to the deep-water reference value. Plots include all measurements of vessels A–C between 17–21 knots. Columns show different sites and rows show different closest point of approach (CPA) distance bins.

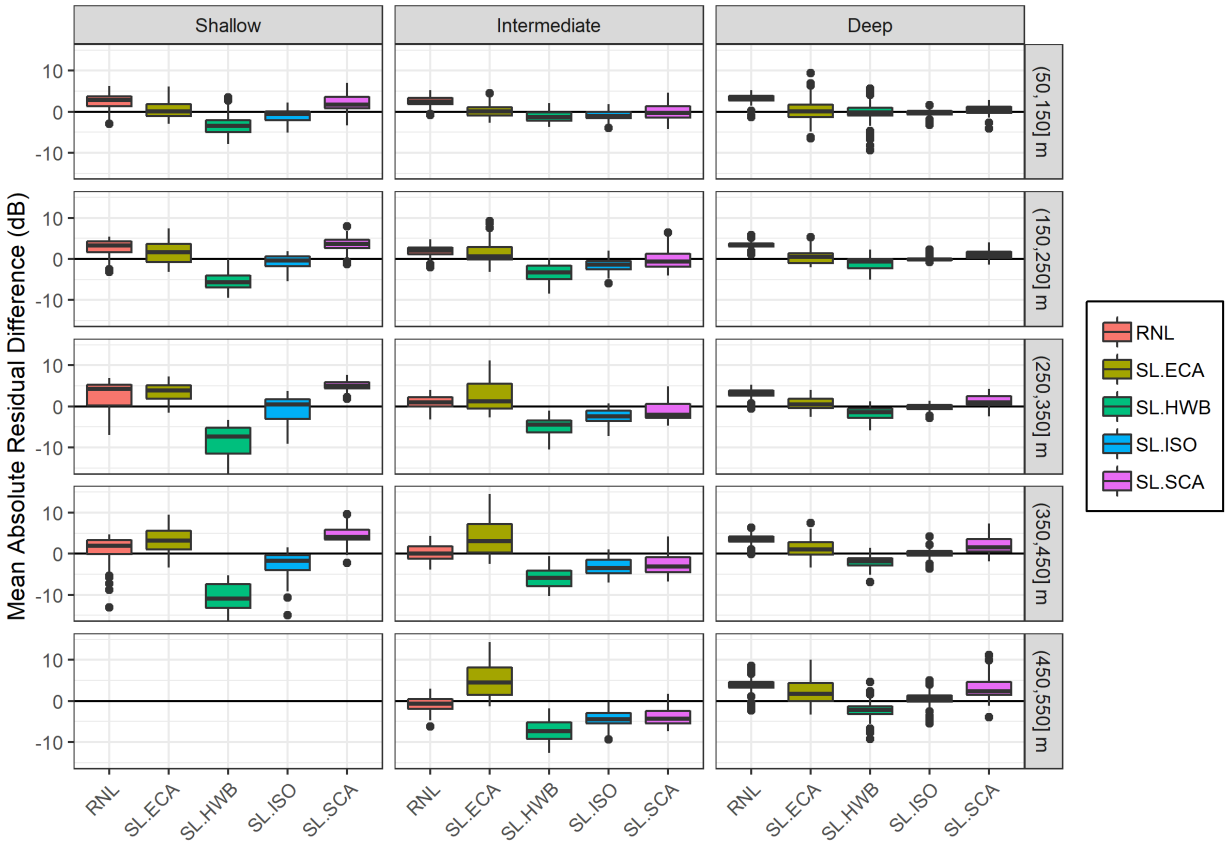

Figure 53. Box-and-whisker plots summarizing residual differences of single-node source level metrics in decidecade bands from 100–800 Hz, relative to the deep-water reference value. Plots include all measurements of vessels A–C between 17–21 knots. Columns show different sites and rows show different closest point of approach (CPA) distance bins.

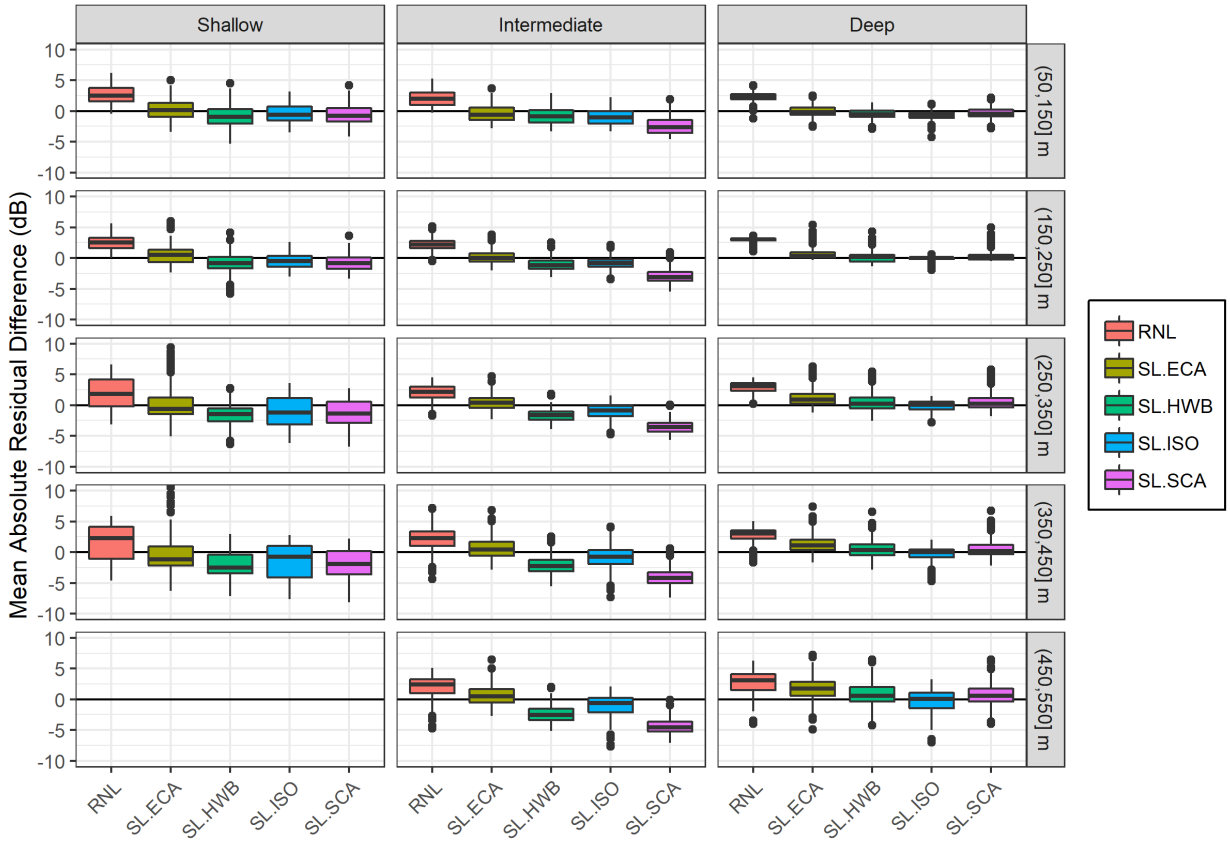

Figure 54. Box-and-whisker plots summarizing residual differences of single-node source level metrics in decidecade bands at 1000 Hz and above, relative to the deep-water reference value. Plots include all measurements of vessels A–C between 17–21 knots. Columns show different sites and rows show different closest point of approach (CPA) distance bins.

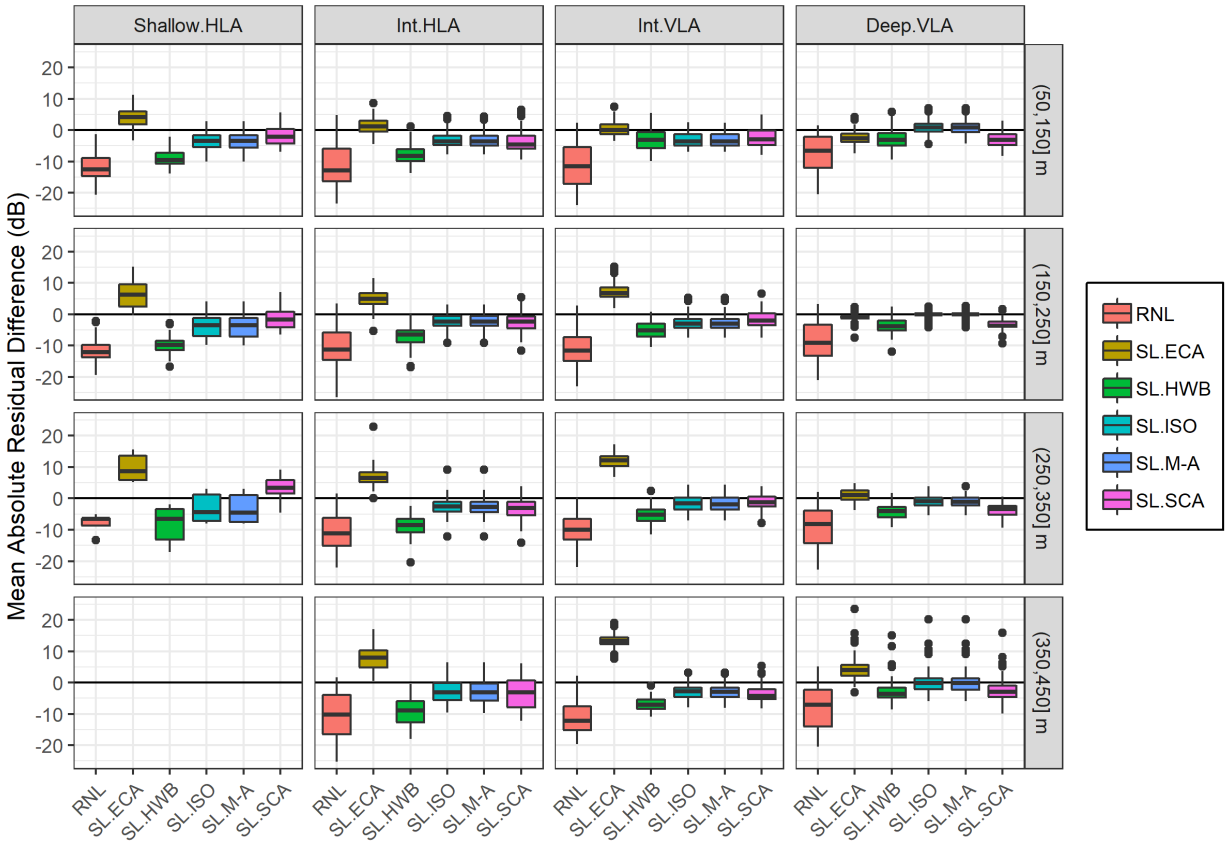

Figure 55. Box-and-whisker plots summarizing residual differences of array-average source level metrics in decidecade bands from 10–80 Hz, relative to the deep-water reference value. Plots include all measurements of vessels A–C between 17–21 knots. Columns show different sites and rows show different closest point of approach (CPA) distance bins.

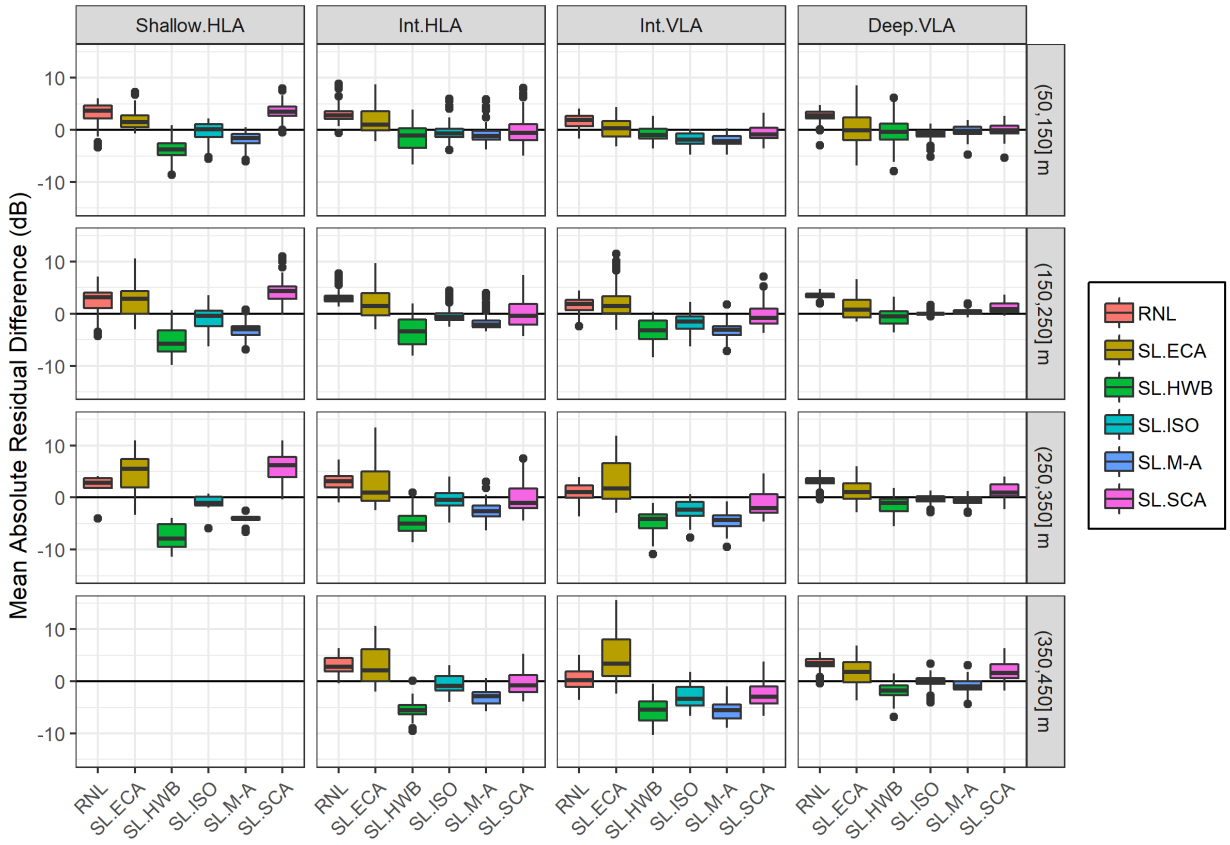

Figure 56. Box-and-whisker plots summarizing residual differences of array-average source level metrics in decidecade bands from 100–800 Hz, relative to the deep-water reference value. Plots include all measurements of vessels A–C between 17–21 knots. Columns show different sites and rows show different closest point of approach (CPA) distance bins.

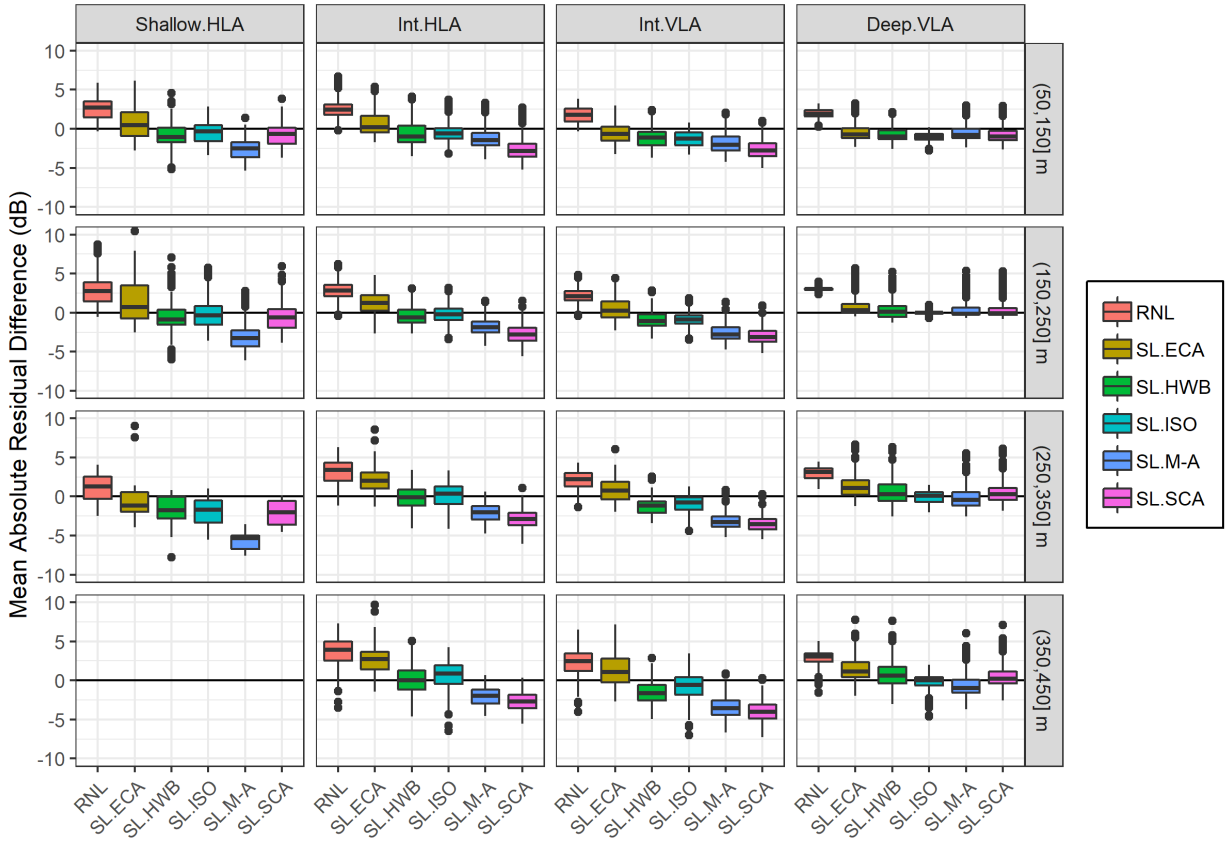

Figure 57. Box-and-whisker plots summarizing residual differences of array-average source level metrics in decidecade bands at 1000 Hz and above, relative to the deep-water reference value. Plots include all measurements of vessels A–C between 17–21 knots. Columns show different sites and rows show different closest point of approach (CPA) distance bins.

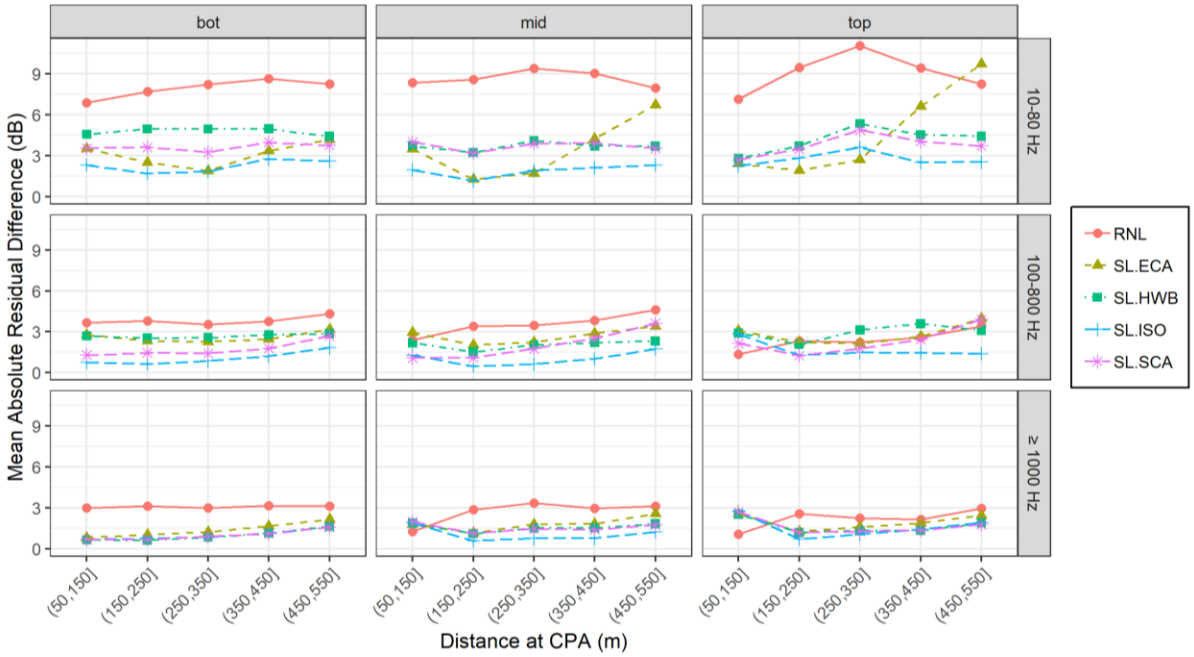

Figure 58. Mean absolute residual differences of single-node source level metrics at the deep site versus closest point of approach (CPA) distance bins. Columns show different array nodes (bot = bottom nodes, mid = middle VLA nodes, top = top VLA nodes) and rows show different decidecade band ranges.

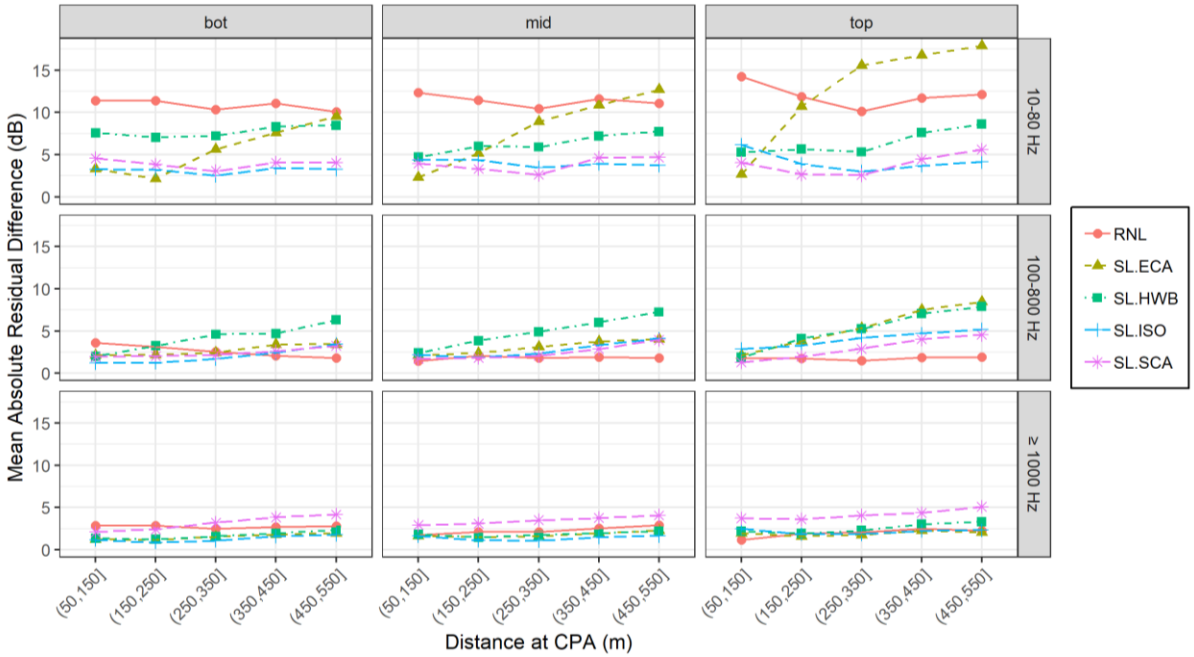

Figure 59. Mean absolute residual differences of single-node source level metrics at the intermediate site versus closest point of approach (CPA) distance bins. Columns show different array nodes (bot = bottom nodes, mid = middle VLA nodes, top = top VLA nodes) and rows show different decidecade band ranges.

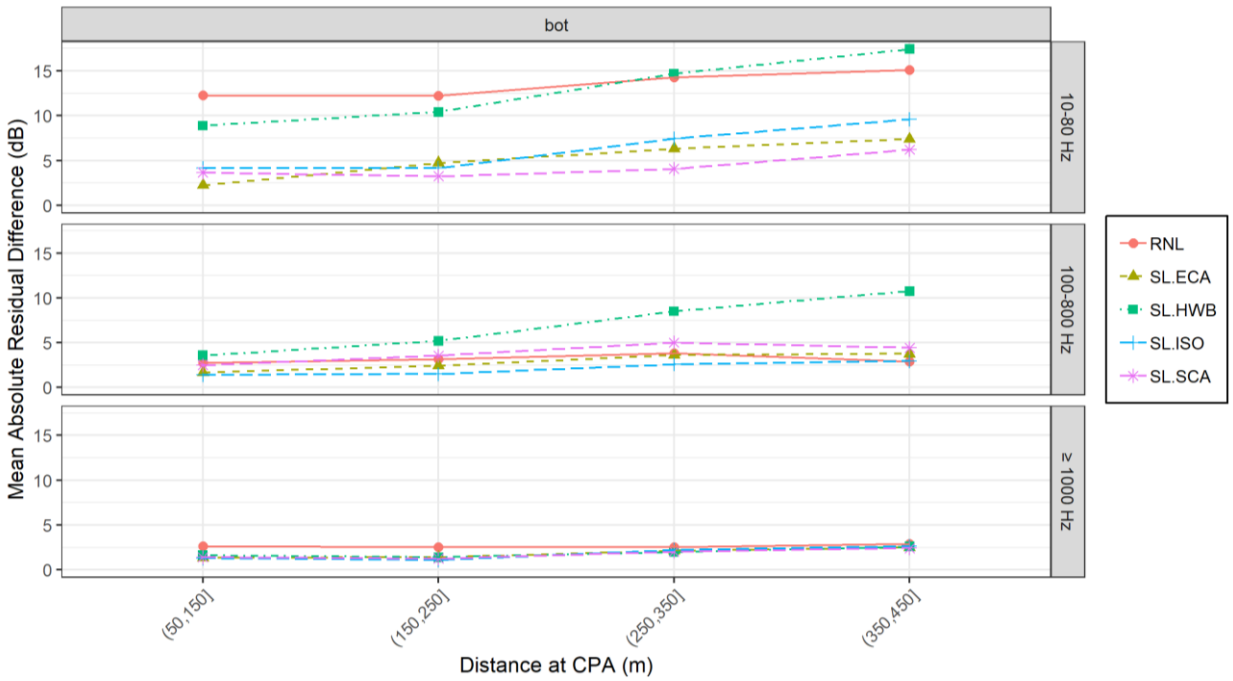

Figure 60. Mean absolute residual differences of single-node source level metrics at the shallow site versus closest point of approach (CPA) distance bins. Note that all hydrophones were bottom nodes at the shallow site. Rows show different decidecade band ranges.

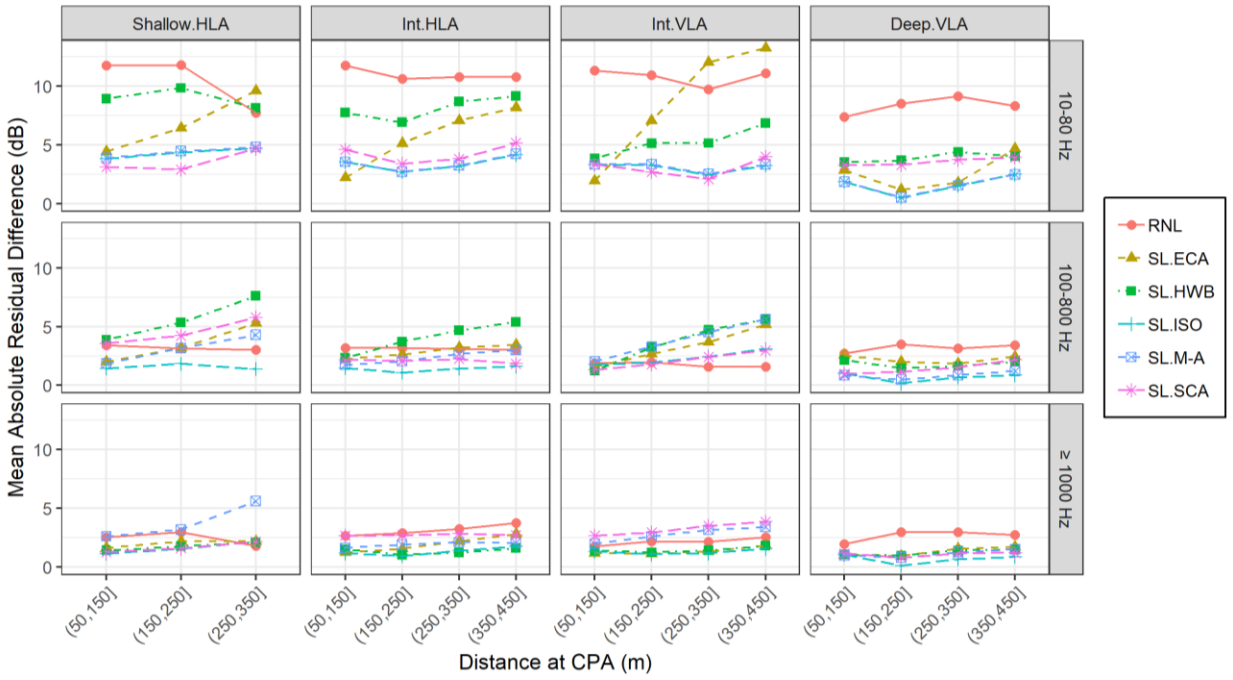

Figure 61. Mean absolute residual differences of array-averaged source level metrics versus closest point of approach (CPA) distance bins. Columns show different arrays and rows show different decidecade band ranges.

4.2.8. Effect of Environmental Mismatch

The effect of environmental mismatch on the SCA and M-A source level metrics was investigated by adjusting parameters related to the influence of the seabed on propagation loss. With the SCA metric (Section 2.3.4), the influence of the seabed is determined by the critical angle parameter, ψ. Three different ψ parameters were evaluated for the SCA metric:

1. The maximum *a posteriori* (MAP) estimate of the frequency-dependent critical angle, $\psi(f)$, as determined by the geoacoustic inversion procedure (see Figure 33). This was the baseline value.
2. A frequency-independent critical angle, $\psi = 33.4°$, representing a homogeneous sand seabed with medium grain size ($\phi = 1.5$) and a sound speed ratio of $\frac{c_P}{c_w} = 1.1978$.
3. A frequency-independent critical angle, $\psi = 17.4°$, representing a homogeneous silt seabed with medium grain size ($\phi = 5.5$) and a sound speed ratio of $\frac{c_P}{c_w} = 1.0479$.

With the M-A metric (Section 2.3.5), the influence of the seabed is determined by the parameter ε, which may be adjusted to represent a soft or hard seabed. Two different ε values were evaluated for the M-A metric:

1. A value of $\varepsilon = 1$, representing a soft sand seabed. This was the baseline value.
2. A value of $\varepsilon = 2$, representing a hard basalt seabed.

Source levels computed using the different seabed parameters were compared on the each of the five different line arrays using URN measurements between 20–21 knots for each vessel, within a fixed range of CPA distances (Figures 62 to 66).

For the SCA metric, source levels were insensitive to environmental mismatch on the deep VLA, which was consistent with the expectation that the seabed's influence on propagation loss is weak in deep water. The seabed type was more influential at the intermediate site, where environmental mismatch appeared to have a greater influence at longer CPA distances (i.e., on I.VLA.350). Interestingly, low-frequency mismatch on the intermediate arrays was improved for the silt ψ parameter, compared to the MAP estimate, although this was not the case at higher frequencies. Sensitivity of the SCA metric to environmental mismatch appeared to be greatest at the shallow HLA, and the alternate ψ values did not appear to improve the mismatch at this site.

For the M-A metric, source levels were equally sensitive to environmental mismatch on all line arrays and at all sites. This was expected because the influence of the ε parameter does not explicitly depend on source-receiver geometry or water depth. In this regard, ε behaves more as an empirical parameter rather than a physical parameter. The $\varepsilon = 2$ seabed model did not improve the mismatch of the M-A source level estimates on any of the arrays, but it should be noted that this represents a basalt seabed type (i.e., with compressional-wave speed of 5.25 km/s), which was significantly different from the inverted seabed properties at the three test sites.

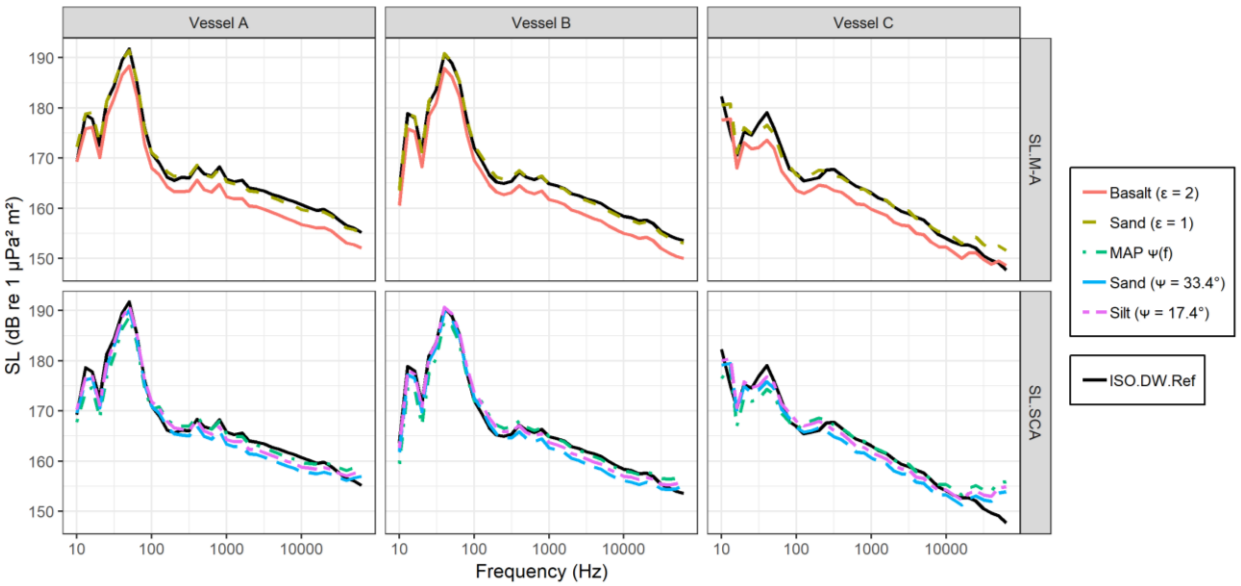

Figure 62. Examination of the effect of environmental mismatch on the SCA and M-A source level metrics on the deep VLA, for measurements with closest point of approach (CPA) distances between 50–250 m and speeds between 20–21 knots. Columns show different vessels and rows show different metrics.

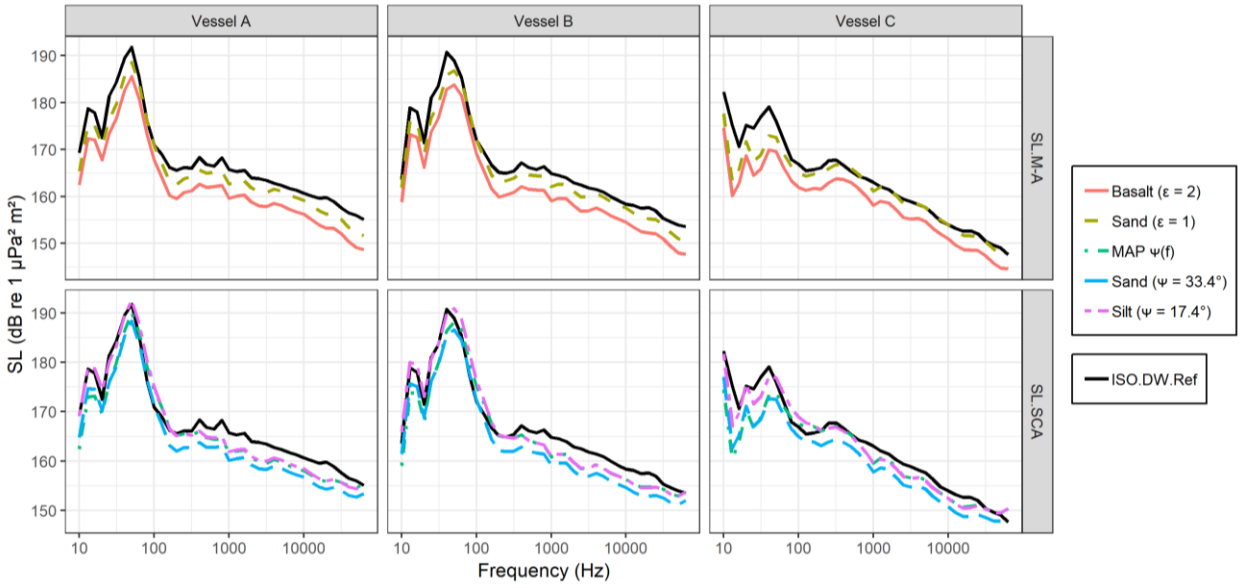

Figure 63. Examination of the effect of environmental mismatch on the SCA and M-A source level metrics on the 121 m intermediate HLA, for measurements with closest point of approach (CPA) distances between 50–250 m and speeds between 20–21 knots. Columns show different vessels and rows show different metrics.

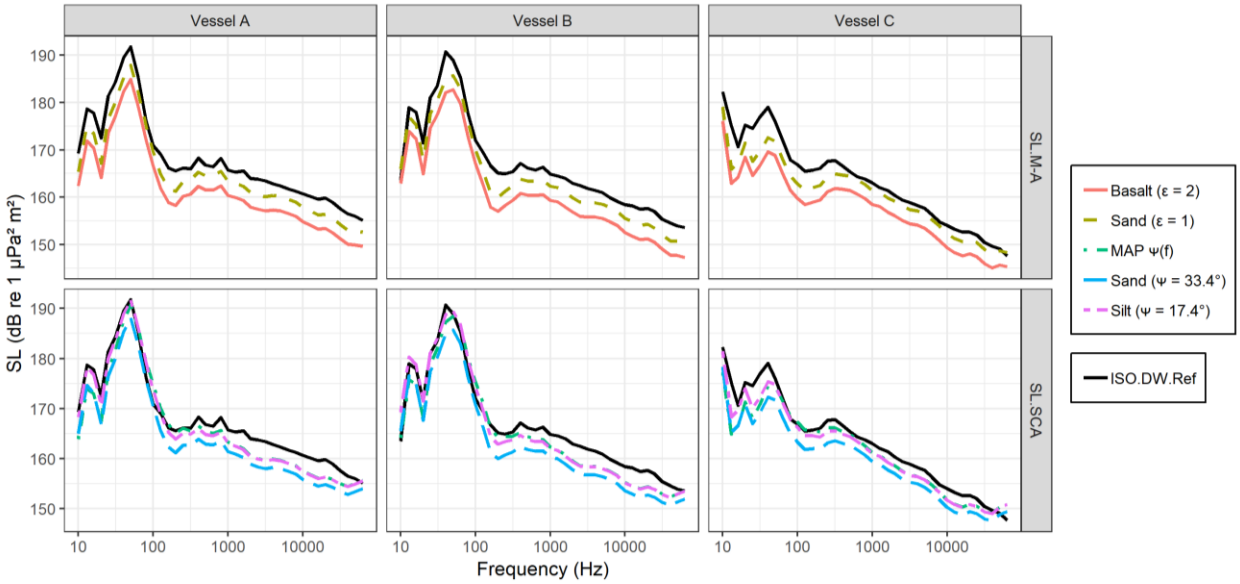

Figure 64. Examination of the effect of environmental mismatch on the SCA and M-A source level metrics on the 150 m intermediate VLA, for measurements with closest point of approach (CPA) distances between 50–250 m and speeds between 20–21 knots. Columns show different vessels and rows show different metrics.

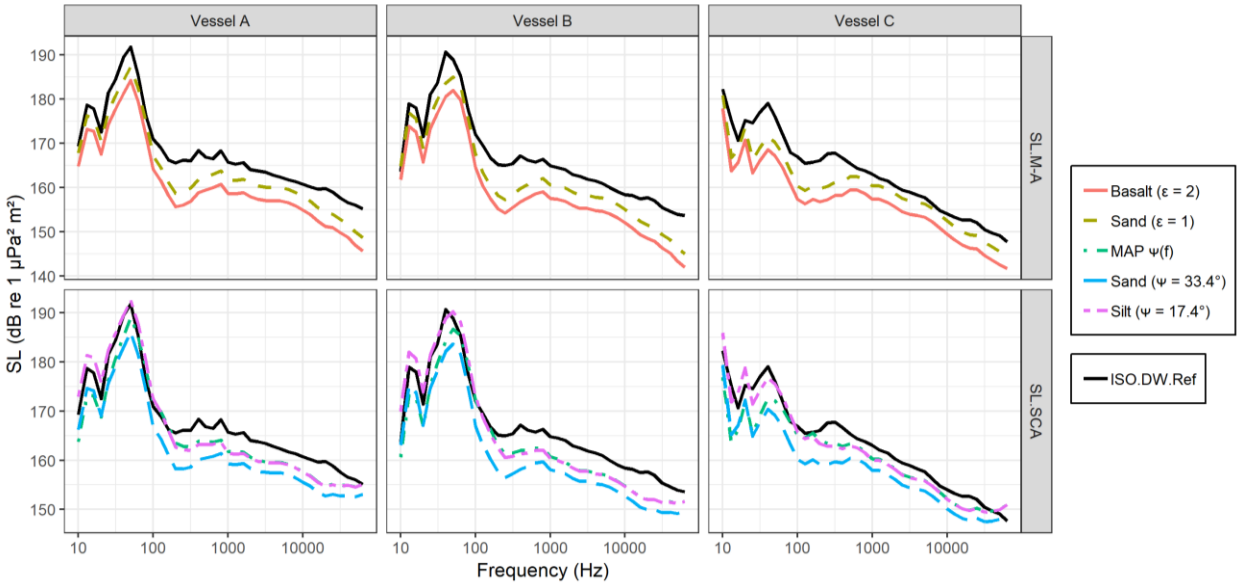

Figure 65. Examination of the effect of environmental mismatch on the SCA and M-A source level metrics on the 350 m intermediate VLA, for measurements with closest point of approach (CPA) distances between 250–450 m and speeds between 20–21 knots. Columns show different vessels and rows show different metrics.

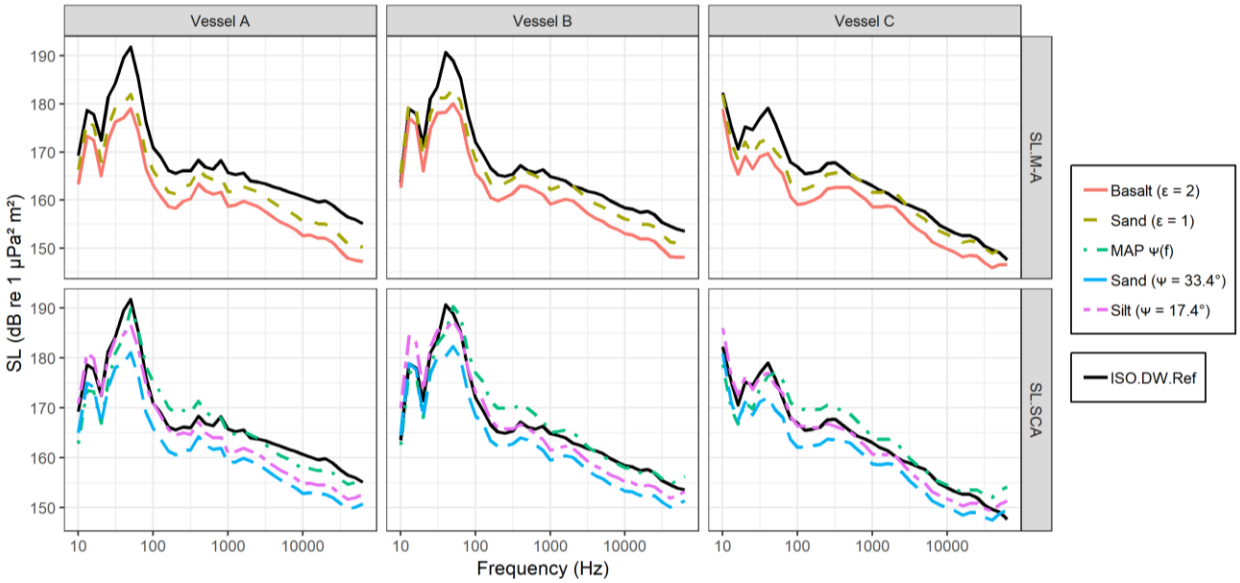

Figure 66. Examination of the effect of environmental mismatch on the SCA and M-A source level metrics on the 150 m shallow HLA, for measurements with closest point of approach (CPA) distances between 50–250 m and speeds between 20–21 knots. Columns show different vessels and rows show different metrics.

4.2.9. Adjusted Source Levels

Adjusted source levels for four of the array-averaged URN metrics (ECA, HWB, SCA, and M-A) were computed according to the methods described in Section 2.3.6 and compared against reference RNL values for vessels A–C (Figure 67). Reference RNL values were based on the adjusted ISO reference source levels from the deep VLA (see Section 4.2.3). Note that adjusted source levels were not computed for the ISO metric, since this is, by definition, equivalent to measured RNL. For each array, the comparisons were based on ten vessel measurements with speeds between 20–21 knots and CPA distances closest to the planned measurement funnel (i.e., those measurements identified in Section 4.2.5).

The performance of the various adjusted source level metrics, in relation to the reference RNL, was effectively identical to their non-adjusted counterparts. This is because the formula used for transforming RNL to ISO source levels is the exact inverse of the formula used for transforming source levels to adjusted source levels (see Section 2.3.6). Thus, any metric that reproduces ISO deep-water source levels in shallow water is expected to perform equally well as an adjusted quantity for reproducing ISO deep-water RNL values. One important difference between RNL and aSL is that the latter incorporates a correction for propagation loss due to sea-water absorption at high frequencies (ΔL_α). Results on the 350 m intermediate VLA indicate that these two metrics start to diverge at 20 kHz. This suggests that accounting for seawater absorption is required for estimating source levels above this frequency.

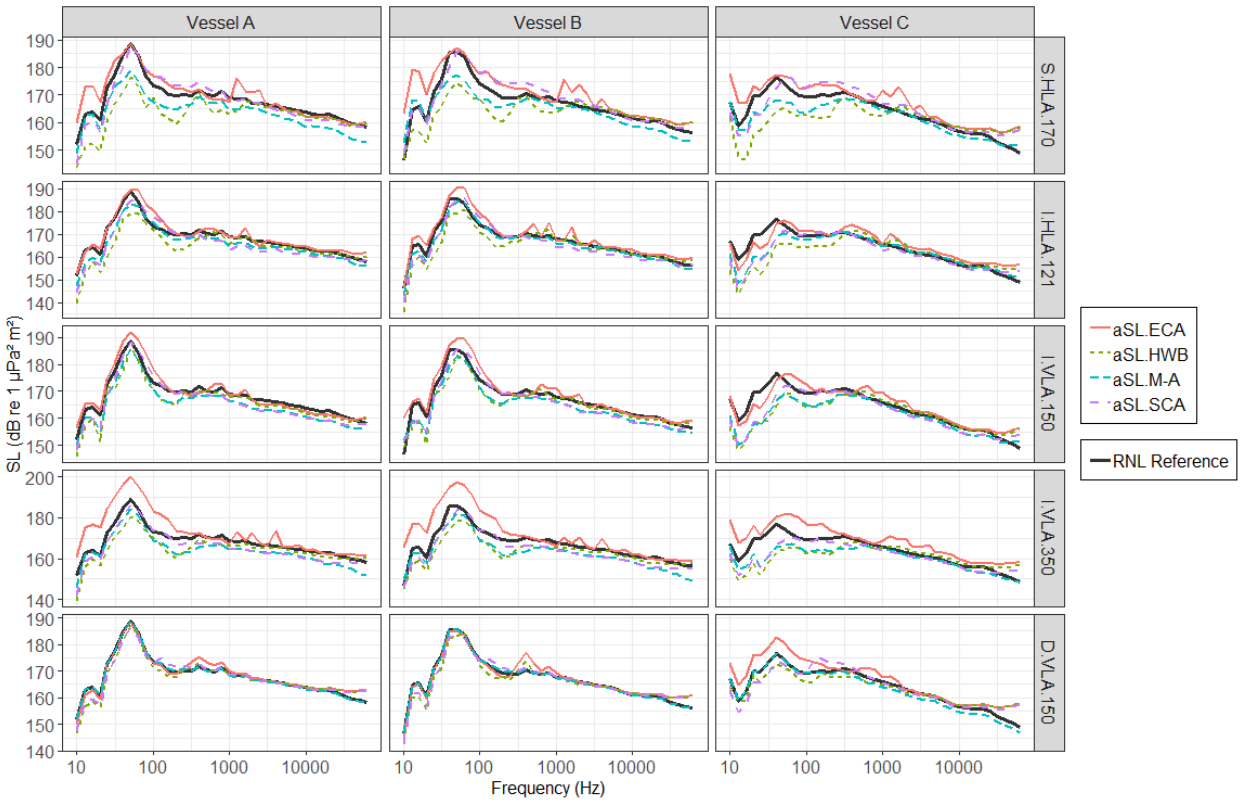

Figure 67. Comparisons of array-averaged adjusted source levels (coloured lines) for vessels A–C to the deep-water reference radiate noise level (RNL; black line). Arithmetic mean values are shown for the ten measurements of each vessel with closest point of approach (CPA) nearest to the measurement funnel with speeds between 20–21 knots (see Figure 47 to 51 captions for mean CPA distance of each vessel). Columns show different vessels and rows show different line arrays.

4.2.10. Comparison of Static and Drift Measurements

Source level measurements collected using the drifting hydrophone array were analyzed separately from the other measurements (Figures 68 to 70; Appendix E). As with the static moorings, source levels for the drift measurements were processed using JASCO's ShipSound software and subjected to quality review by a human analyst. In total, 96 single-node drift measurements were collected during the experiment. Of these measurements, 46 passed the manual quality review, yielding a total of 15 array-averaged measurements for Vessels A and B. Note that the three measurements at the shallow site were collected using a single hydrophone, as the full vertical array could not be deployed in 30 m water depth. The 15 drift measurements spanned a large speed through water (STW) and CPA range, which made direct comparison between measurements unfeasible. The overall quality of the drift measurements was poorer than the static measurements. This was partly due to increased self-noise, caused by wave-induced surface motion and currents, and partly due to difficulties in controlling the measurement geometry, caused by the relative motion of the source vessel and the measurement vessel.

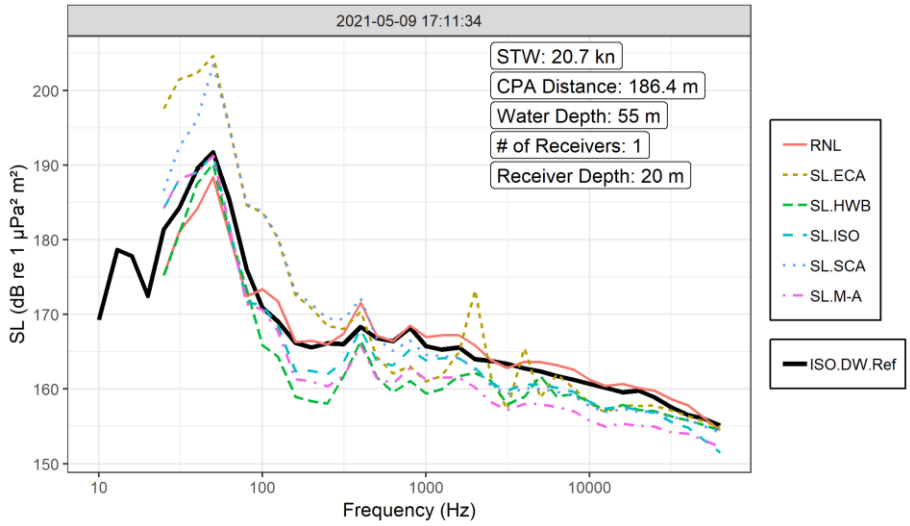

Figure 68. Source level (SL) measurements of vessel A performed at the shallow site using the drifting hydrophone array (coloured lines) compared to the deep-water reference source level (SL.ISO; black line). Annotations indicate vessel speed through water (STW), closest point of approach (CPA) distance, hydrophone, water depth, number of averaged channels, and recording time.

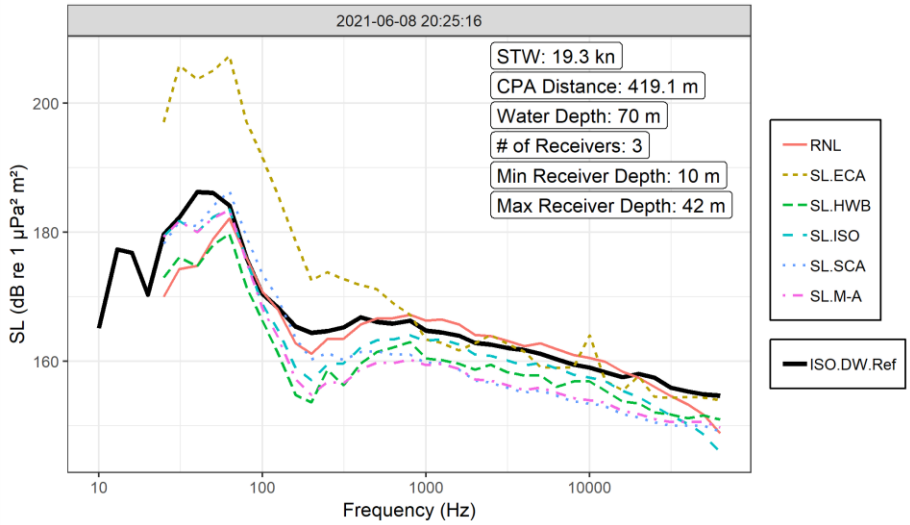

Figure 69. Source level (SL) measurements of vessel B performed at the intermediate site using the drifting hydrophone array (coloured lines) compared to the deep-water reference source level (SL.ISO; black line). Annotations indicate vessel speed through water (STW), closest point of approach (CPA) distance, hydrophone, water depth, number of averaged channels, and recording time.

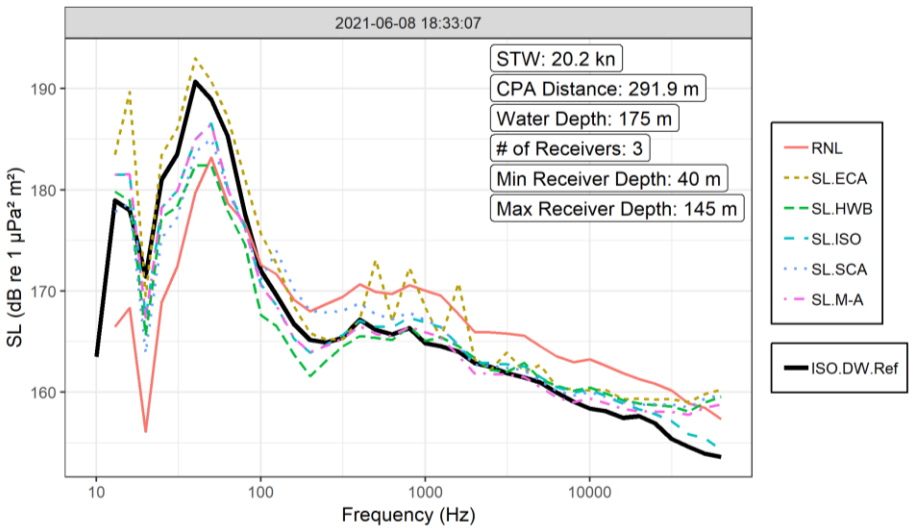

Figure 70. Source level (SL) measurements of vessel B performed at the deep site using the drifting hydrophone array (coloured lines) compared to the deep-water reference source level (SL.ISO; black line). Annotations indicate vessel speed through water (STW), closest point of approach (CPA) distance, hydrophone, water depth, number of averaged channels, and recording time.

4.3. Discussion

4.3.1. Geoacoustic Properties

While the geoacoustic inversion was expected to be a reliable technique for accurately estimating elastic properties of the seabed, the results of the inversion were likely limited to some degree by the frequency range of propagation loss data (600–1200 Hz) compared to the frequency range of the vessel URN data (10–63,000 Hz). This is because the ability of test signals to probe the seabed is dependent on frequency, with lower-frequency signals able to probe to deeper depths and higher-frequency signals able to probe with finer spatial resolution.

The relatively high mismatch of the HWB metric below 1000 Hz at the intermediate and shallow sites suggested that the MAP geoacoustic properties may have underestimated bottom loss at lower frequencies. It is interesting to note, however, that the seabed critical angles estimated from the MAP profiles did not appear to affect the SCA metric to the same degree. Furthermore, there could be other reasons why the wavenumber integration model underestimated propagation loss. For example, Wales and Heitmeyer (2002) found that using a monopole source representation in their PL model introduced artifacts into their source spectrum estimates, which led them to instead use a Gaussian source-depth distribution (see Section 4.1.10). A more detailed sensitivity analysis would be needed to determine how sensitive the HWB method was to variations in the seabed geoacoustic properties and assumed source depth. It also may be possible to directly invert geoacoustic properties using vessel URN data, as recently demonstrated by Tollefsen and Dosso (2020). This topic remains an avenue for future investigation.

4.3.2. Hydrophone Geometry

The experimental data suggested that both horizontal and vertical line arrays were suitable for obtaining consistent source level measurements in water depths less than 100 m over a wide range of frequencies. One advantage of horizontal arrays, however, was that they were not susceptible to knock-down due to ocean currents. In terms of distance from the vessel track, some metrics performed best at shorter CPA distances (ECA, HWB, and ISO), whereas other metrics performed well over a wide range of CPA distances (SCA and M-A). However, comparison of array data from the intermediate site suggested that the two closer line arrays (with 121 and 150 m nominal CPA distance) had overall lower mismatch than the farthest array (with 350 m nominal CPA distance) when considering a wide range of metrics. These results suggest that some flexibility in array geometry is possible when performing vessel URN measurements.

Single-node measurements from the shallow and intermediate sites suggested that performance of many of the metrics was best when hydrophones were 50–150 m from the vessel track. Interestingly, within this CPA distance angle some of the single-node metrics (ECA, SCA, and ISO) performed comparably well to their array-averaged counterparts, particularly for nodes on or near the seabed. This suggests that, with favourable geometry, single-node URN measurements are an acceptable alternative to array-average URN measurements when a slightly lower grade of measurement is acceptable (e.g., as in the Grade C of the ANSI standard S.12-64). It should be noted, however, that there is a trade off with temporal averaging time versus CPA distance (averaging time is proportional to CPA distance), as well as the desire to avoid measuring URN in the near field of the vessel.

Interestingly, results of this experiment suggested that repeatable measurements could be obtained within the minimum CPA distance specified by the current standard (i.e., at CPA distances of less than one vessel length, and as close as 50 m to the source). This suggests that the important noise-generating sources on vessels A–C (e.g., the propellers and engine room) are likely separated by distances shorter than their overall vessel length. Nonetheless, measurements in the acoustic near field should be avoided.

4.3.3. Repeatability of Source Levels

The purpose of following a standard methodology when performing vessel URN measurements is to ensure that the reported source levels are repeatable and consistent. For the current experiment, repeat passes of vessels A–C were performed over three months, presumably under different loading, operating, and weather conditions. This likely led to greater variability in measured source levels than would be observed under a strictly standards-conformant test procedure (i.e., following the strict test sequence described in ISO standard 17208-1). Variance in the URN measurements was reduced experimentally, by binning them into narrow speed ranges and CPA distances and then averaging a number of measurements inside these bins. Nonetheless, some degree of uncertainty remained in the resulting source level estimates due to uncontrollable experimental factors.

Of the three vessels analyzed for this experiment, vessel B had the largest number of accepted measurements and exhibited no strong port/starboard directivity. Hence, vessel B's source levels exhibited the highest degree of repeatability. Vessel A had a lower number of accepted measurements than vessel B and, despite belonging to the same class, exhibited port/starboard directivity, which was not easily controlled for due to uneven sampling of measurement aspects at the shallow and deep sites. Vessel C had the lowest number of accepted measurements and also had lower quality reference measurements than the other two vessels, due to large variations in its CPA distance at the deep site. Thus, results for vessel B had the lowest experimental uncertainty and therefore provided the most reliable assessment of the performance of different URN metrics.

One aspect of uncertainty, not addressed by the current study, is how the choice of source depth (d) affects the repeatability of estimated source levels. Because the calculation is sensitive to source depth, ISO standard 17208-2 specifies that a value equal to 70 % of the vessel draft at the time of measurement be used. However, how this specific choice affects the repeatability of the estimated source levels is unknown and it remains possible that another choice (e.g., based on the propeller geometry, as in Gray and Greeley (1980)) may produce more repeatable estimates. The affect of assumed source depth on estimated source levels is a possible topic of future research that could be addressed using the experimental data from this study.

Another aspect of source level variability not addressed by existing standards is fore/aft directivity of vessel noise emissions. Fore/aft directivity of source levels has been well documented for large vessels (Arveson and Vendittis 2000, Gassmann et al. 2017), though reasons for this variability are less well understood. The existing standards focus on beam-aspect noise emissions, by averaging within a 60° broadside window, but some directivity is possible even inside this range of angles. Source directivity is another future research topic that could be addressed using experimental data from this study.

4.3.4. Robustness of Metrics

Robustness is a desirable property of a source level metric, meaning that errors in estimated source levels should be insensitive to reasonable uncertainties in environmental conditions and source-receiver geometry. Where standards are concerned, a metric that provides a robust measurement is more desirable than one that does not, even if that means the robust metric has lower precision when measurement conditions are known precisely. The experimental data from this study showed that no single source level metric performed best over all water depths, array geometries, CPA distances, and frequency ranges. However, a robust metric should perform well over a wide range of measurement conditions and not just over a narrow range of conditions. This is particularly true where uncertainty in seabed geoacoustic properties is concerned, as these are difficult to measure reliably without considerable effort.

Of the metrics evaluated during this experiment, the SCA and M-A metrics appeared to be the most robust, overall. These metrics both performed well at longer CPA distances compared to the other metrics, although the array geometry comparisons (see Section 4.2.6) suggested the SCA metric had better low-frequency consistency at the shallow site. The robustness of these metrics was likely due to their inclusion of knowledge of the acoustic properties of the seabed,

although they did so in different ways. In shallow water, accounting for the influence of the seabed is more important at longer CPA distances.

Interestingly, the array-average ISO metric also provided robust source level measurements in many instances (similar to the M-A method below 100 Hz), despite not explicitly accounting for the influence of the seabed. This may be contrasted with the ECA metric that is a more general version of the ISO metric: it was accurate at short range but had larger errors at longer CPA distances. The HWB metric was not robust at low frequency, where it struggled to produce consistent source level estimates at longer CPA distances. The relatively poor performance of the HWB metric was surprising, given the sophistication of the method. One possibility is that the results of the geoacoustic inversion were too sensitive to the specific frequency range of the PL measurements (i.e., the PL model may have been over-tuned to the PL data). Another possibility is that the errors were due to the point-source assumption, and that estimates would be improved by using a range of source depths (see Section 4.1.10). Regardless of the explanation, the experimental results suggested that the HWB metric was not as robust as the other methods below 1000 Hz.

An aspect of robustness that was not evaluated during the field trials was sensitivity to estimated source depth. It is well known that low-frequency source levels are very sensitive to errors in estimated source depth, which is one reason for the prevalence of RNL when reporting vessel URN measurements. However, vessels A–C only had very small variations in logged draft during the experiment (see Section 4.2.2). Future research could be undertaken, using data collected from this experiment, to test the sensitivity of the different metrics to variations in source depth.

4.3.5. Drift Measurements

The purpose of the drift measurements was to compare results obtained using a surface-deployed hydrophone array (i.e., as suggested in ISO 17208-1) to results obtained using the moored hydrophone arrays. These comparisons demonstrated that the drift measurements were generally of a lower quality than the moored hydrophone measurements. This was because data from the drift hydrophones were susceptible to contamination from vibration caused by wave-driven surface motion and ocean currents. Furthermore, ocean currents in the study area made it difficult to precisely control the positions of the hydrophones, both in terms of their distances to the source vessel and their depths below the sea-surface. Thus, results from this study suggest that drifting hydrophone measurements should be avoided when tidal currents or waves are present and when shallow water would limit the ability of a vertical array to sample a sufficient range of measurement angles.

4.4. Conclusions

Repeated vessel noise measurements, carried out over a period of three months in British Columbia's Southern Gulf Islands, yielded valuable data to inform the development of an ISO standard for shallow-water vessel URN measurements. Measurements of three anonymized vessels (denoted A, B, and C), were collected on five moored hydrophone arrays, and one drifting hydrophone array, deployed in three different water depths. These measurements

confirmed that it was possible to obtain repeatable vessel source level estimates in shallow water with only a moderate increase in complexity beyond methods codified in existing ISO standards. Nonetheless, the precision of source levels measured in shallow water may be limited to some extent by knowledge of the acoustic properties of the seabed.

The following five source level metrics were evaluated using experimental data from this study, reflecting five different approaches to analyzing vessel URN measurements:

1. ISO (Method for Deep Water Source Levels from ISO 17208-2): This is the method for analyzing deep-water RNL measurements performed according to ISO standard 17208-1 and converting them to source levels using formulae codified in ISO standard 17208-2. It does not account for the influence of the seabed but averages URN over a range of pre-defined grazing angles (15°, 30°, and 45°).
2. HWB (Hybrid Wavenumber Integration & Beam Tracing Method): This is a method for estimating PL of a URN measurement in any water depth using a hybrid model based on low-frequency wavenumber integration and high-frequency beam tracing. This method requires a detailed description of the acoustic properties of the environment (assumed to be range-independent) and sophisticated numerical models. The PL estimate from the numerical models is used to calculate a monopole source level directly from the URN data.
3. ECA (ECHO Certification Alignment Method): This is a method for calculating propagation loss for a URN measurement performed at any grazing angle but which neglects the influence of the seabed. This method is similar in principle to the ISO method, but it does not assume a fixed set of grazing angles and is based on an exact Lloyds mirror PL calculation, integrated over decidecade frequency bands.
4. SCA (Seabed Critical Angle Method): This is a method for calculating source levels from single-node RNL measurements in any water depth by applying physics-based correction factors to account for the critical angle of the seabed (which must be known or estimated) and the water depth. This method can be averaged over multiple hydrophone nodes (i.e., at different grazing angles) to yield a higher-precision source level estimate.
5. M-A (Meyer-Audoly Method): This is a method for calculating source levels from array-averaged RNL measurements in shallow water by applying an empirical correction formula to account for the frequency-dependent influence of the seabed and water depth. This method includes an empirical parameter (ε), which is selected according to the seabed type (which must be known). This method was developed for a vertical array of three hydrophones, spanning the water column.

Of these five metrics, M-A and SCA provided the most robust source level estimates over a wide range of frequencies and water depths while accounting for the influence of the seabed on URN measurements. Performance of these two metrics was similar at the intermediate site, although the SCA method appeared to perform better at the shallow site (where, it should be noted, an HLA was deployed rather than the VLA assumed by the M-A method). Uncertainty regarding the seabed properties was naturally found to affect the accuracy of both these methods.

Of the remaining metrics, the ISO method performed well for estimating array-averaged source levels, especially considering it did not account for the influence of the seabed on shallow-water propagation loss. The ECA method performed well at short CPA distances but not at longer CPA

distances. The HWB method performed well at high frequencies (1000 Hz and above), but it had difficulty estimating low-frequency source levels at longer CPA distances. The reasons for the poor robustness of the HWB method are not yet clear, but they may have been related to the relatively narrow frequency range of PL data (600–1200 Hz) used to the tune the geoacoustic parameters in the HWB model. This is a possible topic for future investigation.

Experimental data indicated that both horizontal line array (HLA) and vertical line array (VLA) geometries performed well in intermediate (~70 m) and shallow (~30 m) water depths, provided they sampled a range of grazing angles. This finding suggested that some flexibility in array geometry could be accommodated in a future standard. The experimental results at the shallow and intermediate sites suggested that single-node measurements may be used to obtain source level estimates that are consistent with the ISO deep-water standard, provided that the hydrophone is deployed at the seabed close to the source (50–150 m range). The experimental results also suggested that it was possible to obtain consistent source level measurements at CPA distances closer than one vessel length from the source (though it remains important to avoid the near field, e.g., not closer than 50 m). Such measurement geometries may be advantageous in shallow water, where bottom loss makes accurate source level measurements difficult at longer CPA distances and surface cancellation makes accurate source level measurements difficult at shallow grazing angles.

Experience from this study suggests that, when ocean currents are a consideration and shallow water is present, moored hydrophone arrays likely allow for more repeatable URN measurements in shallow water. Measurements from drifting hydrophones were more difficult to perform and analyze than measurements from moored hydrophone arrays. This was due several factors: greater difficulty accounting for the relative motion of the source and hydrophones during the test; greater difficulty suspending and retrieving a vertical array of hydrophones; and greater self-noise due to motion and vibration of the measurement platform.

Results of this study are expected to provide valuable information to the ISO working group for developing a standard for shallow-water vessel URN measurements. The findings of this study are believed to be particularly robust, as they are based on a very large data set, consisting of 7675 individual URN measurements of three vessels from 16 individual hydrophone nodes and three different measurement locations. This data set likely has other applications as well, and it may be used to investigate other topics in future. Possible avenues for future research include the following:

1. Investigating methods for measuring directivity of vessel noise;
2. Examining the effect of source depth on source level estimates;
3. Quantifying sources of uncertainty in source level estimates;
4. Investigating whether vessel URN test data may be used to directly estimate seabed geoacoustic properties; and
5. Further investigating adjusted source level (aSL) metrics and their relationship to RNL in shallow water.

5. CONCLUSIONS AND RECOMMENDATIONS TO ISO TC 43/SC 3/WG 1

Based on the results of the MMP2 study, the authors of this report have prepared a set of recommendations to the ISO working group (i.e., ISO TC 43/SC 3/WG 1) to support the development of a new standard for measurement of underwater sound from ships in shallow water:

- Results of this study confirm that it is possible to measure vessel source levels in shallow water that are consistent with those measured in deep-water. Thus, the working group should continue to pursue development of a shallow-water ship noise measurement standard (i.e., ISO 17208-3).
- Both horizontal line array (HLA) and vertical line array (VLA) geometries proved effective for measuring vessel source levels in shallow water. Thus, future standards could consider accommodating both types of arrays. However, in very shallow water (~30 m) it is likely that an HLA deployed at the seabed would be required to measure a sufficiently wide range of grazing angles.
- Data collected during this study suggest that consistent shallow-water source level measurements are possible with single hydrophones nodes if they are deployed at the seabed and at short CPA distances to the source vessel. Results from this study suggest that single hydrophone measurements have slightly greater uncertainty than array-averaged measurements, though additional work would be needed to quantify the difference. Single-hydrophone measurements could be accommodated by including different grades of measurements in a future standard (e.g., as in ANSI S12.64 (2009)).
- Data collected during this study suggest that consistent source level measurements are possible at CPA distances shorter than those permitted by existing standards (i.e., within one vessel length and as close as 50 m). Considering the previous bullet, some consideration should be given to relaxing near-field measurement restrictions from the existing deep-water standard, while still seeking to avoid near-field effects. This possibility could be explored further using data collected from this experiment.
- Experience gained during the field experiments suggested that, in shallow water, measurements performed using drifting hydrophone arrays were more difficult to conduct and analyze than those performed using moored hydrophone arrays. Where currents are a consideration, an HLA deployed on the seabed could be the optimal sensor configuration in shallow water since it is not susceptible to knock-down and self-noise from cable strum.

- Two potential methods for estimating shallow-water source levels were evaluated during this study that accounted for the influence of the seabed on propagation loss, and which the present authors consider simple enough to be codified in a standard:
  1. A more general version of the approximation employed in ISO 17208-2, developed for this study, that includes a correction term for the bottom reflection via the seabed critical angle, as well as an explicit term for the direct path arrival (SL.SCA). These terms depend on grazing angle, water depth, and slant range. The influence of the seabed is determined by a critical angle parameter (ψ) that could be tabulated for common bottom types or determined directly through measurement.
  2. An empirical formula, developed by Meyer and Audoly (2020), to correct RNL measured on a vertical array of hydrophones for the influence of multiple reflections on the sea surface and seafloor in shallow water to obtain source level. The influence of the seabed is determined by an empirical parameter (ε), whose value could be determined for common bottom types via numerical simulations.
- Some knowledge of bottom properties is likely required to accurately estimate source levels in shallow water. Uncertainty regarding bottom properties will introduce uncertainty into the estimated source levels, and such uncertainties should be accounted for in a future standard. Quantifying these uncertainties would likely require conducting a more detailed sensitivity analysis, which could be carried out using either of methods 1 and 2 above using data from this experiment.
- The effect of seawater absorption should be incorporated into future measurement standards to account for excess propagation loss if the frequency range is extended above 20 kHz. A simplified formula, such as Ainslie and McColm (1998) or van Moll et al. (2009), would be suitable.
- Data collected during this study suggest that measurement uncertainties will most likely be greater in shallow water than in deep water, particularly in decidecade bands below 100 Hz. These uncertainties are attributed to uncertainty in propagation loss due to imperfect knowledge of bottom loss. Data collected during this study suggests that such uncertainties increase with CPA distance from the source vessel. Measurements at shorter CPA distances are expected to have lower measurement uncertainties.
- This study demonstrated the feasibility of performing URN measurements in water depths as shallow as 30 m and for decidecade frequency bands between 10–63,000 Hz. It is unknown whether the study findings hold true in shallower water depths or outside the reported frequency range.
- During 2022-2023, the ISO working group may identify other data gaps, beyond those addressed by the MMP2 study. It is expected that many of these gaps will be addressed by the Saturn project (Saturn 2022), which is a parallel, EU-funded research project on the topic of vessel URN. Nonetheless, the working group may consider whether other data gaps could be addressed through additional analyses of the MMP2 dataset.

LITERATURE CITED

[CHS] Canadian Hydrographic Service. 2021. *https://open.canada.ca/data/en/dataset/d3881c4c-650d-4070-bf9b-1e00aabf0a1d* (webpage). Department of Fisheries and Oceans Canada. https://open.canada.ca/data/en/dataset/d3881c4c-650d-4070-bf9b-1e00aabf0a1d. (Accessed 25 May 2022).

[IEC] International Electrotechnical Commission. 2014. *IEC 61260-1:2014 Electroacoustics - Octave-band and fractional-octave-band filters - Part 1: Specifications*. https://webstore.iec.ch/publication/5063.

[ISO] International Organization for Standardization. 2016. *ISO 17208-1:2016. Underwater acoustics – Quantities and procedures for description and measurement of underwater sound from ships – Part 1: Requirements for precision measurements in deep water used for comparison purposes*. https://www.iso.org/standard/62408.html.

[ISO] International Organization for Standardization. 2017. *ISO 18405:2017. Underwater acoustics – Terminology*. Geneva. https://www.iso.org/standard/62406.html.

[ISO] International Organization for Standardization. 2019. *ISO 17208-2:2019. Underwater acoustics – Quantities and procedures for description and measurement of underwater sound from ships – Part 1: Requirements for precision measurements in deep water used for comparison purposes*. https://www.iso.org/standard/62409.html.

Ainslie, M.A. and J.G. McColm. 1998. A simplified formula for viscous and chemical absorption in sea water. *Journal of the Acoustical Society of America* 103(3): 1671-1672. https://doi.org/10.1121/1.421258.

Ainslie, M.A., P.H. Dahl, C.A.F. de Jong, and R.M. Laws. 2014. *Practical Spreading Laws: The Snakes and Ladders of Shallow Water Acoustics*. *UA2014 - 2nd International Conference and Exhibition on Underwater Acoustics*, 22-27 Jun 2014, Island of Rhodes, Greece, pp. 879-886.

Ainslie, M.A., J.L. Miksis-Olds, S.B. Martin, K.D. Heaney, C.A.F. de Jong, A.M. von Benda-Beckmann, and A.P. Lyons. 2018. *ADEON Underwater Soundscape and Modeling Metadata Standard*. Version 1.0. Technical report by JASCO Applied Sciences for ADEON Prime Contract No. M16PC00003. https://doi.org/10.6084/m9.figshare.6792359.v2.

Ainslie, M.A., D.E. Hannay, A.O. MacGillivray, and K. Lucke. 2020a. *Proposed Alignment of Measurement and Analysis for Quiet Ship Certifications*. Document Number 02024, Version 4.0. Technical memorandum by JASCO Applied Sciences for Vancouver Fraser Port Authority.

Ainslie, M.A., S.B. Martin, T.J. Deveau, A.O. MacGillivray, C. Bae, and D. Wittekind. 2020b. *Towards a Standard for Vessel URN Measurement in Shallow Water: Applying Acoustical Propagation Modelling to Inform the Design of a Measurement Program that Determines if Shallow Water URN Measurements can be Comparable to those from Deep Water*. Document Number 02167, Version 1.0. White paper by JASCO Applied Sciences for Transport Canada Innovation Center.

Ainslie, M.A., S.B. Martin, K.B. Trounce, D.E. Hannay, J.M. Eickmeier, T.J. Deveau, K. Lucke, A.O. MacGillivray, V. Nolet, et al. 2022. International harmonization of procedures for measuring and analyzing of vessel underwater radiated noise. *Marine Pollution Bulletin* 174: 113124. https://www.sciencedirect.com/science/article/pii/S0025326X21011589.

ANSI/ASA S12.64/Part 1. 2009. *American National Standard: Quantities and Procedures for Description and Measurement of Underwater Sound from Ships – Part 1: General Requirements*. American National Standards Institute and Acoustical Society of America, NY, USA. https://webstore.ansi.org/Standards/ASA/ANSIASAS12642009Part.

Arveson, P.T. and D.J. Vendittis. 2000. Radiated noise characteristics of a modern cargo ship. *Journal of the Acoustical Society of America* 107(1): 118-129. https://doi.org/10.1121/1.428344.

Baudin, E. and H. Mumm. 2015. *Guidelines for regulation on UW noise from commercial shipping (SONIC Deliverable 5.4)*. Achieve Quieter Oceans by shipping noise footprint reduction, FP7-Grant agreement No 2015. Volume 314227.

Bedford Institute of Oceanography. 2015. *WebTide Tidal Prediction Model (v0.7.1)* (webpage). Government of Canada. http://www.bio-iob.gc.ca/science/research-recherche/ocean/webtide/index-en.php.

Dettmer, J., S.E. Dosso, and C. Holland. 2010. Trans-dimensional geoacoustic inversion. *Journal of the Acoustical Society of America* 128(6): 3393-3405. https://doi.org/10.1121/1.3500674.

Dettmer, J. and S. Dosso. 2012. Trans-dimensional matched-field geoacoustic inversion with hierarchical error models and interacting Markov chains. *Journal of the Acoustical Society of America* 132(4): 2239-2250. https://doi.org/10.1121/1.4746016.

Dosso, S.E., J. Dettmer, G. Steininger, and C.W. Holland. 2014. Efficient trans-dimensional Bayesian inversion for geoacoustic profile estimation. *Inverse Problems* 30(11). https://doi.org/10.1088/0266-5611/30/11/114018.

François, R.E. and G.R. Garrison. 1982a. Sound absorption based on ocean measurements: Part I: Pure water and magnesium sulfate contributions. *Journal of the Acoustical Society of America* 72(3): 896-907. https://doi.org/10.1121/1.388170.

François, R.E. and G.R. Garrison. 1982b. Sound absorption based on ocean measurements: Part II: Boric acid contribution and equation for total absorption. *Journal of the Acoustical Society of America* 72(6): 1879-1890. https://doi.org/10.1121/1.388673.

Gassmann, M., S.M. Wiggins, and J.A. Hildebrand. 2017. Deep-water measurements of container ship radiated noise signatures and directionality. *Journal of the Acoustical Society of America* 142(3): 1563-1574. https://doi.org/10.1121/1.5001063.

Gray, L.M. and D.S. Greeley. 1980. Source level model for propeller blade rate radiation for the world's merchant fleet. *Journal of the Acoustical Society of America* 67(2): 516-522. https://doi.org/10.1121/1.383916.

Green, P.J. 1995. Reversible jump Markov chain Monte Carlo computation and Bayesian model determination. *Biometrika* 82(4): 711-732. https://doi.org/10.1093/biomet/82.4.711.

Hannay, D.E., X. Mouy, and Z. Li. 2016. An automated real-time vessel sound measurement system for calculating monopole source levels using a modified version of ANSI/ASA S12.64-2009. *Canadian Acoustics* 44(3). https://jcaa.caa-aca.ca/index.php/jcaa/article/view/3002.

Jensen, F.B., W.A. Kuperman, M.B. Porter, and H. Schmidt. 2011. *Computational Ocean Acoustics*. 2nd edition. AIP Series in Modern Acourics and Signal Processing. AIP Press - Springer, New York. 794 pp. https://doi.org/10.1007/978-1-4419-8678-8.

Jiang, P., J. Lin, J. Sun, X. Yi, and Y. Shan. 2020. Source spectrum model for merchant ship radiated noise in the Yellow Sea of China. *Ocean Engineering* 216: 107607. https://doi.org/10.1016/j.oceaneng.2020.107607.

Lawrence, C.B., C. Robinson, C.H. Grooms, and S.B. Martin. 2021. *MMP2 May 2021 Deployment Report*. Document Number 02423, Version 1.0. Technical report by JASCO Applied Sciences for Transport Canada.

MacGillivray, A.O., Z. Li, D.E. Hannay, K.B. Trounce, and O. Robinson. 2019. Slowing deep-sea commercial vessels reduces underwater radiated noise. *Journal of the Acoustical Society of America* 146: 340-351. https://doi.org/10.1121/1.5116140.

Martin, S.B., A.O. MacGillivray, C.E. Lumsden, J.J.-Y. Delarue, and T.J. Deveau. 2021. *MMP2 Spring 2021 Trial Plan; Develop Measurement Standard for Shallow Water Vessel Source Level for TC-IC Project MMP2*. Document Number 02268, Version 1.0. Trial Plan by JASCO Applied Sciences for Transport Canada Innovation Centre.

Meyer, V. and C. Audoly. 2020. Accounting for sea floor properties in the assessment of underwater noise radiated from ships in shallow water. *Proceedings of Meetings on Acoustics* 40(1): 070007. https://asa.scitation.org/doi/abs/10.1121/2.0001307.

Porter, M.B. and Y.C. Liu. 1994. Finite-element ray tracing. *In*: Lee, D. and M.H. Schultz (eds.). *International Conference on Theoretical and Computational Acoustics*. Volume 2. World Scientific Publishing Co. pp 947-956.

Quijano, J.E., S.E. Dosso, J. Dettmer, L.M. Zurk, M. Siderius, and C.H. Harrison. 2012. Bayesian geoacoustic inversion using wind-driven ambient noise. *Journal of the Acoustical Society of America* 131(4): 2658-2667. https://doi.org/10.1121/1.3688482.

R: A language and environment for statistical computing. R Foundation for Statistical Computing, Vienna, Austria. http://www.R-project.org/.

Saturn. 2022. *Developing solutions to underwater noise* (webpage). https://www.saturnh2020.eu/.

Steininger, G., J. Dettmer, S. Dosso, and C. Holland. 2013. Trans-dimensional joint inversion of seabed scattering and reflection data. *Journal of the Acoustical Society of America* 133(3): 1347-1357. https://doi.org/10.1121/1.4789930.

Tollefsen, D. and S.E. Dosso. 2020. Ship source level estimation and uncertainty quantification in shallow water via Bayesian marginalization. *Journal of the Acoustical Society of America* 147(4): EL339-EL344. https://doi.org/10.1121/10.0001096.

Traverso, F., T. Gaggero, E. Rizzuto, and A. Trucco. 2015. Spectral analysis of the underwater acoustic noise radiated by ships with controllable pitch propellers. *OCEANS 2015 - Genova*. 18-21 May 2015, Genova, Italy. pp 1-6. https://doi.org/10.1109/OCEANS-Genova.2015.7271483.

van Moll, C.A.M., M.A. Ainslie, and R. van Vossen. 2009. A Simple and Accurate Formula for the Absorption of Sound in Seawater. *IEEE Journal of Oceanic Engineering* 34(4): 610-616. https://doi.org/10.1109/JOE.2009.2027800.

Wales, S.C. and R.M. Heitmeyer. 2002. An ensemble source spectra model for merchant ship-radiated noise. *Journal of the Acoustical Society of America* 111(3): 1211-1231. https://doi.org/10.1121/1.1427355.

Wenz, G.M. 1962. Acoustic Ambient Noise in the Ocean: Spectra and Sources. *Journal of the Acoustical Society of America* 34(12): 1936-1956. https://doi.org/10.1121/1.1909155.

APPENDIX A. STANDARD FREQUENCY BANDS

Standard bands are arranged logarithmically in frequency and are based on powers of ten around a centre frequency of 1000 Hz. Multiplying this centre frequency by integer powers of ten gives 10, 100, 1000, and 10,000 Hz. The band between each successive factor of 10 (e.g., from 100 to 1000 kHz) is a decade. It is customary to divide each decade band into ten equal sub-bands, each one tenth of a decade (i.e., one decidecade) wide. Table A-1, based on the *ADEON Soundscape Specification* (Ainslie et al. 2018), shows decidecade (ddec) bands according to IEC (2014), for decidecade frequency bands with centre frequencies 10 Hz ($n = -20$) Hz to 100 kHz ($n = +20$). Each decidecade band in the table is identified by a unique integer index between $n = -20$ (10 Hz) and $+20$ (100 kHz), with $n = 0$ corresponding to 1 kHz.

Table A-1. Decidecade frequency bands, as defined by IEC (2014), with centre frequencies between 10 Hz ($n = -20$) and 100 kHz ($n = +20$). Band edge and centre frequencies are stated to five significant figures. Centre frequencies of nominal octave-bands (the precise bandwidth of which is 3 ddec) are bold. Alternate dark and light shading shows ADEON decade bands B to E (Ainslie et al. 2018).

Band index (n)	Lower bound (f_{min}/Hz)	Centre frequency (f_{C}/Hz)	Upper bound (f_{max}/Hz)	Nominal centre frequency ($f_{\mathrm{c,nom}}$/Hz)
−20	8.9125	10.000	11.220	10
−19	11.220	12.589	14.125	12.5
−18	14.125	**15.849**	17.783	16
−17	17.783	19.953	22.387	20
−16	22.387	25.119	28.184	25
−15	28.184	**31.623**	35.481	32
−14	35.481	39.811	44.668	40
−13	44.668	50.119	56.234	50
−12	56.234	**63.096**	70.795	63
−11	70.795	79.433	89.125	80
−10	89.125	100.00	112.20	100
−9	112.20	**125.89**	141.25	125
−8	141.25	158.49	177.83	160
−7	177.83	199.53	223.87	200
−6	223.87	**251.19**	281.84	250
−5	281.84	316.23	354.81	320
−4	354.81	398.11	446.68	400
−3	446.68	**501.19**	562.34	500
−2	562.34	630.96	707.95	630
−1	707.95	794.33	891.25	800
0	891.25	**1000.0**	1122.0	$1{\cdot}10^3$
1	1122.0	1258.9	1412.5	$1.25{\cdot}10^3$
2	1412.5	1584.9	1778.3	$1.6{\cdot}10^3$
3	1778.3	**1995.3**	2238.7	$2{\cdot}10^3$

4	2238.7	2511.9	2818.4	$2.5 \cdot 10^3$
5	2818.4	3162.3	3548.1	$3.2 \cdot 10^3$
6	3548.1	**3981.1**	4466.8	$4 \cdot 10^3$
7	4466.8	5011.9	5623.4	$5 \cdot 10^3$
8	5623.4	6309.6	7079.5	$6.3 \cdot 10^3$
9	7079.5	**7943.3**	8912.5	$8 \cdot 10^3$
10	8912.5	10000	11220	$10 \cdot 10^3$
11	11220	12589	14125	$12.5 \cdot 10^3$
12	14125	**15849**	17783	$16 \cdot 10^3$
13	17783	19953	22387	$20 \cdot 10^3$
14	22387	25119	28184	$25 \cdot 10^3$
15	28184	**31623**	35481	$32 \cdot 10^3$
16	35481	39811	44668	$40 \cdot 10^3$
17	44668	50119	56234	$50 \cdot 10^3$
18	56234	**63096**	70795	$63 \cdot 10^3$
19	70795	79433	89125	$80 \cdot 10^3$
20	89125	100000	112200	$100 \cdot 10^3$

A decidecade (0.1 dec) is approximately equal to one third of an octave, and for this reason is referred to by IEC (2014) as a ‘one-third octave’ (Table A-2).

Table A-2. Fractional octave and fractional decade frequency bands.

Frequency ratio	IEC 61260: 1995	IEC 61260-1:2014	ISO 18405	ISO 80000-8	Notes
2	octave	-	octave	octave	
$2^{1/3}$	one-third octave	-	one-third octave one-third octave (base 2)		
10	-	-	decade	decade	
$10^{1/10}$	one-third octave	one-third octave	decidecade one-third octave (base 10)		an alternative name for this frequency ratio is ‘one-tenth decade’ (ANSI S1.6-2016)

APPENDIX B. MEMORANDUM: WHAT IS ADJUSTED RNL?

From: Michael Ainslie
To: Alex MacGillivray
Cc: Bruce Martin
Date: 27 January 2022

B.1. Purpose and Approach

The purpose of this memorandum is to resolve a discrepancy between the respective equations for adjusted RNL (aRNL) presented in Ainslie et al. (2020a) and Ainslie et al. (2022). The concept of aRNL was proposed by Ainslie et al. (2020a) but was not clearly defined. There are at least three versions in circulation (Ainslie et al. 2020a, Ainslie et al. 2022). Which one is correct? RNL in deep water is equal to adjusted SL (aSL), so the correct definition is the one that most closely resembles aSL. I derived an expression for aRNL based on the requirement that it should be approximately equal to aSL. This led to a fourth expression that differs from all three previous versions.

B.2. Derivation

The heuristic approach of Ainslie et al. (2020a) was improved in Ainslie et al. (2020a) with a more rigorous derivation, but both memorandums lack a clear *definition* of aRNL. For the purpose of deciding which equation to recommend I decided derive a formula for aRNL starting from the principle that it should be equal to aSL. The end result is a fourth equation, different from the three previous versions. The one that is closest is the from Ainslie et al. (2020a), but there are some important differences.

To start, we want aRNL to be a simple but accurate approximation to aSL. The aSL is the dipole source level at a specified angle. For convenience, we adopt the equation:

$$L'_{\mathrm{S}} = L_{\mathrm{S}} + 10\log_{10}\bar{\sigma}\,\mathrm{dB}\,. \tag{B-1}$$

Equation B-1 is not the definition of aSL, but it is sufficient for the present purpose.

SL and SPL are related by (F = propagation factor):

$$L_{\mathrm{S}} = L_p + 10\log_{10}\frac{F^{-1}}{r_0^2}\,\mathrm{dB}\,, \tag{B-2}$$

expanding SL as SPL −10log$_{10}$F:

$$L'_{\mathrm{S}} \approx L_{\mathrm{RN}}(\theta_1) - 10\log_{10}(Fr^2)\,\mathrm{dB} + 10\log_{10}\bar{\sigma}\,\mathrm{dB}\,. \tag{B-3}$$

Write incoherent propagation factor for water depth H and critical angle ψ (neglecting absorption for simplicity):

$$F \approx \frac{2}{r^2} + \frac{2\psi}{rH}\,. \tag{B-4}$$

Use of equation B-4 in equation B-3 does not reproduce the deep-water RNL because of missing Lloyds mirror interference (essential at low frequency). Correcting for this, we have:

$$F \approx \frac{\sigma_1}{r^2} + \frac{2\psi}{rH}. \tag{B-5}$$

Equation B-5 works in deep water. In shallow water, it works at short range or high frequency but fails for low frequency at long range because the cylindrical spreading term is not applicable to a dipole source. Correcting a factor 4 error in the dipole correction from Ainslie et al. (2014):

$$F \approx \frac{1}{r^2}\sigma_1 + \frac{\psi}{rH}\sigma_\psi, \tag{B-6}$$

where sigma is given by equation B-19. Substituting equation B-6 into equation B-3 gives:

$$L'_{\mathrm{S}} \approx L_{\mathrm{RN}}(\theta_1) - 10\log_{10}\left(\sigma_1 + \frac{\psi r}{H}\sigma_\psi\right)\mathrm{dB} + 10\log_{10}\bar{\sigma}\,\mathrm{dB}. \tag{B-7}$$

One could define aRNL as aSL, but then it would be better to call it aSL (not aRNL).[7] An alternative approach that distinguishes between aSL and aRNL is to define aRNL as the RHS of equation B-7, i.e.,

$$L'_{\mathrm{RN}} = L_{\mathrm{RN}}(\theta_1) + \Delta L_{\mathrm{S}} - 10\log_{10}\left(\sigma_1 + \frac{\psi r}{H}\sigma_\psi\right)\mathrm{dB}. \tag{B-8}$$

Equation B-8 is proposed as the definition of aRNL.

As a by-product, the derivation also yields an approximation to PL:

$$N_{\mathrm{PL}} = 10\log_{10}\frac{F^{-1}}{r_0^2}\ \mathrm{dB\ and} \tag{B-9}$$

$$N_{\mathrm{PL}} = 10\log_{10}\frac{\left(\frac{1}{r^2}\sigma_1 + \frac{\psi}{rH}\sigma_\psi\right)^{-1}}{r_0^2}\ \mathrm{dB}. \tag{B-10}$$

This formula is illustrated for a deep-water example (Figure B-1, for 300 m water depth) for (left) sand sediment and (right) silt sediment. Also included for comparison is the formula from Meyer & Audoly, which underestimates PL at low frequency, perhaps because their formula assumes a specific hydrophone geometry. The applicability of equation B-10 is not restricted to any one geometry.

[7] There would be no need for two names (aRNL and aSL) because the two quantities would be identical. While on the subject of names, it is worth recalling that the concept of RNL is not well defined in shallow water. It could be re-defined as equal to the aRNL proposed here, in which case we are left with three distinct terms: 1) source level (SL), 2) adjusted source level (aSL), and 3) radiated noise level (RNL). With these definitions, aSL and RNL would be approximately equal.

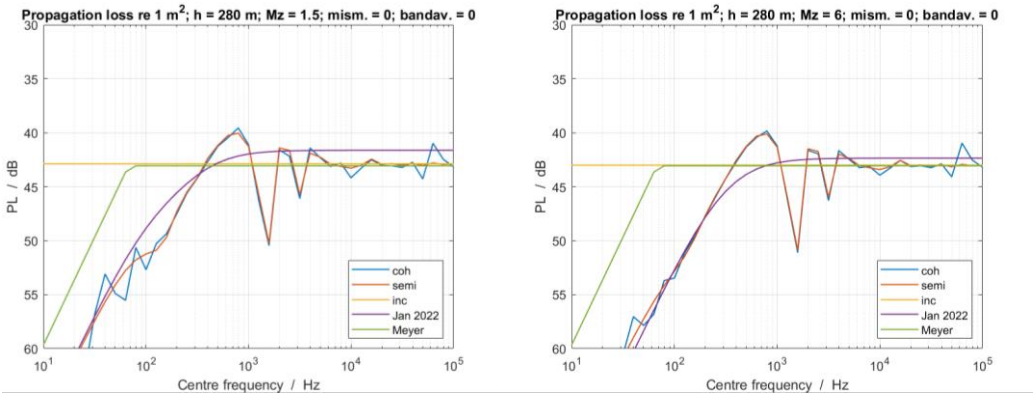

Figure B-1. Deep-water propagation loss (re 1 ∝Pa^2) for (left) sand sediment and (right) silt sediment. The magenta curve is calculated using equation B-10 from this memo. The blue (red) curve is calculated using a coherent (semi-coherent) image sum.

This formula is illustrated for a shallow-water example (Figure B-2, for 30 m water depth). The Meyer-Audoly formula works for (left) sand and underestimates PL for (right) silt.

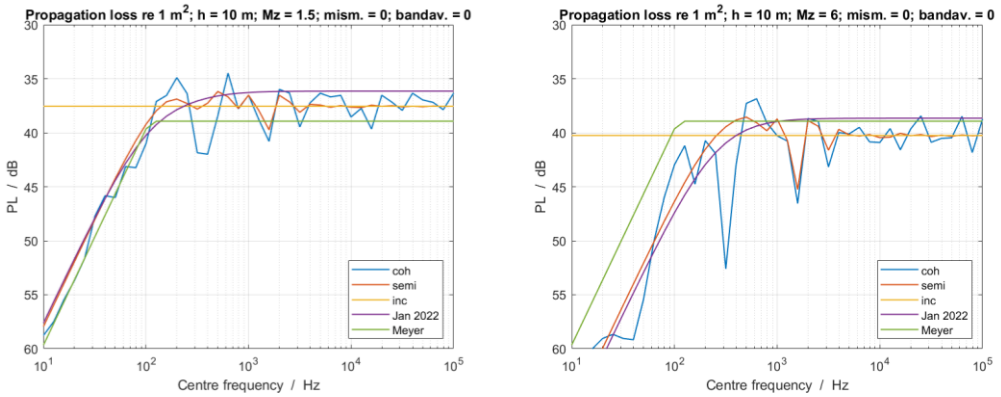

Figure B-2. Shallow-water propagation loss (re 1 ∝Pa^2) for (left) sand sediment and (right) silt sediment. The magenta curve is calculated using equation B-10 from this memo. The blue (red) curve is calculated using a coherent (semi-coherent) image sum.

Source level (Figure B-3) follows using equation B-10 with

$$L_S = L_p + N_{PL}\,. \tag{B-11}$$

Undesirable oscillations of amplitude 2–4 dB around the correct value (120 dB) can be damped by averaging over frequency. The right-hand graph shows the effect of power-averaging over three successive decidecade bands.

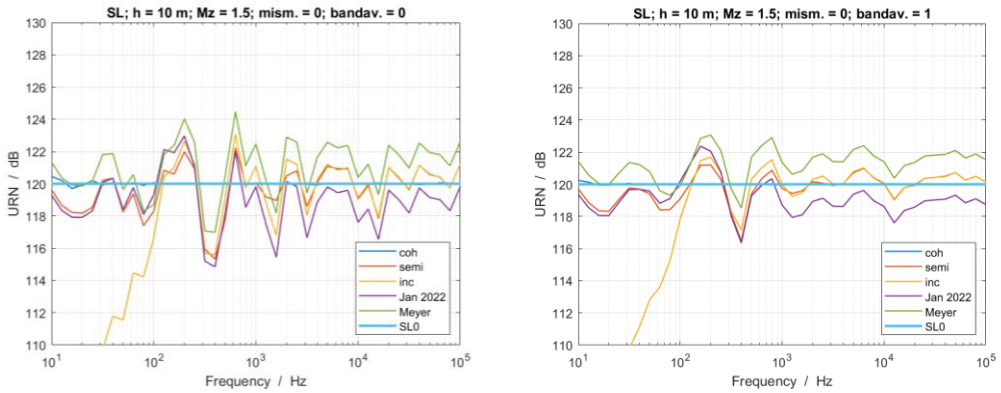

Figure B-3. (Left) Unaveraged and (right) averaged: Effect of 3-band averaging on shallow-water source level (re 1 $\propto$Pa^2 m^2) for sand sediment. The correct source level is 120 dB. The magenta curve is calculated using equation B-11 from this memo. The blue (red) curve is calculated using a coherent (semi-coherent) image sum.

Figure B-3 assumes perfect knowledge of environment and geometry. The effect of mismatch is shown in Figure B-4.

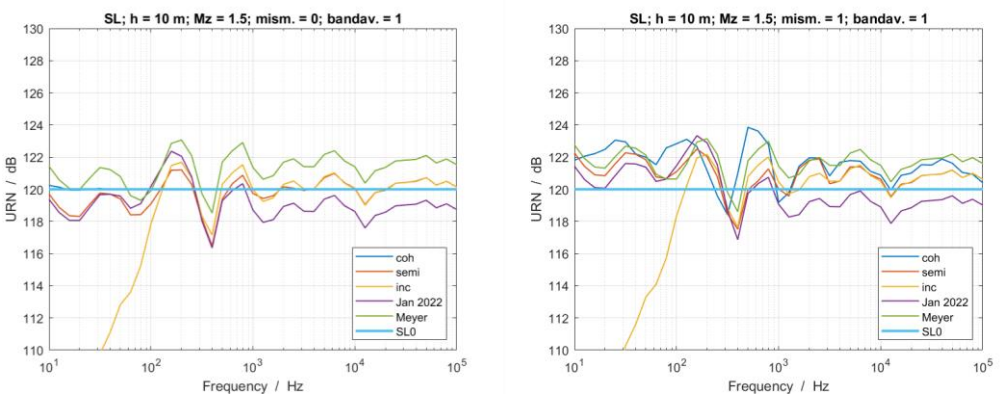

Figure B-4. (Left) No mismatch and (right) with mismatch: Effect of mismatch on 3-band average shallow-water source level (re 1 $\propto$Pa^2 m^2) for sand sediment. The correct source level is 120 dB (bold blue line). The magenta curve is calculated using equation B-11 from this memo. The blue (red) curve is calculated using a coherent (semi-coherent) image sum.

Given SL, one can calculate aSL using (Figure B-5):

$$L'_S = L_S + \Delta L_S\,, \tag{B-12}$$

where ΔL_S is given by equation B-15. If equation B-10 is used for PL, the right-hand side of equation B-12 is equal to aRNL

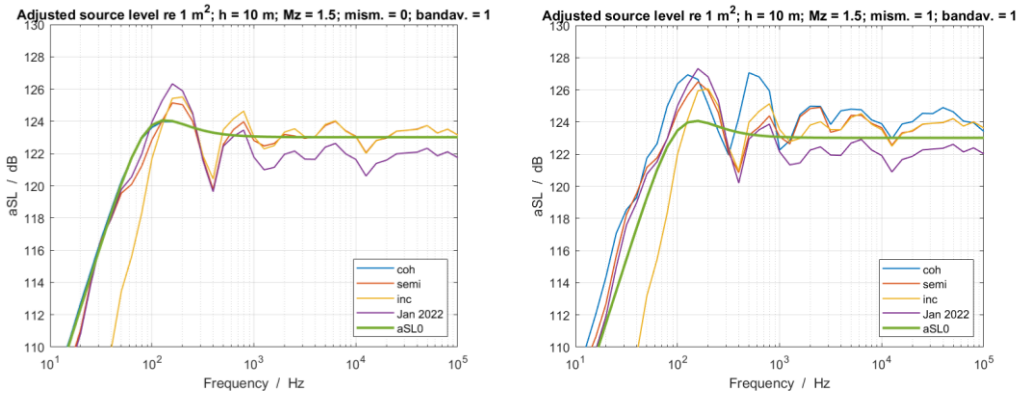

Figure B-5. (Left) No mismatch and (right) with mismatch: Effect of mismatch on 3-band average aSL (re 1 ∝Pa² m²) for sand sediment. The correct aSL is the bold green line. The magenta curve is calculated using equation B-12 from this memo, with equation B-10 for PL, and corresponds to the proposed aRNL formula equation B-13 to equation B-17, with $\alpha = 0$). The blue (red) curve is calculated using a coherent (semi-coherent) image sum.

B.3. Conclusion

The recommended formula for aRNL (reinstating the absorption term omitted from equation B-8 for simplicity) is:

$$L'_{\mathrm{RN}} = L_{\mathrm{RN}}(\theta_1) + \Delta L_{\mathrm{S}} + \Delta L_H + \Delta L_\alpha \,, \tag{B-13}$$

where (for sound pressure level L_p, slant range r, and reference distance r_0):

$$L_{\mathrm{RN}}(\theta_1) = L_p + 10 \log_{10} \frac{r^2}{r_0^2} \,\mathrm{dB} \,, \tag{B-14}$$

$$\Delta L_{\mathrm{S}} = 10 \log_{10} \bar{\sigma} \,\mathrm{dB}, \tag{B-15}$$

$$\Delta L_H = -10 \log_{10} \left(\sigma_1 + \frac{\psi r}{H} \sigma_\psi \right) \mathrm{dB} \,, \tag{B-16}$$

and (for attenuation coefficient α):

$$\Delta L_\alpha = \alpha r \,, \tag{B-17}$$

where ψ is sediment critical angle and H is water depth. (In the remainder of this memorandum, the absorption coefficient is assumed to be negligible and α is set to zero).

Other parameters are:

$$\sigma_1 \approx \left(\frac{1}{2} + \frac{1}{4\eta \sin^2 \theta_1}\right)^{-1}, \tag{B-18}$$

and[8]

$$\sigma_\psi \approx \left(\frac{1}{2} + \frac{3}{4\eta \sin^2 \psi}\right)^{-1}, \tag{B-19}$$

where (θ_1) is the elevation angle (from the sea surface) at which the measurement is made (for horizontal distance x):

$$\cos \theta_1 = \frac{x}{r}, \tag{B-20}$$

$\bar{\sigma}$ is the ratio of dipole to monopole source factor used by ISO 17208-2 (for angular wavenumber k, source depth d):

$$\bar{\sigma} = \frac{14\eta + 2\eta^2}{14 + 2\eta + \eta^2}, \tag{B-21}$$

$$\eta = k^2 d^2 . \tag{B-22}$$

[8] A more precise formula can be obtained by replacing $\sin^2 \psi$ with $\frac{3}{2}\left(1 - \frac{\sin 2\psi}{2\psi}\right)$. (I have discovered a truly marvelous proof of this, which this footnote is too small to contain).

APPENDIX C. MEASURING SEDIMENT PROPERTIES BY INVERSION

C.1. Measured Propagation Loss Data

An underwater sound projector played acoustic sweeps over frequency as it drifted past a near-seabed AMAR at each site (see Section 4.1.4). Figure C-1 shows the projector drift track and the AMAR location for the deep site. Figure C-2 shows the projector drift tracks and the AMAR locations for the Intermediate and Shallow sites.

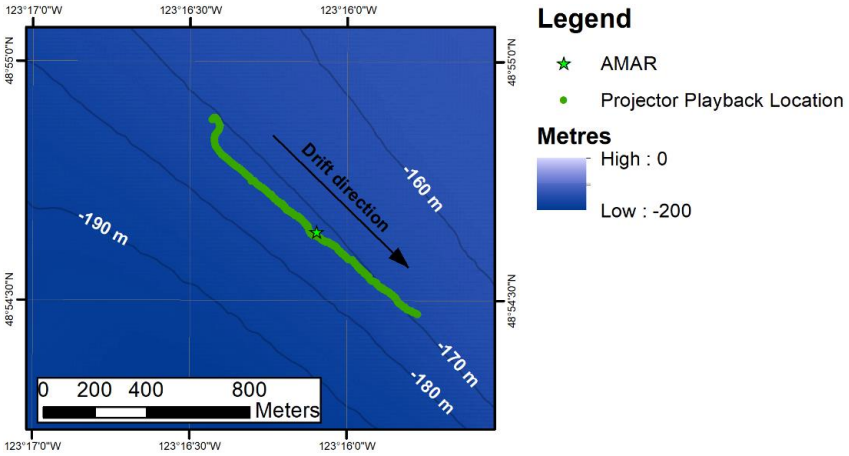

Figure C-1. Map showing the deep site propagation loss (PL) study drift tracks and bathymetry.

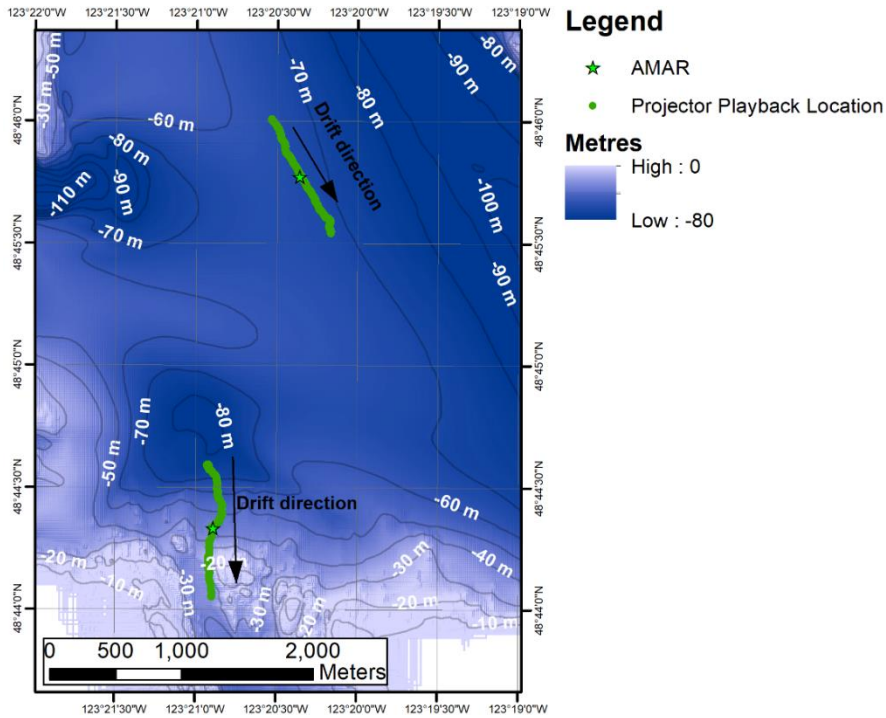

Figure C-2. Map showing the deep site propagation loss (PL) study drift tracks and bathymetry.

Recordings from the AMAR and an OSM with hydrophone 1 m from the projector were processed to calculate sound levels in 100 Hz wide bands. The 2 s long sweeps were played every 10 s and sound levels were computed for every second in the recordings. For each frequency band and over each 11 s window of the recordings, the 'signal' level was set to the maximum 1 s SPL and the 'background' level was set to the median of the 1 s SPL within the 11 s window. Figure C-3 shows the sound levels from the AMAR as a function of range. Background sound levels increased substantially during portions of the measurements because the source vessel occasionally had to engage its engine to maintain a suitable drift speed and direction. To avoid contamination from the measurement vessel, the signal to background noise ratio (SNR) was calculated for each time window and measurements where the ratio was less than 10 dB were discarded from further analysis.

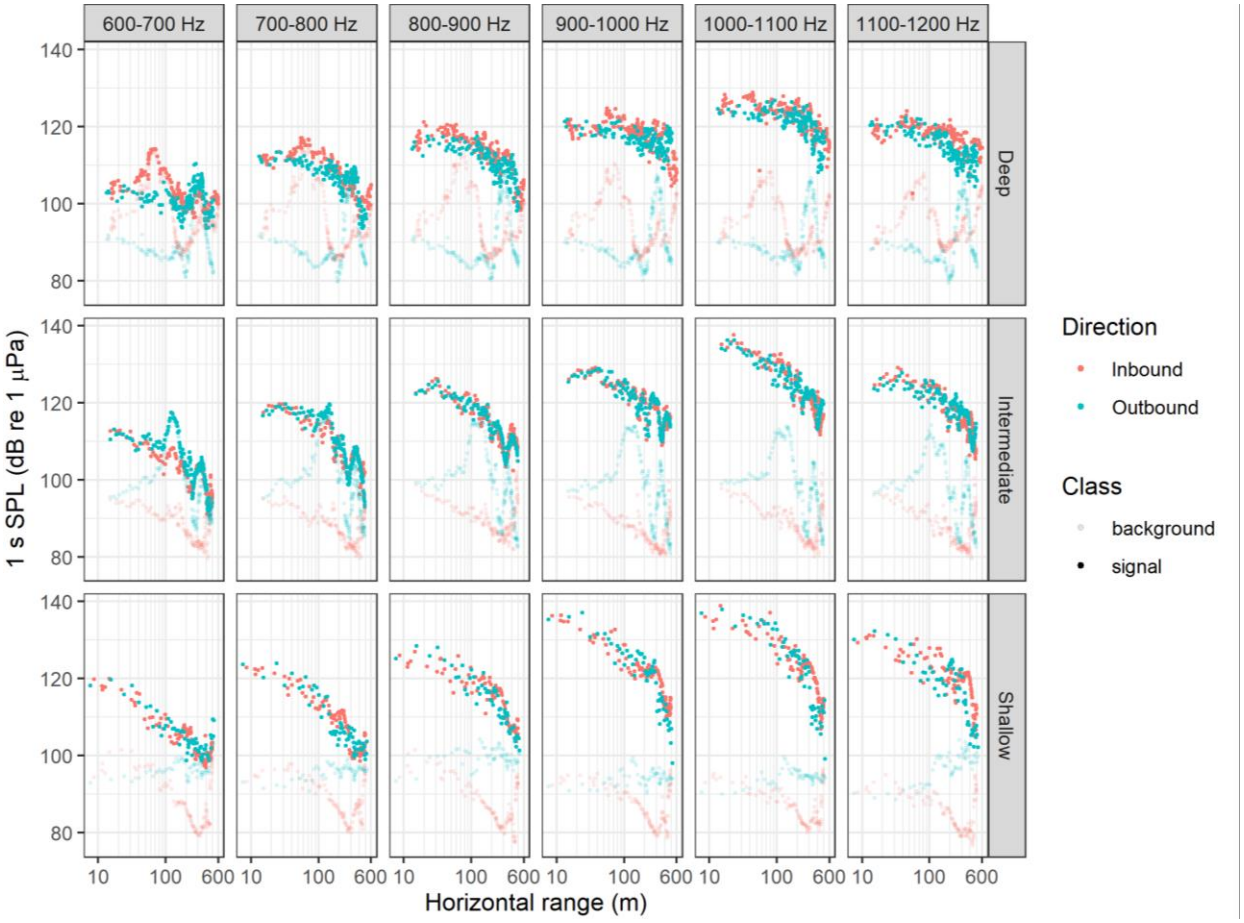

Figure C-3. AMAR measured signal and background sound pressure level (SPL) as a function of range during the propagation loss (PL) experiment.

Figure C-4 shows the sound levels from the 1 m hydrophone (OSM) recordings. The signal levels were generally consistent throughout the experiment but there were occasional shifts in levels. Signal levels consistently exceeded background levels by at least 30 dB.

Figure C-4. OSM (1 m hydrophone) measured signal and background sound pressure level (SPL) as a function of range during the propagation loss (PL) experiment.

Propagation loss was then calculated by matching the SNR-filtered AMAR SPL and 1 m SPL by time and subtracting (equation 32). Figure C-5 shows the calculated PL for each site.

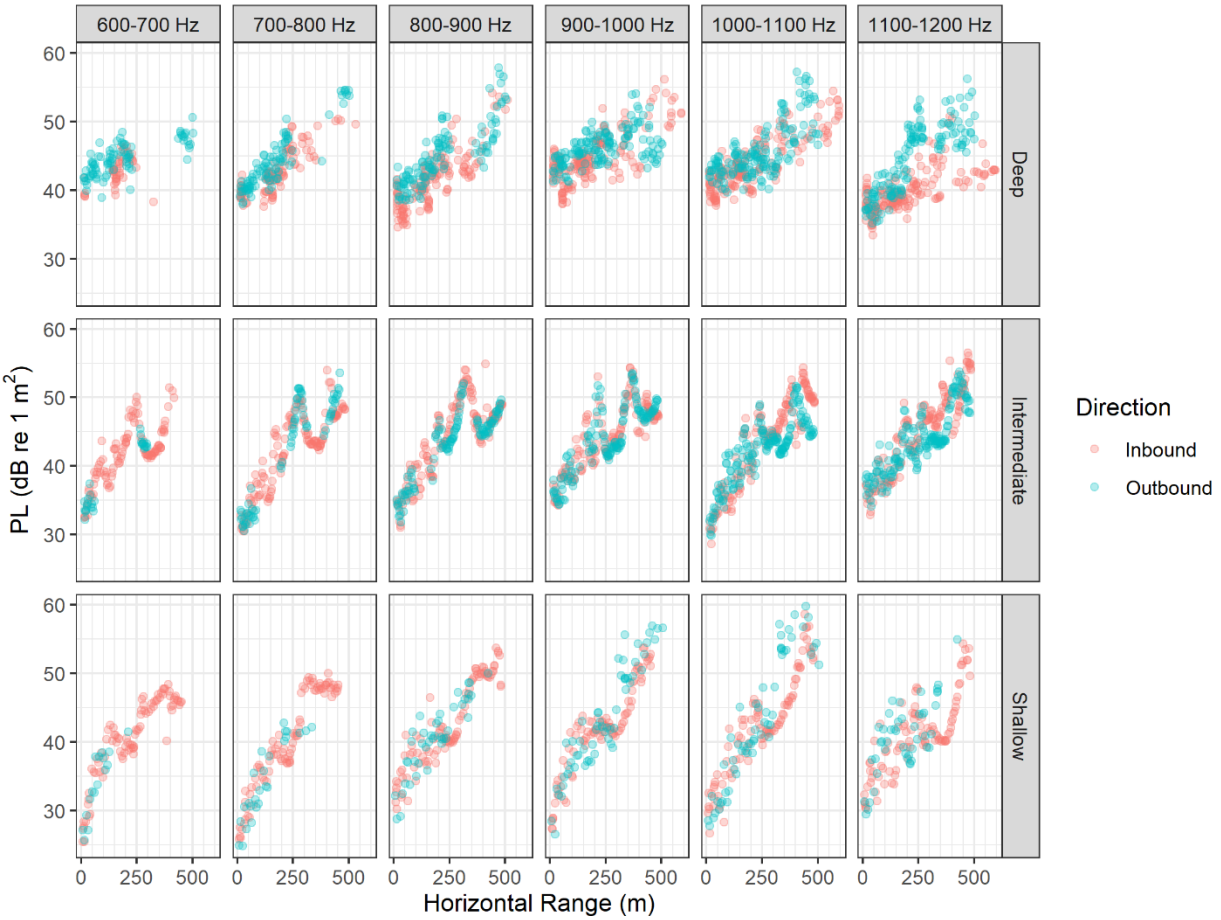

Figure C-5. Measured propagation loss as a function of distance.

The bathymetry at the Deep and Intermediate sites was essentially flat. The water depth at the Deep site was approximately 170 m and the water depth at the intermediate site was approximately 66 m. The bathymetry at the Shallow site was more complex (Figure C-2). The water depth decreased as the projector approached the AMAR (the slope was ~4.3°; Figure C-6). As the projector drifted past the AMAR, the water depth continued to decrease until approximately 275 m distance but then increased at farther distances. PL measurements at the shallow site obtained after reaching the closest point of approach were discarded prior to running the inversion to simplify the approach and to limit potential issues with range-dependent geoacoustic properties. Therefore, only the inbound PL data from the shallow site was used in the inversion.

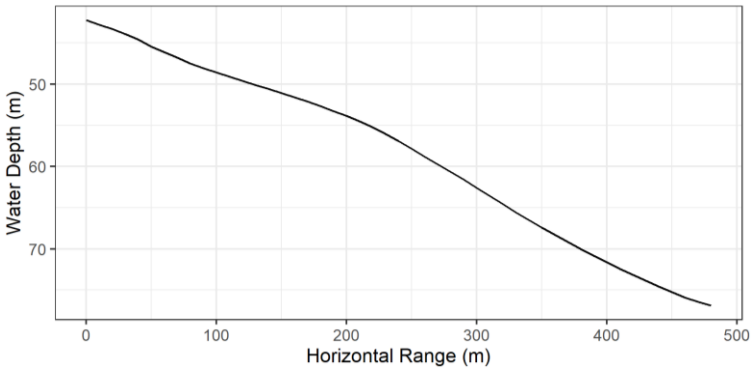

Figure C-6. Water depth at the shallow site as the projector approached the Autonomous Multichannel Acoustic Recorder (AMAR) during the propagation loss (PL) study.

C.2. Nonlinear Bayesian Inversion

The propagation loss indicated in Figure C-5 can be inverted for geoacoustic properties. The inversion method used here uses a trans-Dimensional (trans-D) formulation to determine the number of seabed layers, the layer properties, and the presence of autocorrelated errors, separately for each site. The formulation closely follows that used in other geoacoustic inversion research (Dettmer et al. 2010, Dettmer and Dosso 2012, Steininger et al. 2013, Dosso et al. 2014).

The environmental model uses a known (fixed) water sound speed profile with an unknown number of homogeneous layers overlaying an unknown halfspace. Each layer has a thickness and depth-linear gradients for the compressional wave sound speed, density, and compressional wave attenuation. Single values for the shear wave sound speed and attenuation are applied to the entire subbottom (i.e., they are independent of subbottom depth and layering). The bathymetry is considered known at each site, but an unknown depth offset is estimated in the inversion. Easting and northing offsets are also estimated to account for systematic differences between the drifting GPS and projector location throughout the drift measurements.

The inversion involves applying Bayes theorem to update prior beliefs (probabilities) of parameter values with information obtained from the data using a likelihood function. The distributions representing prior beliefs were assumed to be uniform between lower and upper bounds as specified in Table C-1. Compressional wave speed and density were further constrained to physically realistic combinations as described in Quijano et al. (2012).

Table C-1. Prior model parameter bounds for the geoacoustic inversion.

Parameter	Units	Prior bounds
Number of layers	-	[0,4]
Layer interface depth	m	[0.1,50]
Layer compressional wave speed	m/s	[1450, 2500]
Layer density	g/cm^3	[1.3, 2.5]
Layer compressional wave attenuation	dB/λ	[0.01, 1]
Shear wave speed	m/s	[0.1, 750]
Shear wave attenuation	dB/λ	[0.01, 4]
Easting offset	m	[-20, 20]
Northing offset	m	[-20, 20]
Water depth offset	m	[-10, 10] (Deep site) [-6, 6] (Intermediate site) [-20, 5] (Shallow site)

For the likelihood function, we assume autocorrelated gaussian-distributed errors between PL model predictions and observed data that have the same standard deviation within each frequency band but may differ between bands. The likelihood function is therefore:

$$L(k, \boldsymbol{m}_k) = [(2\pi)^N |\boldsymbol{C}_d|]^{-1/2} \times \exp\left[-\frac{1}{2}\boldsymbol{r}^T \boldsymbol{C}_d^{-1} \boldsymbol{r}\right], \quad \text{(C-1)}$$

where k is the number of geoacoustic layers, $\boldsymbol{m}_k$ is the vector of model parameters (environmental and non-environmental), N is the number of PL measurements, $\boldsymbol{C}_d$ is a diagonal covariance matrix, and $\boldsymbol{r}$ is a vector of data residuals. The data residuals are given by:

$$r_i = d_i - d_i(\boldsymbol{m}_k) - d_i(a) \text{ and } d_i(a) = a[d_{i-1} - d_{i-1}(\boldsymbol{m}_k)], \quad \text{(C-2)}$$

where d_i is measured propagation loss for the ith measurement within a frequency band, $d_i(\boldsymbol{m}_k)$ is the corresponding modelled propagation loss, and *a* is the autoregressive parameter for the specified frequency band.

Propagation loss was modelled using JASCO's Parabolic Equation (PE) Marine Operations Noise Model (MONM). Some of the near-range PL measurements at the Deep and Intermediate sites could not be modelled efficiently because the receivers were outside the valid angles of the PE model. To avoid this issue, we excluded PL measurements within 75 m (horizontal distance) from the Deep and Intermediate sites.

The complete solution to the Bayesian inversion is the posterior probability density (PPD) of the model parameters given the measured data and prior distribution. A reversible-jump Markov Chain Monte Carlo (rjMCMC) algorithm was applied to sample the PPD where model transitions were probabilistically accepted according to the Metropolis-Hastings-Green criterion (Green 1995). Properties of the PPD can be used to estimate model parameters and their uncertainties. In this study, convergence of the PPD could not be achieved given time constraints so parameter uncertainty estimates could not be made. However, measured PL data were fit well at all three sites and the corresponding maximum *a posteriori* (MAP) models were used to define the geoacoustic properties.

C.3. Bottom Loss Versus Frequency

The geoacoustic properties from the MAP models were used to calculate bottom loss versus grazing angle and frequency at each site (Figures C-7 to C-9). Bottom loss was calculated by approximating the geoacoustic model at each site by a two-layer elastic system, consisting of a top sediment layer over a semi-infinite basement. Geoacoustic properties were assumed to vary linearly with depth in the sediment layer and to be uniform with depth in the basement layer. The bottom loss function was used to determine the grazing angle as a function of frequency at each site (see Section 4.2.1). The grazing angle was required for calculating vessel source levels using the seabed critical angle method (see Section 2.3.4).

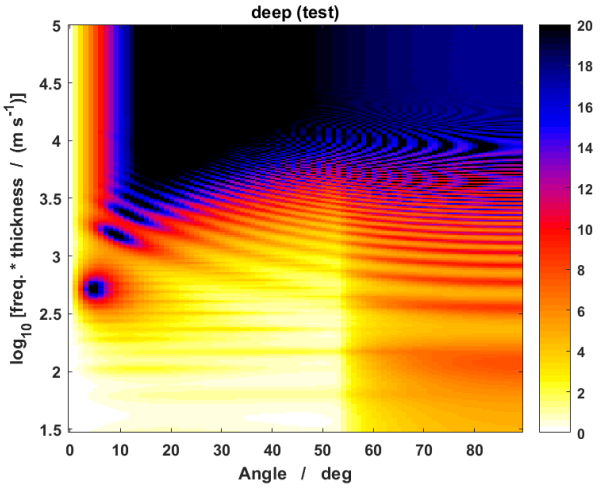

Figure C-7. Deep site: Seabed reflection loss (dB) versus the logarithm of a dimensionless frequency, $\log_{10}(fh/(\text{m s}^{-1}))$, where fh is the product of frequency f and sediment thickness h. Thickness of the top sediment layer at the deep site was assumed to be $h = 2.78\ m$.

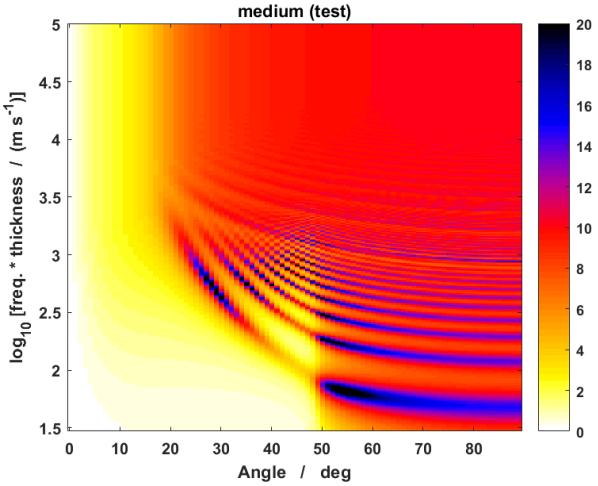

Figure C-8. Intermediate site: Seabed reflection loss (dB) versus the logarithm of a dimensionless frequency, $\log_{10}(fh/(\text{m s}^{-1}))$, where fh is the product of frequency f and sediment thickness h. Thickness of the top sediment layer at the intermediate site was assumed to be $h = 10.34\ m$.

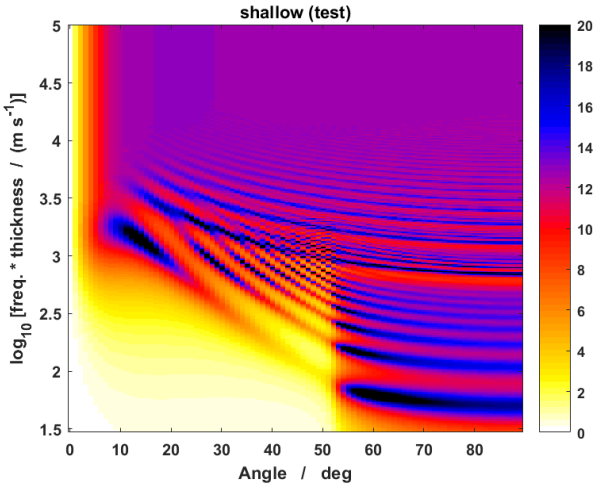

Figure C-9. Shallow site: Seabed reflection loss (dB) versus the logarithm of a dimensionless frequency, $\log_{10}(fh/(\text{m s}^{-1}))$, where fh is the product of frequency f and sediment thickness h. Thickness of the top sediment layer at the deep site was assumed to be $h = 13.18\ m$.

APPENDIX D. DETAILED SOURCE LEVEL COMPARISONS

D.1. Single-Node URN Measurements

Plots in this appendix show curves of mean source level versus frequency for single-node hydrophone measurements of vessels A–C, for speeds from 17–21 knots. Columns show different sites and rows show different SL metrics. Coloured lines show different CPA distance bins. Black lines show reference measurements (SL.ISO) from the deep VLA. The *n* values indicate the number of individual measurements contributing to the average.

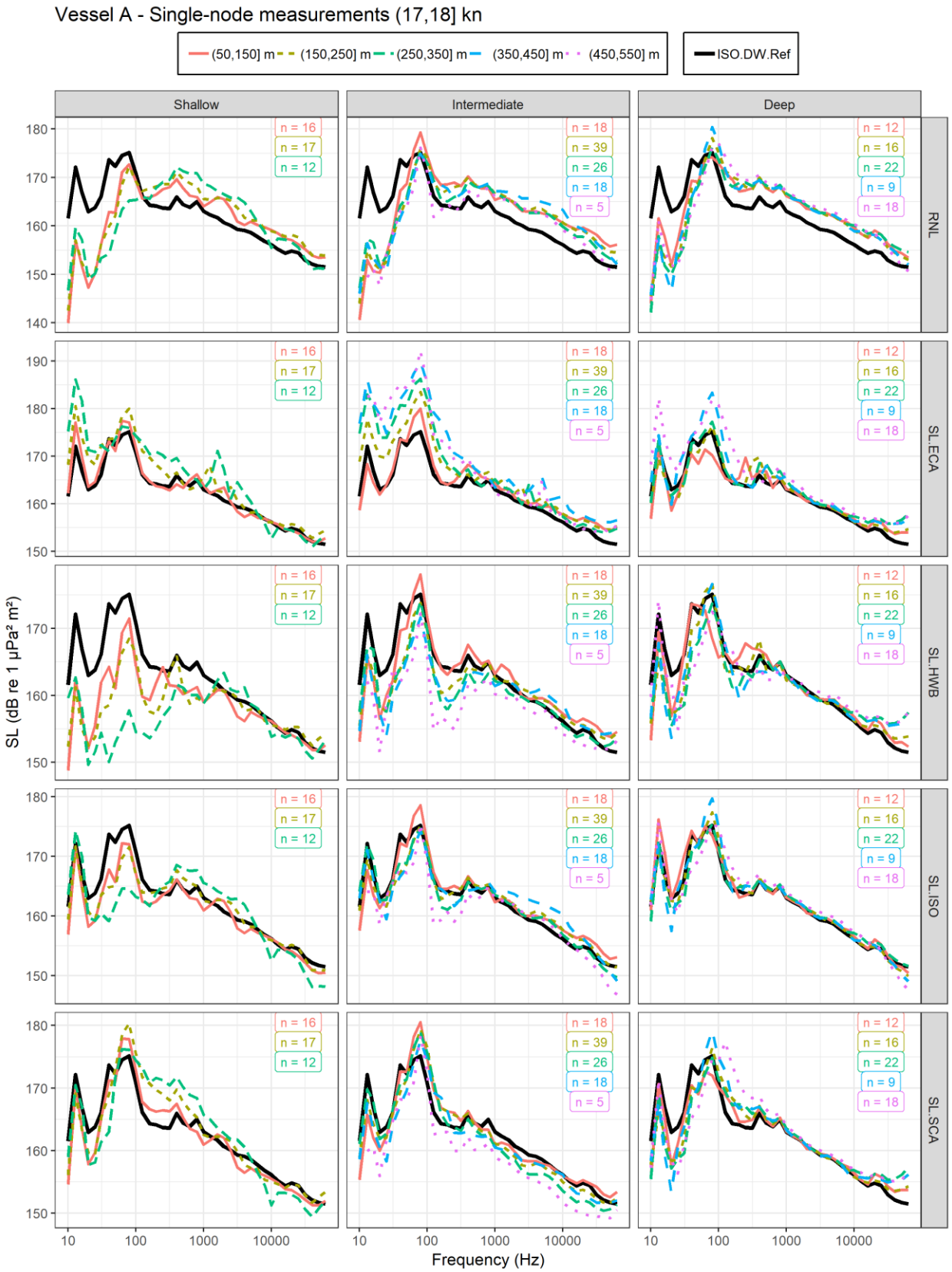
Vessel A - Single-node measurements (17,18] kn
(50,150] m
(150,250] m
(250,350] m
(350,450] m
(450,550] m
ISO.DW.Ref
Shallow
Intermediate
Deep
RNL
SL.ECA
SL.HWB
SL.ISO
SL.SCA
SL (dB re 1 µPa² m²)
Frequency (Hz)
n = 16
n = 17
n = 12
n = 18
n = 39
n = 26
n = 5
n = 22
n = 9

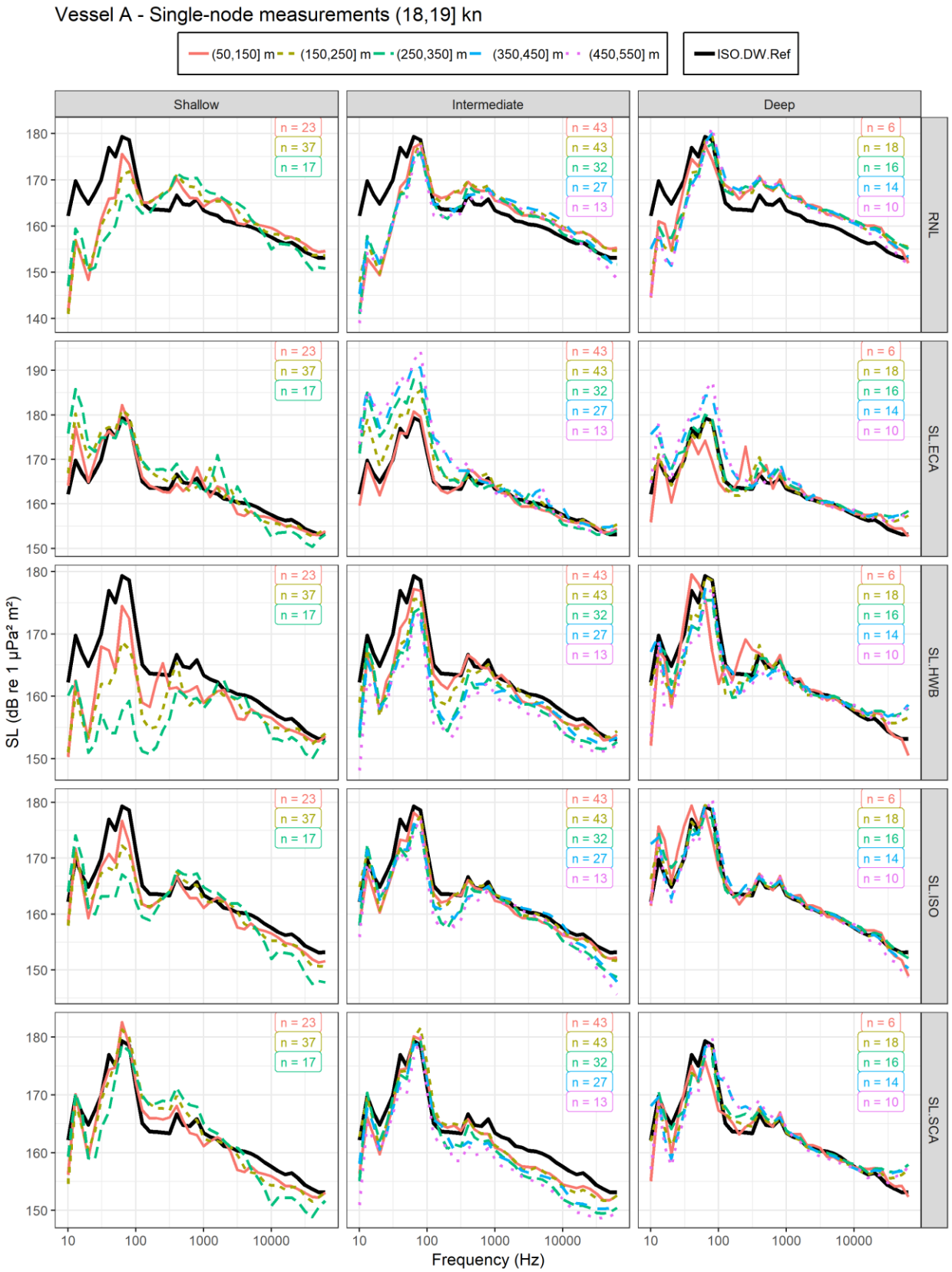
Vessel A - Single-node measurements (18,19] kn
(50,150] m
(150,250] m
(250,350] m
(350,450] m
(450,550] m
ISO.DW.Ref
Shallow
Intermediate
Deep
RNL
SL.ECA
SL.HWB
SL.ISO
SL.SCA
SL (dB re 1 µPa² m²)
Frequency (Hz)
n = 23
n = 37
n = 17
n = 43
n = 43
n = 32
n = 27
n = 13
n = 6
n = 18
n = 16
n = 14
n = 10

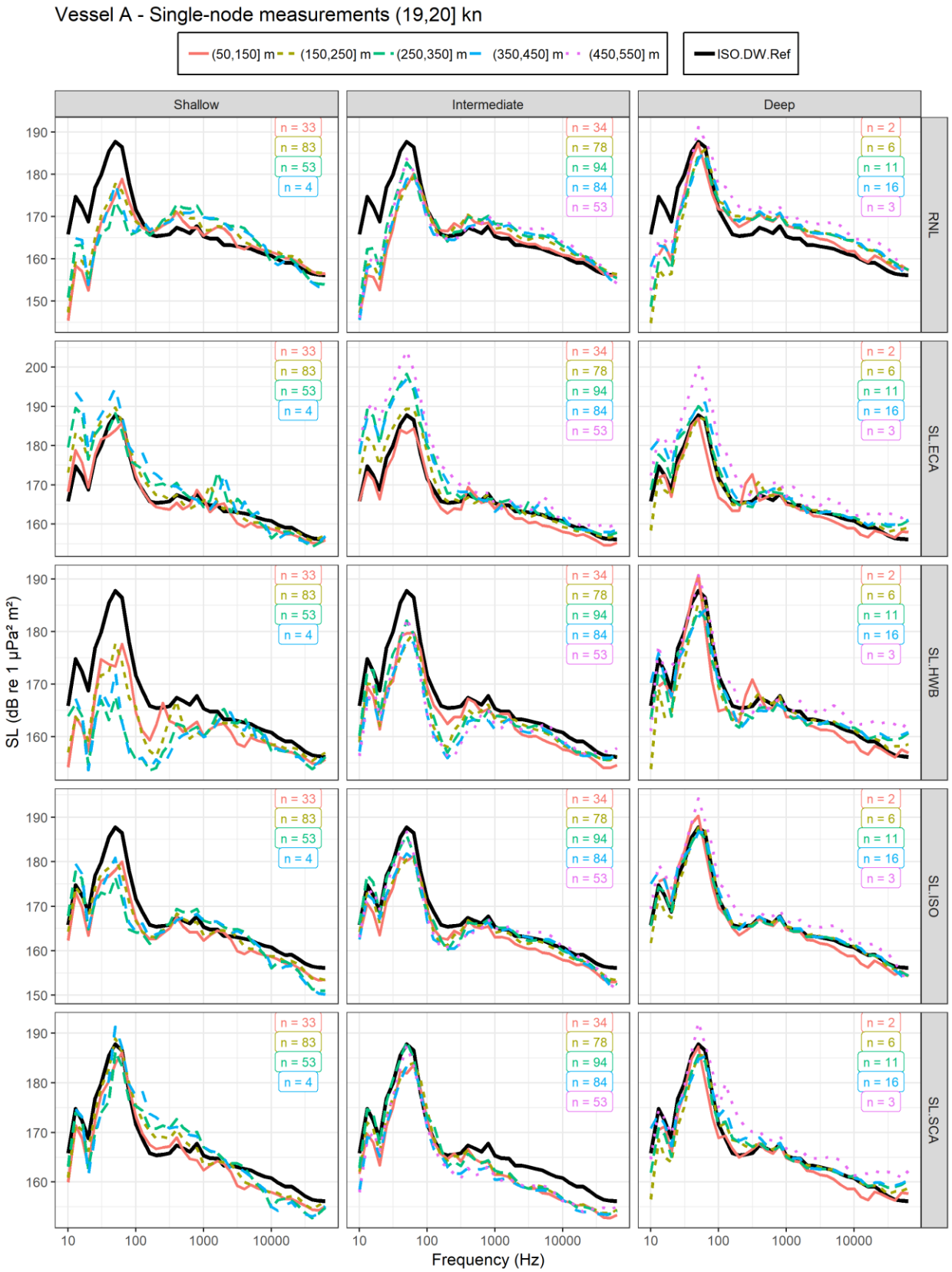
Vessel A - Single-node measurements (19,20] kn
(50,150] m
(150,250] m
(250,350] m
(350,450] m
(450,550] m
ISO.DW.Ref
Shallow
Intermediate
Deep
RNL
SL.ECA
SL.HWB
SL.ISO
SL.SCA
SL (dB re 1 µPa² m²)
Frequency (Hz)
n = 33
n = 83
n = 53
n = 4
n = 34
n = 78
n = 94
n = 84
n = 53
n = 2
n = 6
n = 11
n = 16
n = 3

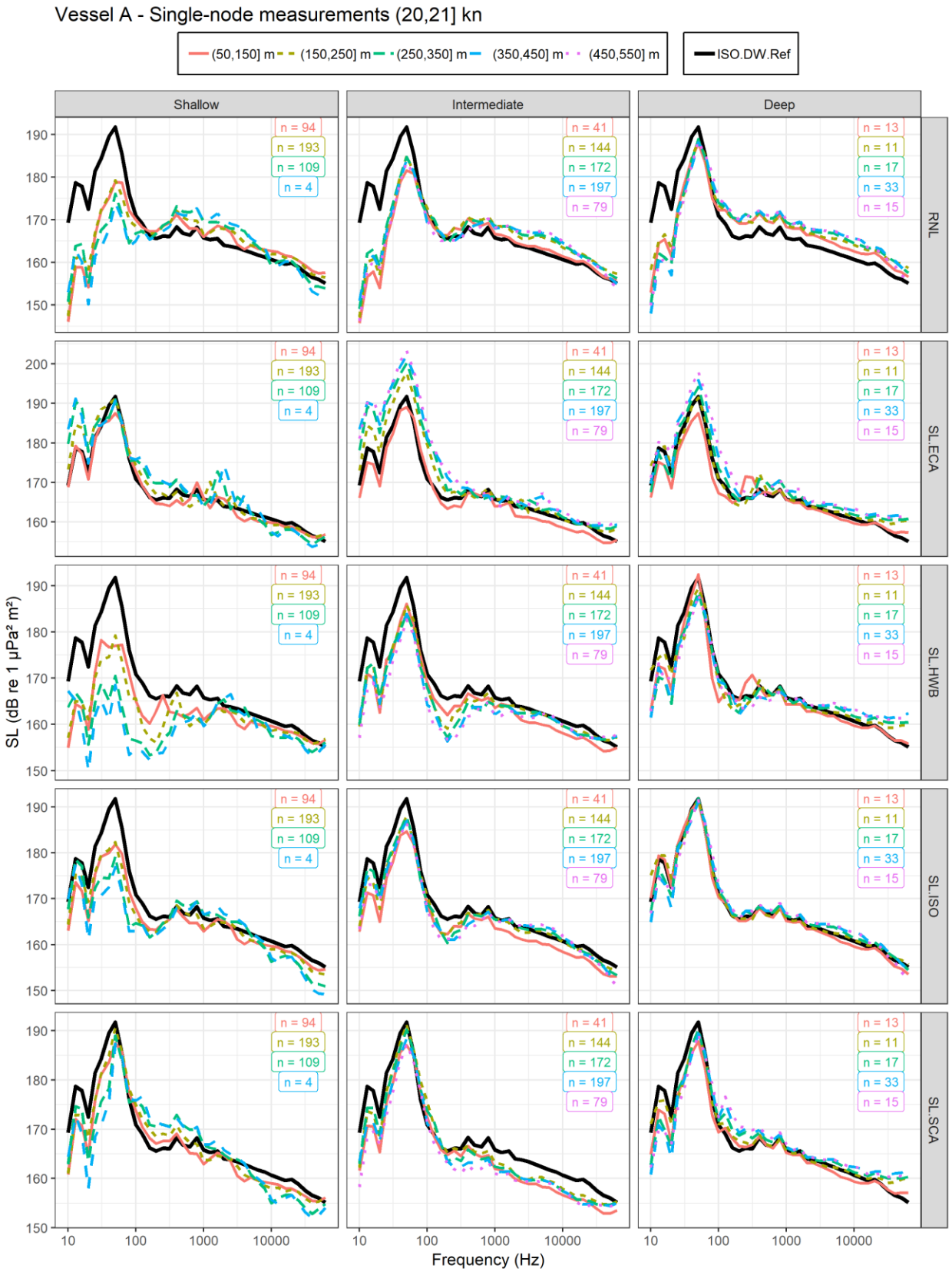
Vessel A - Single-node measurements (20,21] kn
(50,150] m
(150,250] m
(250,350] m
(350,450] m
(450,550] m
ISO.DW.Ref
Shallow
Intermediate
Deep
RNL
SL.ECA
SL.HWB
SL.ISO
SL.SCA
n = 94
n = 193
n = 109
n = 4
n = 41
n = 144
n = 172
n = 197
n = 79
n = 13
n = 11
n = 17
n = 33
n = 15
SL (dB re 1 µPa² m²)
Frequency (Hz)
10
100
1000
10000

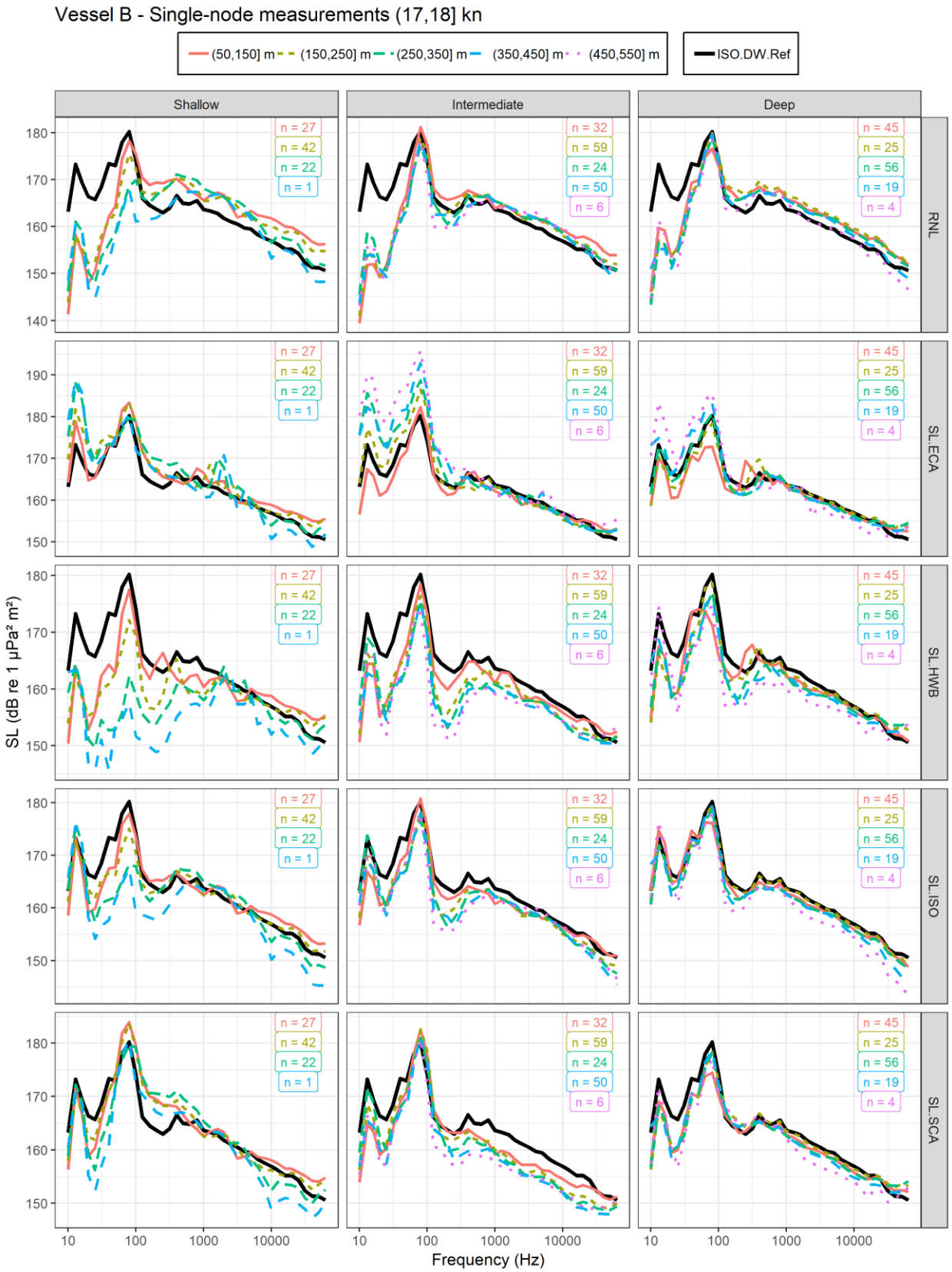
Vessel B - Single-node measurements (17,18] kn
(50,150] m
(150,250] m
(250,350] m
(350,450] m
(450,550] m
ISO.DW.Ref
Shallow
Intermediate
Deep
RNL
SL.ECA
SL.HWB
SL.ISO
SL.SCA
SL (dB re 1 µPa² m²)
Frequency (Hz)
n = 27
n = 42
n = 22
n = 1
n = 32
n = 59
n = 24
n = 50
n = 6
n = 45
n = 25
n = 56
n = 19
n = 4

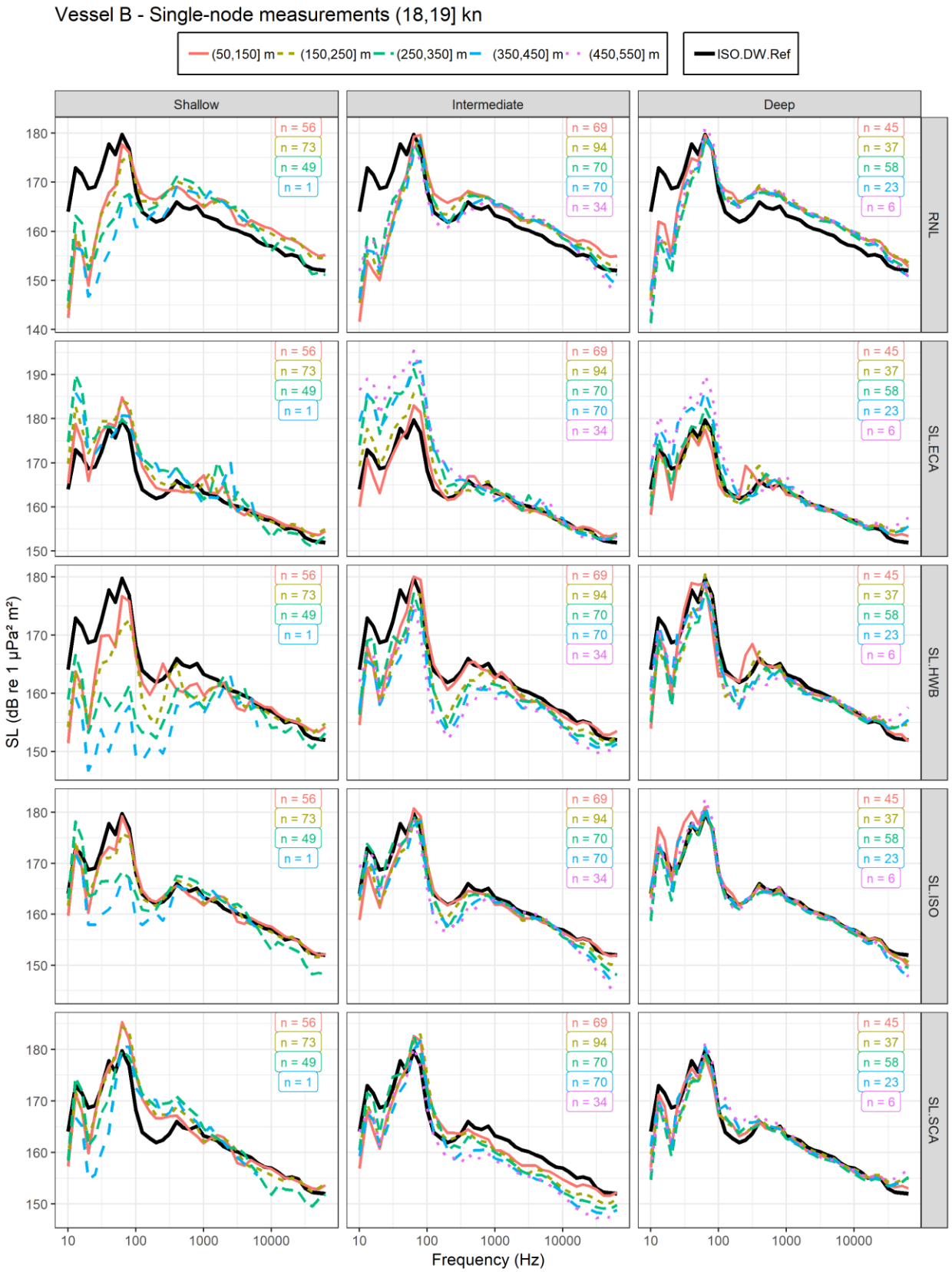
Vessel B - Single-node measurements (18,19] kn
(50,150] m
(150,250] m
(250,350] m
(350,450] m
(450,550] m
ISO.DW.Ref
Shallow
Intermediate
Deep
RNL
SL.ECA
SL.HWB
SL.ISO
SL.SCA
SL (dB re 1 µPa² m²)
Frequency (Hz)
n = 56
n = 73
n = 49
n = 1
n = 69
n = 94
n = 70
n = 34
n = 45
n = 37
n = 58
n = 23
n = 6

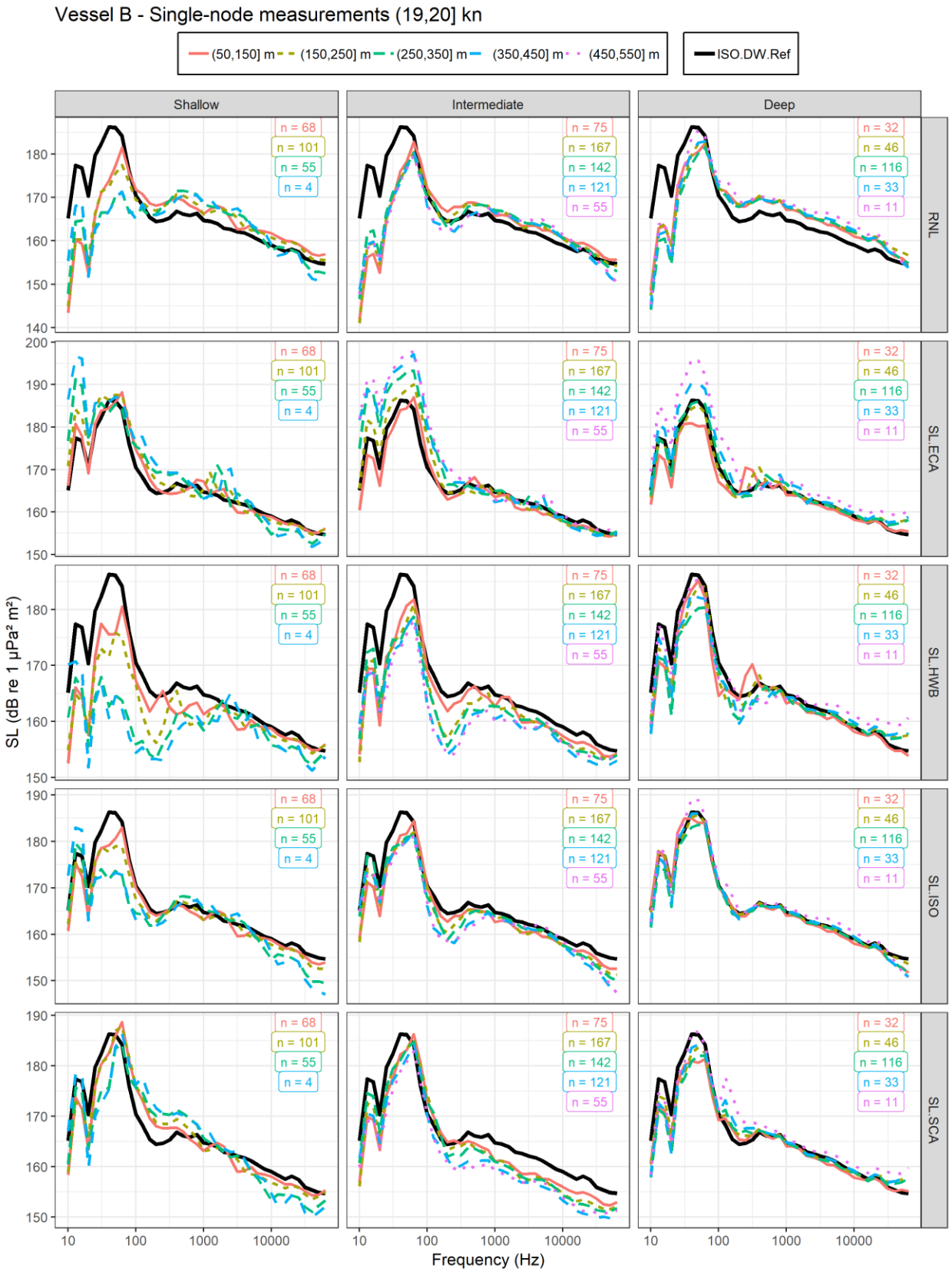
Vessel B - Single-node measurements (19,20] kn
(50,150] m
(150,250] m
(250,350] m
(350,450] m
(450,550] m
ISO.DW.Ref
Shallow
Intermediate
Deep
RNL
SL.ECA
SL.HWB
SL.ISO
SL.SCA
n = 68
n = 101
n = 55
n = 4
n = 75
n = 167
n = 142
n = 121
n = 55
n = 32
n = 46
n = 116
n = 33
n = 11
SL (dB re 1 µPa² m²)
Frequency (Hz)
10
100
1000
10000

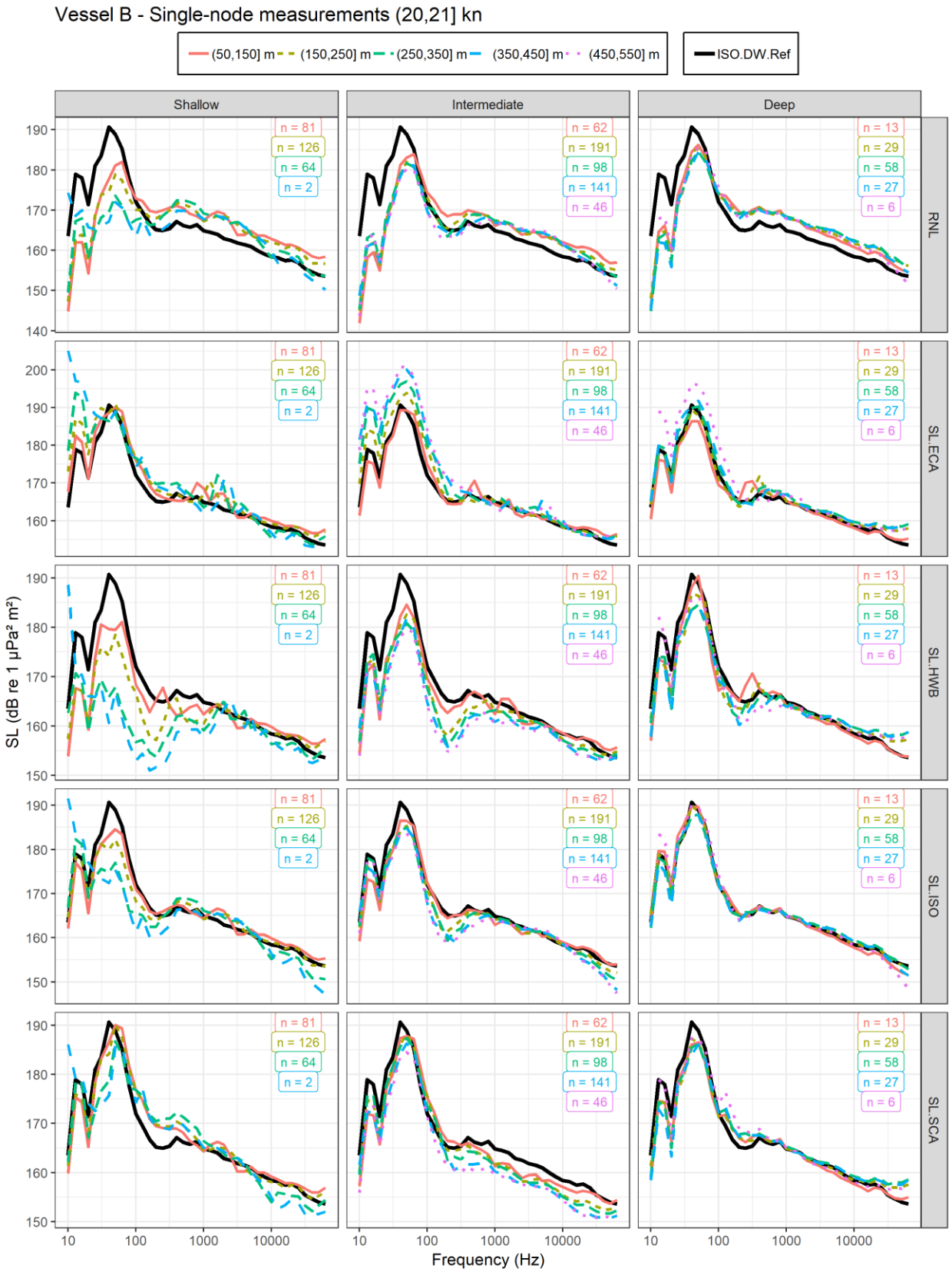
Vessel B - Single-node measurements (20,21] kn
(50,150] m
(150,250] m
(250,350] m
(350,450] m
(450,550] m
ISO.DW.Ref
Shallow
Intermediate
Deep
RNL
SL.ECA
SL.HWB
SL.ISO
SL.SCA
n = 81
n = 126
n = 64
n = 2
n = 62
n = 191
n = 98
n = 141
n = 46
n = 13
n = 29
n = 58
n = 27
n = 6
SL (dB re 1 µPa² m²)
Frequency (Hz)


Vessel C - Single-node measurements (17,18] kn
(50,150] m
(150,250] m
(250,350] m
(350,450] m
(450,550] m
ISO.DW.Ref
Shallow
Intermediate
Deep
RNL
SL.ECA
SL.HWB
SL.ISO
SL.SCA
SL (dB re 1 µPa² m²)
Frequency (Hz)
10
100
1000
10000

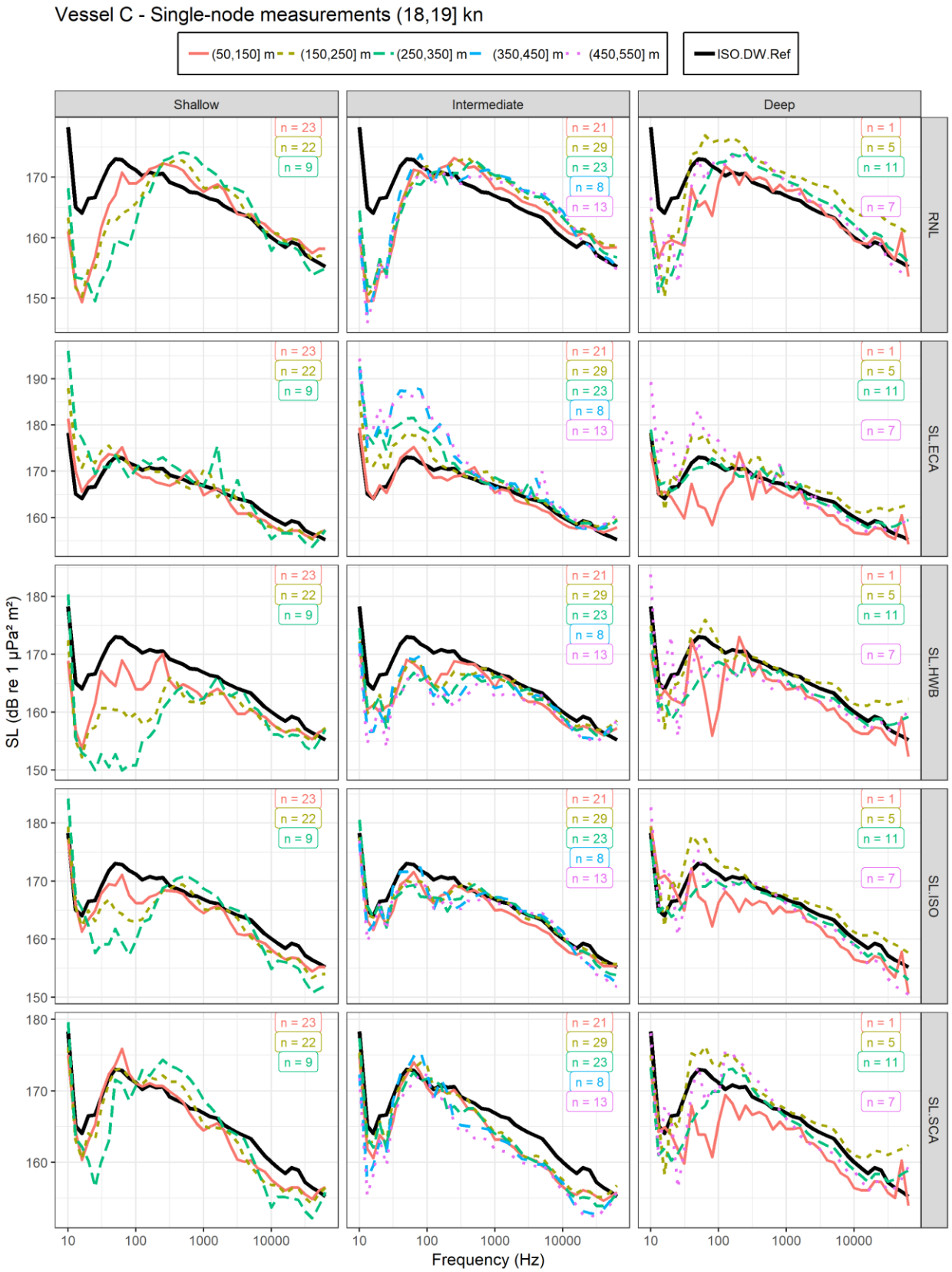
Vessel C - Single-node measurements (18,19] kn
(50,150] m
(150,250] m
(250,350] m
(350,450] m
(450,550] m
ISO.DW.Ref
Shallow
Intermediate
Deep
RNL
SL.ECA
SL.HWB
SL.ISO
SL.SCA
SL (dB re 1 µPa² m²)
Frequency (Hz)
10
100
1000
10000


Vessel C - Single-node measurements (19,20] kn
(50,150] m
(150,250] m
(250,350] m
(350,450] m
(450,550] m
ISO.DW.Ref
Shallow
Intermediate
Deep
RNL
SL.ECA
SL.HWB
SL.ISO
SL.SCA
SL (dB re 1 µPa² m²)
Frequency (Hz)
10
100
1000
10000


Vessel C - Single-node measurements (20,21] kn
(50,150] m
(150,250] m
(250,350] m
(350,450] m
(450,550] m
ISO.DW.Ref
Shallow
Intermediate
Deep
RNL
SL.ECA
SL.HWB
SL.ISO
SL.SCA
n = 45
n = 39
n = 15
n = 35
n = 55
n = 37
n = 29
n = 11
n = 3
n = 5
n = 6
n = 18
SL (dB re 1 µPa² m²)
Frequency (Hz)
10
100
1000
10000

D.2. Array-Average URN Measurements

Plots in this appendix show curves of mean source level versus frequency for array-average hydrophone measurements of vessels A–C, for speeds from 17–21 knots. Columns show different SL metrics and rows show different CPA bins from the arrays. Coloured lines show different HLA and VLA combinations. Black lines show reference measurements (SL.ISO) from the deep VLA. The n values indicate the number of individual measurements contributing to the average.

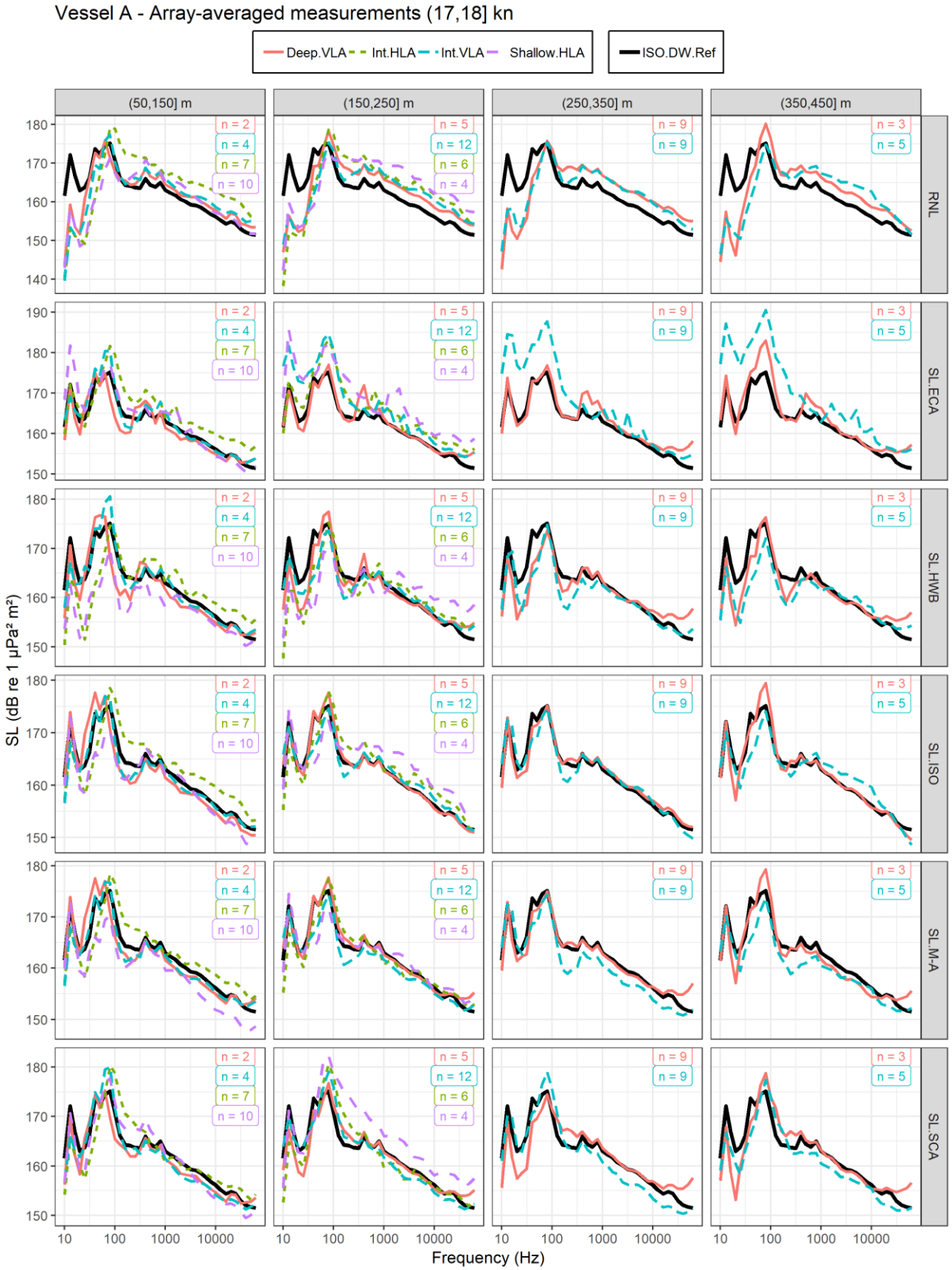
Vessel A - Array-averaged measurements (17,18] kn
Deep.VLA
Int.HLA
Int.VLA
Shallow.HLA
ISO.DW.Ref
(50,150] m
(150,250] m
(250,350] m
(350,450] m
RNL
SL.ECA
SL.HWB
SL.ISO
SL.M-A
SL.SCA
SL (dB re 1 µPa² m²)
Frequency (Hz)

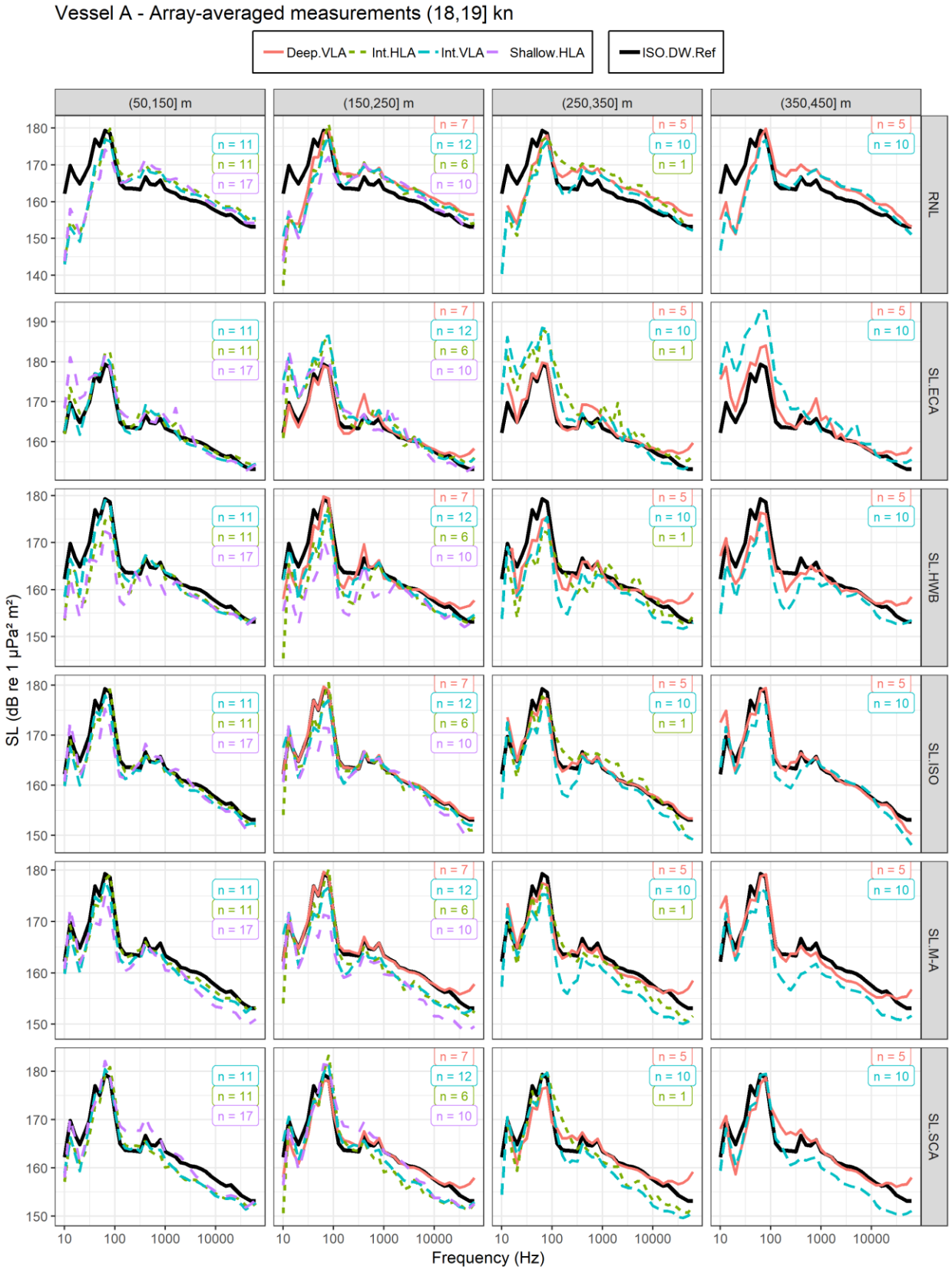
Vessel A - Array-averaged measurements (18,19] kn
Deep.VLA
Int.HLA
Int.VLA
Shallow.HLA
ISO.DW.Ref
(50,150] m
(150,250] m
(250,350] m
(350,450] m
RNL
SL.ECA
SL.HWB
SL.ISO
SL.M-A
SL.SCA
SL (dB re 1 µPa² m²)
Frequency (Hz)

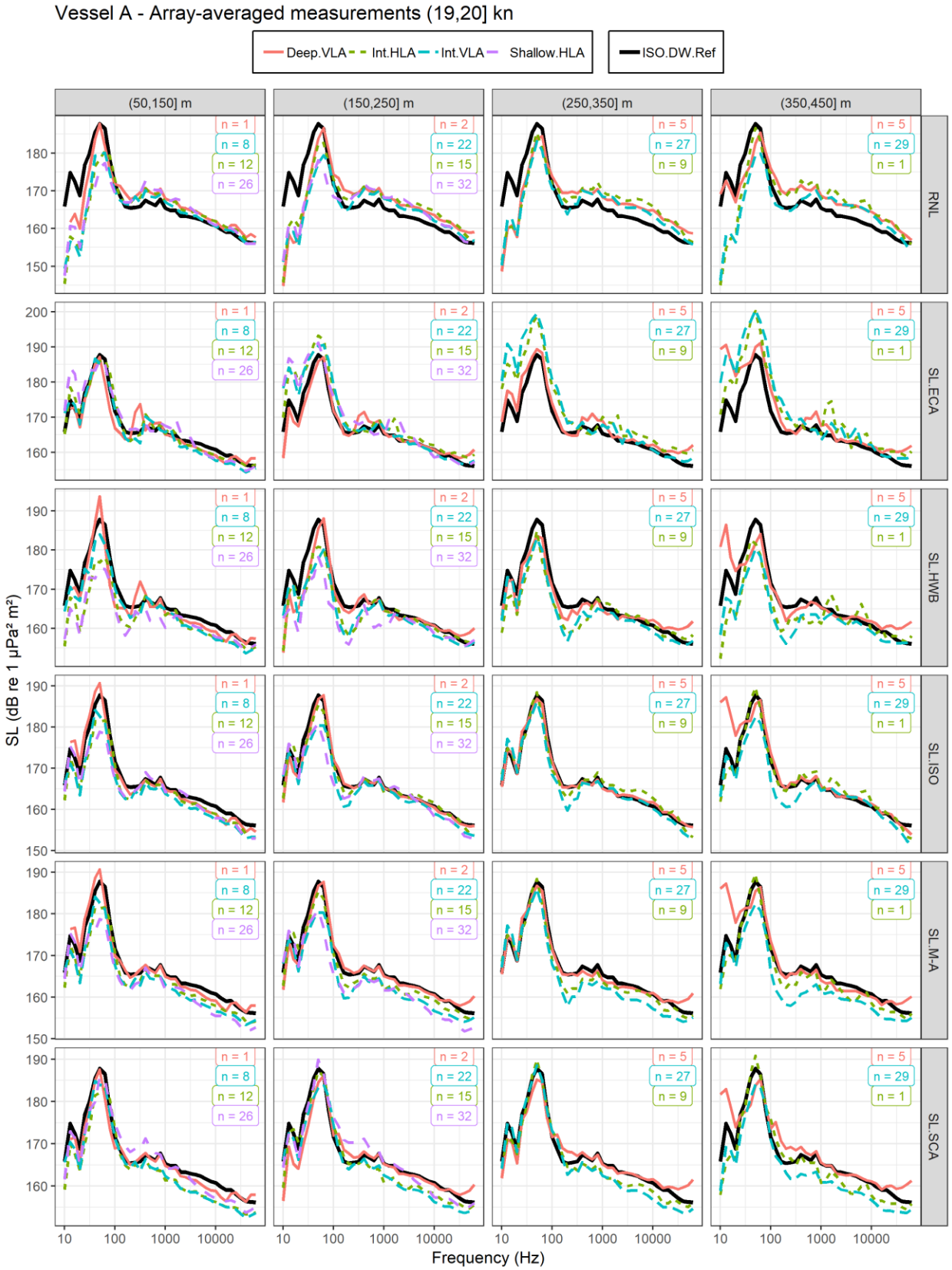
Vessel A - Array-averaged measurements (19,20] kn
Deep.VLA
Int.HLA
Int.VLA
Shallow.HLA
ISO.DW.Ref
(50,150] m
(150,250] m
(250,350] m
(350,450] m
RNL
SL.ECA
SL.HWB
SL.ISO
SL.M-A
SL.SCA
SL (dB re 1 µPa² m²)
Frequency (Hz)

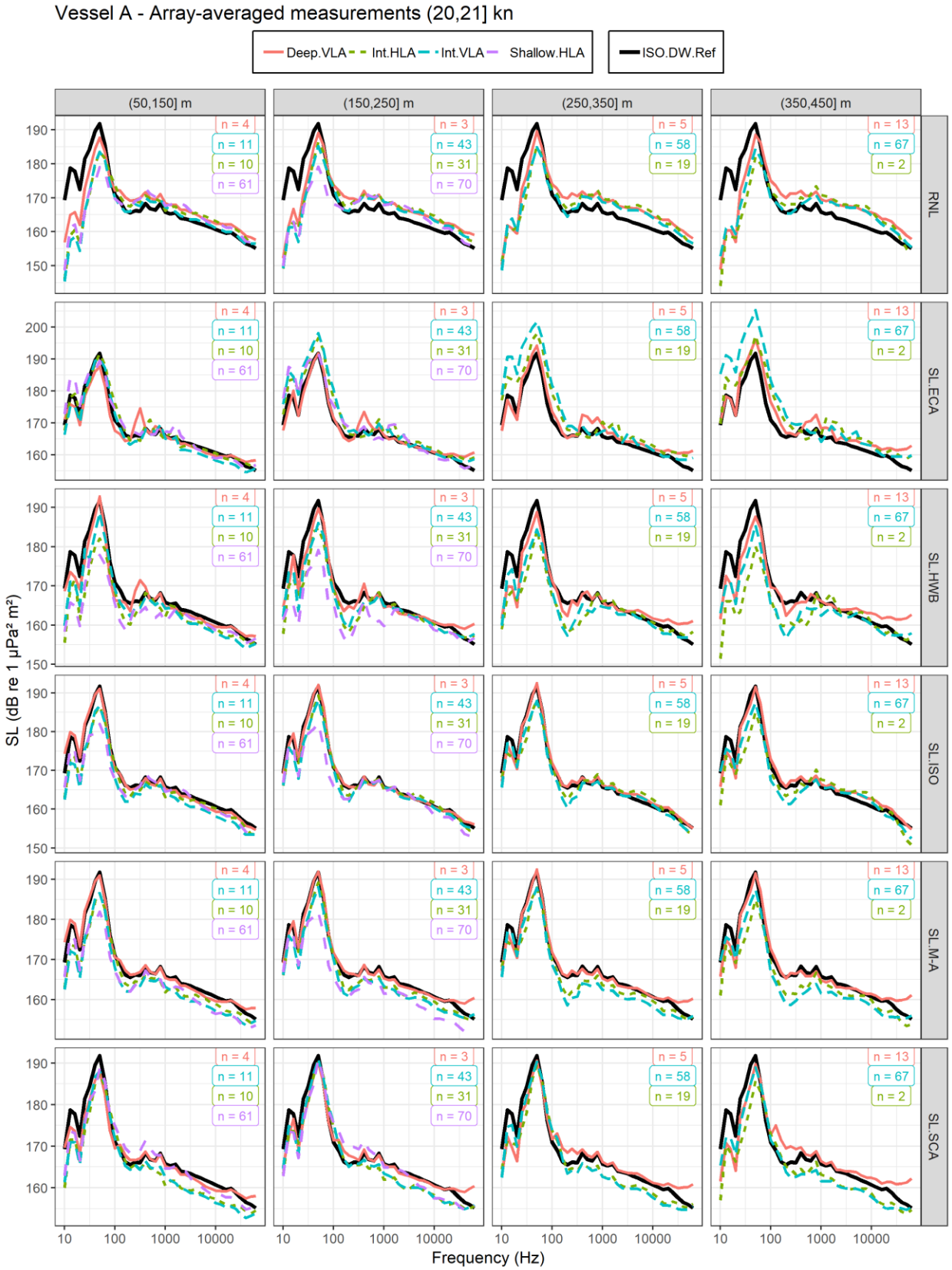
Vessel A - Array-averaged measurements (20,21] kn
Deep.VLA
Int.HLA
Int.VLA
Shallow.HLA
ISO.DW.Ref
(50,150] m
(150,250] m
(250,350] m
(350,450] m
RNL
SL.ECA
SL.HWB
SL.ISO
SL.M-A
SL.SCA
SL (dB re 1 µPa² m²)
Frequency (Hz)

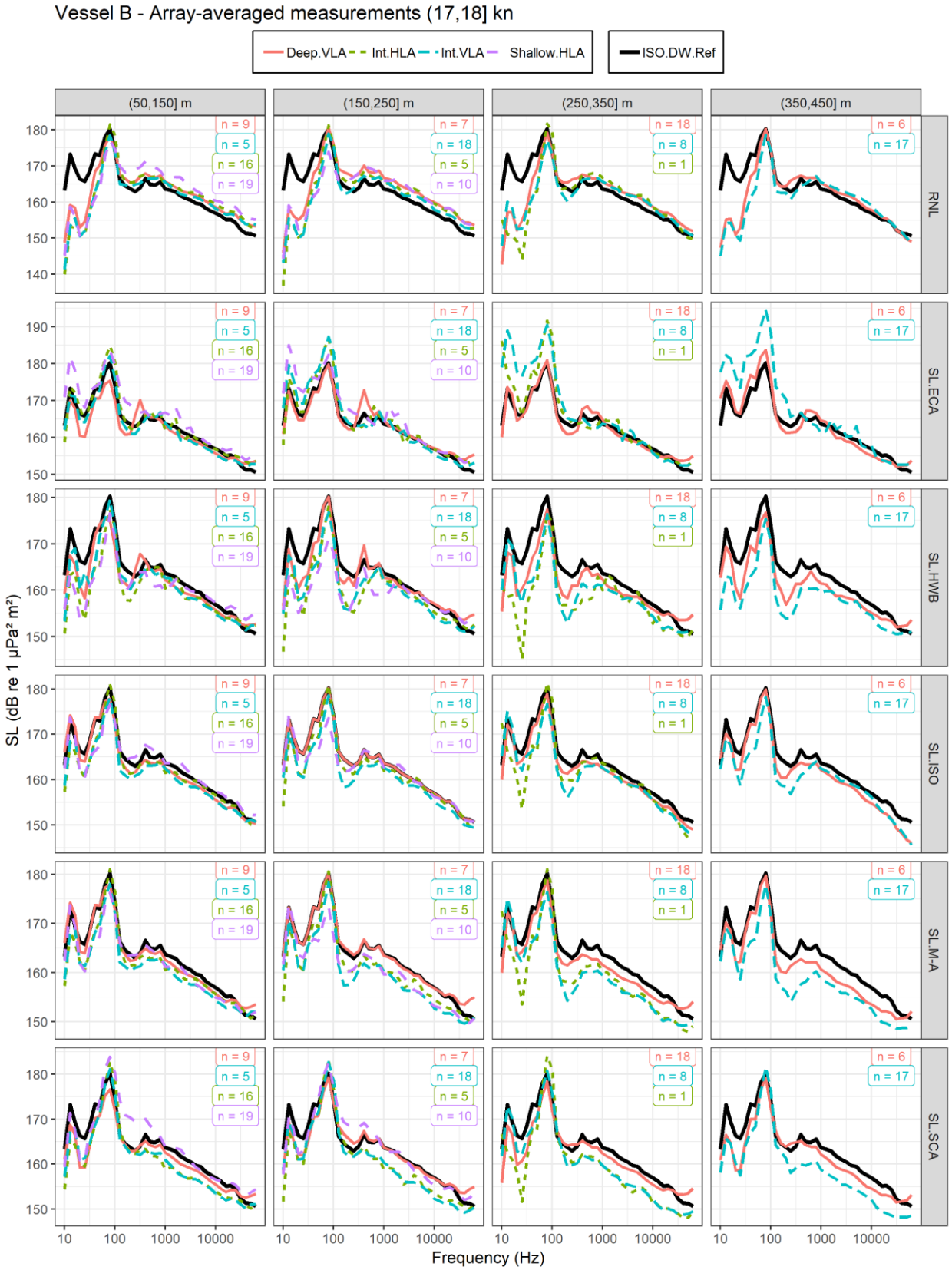
Vessel B - Array-averaged measurements (17,18] kn
Deep.VLA
Int.HLA
Int.VLA
Shallow.HLA
ISO.DW.Ref
(50,150] m
(150,250] m
(250,350] m
(350,450] m
RNL
SL.ECA
SL.HWB
SL.ISO
SL.M-A
SL.SCA
SL (dB re 1 µPa² m²)
Frequency (Hz)

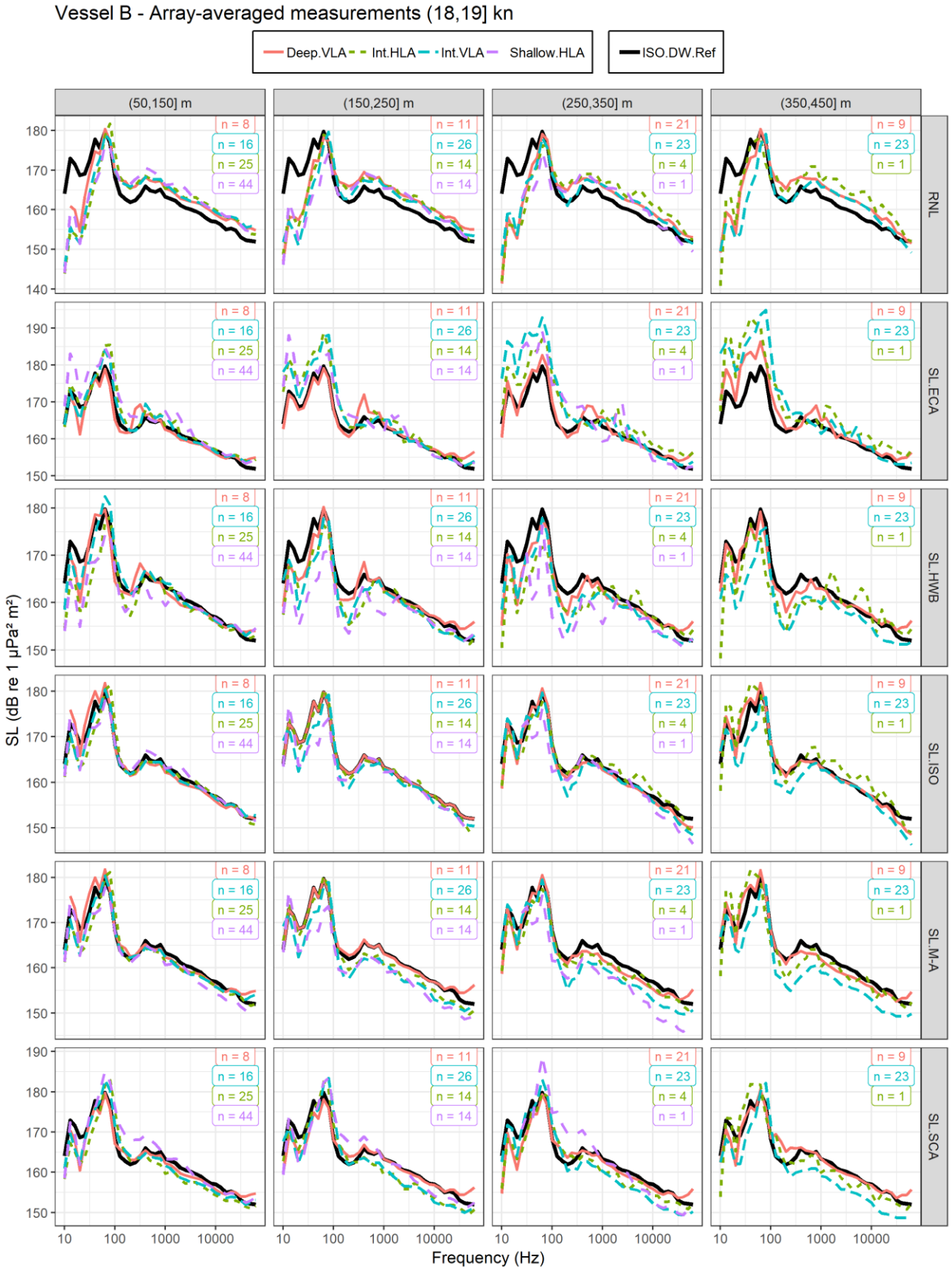
Vessel B - Array-averaged measurements (18,19] kn
Deep.VLA
Int.HLA
Int.VLA
Shallow.HLA
ISO.DW.Ref
(50,150] m
(150,250] m
(250,350] m
(350,450] m
RNL
SL.ECA
SL.HWB
SL.ISO
SL.M-A
SL.SCA
SL (dB re 1 µPa² m²)
Frequency (Hz)

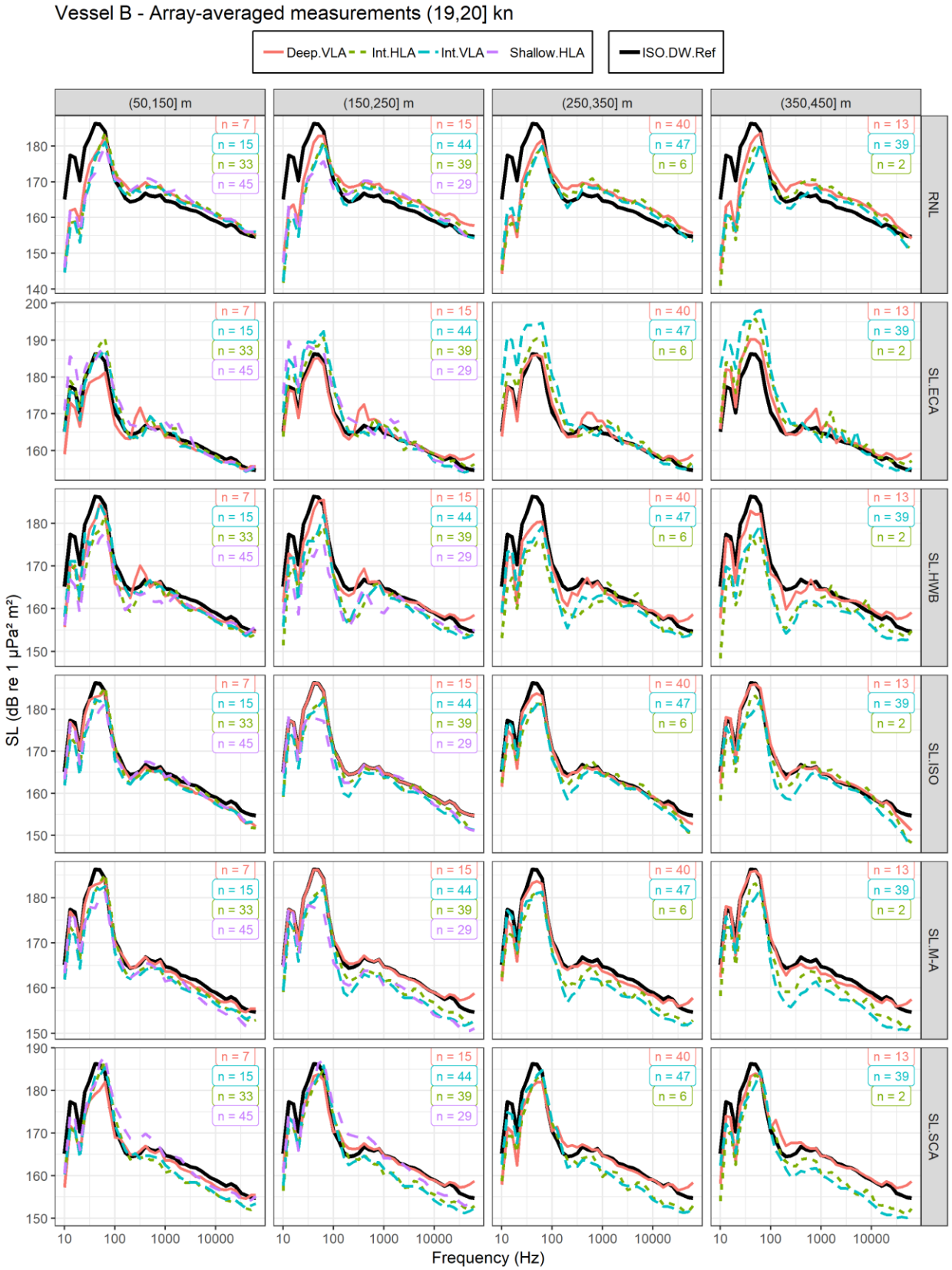
Vessel B - Array-averaged measurements (19,20] kn
Deep.VLA
Int.HLA
Int.VLA
Shallow.HLA
ISO.DW.Ref
(50,150] m
(150,250] m
(250,350] m
(350,450] m
RNL
SL.ECA
SL.HWB
SL.ISO
SL.M-A
SL.SCA
SL (dB re 1 µPa² m²)
Frequency (Hz)

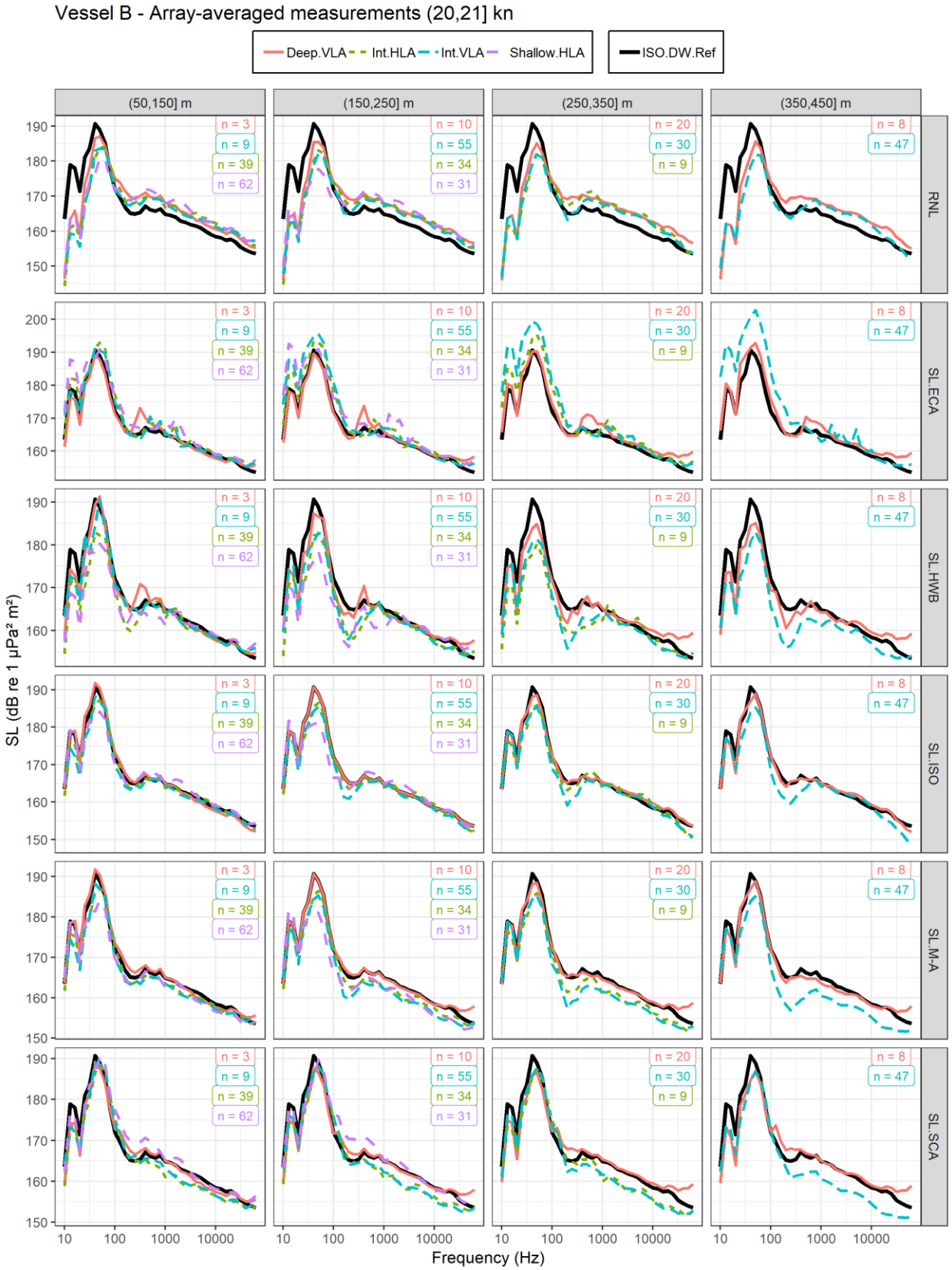
Vessel B - Array-averaged measurements (20,21] kn
Deep.VLA
Int.HLA
Int.VLA
Shallow.HLA
ISO.DW.Ref
(50,150] m
(150,250] m
(250,350] m
(350,450] m
RNL
SL.ECA
SL.HWB
SL.ISO
SL.M-A
SL.SCA
SL (dB re 1 µPa² m²)
Frequency (Hz)

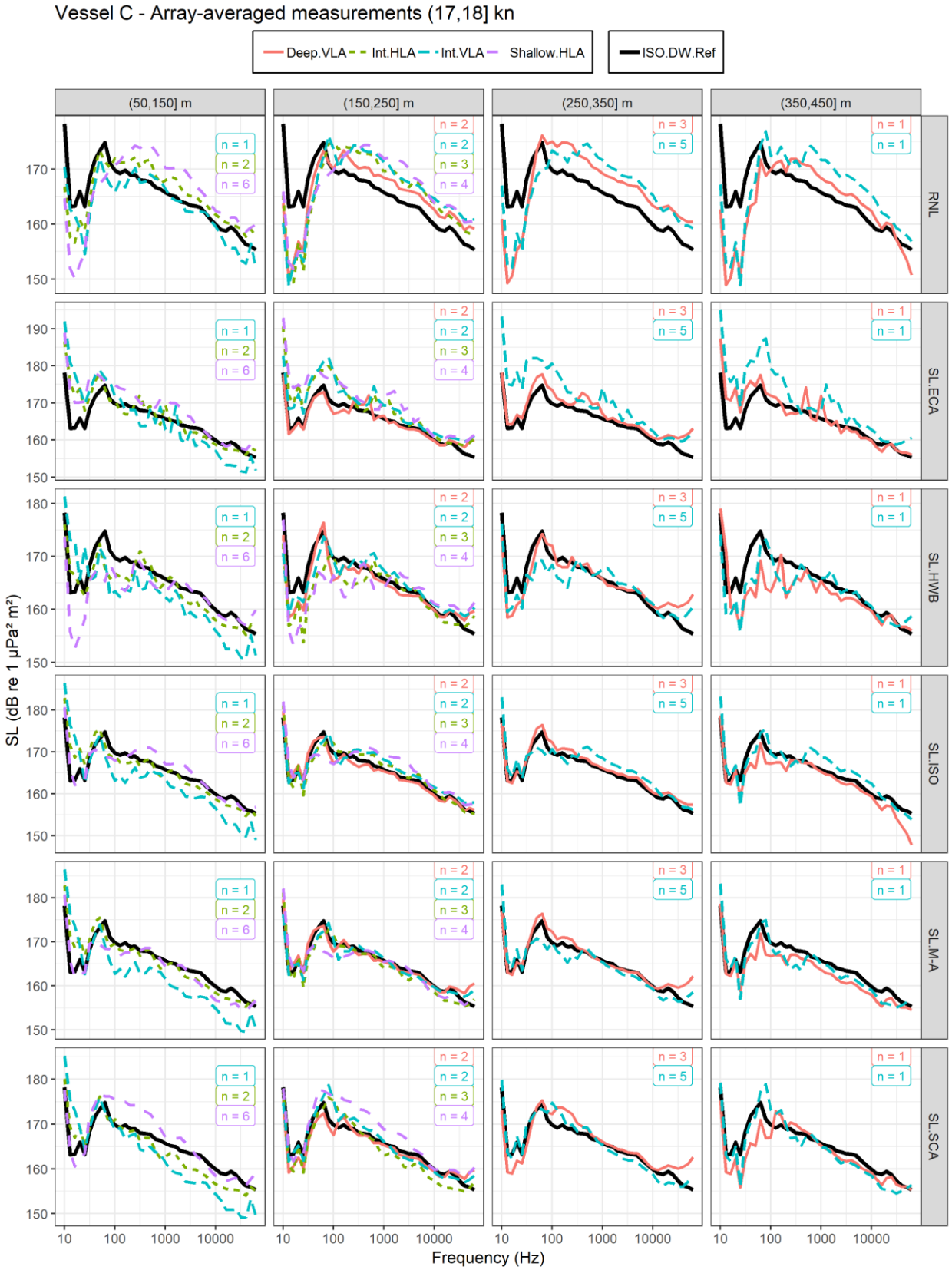
Vessel C - Array-averaged measurements (17,18] kn
Deep.VLA
Int.HLA
Int.VLA
Shallow.HLA
ISO.DW.Ref
(50,150] m
(150,250] m
(250,350] m
(350,450] m
RNL
SL.ECA
SL.HWB
SL.ISO
SL.M-A
SL.SCA
SL (dB re 1 µPa² m²)
Frequency (Hz)

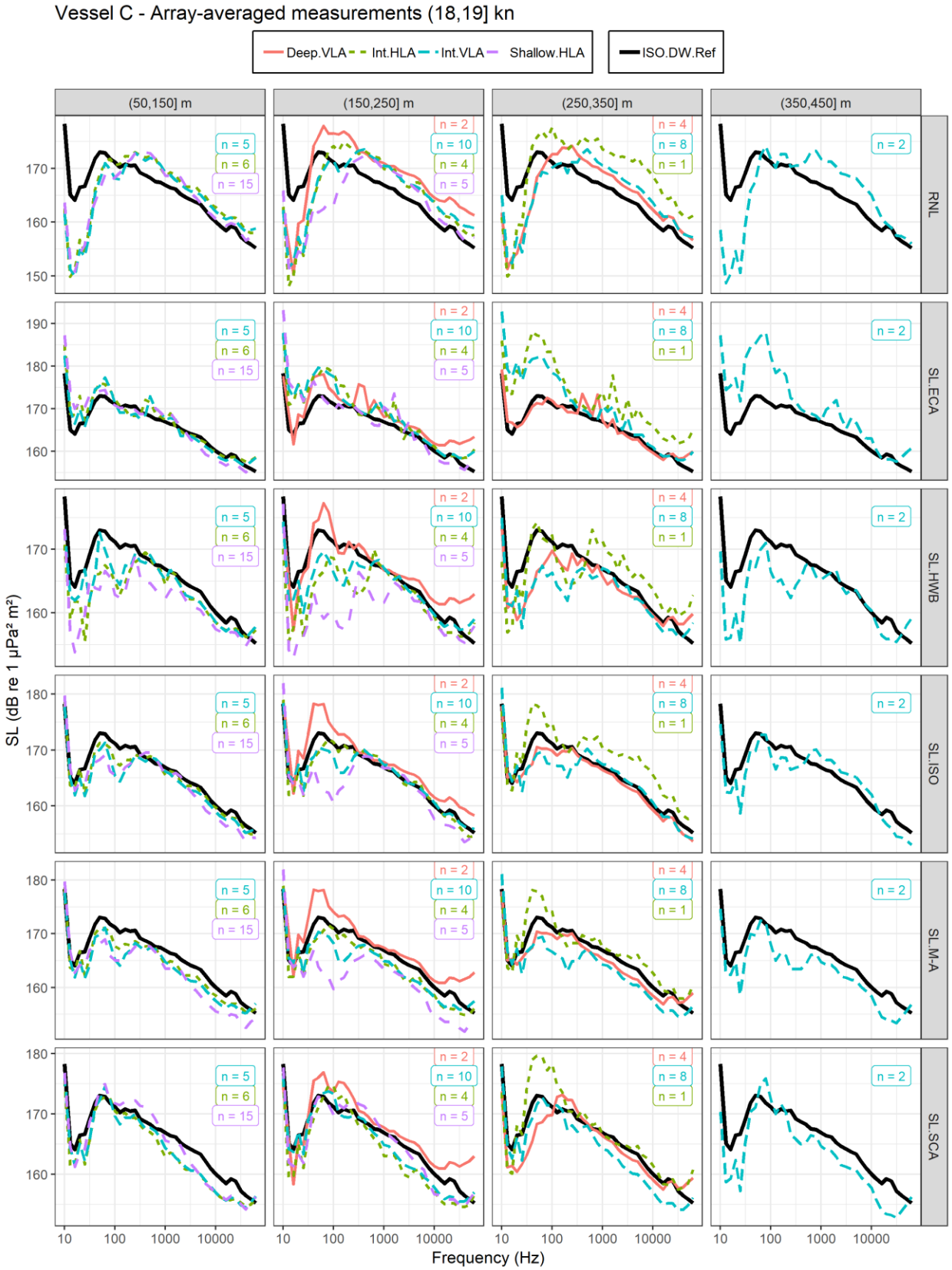
Vessel C - Array-averaged measurements (18,19] kn
Deep.VLA
Int.HLA
Int.VLA
Shallow.HLA
ISO.DW.Ref
(50,150] m
(150,250] m
(250,350] m
(350,450] m
RNL
SL.ECA
SL.HWB
SL.ISO
SL.M-A
SL.SCA
n = 5
n = 6
n = 15
n = 2
n = 10
n = 4
n = 5
n = 8
n = 1
SL (dB re 1 µPa² m²)
Frequency (Hz)
10
100
1000
10000

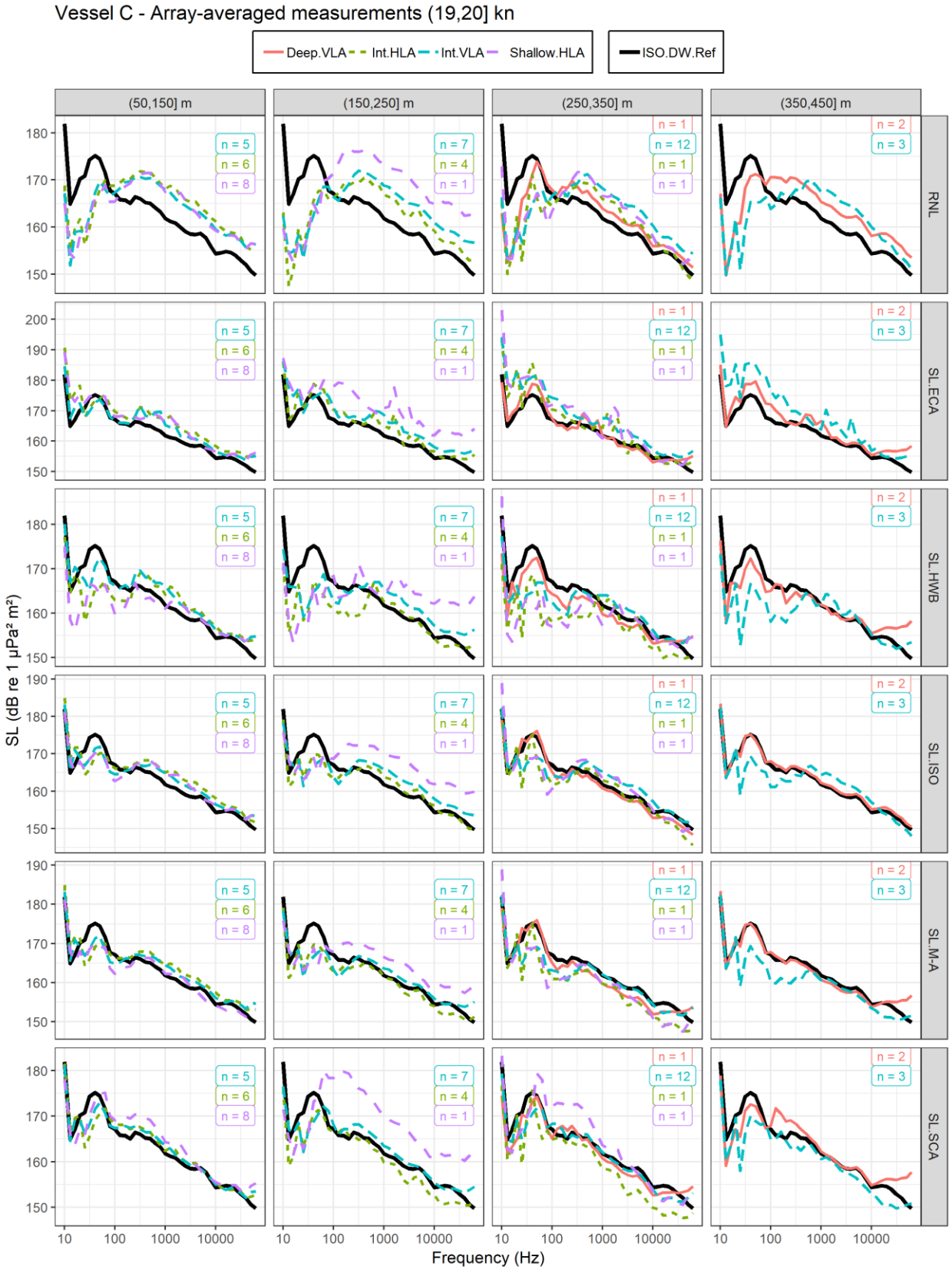
Vessel C - Array-averaged measurements (19,20] kn
Deep.VLA
Int.HLA
Int.VLA
Shallow.HLA
ISO.DW.Ref
(50,150] m
(150,250] m
(250,350] m
(350,450] m
RNL
SL.ECA
SL.HWB
SL.ISO
SL.M-A
SL.SCA
SL (dB re 1 µPa² m²)
Frequency (Hz)

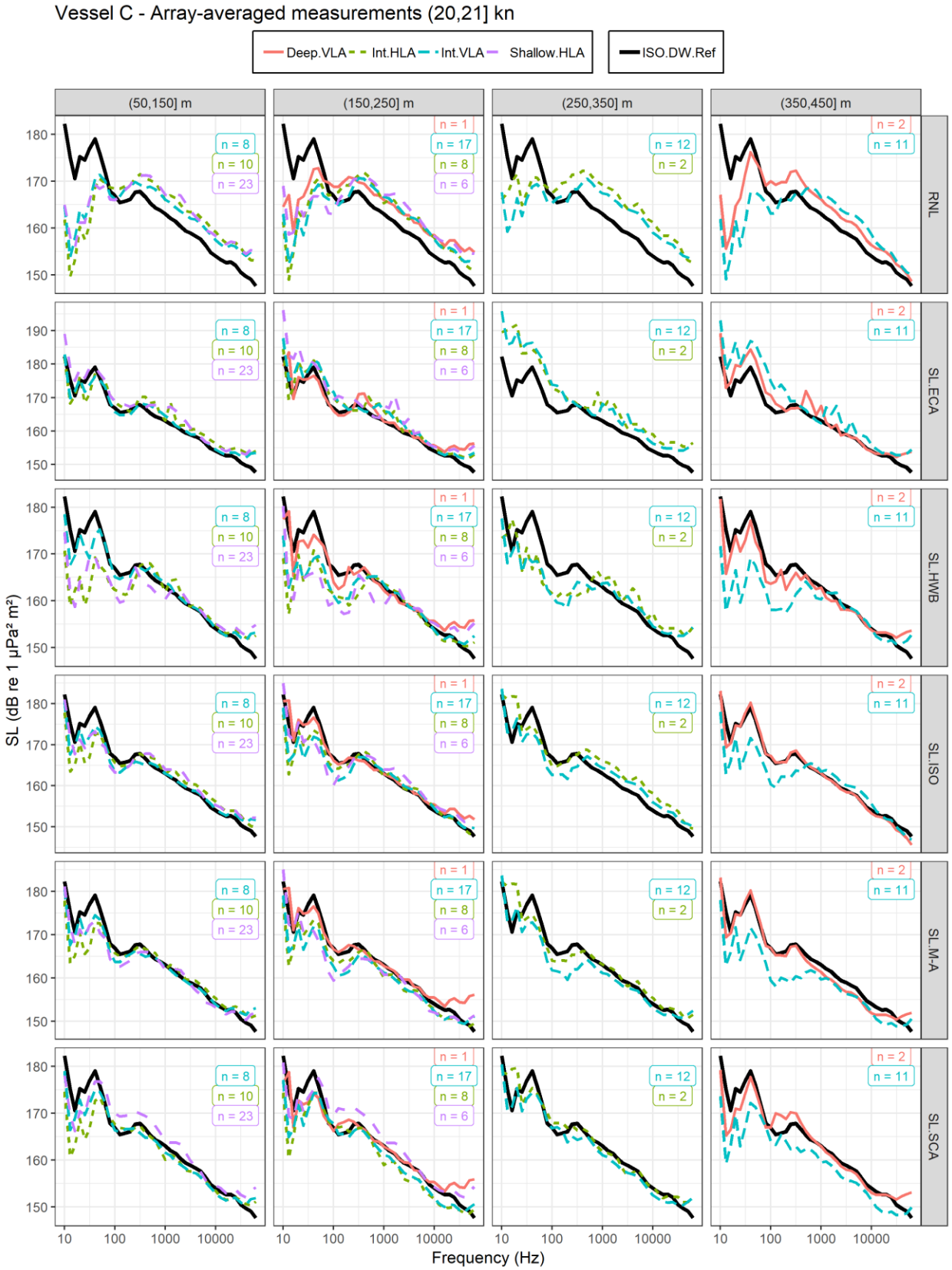
Vessel C - Array-averaged measurements (20,21] kn
Deep.VLA
Int.HLA
Int.VLA
Shallow.HLA
ISO.DW.Ref
(50,150] m
(150,250] m
(250,350] m
(350,450] m
RNL
SL.ECA
SL.HWB
SL.ISO
SL.M-A
SL.SCA
SL (dB re 1 µPa² m²)
Frequency (Hz)

APPENDIX E. COMPARISONS BETWEEN HYDROPHONE ARRAY CHANNELS

Plots in this appendix (Figures E-1 to E-5) have been included as a supplement to results presented in Section 4.2.6. Data presented in this appendix are the same as those shown in Section 4.2.6, but the presentation has been modified to show frequency-dependent differences between individual channels in the array-averaged measurements. These results are intended to show how measurements from individual array nodes contribute to the array-average values for the different VLA and HLA geometries tested during the experimental field trials.

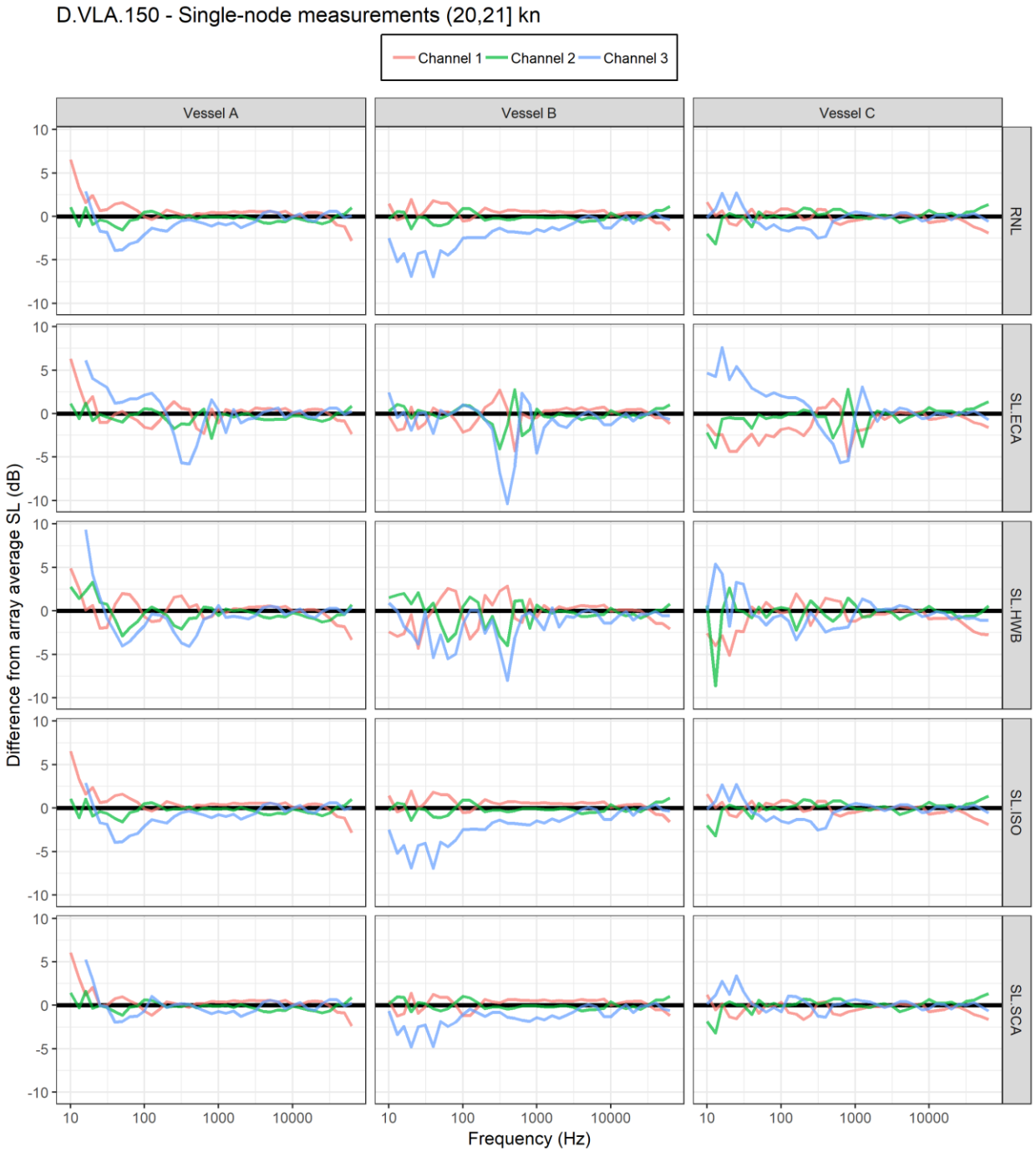

Figure E-1. Differences of single-node source levels from the array-average value for measurements of vessels A–C on the deep VLA (D.VLA.150). Average values are shown for the ten measurements of each vessel with closest point of approach (CPA) closest to 215 m from the VLA and speeds through water between 20–21 knots. Channels 1, 2, and 3 refer to the bottom, middle, and top hydrophones, respectively.

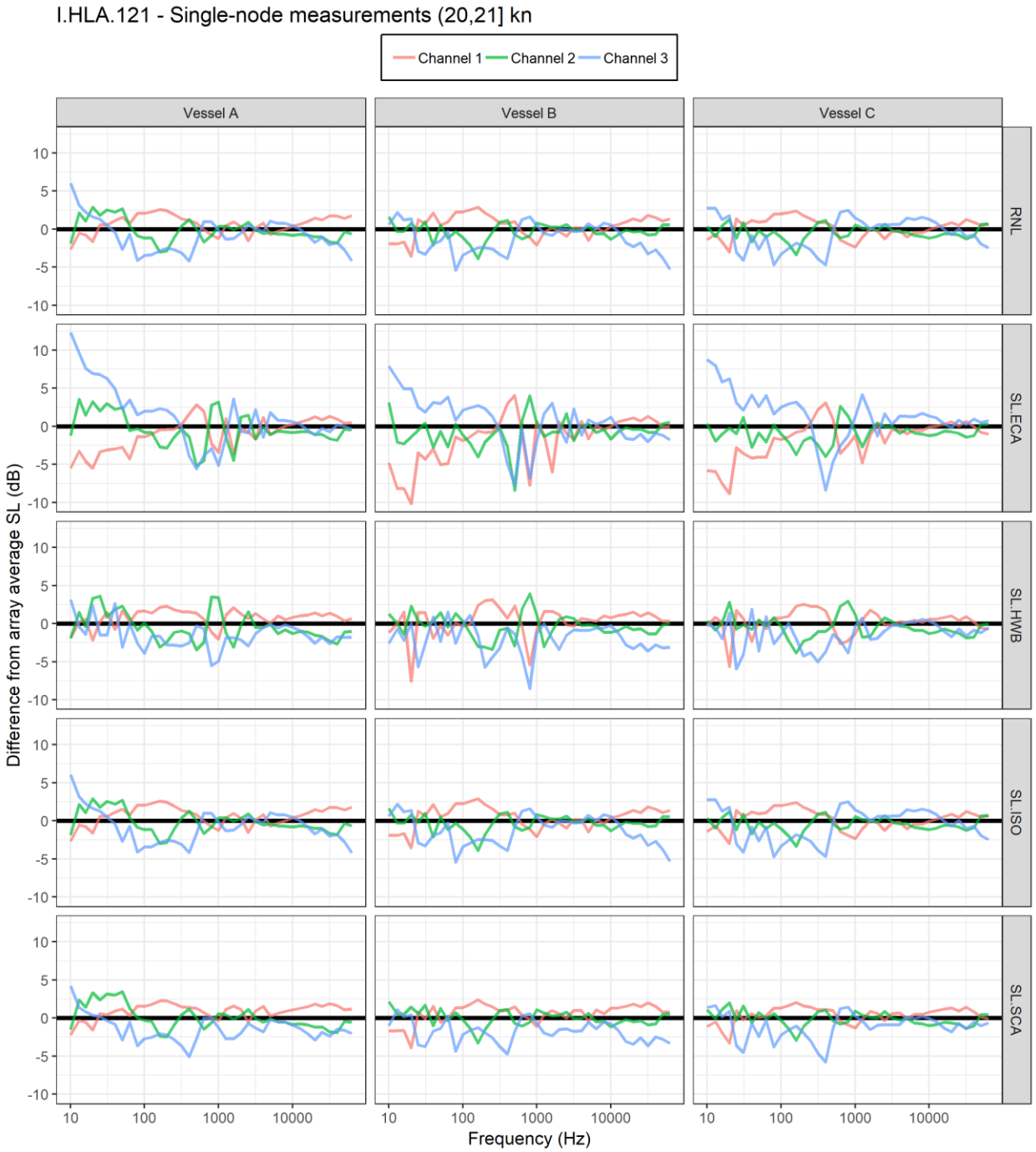

Figure E-2. Differences of single-node source levels from the array-average value for measurements of vessels A–C on the 121 m intermediate HLA (I.HLA.121). Average values are shown for the ten measurements of each vessel with closest point of approach (CPA) closest to 121 m from the VLA and speeds through water between 20–21 knots. Channels 1, 2, and 3 refer to the closest, middle, and farthest hydrophones from the vessel track, respectively.

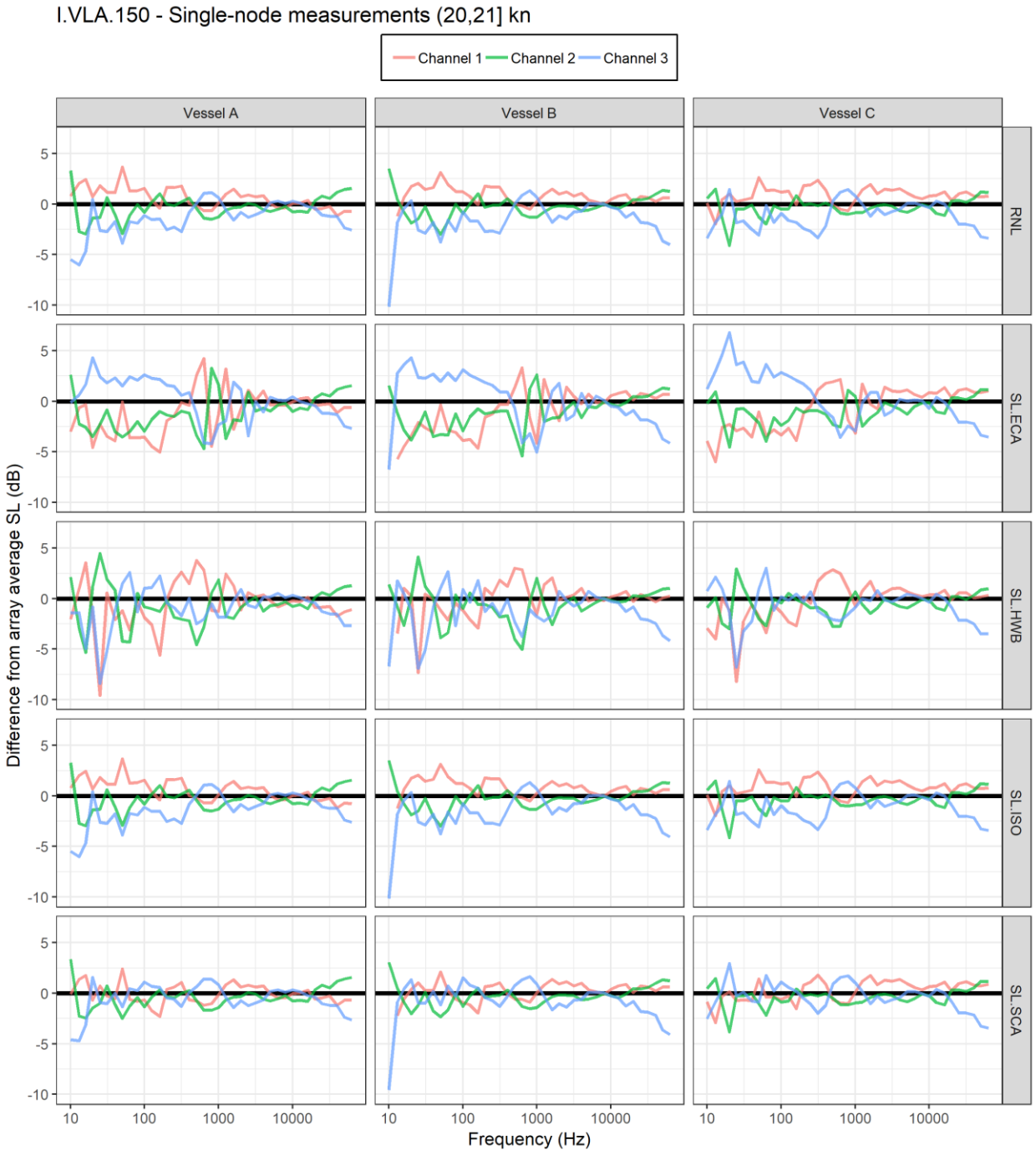

Figure E-3. Differences of single-node source levels from the array-average value for measurements of vessels A–C on the 150 m intermediate VLA (I.VLA.150). Average values are shown for the ten measurements of each vessel with closest point of approach (CPA) closest to 150 m from the VLA and speeds through water between 20–21 knots. Channels 1, 2, and 3 refer to the bottom, middle, and top hydrophones, respectively.

Figure E-4. Differences of single-node source levels from the array-average value for measurements of vessels A–C on the 350 m intermediate VLA (I.VLA.350). Average values are shown for the ten measurements of each vessel with closest point of approach (CPA) closest to 350 m from the VLA and speeds through water between 20–21 knots. Channels 1, 2, and 3 refer to the bottom, middle, and top hydrophones, respectively.

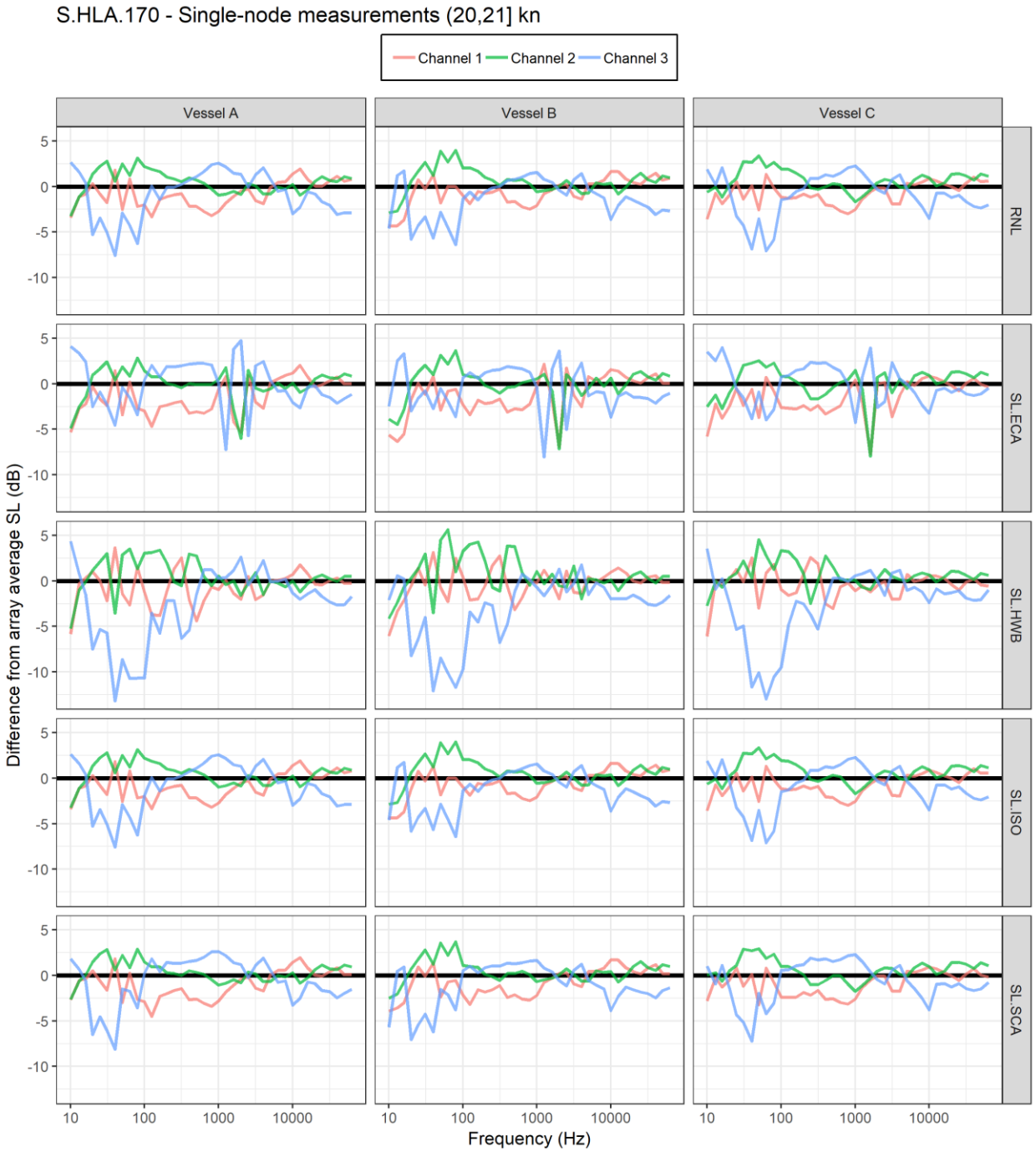

Figure E-5. Differences of single-node source levels from the array-average value for measurements of vessels A–C on the 170 m shallow HLA (S.HLA.170). Average values are shown for the ten measurements of each vessel with closest point of approach (CPA) closest to 170 m from the VLA and speeds through water between 20–21 knots. Channels 1, 2, and 3 refer to the closest, middle, and farthest hydrophones from the vessel track, respectively.

APPENDIX F. DRIFTING ARRAY MEASUREMENTS

Plots in this appendix show source level versus frequency curves for vessels A and B collected using the drifting hydrophone array. Coloured lines show array-averaged drift measurements and black lines show deep-water reference measurements (SL.ISO). Annotations indicate vessel STW, CPA distance, hydrophone, water depth, number of averaged channels, and recording time.

F.1. Vessel A Drifting URN Measurements

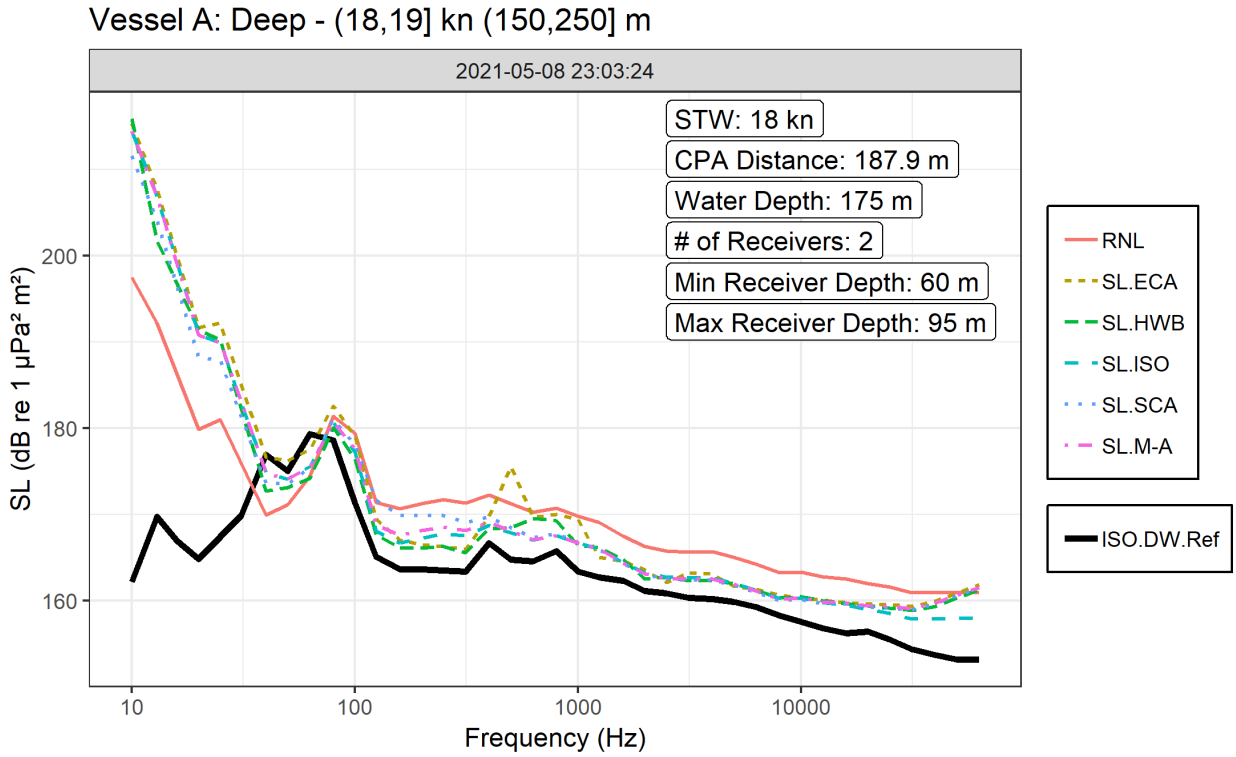

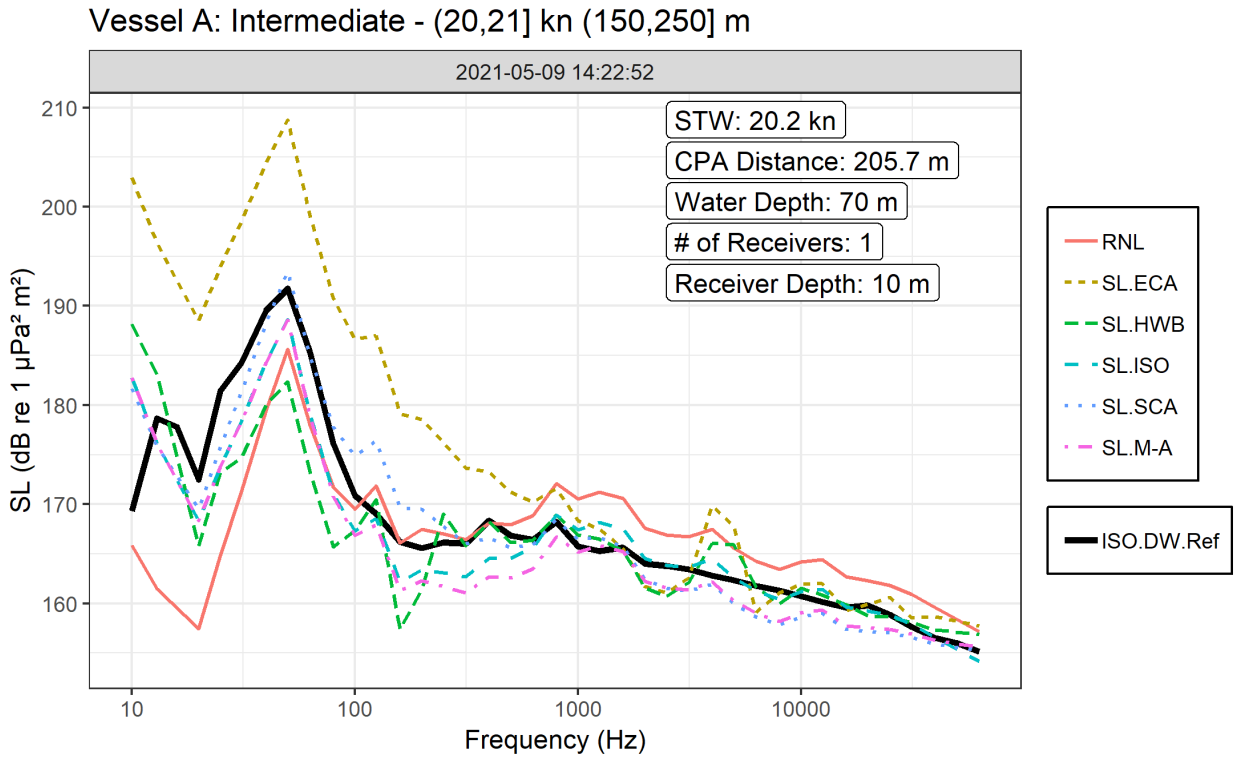
Vessel A: Intermediate - (20,21] kn (150,250] m
2021-05-09 14:22:52
STW: 20.2 kn
CPA Distance: 205.7 m
Water Depth: 70 m
# of Receivers: 1
Receiver Depth: 10 m
SL (dB re 1 µPa² m²)
Frequency (Hz)
RNL
SL.ECA
SL.HWB
SL.ISO
SL.SCA
SL.M-A
ISO.DW.Ref

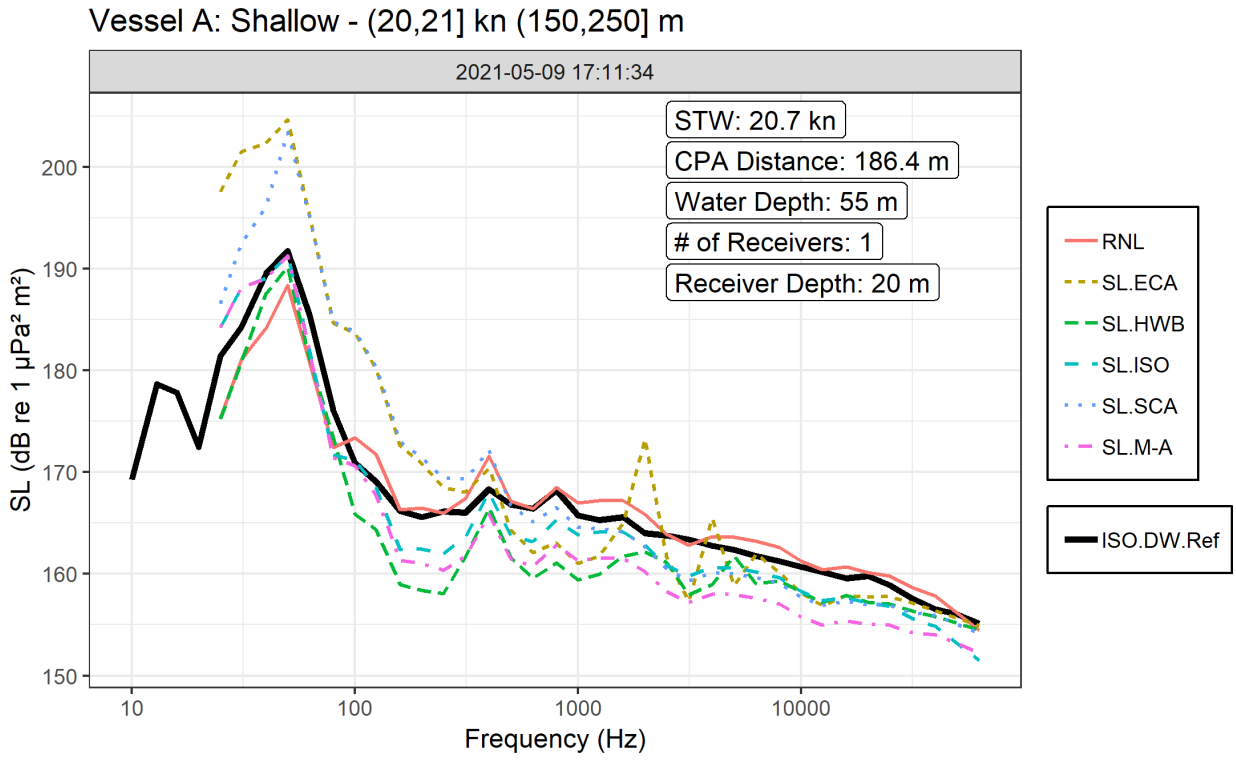
Vessel A: Shallow - (20,21] kn (150,250] m
2021-05-09 17:11:34
STW: 20.7 kn
CPA Distance: 186.4 m
Water Depth: 55 m
# of Receivers: 1
Receiver Depth: 20 m
SL (dB re 1 µPa² m²)
Frequency (Hz)
RNL
SL.ECA
SL.HWB
SL.ISO
SL.SCA
SL.M-A
ISO.DW.Ref

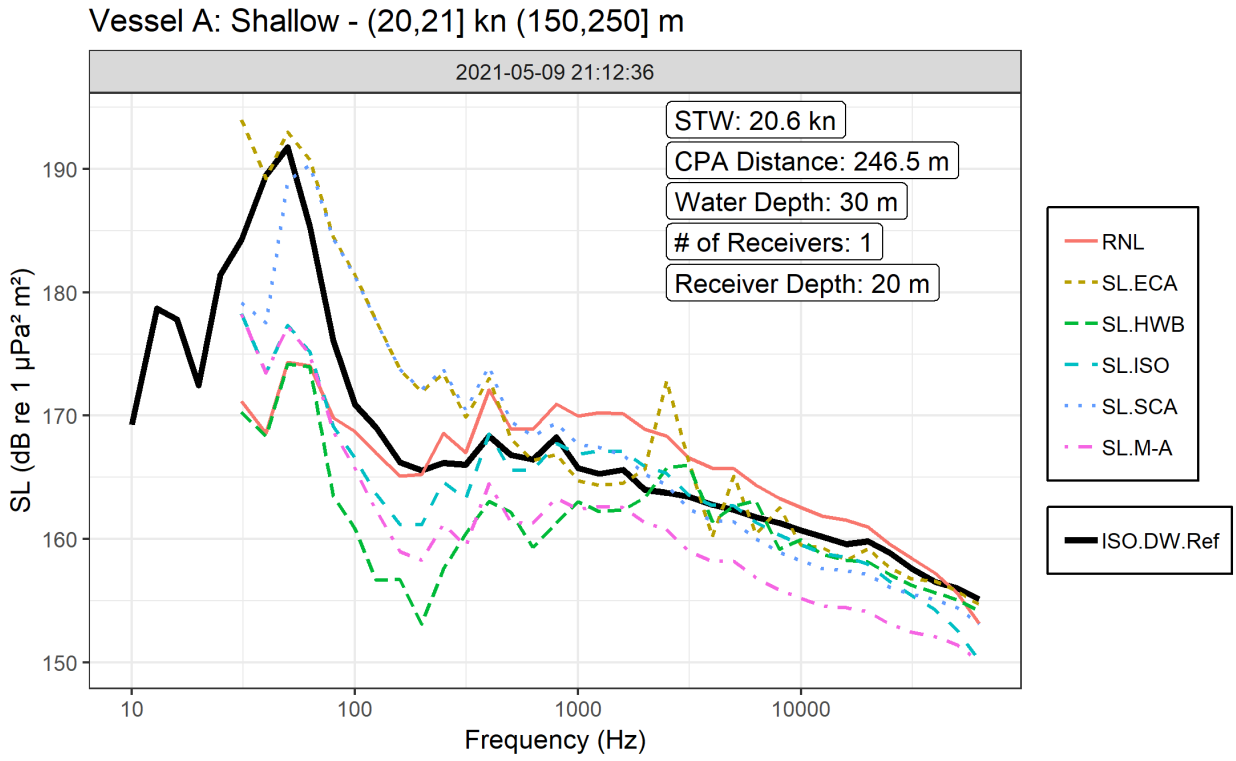
Vessel A: Shallow - (20,21] kn (150,250] m
2021-05-09 21:12:36
STW: 20.6 kn
CPA Distance: 246.5 m
Water Depth: 30 m
# of Receivers: 1
Receiver Depth: 20 m
SL (dB re 1 µPa² m²)
190
180
170
160
150
10
100
1000
10000
Frequency (Hz)
RNL
SL.ECA
SL.HWB
SL.ISO
SL.SCA
SL.M-A
ISO.DW.Ref

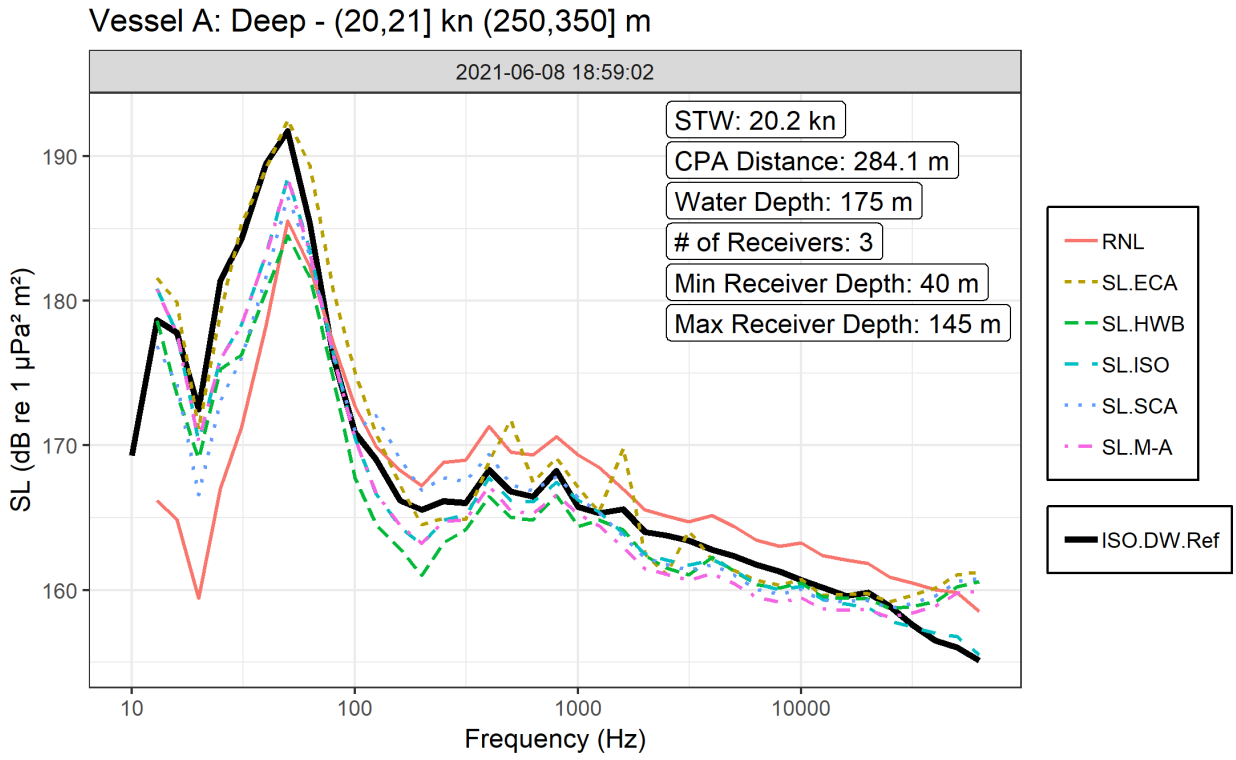
Vessel A: Deep - (20,21] kn (250,350] m
2021-06-08 18:59:02
STW: 20.2 kn
CPA Distance: 284.1 m
Water Depth: 175 m
# of Receivers: 3
Min Receiver Depth: 40 m
Max Receiver Depth: 145 m
SL (dB re 1 µPa² m²)
190
180
170
160
10
100
1000
10000
Frequency (Hz)
RNL
SL.ECA
SL.HWB
SL.ISO
SL.SCA
SL.M-A
ISO.DW.Ref

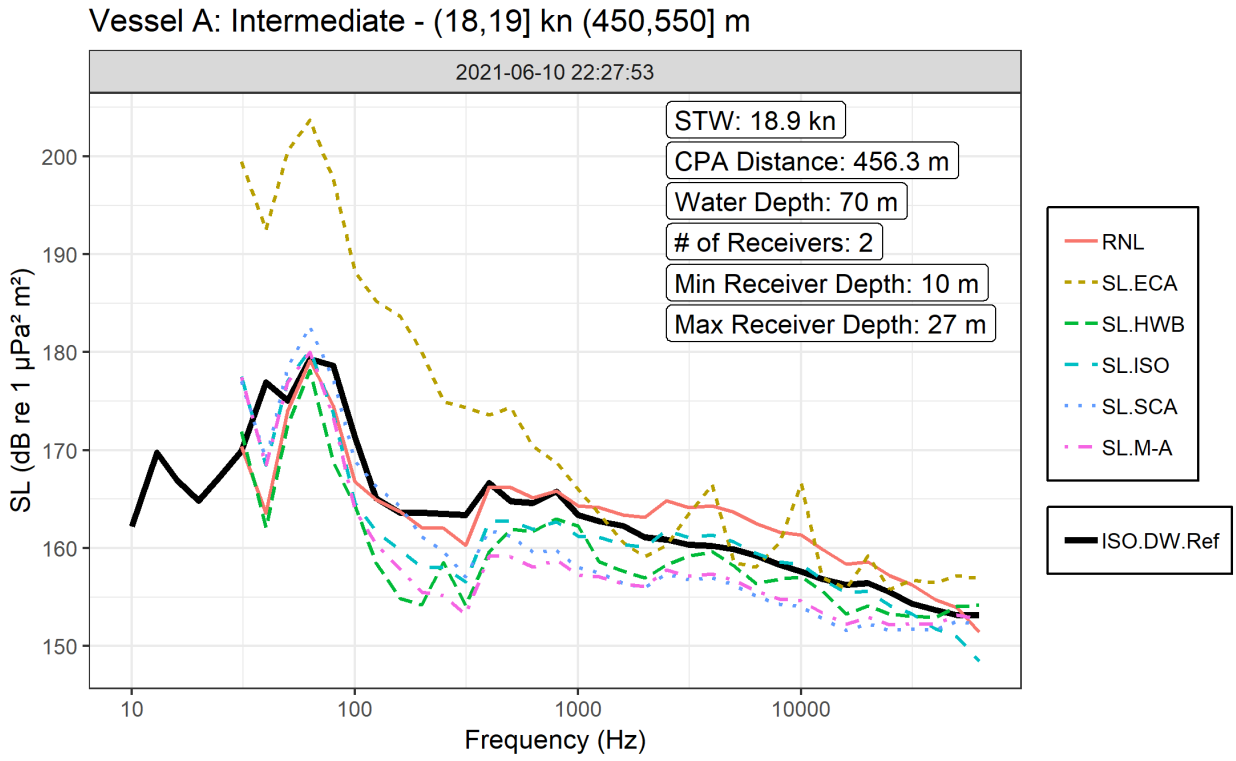
Vessel A: Intermediate - (18,19] kn (450,550] m
2021-06-10 22:27:53
STW: 18.9 kn
CPA Distance: 456.3 m
Water Depth: 70 m
# of Receivers: 2
Min Receiver Depth: 10 m
Max Receiver Depth: 27 m
SL (dB re 1 µPa² m²)
200
190
180
170
160
150
10
100
1000
10000
Frequency (Hz)
RNL
SL.ECA
SL.HWB
SL.ISO
SL.SCA
SL.M-A
ISO.DW.Ref

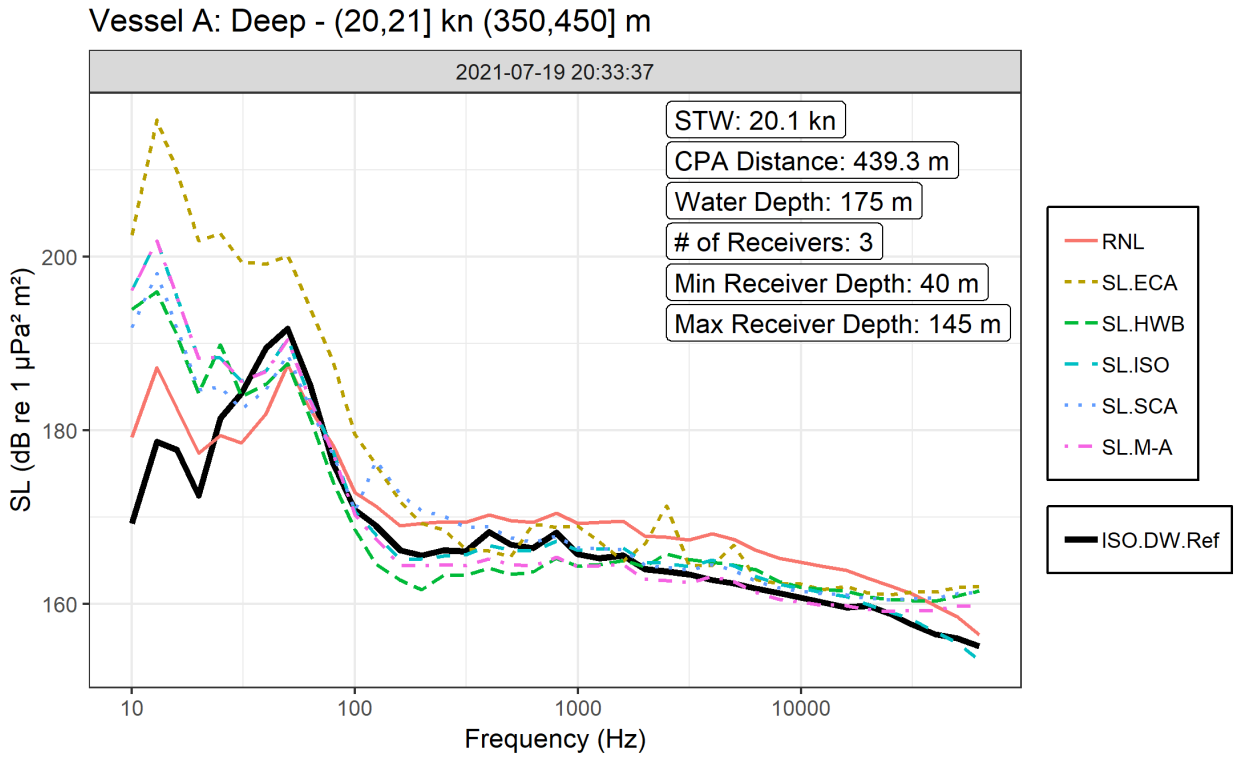
Vessel A: Deep - (20,21] kn (350,450] m
2021-07-19 20:33:37
STW: 20.1 kn
CPA Distance: 439.3 m
Water Depth: 175 m
# of Receivers: 3
Min Receiver Depth: 40 m
Max Receiver Depth: 145 m
SL (dB re 1 µPa² m²)
200
180
160
10
100
1000
10000
Frequency (Hz)
RNL
SL.ECA
SL.HWB
SL.ISO
SL.SCA
SL.M-A
ISO.DW.Ref

F.2. Vessel B Drifting URN Measurements

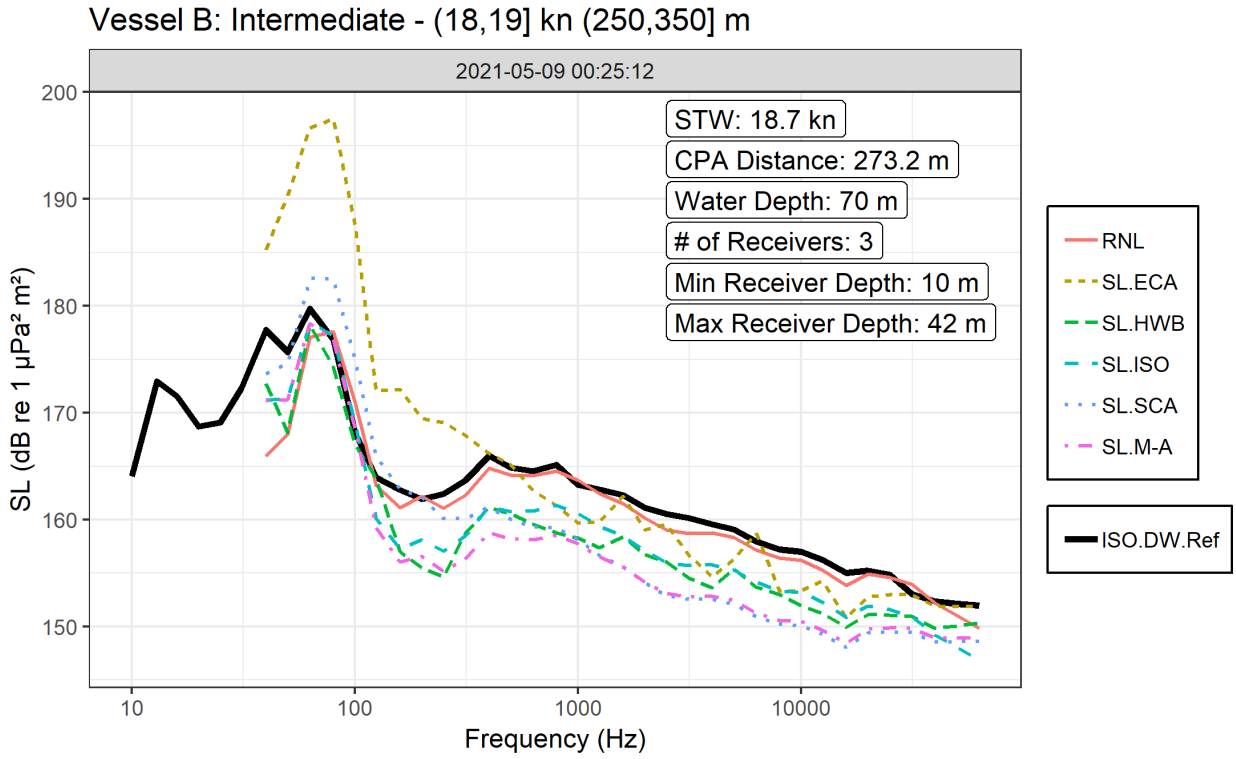

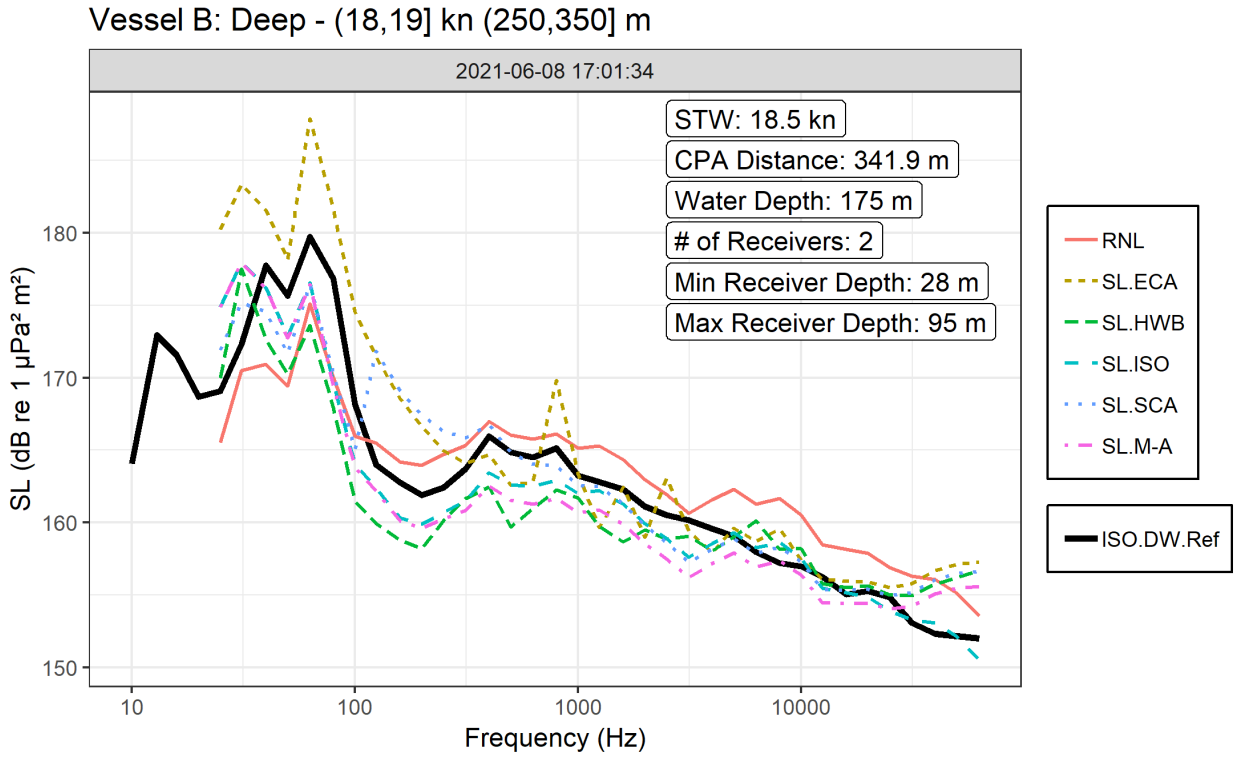

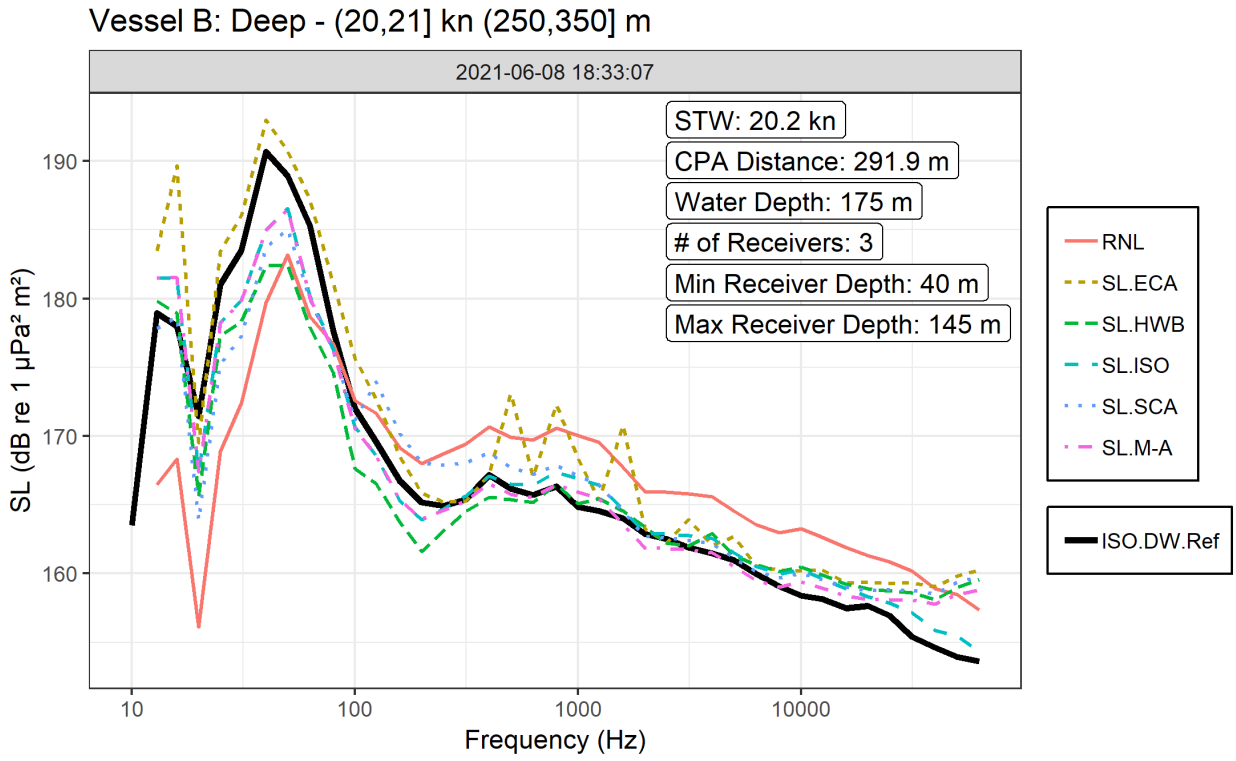
Vessel B: Deep - (20,21] kn (250,350] m
2021-06-08 18:33:07
STW: 20.2 kn
CPA Distance: 291.9 m
Water Depth: 175 m
# of Receivers: 3
Min Receiver Depth: 40 m
Max Receiver Depth: 145 m
SL (dB re 1 µPa² m²)
190
180
170
160
10
100
1000
10000
Frequency (Hz)
RNL
SL.ECA
SL.HWB
SL.ISO
SL.SCA
SL.M-A
ISO.DW.Ref

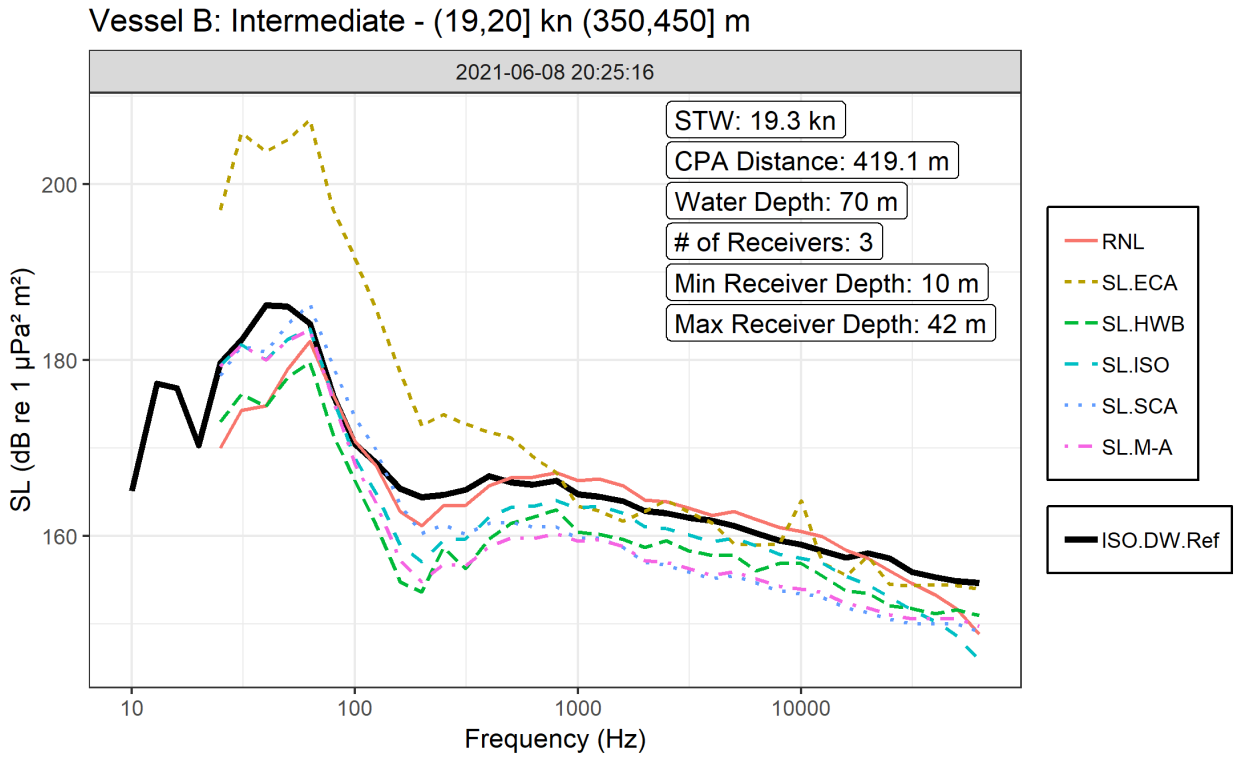
Vessel B: Intermediate - (19,20] kn (350,450] m
2021-06-08 20:25:16
STW: 19.3 kn
CPA Distance: 419.1 m
Water Depth: 70 m
# of Receivers: 3
Min Receiver Depth: 10 m
Max Receiver Depth: 42 m
SL (dB re 1 µPa² m²)
200
180
160
10
100
1000
10000
Frequency (Hz)
RNL
SL.ECA
SL.HWB
SL.ISO
SL.SCA
SL.M-A
ISO.DW.Ref

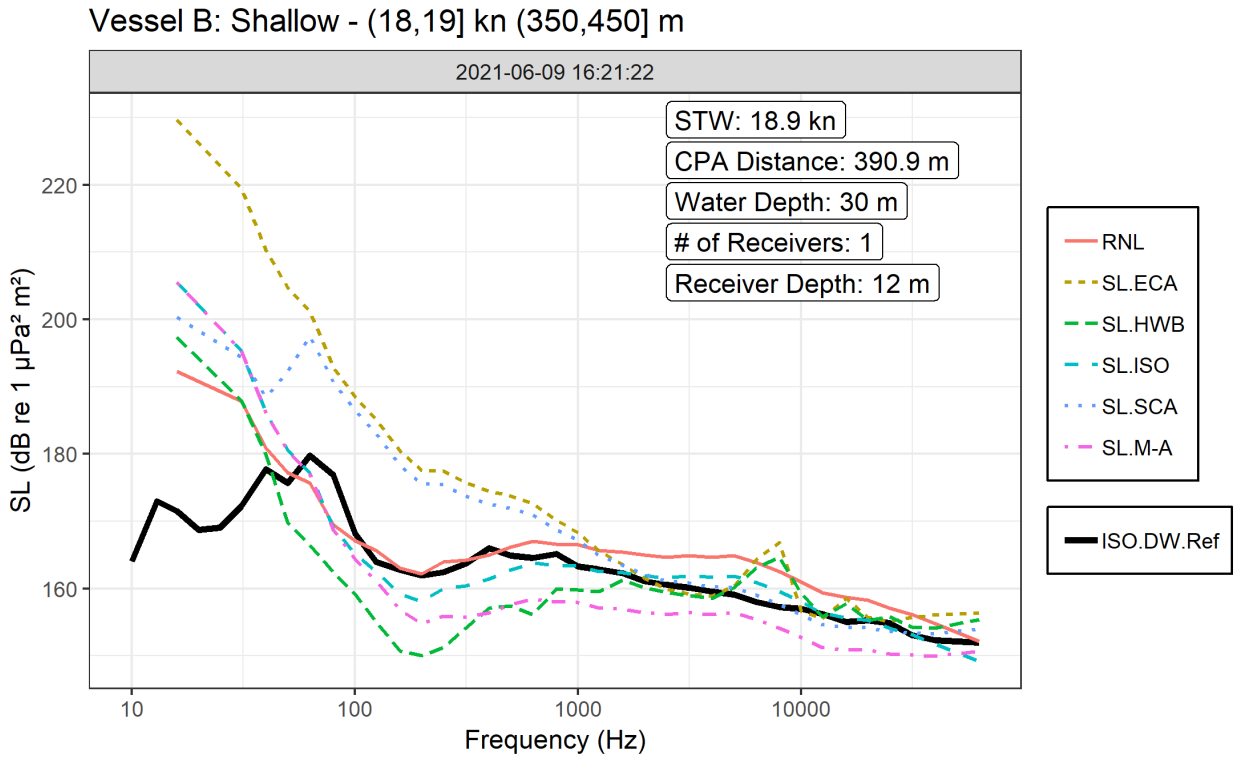
Vessel B: Shallow - (18,19] kn (350,450] m
2021-06-09 16:21:22
STW: 18.9 kn
CPA Distance: 390.9 m
Water Depth: 30 m
# of Receivers: 1
Receiver Depth: 12 m
SL (dB re 1 µPa² m²)
220
200
180
160
10
100
1000
10000
Frequency (Hz)
RNL
SL.ECA
SL.HWB
SL.ISO
SL.SCA
SL.M-A
ISO.DW.Ref

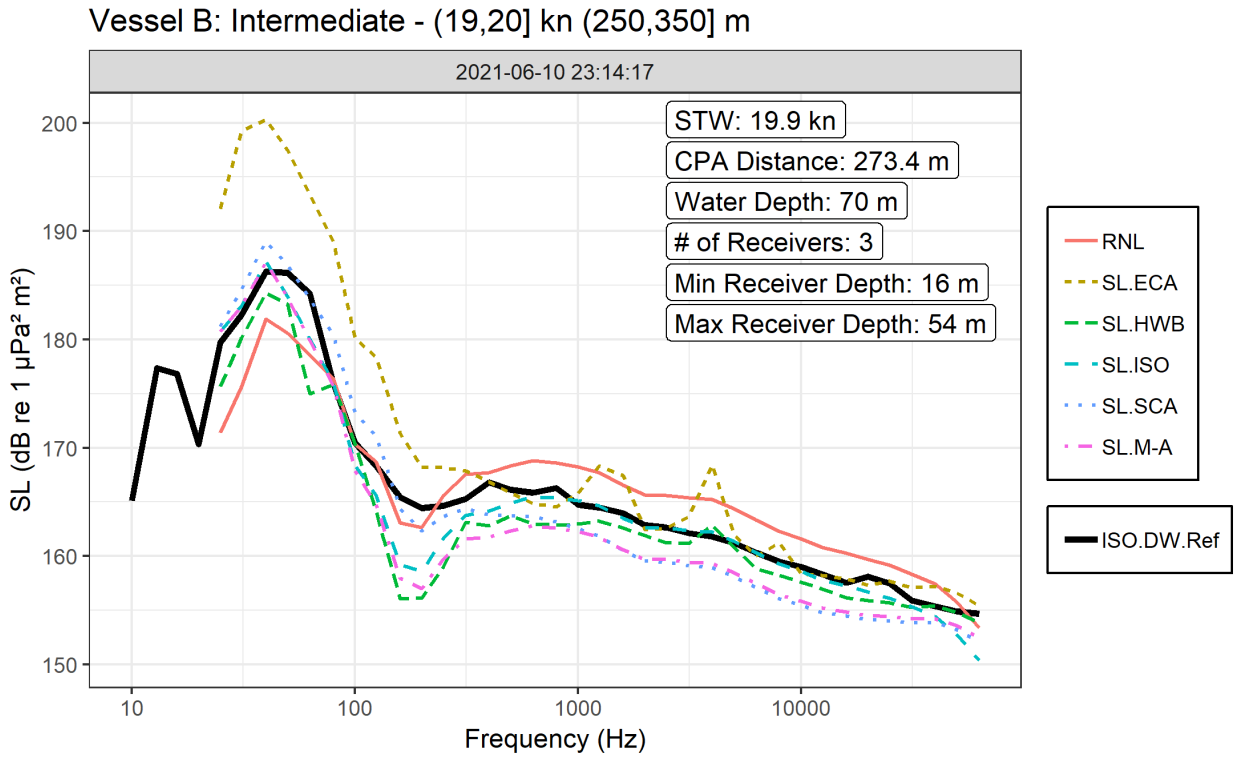
Vessel B: Intermediate - (19,20] kn (250,350] m
2021-06-10 23:14:17
STW: 19.9 kn
CPA Distance: 273.4 m
Water Depth: 70 m
# of Receivers: 3
Min Receiver Depth: 16 m
Max Receiver Depth: 54 m
SL (dB re 1 µPa² m²)
200
190
180
170
160
150
10
100
1000
10000
Frequency (Hz)
RNL
SL.ECA
SL.HWB
SL.ISO
SL.SCA
SL.M-A
ISO.DW.Ref

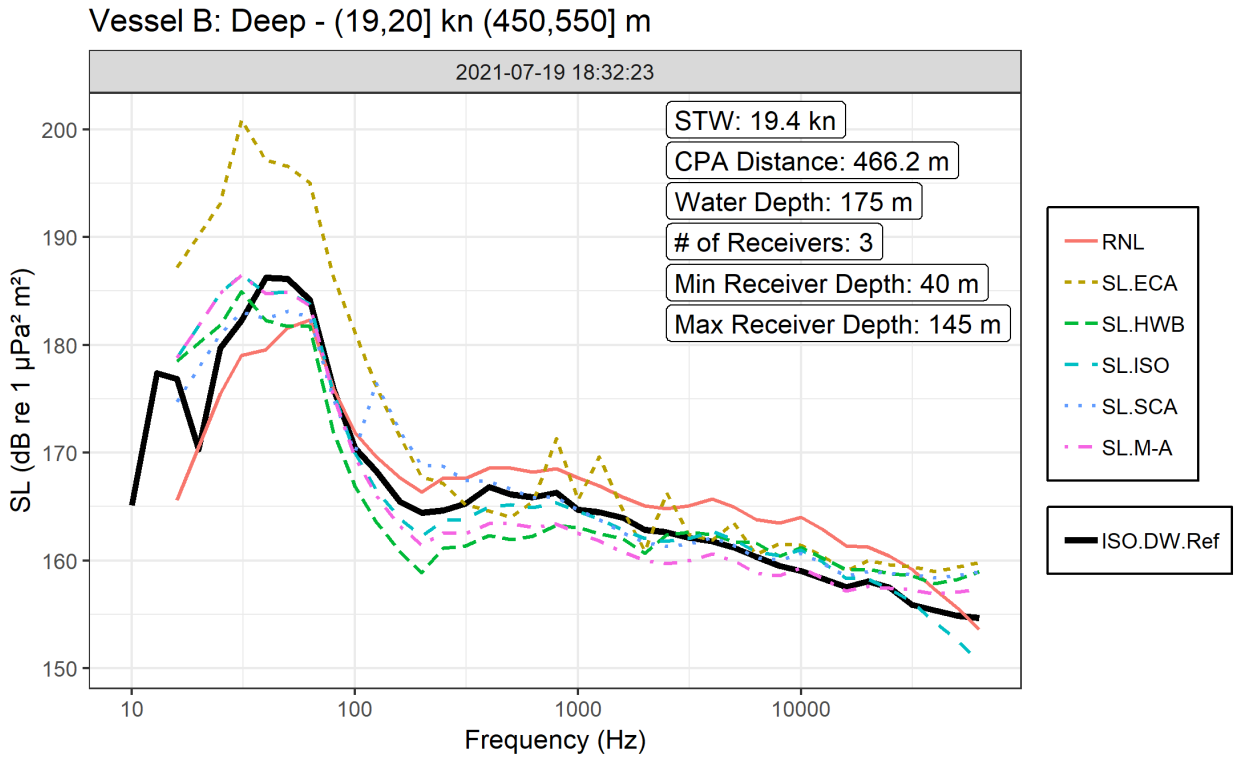
Vessel B: Deep - (19,20] kn (450,550] m
2021-07-19 18:32:23
STW: 19.4 kn
CPA Distance: 466.2 m
Water Depth: 175 m
# of Receivers: 3
Min Receiver Depth: 40 m
Max Receiver Depth: 145 m
SL (dB re 1 µPa² m²)
Frequency (Hz)
RNL
SL.ECA
SL.HWB
SL.ISO
SL.SCA
SL.M-A
ISO.DW.Ref

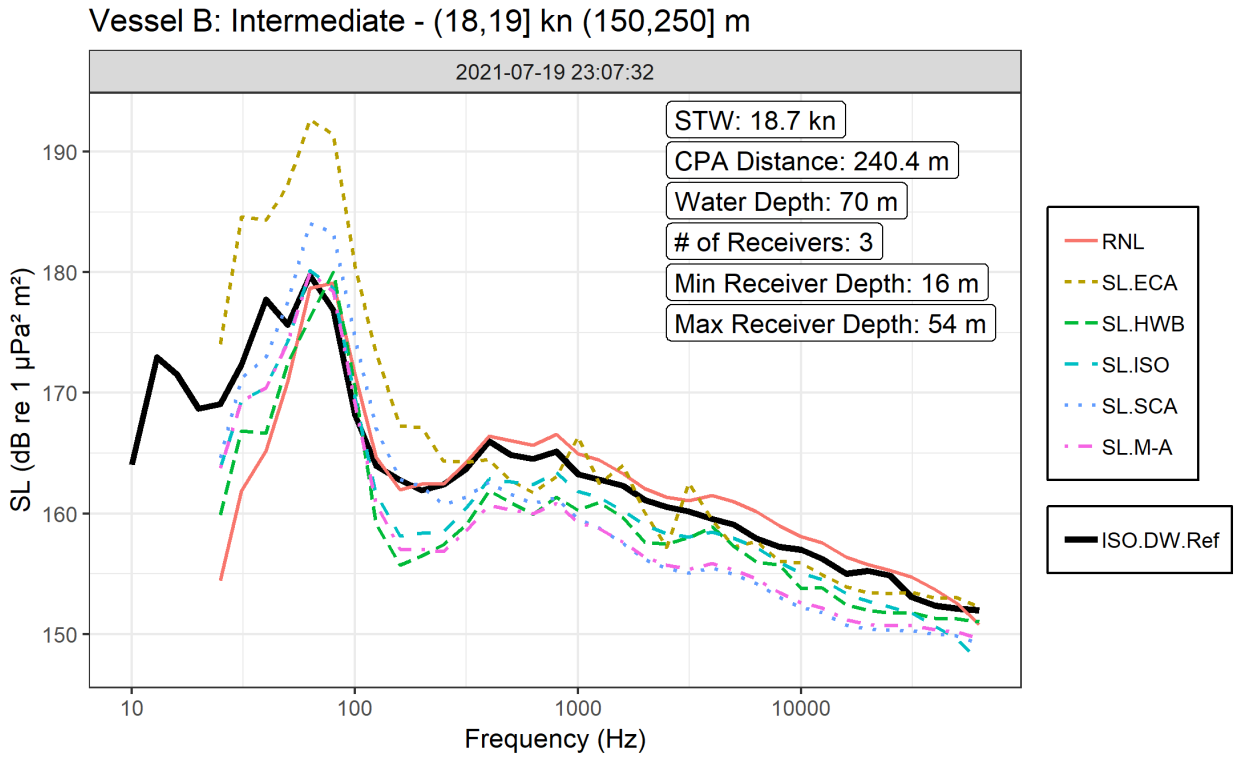
Vessel B: Intermediate - (18,19] kn (150,250] m
2021-07-19 23:07:32
STW: 18.7 kn
CPA Distance: 240.4 m
Water Depth: 70 m
# of Receivers: 3
Min Receiver Depth: 16 m
Max Receiver Depth: 54 m
SL (dB re 1 µPa² m²)
Frequency (Hz)
RNL
SL.ECA
SL.HWB
SL.ISO
SL.SCA
SL.M-A
ISO.DW.Ref